2010

Biodegradation of Groundwater Pollutants (Chlorinated Hydrocarbons) in Vegetated Wetlands: Role of Aerobic Microbes Naturally Associated with Roots of Common Plants

Christina Lynn Powell
Wright State University

BIODEGRADATION OF GROUNDWATER POLLUTANTS (CHLORINATED HYDROCARBONS) IN VEGETATED WETLANDS: ROLE OF AEROBIC MICROBES NATURALLY ASSOCIATED WITH ROOTS OF COMMON PLANTS

A dissertation submitted in partial fulfillment of the
requirements for the degree of
Doctor of Philosophy

By

CHRISTINA LYNN POWELL
M.S., Texas A&M University, 2005

2010
Wright State University

WRIGHT STATE UNIVERSITY
SCHOOL OF GRADUATE STUDIES

September 27, 2010

I HEREBY RECOMMEND THAT THE DISSERTATION PREPARED UNDER MY SUPERVISION BY Christina Lynn Powell ENTITLED Biodegradation of Groundwater Pollutants (Chlorinated Hydrocarbons) in Vegetated Wetlands: Role of Aerobic Microbes Naturally Associated with Roots of Common Plants BE ACCEPTED IN PARTIAL FULFILLMENT OF THE REQUIREMENTS FOR THE DEGREE OF Doctor of Philosophy.

Abinash Agrawal, Ph.D.
Dissertation Director

Don F. Cipollini, Ph.D.
Director, Environmental Sciences
Ph.D. Program

Andrew T. Hsu, Ph.D.
Dean, School of Graduate Studies

Committee on
Final Examination

Abinash Agrawal, Ph.D.

Songlin Cheng, Ph.D.

Don F. Cipollini, Ph.D.

Mark N. Goltz, Ph.D.

Patrick J. Megonigal, Ph.D.

ABSTRACT

Powell, Christina, L. Ph.D. Environmental Sciences Ph.D. Program, Wright State University, 2010. Biodegradation of Groundwater Pollutants (Chlorinated Hydrocarbons) in Vegetated Wetlands: Role of Aerobic Microbes Naturally Associated with Roots of Common Plants.

Chlorinated aliphatic hydrocarbons (CAHs) are often found as groundwater contaminants because of past industrial activities and disposal practices. CAHs pose a threat to human health and thus, create a need to find both natural and engineered processes that can remove these chlorinated compounds from the environment. Natural attenuation by oxidative biodegradation is especially important because it can allow for mineralization to carbon dioxide, a nontoxic end-product. The goal of this research was to evaluate the potential oxidative biodegradation of CAHs by microorganisms that are naturally associated with wetland plant roots. The research was divided into field work and laboratory batch studies.

The field work consisted of using newly designed pore water samplers to provide a biogeochemical characterization of a constructed wetland environment with an emphasis on the shallow vegetated zone. Reducing conditions were found at the bottom of the wetland with overlapping zones of nitrate, iron, and sulfate reduction and methanogenesis. More oxidizing conditions were found closer to the surface and in the root zone. There was evidence of tetrachloroethene (PCE) degradation by its removal and formation of daughter products, trichloroethene (TCE) and vinyl chloride (VC), both of which disappeared by possible oxidative processes in the near surface environment and root zone.

The laboratory work was done using a unique approach with microcosms containing soil-free washed wetland plant roots. The activity and TCE degradation potential by aerobic methane- and ammonia-oxidizing microorganisms naturally associated with *Carex comosa* roots was investigated. Methane oxidation developed faster than ammonia oxidation during the respective enrichment periods. After enrichment, methane oxidizers were able to degrade TCE in contrast to ammonia oxidizers, which were rapidly and completely inhibited, perhaps due to the presence of TCE or TCE degradation products. The root morphology, methane-oxidizing activity, and TCE degradation potential was compared between *Carex comosa* and *Scirpus atrovirens. Carex comosa* roots were found to have shorter and thicker roots compared to *Scirpus atrovirens*, which grew longer and were more fibrous. Initial methane oxidation was greater with the *Carex comosa* roots compared to the *Scirpus atrovirens* roots, however, TCE degradation was quite similar with roots from both species. The potential for methane oxidizers naturally associated with *Carex comosa* roots to degrade *cis*-1,2-dichloroethene (*cis*DCE), TCE, and 1,1,1-trichloroethane (1,1,1TCA) was investigated and the degradation rates were determined. TCE and *cis*DCE were both significantly degraded with first order kinetics while 1,1,1TCA degradation was not observed in the presence of active methane oxidizers. Overall, the results presented suggest that microorganisms associated with wetland plant roots have the intrinsic ability to naturally attenuate TCE and *cis*DCE in contaminated aquatic environments.

TABLE OF CONTENTS

LIST OF FIGURES

LIST OF TABLES

ACKNOWLEDGMENTS

I would like to thank my advisor, Dr. Agrawal, and everyone that worked in the Agrawal lab, especially Sarah Tritschler, for their help and support. My committee members, Dr. Don Cipollini, Dr. Songlin Cheng, Dr. Mark Goltz, and Dr. Pat Megonigal, have provided much appreciated advice, and I sincerely thank them for their time and effort. Dr. Jim Amon, Dr. Geraldine Nagaro, and Dr. Garrett Struckoff provided technical advice and field assistance. My family, especially Jeff and Adelaide Powell, for providing support at home. I received funding from Wright State University and the US Environmental Protection Agency's Greater Research Opportunities Fellowship program (#91684601).

1 BACKGROUND

Chlorinated ethenes (CEs) and chlorinated ethanes (CAs) are chlorinated aliphatic hydrocarbons (CAHs) that have been widely used in industrial applications(Pankow & Cherry 1996) as cleaning solvents. Due to widespread usage and disposal practices in recent decades, CAHs have become groundwater contaminants of major concern. These contaminants have been found to pose threat to human health, being known or suspected carcinogens. Common CEs and CAs discussed in this paper are listed in Table 1.1.

CAHs in the contaminated groundwater can be affected by several processes such as sorption, dilution, volatilization, and chemical and microbiological transformations. Among these, an indepth understanding of the microbiological transformation or biodegradation processes affecting CAH compounds is especially important because it affects the environmental fate of CAHs in the environment. It can also be applied for the treatment of groundwater contaminated with CAHs, by both oxidative and reductive pathways, in a natural, cost-effective remediation approach. Highly-chlorinated CAHs, such as perchloroethene (PCE) and tetrachloroethane (TeCA), have the tendency to undergo biodegradation through reduction pathways, whereas, less-chlorinated CAHs, such as vinyl chloride (VC) and mono chloroethane (mCA), have the tendency to undergo biodegradation through oxidative pathways (Vogel et al. 1987; Bradley 2000;).

Studies have found that wetlands provide unique environments for coupled oxidative and reductive biodegradation of CAHs (Amon et al. 2007). Wetland environments are favorable for reductive biodegradation because of the hydric soil and abundant supply of natural organic carbon that can provide electron donors such as

hydrogen (H_2) and volatile fatty acids (Westermann 1994; Conrad 1999; Kao & Lei 2000; Kassenga et al. 2004; Kassenga & Pardue 2006; Amon et al. 2007). These electron donors can support metabolic microbial reduction by the process known as halorespiration where the CAHs act as the terminal electron acceptors (Kassenga et al. 2004). CAHs can also be degraded cometabolically in anaerobic conditions: Fe(III)-reducing (Aulenta et al. 2006), sulfate-reducing, methanogenic, or acetogenic conditions (Bradley 2000; Kassenga et al. 2004). Of these, methanogenic conditions have been found to result in more complete degradation to non-toxic end products, ethane and ethene (Freedman & Gossett 1989). Pathways for microbial reductive degradation are shown in Figure 1.1.

When complete degradation of CAHs does not occur through reductive biodegradation, less-chlorinated daughter CAHs can accumulate in the anaerobic zones of wetland environments (Lorah 1999; Lorah & Olsen 1999; Lorah & Voytek 2004). However, these products (dichloroethenes (DCEs), VC, 1,2-dichloroethane (1,2-DCA), mCA) have the potential to degrade oxidatively in aerobic environments: either by serving as electron donors for microbial metabolism (Stucki et al. 1983; Janssen et al. 1985; Davis & Carpenter 1990; Janssen & Dekoning 1995; Janssen et al. 1995; Bradley & Chapelle 1998; Klecka et al. 1998; Hage & Hartmans 1999; Klier et al. 1999; Bradley 2000; Bradley & Chapelle 2000; Hage et al. 2001; Coleman et al. 2002a; Coleman et al. 2002b; Broholm et al. 2005; Fathepure et al. 2005) or by cometabolic processes in the presence of numerous growth substrates.

Aerobic oxidative degradation of CAHs can take place not only in the near-surface environments of the wetland if oxygen (O_2) is available, but can also be

facilitated in the root zone, particularly in the rhizosphere, of wetland plants (Anderson et al. 1993; Anderson & Walton 1995; Bankston et al. 2002). Wetland plants have special tissues that can transport O_2 from the leaves to the roots (Mitsch & Gosselink 2000). Some of this O_2 can leak into the rhizosphere and facilitate CAH oxidation by microorganisms inhabiting the roots. This process has been evaluated in bench-scale microcosms created with root zone soil (Bankston et al. 2002), and speculated to occur during recent field studies (Amon et al. 2007). However, this has not been investigated with respect to microbial activity directly associated with wetland plant roots.

The research presesented in this dissertation examines the transformation potential of CAHs by aerobic cometabolic pathways by microbial activity directly associated with wetland plant roots. Specifically, the focus of the investigation was with plant species, *Carex comosa* and *Scirpus atrovirens* and the contaminants evaluated were 1,2-dichloroethene (*cis*DCE), 1,1,1-tricholoethane, and trichloroethene (TCE). The cometabolic growth substrates evaluated were methane and ammonia.

1.1 OXIDATIVE ENVIRONMENT IN WETLAND PLANT ROOTS

In this section, a brief review of the oxidation potential of reduced species in the root zone of wetland plants, mechanisms of oxidation for CAHs through metabolic and cometabolic pathways, and the potential for methane and ammonia production in wetland environments is presented.

Plants growing in waterlogged, anaerobic wetland soils must themselves provide O_2 to their roots because of the slow diffusion and solubility of oxygen in water and its high demand in wetland soil. This is accomplished via a high-porosity continuous gas

space within the plant tissue called the *aerenchyma*, a specialized tissue that supports enhanced longitudinal transport of O_2 from plant shoots to their roots, allowing the gas to diffuse from the aerial parts of the plants to the tips of the roots (Justin & Armstrong 1987; Armstrong et al. 2000; Colmer 2003). In the process, some of the O_2 can leak into the immediate soil environment surrounding the roots by diffusing across the root wall; this process is referred to as *radial oxygen loss* (ROL) (Hinsinger et al. 2006). ROL can provide an aerobic microenvironment surrounding the plant roots (rhizosphere) in an otherwise anaerobic soil. The release of O_2 can affect the rhizosphere by reacting with reduced solutes and chemical constituents that may diffuse from the surrounding reduced soil, which can set up concentration gradients, drive mass fluxes in the rhizosphere and facilitate oxidative reactions (for example, see Figure 1.2). The release of O_2 from the roots can help maintain high redox potential conditions in the rhizosphere (Flessa & Fischer 1992; Kristensen & Alongi 2006), as is evident by precipitation of Fe(III) solids as iron plaque on the root's surface; oxidation of Fe(II) and formation of iron plaque is quite commonplace in the rhizosphere of plants inhabiting most flooded soils (Begg et al. 1994).

1.2 CAH OXIDATION BY MICROBIAL PROCESSES

The organic nature of CAH compounds may allow them to act as electron acceptors or electron donors and undergo reduction or oxidation; however, their potential for reduction or oxidation may depend on the individual CAH compound. The more reduced and less chlorinated the CAH, the more likely it will undergo oxidation. Likewise, the more oxidized and more chlorinated the CAH, the less likely it will undergo oxidation; these compounds are more likely to be reduced (Vogel et al. 1987).

The pathway for oxidation is largely unknown for many CAHs but can be assumed to be initiated by one of the following three general mechanisms that occur in mammalian systems: (a) incorporation of oxygen in the carbon-hydrogen bond (i.e., α-hydroxylation); (b) oxidation of a halogen substitution; and (c) oxidation of a carbon-carbon bond via epoxidation (Vogel et al. 1987). For chlorinated ethenes (CEs), the initial step in oxidation is generally assumed to be epoxidation of the carbon-carbon bond (Bhatt et al. 2007), and for chlorinated ethanes (CAs), the cleavage of the carbon-hydrogen bond occurs first (Hirschorn et al. 2007). These pathways lead to formation of alcohols or free radicals as intermediate products during oxidation of CAs, and epoxides as intermediate products during oxidation of CEs (Vlieg & Janssen 2001). The epoxides can be transformed by reacting with cellular nucleophiles, rearranging to chlorinated acids or acetaldehydes, or hydrolyze to other unstable chlorinated intermediate (Vlieg & Janssen 2001). Subsequent degradation of these intermediate compounds may result into their net mineralization to CO_2.

CAH mineralization is catalyzed by special enzymes produced by the microorganisms capable of oxidation (Bhatt et al. 2007). In aerobic conditions, molecular O_2 can be introduced into the CAHs by enzymes called oxygenases (either monooxygenase or dioxygenase) that catalyze the degradation by incorporating one or two oxygen atoms into the compound respectively (Fetzner & Lingens 1994). CAHs oxidized via a hydroxylation process utilize enzymes called hydroxylases, which catalyze the incorporation of a hydroxyl group into the compound (Fetzner & Lingens 1994). In some cases, complete mineralization can occur by the same enzyme, whereas in other cases more than one enzyme is required (Janssen & Dekoning 1995). When epoxides are

formed, their conversion can be brought about by enzymes such as glutathione *S*-transferase, epoxide carboxylases, epoxide dehydrogenases, or epoxide hydrolases (Vlieg & Janssen 2001).

Oxidation of CAHs can occur aerobically or anaerobically depending on the presence or absence of oxygen. In the shallow zones of the wetland, the O_2 released from the plant roots can serve two functions in CAH oxidation: it either acts as an acceptor of the electrons released during oxidation, or it can react directly with the CAHs (Bouwer & Zehnder 1993). As an electron acceptor, O_2 can control the microbial metabolism for aerobic processes as it is leaked from the plant roots, and O_2 typically provides the maximum free energy during electron transfer (Bouwer & Zehnder 1993; Bhatt et al. 2007). As the O_2 gets depleted, it can be replaced by other oxidized inorganic compounds as electron acceptors for reactions facilitated by anaerobic microorganisms (Bouwer & Zehnder 1993); nitrate, Mn (IV), Fe(III), sulfate, and CO_2 are other possible electron acceptors listed in the order of their redox potential.

1.2.1 CAH Biodegradation by Metabolic Processes

When CAHs are degraded metabolically, microorganisms use these compounds as the sole carbon source for energy and growth, where the CAHs act as the electron donor, balanced by the molecular O_2 released from the roots acting as the electron acceptor. This process can yield significant amounts of energy (Janssen & Dekoning 1995; Vlieg & Janssen 2001). This is evident in Table 1.2 by the Gibbs free energy values calculated for the aerobic mineralization of CAHs to water, CO_2, and hydrochloric acid. Overall, these

values indicate that the Gibbs free energy increases as the number of chlorine substitutes decreases.

Although, based on thermodynamic principles, microbial growth on nearly all chlorinated compounds is possible, yet there is a greater potential for the mineralization of less-chlorinated CAHs (Janssen & Dekoning 1995; Vlieg & Janssen 2001). Only two less-chlorinated CEs and one CA have been reported in the literature as the sole carbon source for microbial metabolism. Of the chlorinated ethenes, most studies have focused on the epoxidation process of VC (Davis & Carpenter 1990; Coleman et al. 2002b; Fathepure et al. 2005), with a few studies researching DCEs (Bradley & Chapelle 1998; Klier et al. 1999; Bradley 2000; Bradley & Chapelle 2000; Coleman et al. 2002a; Broholm et al. 2005). 1,2-DCA has been reported as the only chlorinated ethane capable of serving as a growth substrate for aerobic bacteria metabolism (Stucki et al. 1983; Vandenbergh & Kunka 1988; Vandenwijngaard et al. 1992; Janssen & Dekoning 1995; Janssen et al. 1985; Janssen et al. 1995; Klecka et al. 1998; Hage & Hartmans 1999; Hage et al. 2001)

1.2.2 CAH Biodegradation by Cometabolic Processes

As opposed to metabolic transformations, a wider range of CAHs can undergo cometabolic transformations under aerobic conditions. Most CAHs can be cometabolically oxidized by bacteria that produce non-specific oxygenase enzymes (Anderson & McCarty 1997). Cometabolic transformations of CAHs yield no carbon or energy benefits to the microorganisms and can have several limitations, including substrate competition, enzyme inactivation, and toxicity to the organism (Oldenhuis et al.

1991; Rasche et al. 1991; Alvarez-Cohen & McCarty 1991; Dolan & McCarthy 1995; Alvarez-Cohen & Speitel 2001; Arp et al. 2001). Even with these limitations, studies have found that cometabolic oxidation is not only possible but effective and can occur with several different growth substrates, discussed below.

Growth substrates are needed for cometabolic reactions to take place. These substances provide an energy source and induce production of the oxygenase-expressing cometabolic enzymes (Alvarez-Cohen & Speitel 2001). Growth substrates have been found to include methane (CH_4) (Colby et al. 1977; Colby & Dalton 1979; Woodland & Dalton 1984; Wilson & Wilson 1985; Fogel et al. 1986; Henson et al. 1988; Janssen et al. 1988; Little et al. 1988; Fox et al. 1989; Green & Dalton 1989; Henson et al. 1989; Oldenhuis et al. 1989; Strandberg et al. 1989; Tsien et al. 1989; Fox et al. 1990; Strand et al. 1990; Alvarez-Cohen & McCarty 1991; Arvin 1991; Fox et al. 1991; Henry & Grbicgalic 1991; Oldenhuis et al. 1991; Nakajima et al. 1992; Phelps et al. 1992; Malachowsky et al. 1994; Dolan & McCarthy 1995; Arcangeli et al. 1996; Chang & Alvarez-Cohen 1996; Hanson & Hanson 1996; Anderson & McCarty 1997; Lontoh & Semrau 1998; Aziz et al. 1999; Shigematsu et al. 1999; Alvarez-Cohen & Speitel 2001; Arp et al. 2001; Broholm et al. 2005; Frascari et al. 2006), propane (Fliermans et al. 1988; Phelps et al. 1991; Wackett et al. 1989), propene (Ensign et al. 1992), isoprene (Ewers et al. 1990), toluene (Wackett & Gibson 1988; Shields et al. 1989a; Shields et al. 1989b; Zylstra et al. 1989; Ryoo et al. 2000; Shim et al. 2001), phenol (Folsom et al. 1990; Harker & Kim 1990; Hopkins et al. 1993a; Hopkins et al. 1993b; Anderson & Walton 1995; Fries et al. 1997a; Fries et al. 1997b; Ishida & Nakamura 2000; Futamata et al. 2001; Futamata et al. 2003; Chen et al. 2004;), ethene (Debont & Harder 1978;

Hartmans et al. 1991; Weber et al. 1992; Freedman & Herz 1996; Koziollek et al. 1999; Verce et al. 2001), ammonia (Hyman et al. 1988; Rasche et al. 1990; Vannelli et al. 1990; Rasche et al. 1991; Ely et al. 1995; Hyman et al. 1995; Ely et al. 1997; Moran & Hickey 1997; Hommes et al. 1998; Yang et al. 1999; Kocamemi & Cecen 2005; Kocamemi & Cecen 2007), VC (Hartmans & Debont 1992; Verce et al. 2000; Verce et al. 2001; Verce et al. 2002; Singh et al. 2004; Broholm et al. 2005; Fathepure et al. 2005), and several others.

The cometabolic activity of methanotrophs has been studied extensively. Methanotrophs are a group of gram-negative bacteria that produce an enzyme called methane monooxygenase (MMO) that catalyzes the incorporation of molecular oxygen into CH_4 to produce methanol (Hanson & Hanson 1996). Three general categories of methanotrophs have been identified (type I, type II, and type X) based on the structures of their internal membranes and carbon assimilation pathways (Hanson & Hanson 1996; Lontoh & Semrau 1998). Type I methanotrophs produce an insoluble form of the MMO enzyme (pMMO), and are thought to proliferate under high-oxygen, low CH_4 conditions (Hanson & Hanson 1996; Auman & Lidstrom 2002; Costello et al. 2002). Type II methanotrophs produce a pMMO enzyme, and have the ability to produce a more reactive soluble form of the MMO enzyme (sMMO) under copper-limiting conditions, and thrive under high methane-to-oxygen ratios (Hanson & Hanson 1996). Type X methanotrophs, such as *Methylococcus capsulatus* Bath, possess characteristics of both Type I and Type II methanotrophs.

Both pMMO and sMMO are capable of CAH oxidation, but sMMO is much more non-specific with respect to potential substrates; it can rapidly oxidize all the CEs except

PCE (Fox et al. 1990). Of those methanotrophs that produce sMMO, *Methylosinus trichosporium* OB3b has been the focus of many studies (Fox et al. 1989; Fox et al. 1991; Janssen & Dekoning 1995; Chang & Alvarez-Cohen 1996; Sullivan et al. 1998; Tsien et al. 1989; Aziz et al. 1999; Lee et al. 2006;). Not only can *Methylosinus trichosporium* OB3b produce sMMO but it can also switch between sMMO and pMMO under different oxygen and copper concentrations (Sullivan et al. 1998).

The sMMO enzymes produced by methanotrophic bacteria catalyze a wide range of oxidative reactions, including the epoxidation of alkenes, and the hydroxylation of alkanes (Colby et al. 1977; Patel et al. 1982; Alvarez-Cohen & McCarty 1991;). Of these, the oxidation of TCE has been widely studied with high rates of cometabolic degradation found by sMMO-producing methanotrophs. The pathway for CH_4 oxidation and TCE cometabolic degradation is shown in Figure 1.3. The oxidation of methane yields methanol, which can subsequently be oxidized to formaldehyde, then formic acid, and finally to CO_2 (equations 1a-d) (Sullivan et al. 1998). Equation 1 represents the overall reaction.

$$CH_4 + {}^1/_2O_2 \rightarrow CH_3OH \quad (1a)$$

$$CH_3OH + {}^1/_2O_2 \rightarrow HCHO + H_2O \quad (1b)$$

$$HCHO + {}^1/_2O_2 \rightarrow HCOOH \quad (1c)$$

$$HCOOH + {}^1/_2O_2 \rightarrow CO_2 + H_2O \quad (1d)$$

$$CH_4 + 2O_2 \rightarrow CO_2 + 2H_2O \quad (1)$$

The cometabolic oxidation of TCE by methanotrophs is mostly an epoxidation process initiated by the sMMO with NADH as an intermediate energy source (equation 2) (Chang & Alvarez-Cohen 1995; Fox et al. 1990). With a half-life of 12 s, TCE

epoxide spontaneously breaks down in water to form dichloroacetic acid (equation 3), glyoxylic acid (equation 4), or one-carbon compounds such as formic acid or carbon monoxide (CO) (equation 5) (Miller & Guengerich 1982; Fogel et al. 1986; Nelson et al. 1987; Little et al. 1988; Fox et al. 1989; Oldenhuis et al. 1989; Tsien et al. 1989; Fox et al. 1990; Alvarez-Cohen & Speitel 2001). Formic acid and CO can be further oxidized by methanotrophic bacteria to CO_2 (Little et al. 1988). The other non-chlorinated oxidation products can then be easily mineralized by the heterotrophic bacteria.

$$HClC\text{-}CCl_2 + H_2O \rightarrow HClCOCCl_2 \text{ (TCE expoxide)} + 2H^+ + 2e^- \quad (2)$$

$$HClCOCCl_2 + H_2O \rightarrow HCl_2C\text{-}COOH \text{ (dichloroacetic acid)} + HCl \quad (3)$$

$$HClCOCCl_2 + 2H_2O \rightarrow HCO\text{-}COOH \text{ (glyoxylic acid)} + 3HCl \quad (4)$$

$$HClCOCCl_2 + 2H_2O \rightarrow HCOOH \text{ (formic acid)} + CO + 3HCl \quad (5)$$

In addition to the epoxide, TCE can less commonly be converted into CO_2 by equation 2, which proceeds through chloral hydrate (equation 6a) and then trichloroethanol and trichloroacetic acid, and finally to CO_2 (equations 6 b-c) (Fetzner & Lingens 1994).

$$HClC\text{-}CCl_2 + 2H_2O \rightarrow Cl_3C\text{-}C(OH)_2 \text{ (chloral hydrate)} + 2H^+ + 2e^- \quad (6a)$$

$$Cl_3C\text{-}C(OH)_2 + 2H^+ + 2e^- \rightarrow Cl_3C\text{-}CH_2OH \text{ (trichloroethanol)} + H_2O \quad (6b)$$

$$Cl_3C\text{-}CH_2OH + {}^1/_2O_2 \rightarrow Cl_3C\text{-}COOH \text{ (trichloracetic acid)} + 2H^+ + 2e^- \quad (6c)$$

$$Cl_3C\text{-}COOH + O_2 + 2H^+ + 2e^- \rightarrow 2CO_2 + 3HCl \quad (6d)$$

$$HClC\text{-}CCl_2 + H_2O + {}^3/_2O_2 \rightarrow 2CO_2 + 3HCl \quad (6)$$

Other CAHs have been found to be oxidized cometabolically with CH_4 as the growth substrate (Fogel et al. 1986; Aziz et al. 1999; Lee et al. 2006). Although specific pathways and degradation products are not clealy identified in the literature, studies have found cometabolic oxidation of CAs such as 1,2-DCA, 1,1,2-TCA, 1,1,1-TCA, and even

1,1,2,2-TeCA, which is usually considered non-biodegradable in aerobic metabolic conditions (Chang & Alvarez-Cohen 1996; Frascari et al. 2006).

A reaction sequence similar to TCE degradation has been proposed for cometabolic degradation of VC by methanotrophs; in this degradation sequence VC is oxidized by the sMMO to chlorooxirane, which can rapidly rearrange to chloroacetaldehyde or hydrolyze to glycoaldehyde (Guengerich et al. 1979), both of which can be metabolized by heterotrophic bacteria (Fogel et al. 1986). Studies have also found that DCE isomers can also form epoxides (Janssen et al. 1988; Oldenhuis et al. 1989; Arvin 1991; Lauritsen & Gylling 1995; Arcangeli et al. 1996). Similarly, it has been suggested that *trans*-1,2-DCE-epoxide, gets hydrolyzed to glyoxal, and then further mineralized (Janssen et al. 1988).

CAHs have been found to be transformed cometabolically with ammonia as the growth substrate and oxygen as the electron acceptor. The investigations of ammonia as growth substrate for aerobic cometabolic CAH degradation is fewer than studies with CH_4, most such studies focused on pure or enriched cultures of *Nitrosomonas europaea* (Hyman et al. 1988; Rasche et al. 1990; Vannelli et al. 1990; Rasche et al. 1991; Hopkins et al. 1993a; Hopkins et al. 1993b; Hyman et al. 1995; Ely et al. 1997; Moran & Hickey 1997; Yang et al. 1999; Kocamemi & Cecen 2005). *Nitrosomonas europaea* is an obligate chemolithotroph generally found in environments with high ammonia concentrations (Koops & Pommerening-Roser 2001), and it can cometabolically oxidize a wide variety of CAHs with varying efficiencies, as summarized below. Rasche et al. (1991) examined. The cometabolic oxidation of 16 CAHs by *Nitrosomonas europaea* with ammonia was examined, and grouped them into three categories based on their

behavior and effects on the bacteria. PCE was in the *category I* since it was not oxidized cometabolically. In *category II*, CAH compounds, chloroethane and 1,2-DCA were cometabolically transformed by *Nitrosomonas europaea* without significant cellular injury. Finally, *category III* CAH compounds, TCE, DCE isomers, VC, 1,1,1,2-PCA, 111- and 112-TCAs, and 1,1-DCA were transformed by the bacteria but caused substantial cellular injury in the process. Studies with aerobic cometabolic TCE oxidation in nitrifying conditions has been the focus of much research, first demonstrated by Arciero et al. (1989) followed by several additional studies (Hyman et al. 1988; Rasche et al. 1990; Rasche et al. 1991; Ely et al. 1995; Hyman et al. 1995; Ely et al. 1997; Moran & Hickey 1997; Hommes et al. 1998; Yang et al. 1999; Kocamemi & Cecen 2005; Kocamemi & Cecen 2007).

The cometabolic oxidation of CAHs is indicated by substrate depletion, chloride release, and product formation (Rasche et al. 1991). The products formed is consistent with a reaction pathway involving simple hydroxylation of a carbon-hydrogen bond, or an oxidative dehalogenation (Rasche et al. 1991). Some of the products from CA oxidation that have been identified include the following: acetaldehyde from chloroethane (Rasche et al. 1990; Hommes et al. 1998), 2,2,2-trichloroethanol from 1,1,1-TCA (Hommes et al. 1998), chloroacetaldehyde from 1,2-DCA (Rasche et al. 1991); and chloral hydrate from 1,1,1,2-PCA (Rasche et al. 1991). Further, the TCE oxidation by ammonia monooxygenase has been suggested to results in a chlorinated epoxide similar to its oxidation with sMMO (Rasche et al. 1991) (Figure 1.3).

1.3 METHANE AND AMMONIA IN WETLAND

Wetlands are a major source of atmospheric CH_4 due to the abundance of labile organic material within the wetland soil. CH_4 producing bacteria or methanogens can use this organic material for CH_4 production in the anaerobic portions of the wetland where alternative electron acceptors (nitrate, Fe(III), and sulfate) have been depleted. CH_4 production or methanogenesis requires a series of reaction steps, involving two main substrates (H_2 coupled to CO_2, and acetate) that are derived from the breakdown of organic material by hydrolytic and fermenting bacteria (Whalen 2005). Acetotrophic methanogens produce CH_4 through a fermentative breakdown of acetate shown in equation 7, while hydrogenotrophic methanogens utilize H_2 as an electron donor for the reduction of CO_2 as shown in equation 8 below (Whalen 2005):

$$CH_3COOH \rightarrow CH_4 + CO_2 \quad (7)$$

$$4H_2 + CO_2 \rightarrow CH_4 + 2H_2O \quad (8)$$

CH_4 emissions from the wetlands can be reduced by its oxidation by microbial processes in near surface aerobic environments. In vegetated and waterlogged wetlands, CH_4 oxidation in the presence of oxygen occurs either at the sediment-floodwater interface or in the rhizosphere where oxygen leaks from the roots of emergent plants (Armstrong & Armstrong 1991; Frenzel et al. 1992; Popp et al. 2000; Broholm et al. 2005). As CH_4 diffuses from the bulk soil into the rhizosphere, the CH_4-oxidizing (methanotrophic) bacteria inhabiting the surface of the plant roots can facilitate CH_4 oxidation in the presence of O_2 (Shannon et al. 1996; Bosse & Frenzel 1998; Brune et al. 2000; Ding et al. 2005). The methanotrophic bacteria in the plant rhizosphere can

consume a substantial portion of the CH_4 produced in the bulk wetland soil (King 1996; Calhoun & King 1997; Bosse & Frenzel 1998).

Type I methanotrophs are more common in the water columns of lakes and in the upper portion of lake sediment; whereas, Type II are more likely found in areas such as the roots of wetland plants. Most studies have found Type II populations, mainly *Methylocystis* spp., primarily dominate in wetland sediments (Gilbert & Frenzel 1998; van Bodegom et al. 2001; Horz et al. 2002) and on wetland plant roots (Calhoun & King 1997). However, in another study approximately equal numbers of Type I and Type II methanotrophs were found with wetland sediments (DeJournett et al. 2007).

Wetlands rich in organic matter can result in the production of ammonia during breakdown of organic matter via ammonification, where the organic nitrogen is converted to ammonia (Atlas 1993). Ammonia that accumulates in the anaerobic areas of the wetland can diffuse upward along concentration gradient or advect with flowing groundwater into the shallow zones of the vegetated wetland and pass through the root zone (Reddy et al. 1989). In the presence of O_2, ammonia is oxidized to nitrite and then to nitrate facilitated by the microbial process commonly known as nitrification. This multistep reaction is catalyzed by the action of two enzymes: (1) ammonia monooxygenase, which oxidizes ammonia to hydroxylamine in a reductant-dependent reaction, and (2) hydroxylamine oxidoreductase, which oxidizes hydroxylamine to nitrite (Atlas 1993). The biological oxidation of ammonia to nitrite is shown in equation 9, and nitrite oxidation to nitrate is shown in equation 10.

$$NH_4^+ + {}^3/_2O_2 \rightarrow 2H^+ + H_2O + NO_2^- \quad (9)$$

$$NO_2^- + \tfrac{1}{2}O_2 \rightarrow NO_3^- \quad (10)$$

1.4 CAH BIODEGRADATION IN WETLANDS: FIELD INVESTIGATIONS AT WRIGHT-PATTERSON AFB RESEARCH SITE

An upward-flowing wetland research facility was constructed in the year 2000, at the Wright-Patterson Air Force Base or WPAFB (Dayton, OH), for the removal of PCE in the groundwater, found at roughly 35μg L^{-1} in the nearby contaminated aquifer (Amon et al. 2007). The project was initiated in 1999 by a team of interdisciplinary scientists (Professors J.P. Amon and A. Agrawal of Wright State University, and Professor M.L. Shelley of the Air Force Institute of Technology, Ohio) with seed funding from the Ohio Board of Regents, the Ohio Environmental Protection Agency, and the US Department of Defense. The concept of a constructed wetland for the passive treatment of groundwater contaminated with toxic chlorinated organic compounds was novel and high-risk, as it was based on just one study that demonstrated the ability of a natural wetland to attenuate chlorinated organic chemicals (Lorah 1999; Jones 2004; Lorah & Voytek 2004). Several reports have been published since then (Richard 2004) about the field study and bench-scale validations, which provide the microbiological and geochemical basis for the degradation of the toxic chlorinated organics at a natural wetland site in Aberdeen Proving Grounds, MD. In 2004, preliminary results of applying a constructed wetland for the treatment of TCE-contaminated groundwater were reported (Slusser 2001; Bugg 2002; Entingh 2002; Opperman 2002; Clemmer 2003; Kovacic 2003; Bondurant 2004; Lach 2004; Sobolewski 2004; Mohamud 2007).

The pilot-scale treatment wetland at WPAFB was constructed in an excavated-pit (37m x 18m, & 1.5m deep), lined with a 12-inch thick clay layer and PVC geomembrane for hydraulic isolation from the underlying soil/aquifer. The excavated pit was then filled with a gravel layer at the bottom, and 3 layers of hydric soil obtained from a nearby

drained wetland. The plumbing at the site allows the PCE-contaminated groundwater to be pumped into this system at the bottom. The water flows upward through the hydric soil zones, emerging at the wetland surface and flowing into a sewer. The residence time of the water within the treatment wetland is ~4 days. The WPAFB constructed wetland has 66 clusters of piezometers, installed in a 6x11 grid, and each cluster has 3 stainless-steel drive-point piezometers (Solinst Model 615S) screened at different depths for groundwater sampling. The depths of the piezometer screens (137, 90 and 46 cm below ground surface) correspond to the gravel, lower, and middle layers of the wetland soil. The site was planted with multiple species and some roots now extend the full depth of the wetland.

Field investigation at the site began in Dec. 2001. The groundwater samples were sampled during two different seasons; during plant dormancy in the late fall and winter months (2001-‘03) and during active plant growth in the summer and early fall (Jul and Sept. 2003). The results from these studies were published in several MS theses (Clemmer 2003; Lach 2004; Sobolewski 2004) and a compilation of the work is in the Ecological Engineering Journal (Amon et al. 2007). Vertical profiles of terminal electron acceptors and other dissolved species from pore water analysis have provided evidence that a normal sequence of electron accepting conditions exists with nitrate reduction in the gravel layer and lower layer followed by overlapping zones of sulfate and Fe(III) reduction and methongenesis in the lower layer. At the shallower depth, the redox conditions become more oxidizing as evident from a sharp drop in methane and Fe(II) concentrations (Lorah & Olsen 1999). The recent results indicate influence of season and vegetation on redox conditions; generally lower concentrations of electron acceptors were

observed in the warmer months, suggesting the role of vegetation on microbially-mediated redox processes.

The geochemical data collected from the treatment wetland site in 2003 showed (Lorah & Olsen 1999) PCE degradation in the treatment wetland, as measured by its disappearance along with formation of its daughter products, e.g., TCE, DCEs, and VC. There is increasing evidence in 2005-'06 that the degradation of PCE and its daughter products may occur more rapidly and perhaps differently than in a typical shallow aquifer by processes and pathways characteristic only to a wetland. In the deeper, anaerobic portions of the wetland that are dominated by sulfate reducing and methanogenic conditions, PCE degradation into daughter CEs may occur by hydrogenolysis (Lach 2004; Amon et al. 2007). However, daughter CEs appear to readily degrade at the shallower depths at this site.

1.5 RESEARCH GOALS AND OBJECTIVES

- Develop sampling procedures for wetland field application of newly designed pore water samplers.
- Provide a high-resolution biogeochemical characterization of pore water parameters including electron accepting conditions and PCE degradation potential in the WPAFB constructed wetland using newly designed pore water samplers.
- Compare the activities and TCE degradation potential of methane oxidizers and ammonia oxidizers naturally associated with washed soil-free roots of the wetland plants species, *Carex comosa.*

- Evaluate the root morphology of two wetland sedge plants, *Carex comosa* and *Scirpus atrovirens,* and the corresponding influences on methane-oxidizing activity and TCE degradation potential in the presence of methane.
- Determine the degradation potential and kinetics of TCE, *cis*DCE, and 1,1,1TCA by methane oxidizers naturally associated with the roots of *Carex comosa*.

1.6 REFERENCES

Alvarez-Cohen L, Speitel GE (2001) Kinetics of aerobic cometabolism of chlorinated solvents. Biodegradation 12(2): 105-126

Alvarez-Cohen L, McCarty PL (1991) Effects of Toxicity, Aeration, and Reductant Supply on Trichloroethylene Transformation by a Mixed Methanotrophic Culture. Applied and Environmental Microbiology 57(1): 228-235

Amon JP, Agrawal A, Shelley ML, Opperman BC, Enright MP, Clemmer ND, Slusser T, Lach J, Sobolewski T, Gruner W, Entingh AC (2007) Development of a wetland constructed for the treatment of groundwater contaminated by chlorinated ethenes. Ecol. Eng. 30(1): 51-66

Anderson JE, McCarty PL (1997) Transformation yields of chlorinated ethenes by a methanotrophic mixed culture expressing particulate methane monooxygenase. Appl. Environ. Microbiol. 63(2): 687-693

Anderson TA, Guthrie EA, Walton BT (1993) Bioremediation in the Rhizosphere. Environmental Science & Technology 27(13): 2630-2636

Anderson TA, Walton BT (1995) Comparative Fate of [C-14] Trichloroethylene in the Root-Zone of Plants from a Former Solvent Disposal Site. Environmental Toxicology and Chemistry 14(12): 2041-2047

Arcangeli JP, Arvin E, Mejlhede M, Lauritsen FR (1996) Biodegradation of cis-1,2-dichloro-ethylene at low concentrations with methane-oxidizing bacteria in a biofilm reactor. Water Res. 30(8): 1885-1893

Arciero D, Vannelli T, Logan M, Hooper AB (1989) Degradation of Trichloroethylene by the Ammonia-Oxidizing Bacterium Nitrosomonas-Europaea. Biochemical and Biophysical Research Communications 159(2): 640-643

Armstrong J, Armstrong W (1991) A Convective through-Flow of Gases in Phragmites-Australis (Cav) Trin Ex Steud. Aquat. Bot. 39(1-2): 75-88

Armstrong W, Cousins D, Armstrong J, Turner DW, Beckett PM (2000) Oxygen distribution in wetland plant roots and permeability barriers to gas-exchange with the rhizosphere: a microelectrode and modelling study with Phragmites australis. Annals of Botany 86(3): 687-703

Arp DJ, Yeager CM, Hyman MR (2001) Molecular and cellular fundamentals of aerobic cometabolism of trichloroethylene. Biodegradation 12(2): 81-103

Arvin E (1991) Biodegradation Kinetics of Chlorinated Aliphatic-Hydrocarbons with Methane Oxidizing Bacteria in an Aerobic Fixed Biofilm Reactor. Water Res. 25(7): 873-881

Atlas RaB, R. (1993) Microbial Ecology. The Benjamin Cummings Publishing Company, Redwood City

Aulenta F, Majone M, Tandoi V (2006) Enhanced anaerobic bioremediation of chlorinated solvents: environmental factors influencing microbial activity and their relevance under field conditions. Journal of Chemical Technology and Biotechnology 81(9): 1463-1474

Auman AJ, Lidstrom ME (2002) Analysis of sMMO-containing Type I methanotrophs in Lake Washington sediment. Environmental Microbiology 4(9): 517-524

Aziz CE, Georgiou G, Speitel GE (1999) Cometabolism of chlorinated solvents and binary chlorinated solvent mixtures using M-trichosporium OB3b PP358. Biotechnology and Bioengineering 65(1): 100-107

Bankston JL, Sola DL, Komor AT, Dwyer DF (2002) Degradation of trichloroethylene in wetland microcosms containing broad-leaved cattail and eastern cottonwood. Water Res. 36(6): 1539-1546

Begg CBM, Kirk GJD, Mackenzie AF, Neue HU (1994) Root-Induced Iron Oxidation and Ph Changes in the Lowland Rice Rhizosphere. New Phytologist 128(3): 469-477

Bhatt P, Kumar MS, Mudliar S, Chakrabarti T (2007) Biodegradation of chlorinated compounds - A review. Critical Reviews in Environmental Science and Technology 37(2): 165-198

Bondurant C (2004) Characterizatin of Microbial Processes that Degrade Chlorinated Solvents in a Constructed Wetland using Organic Acid and Inorganic Anion Concentration Profiles. In: AFIT/GEE/ENV/04M-03. Graduate School of

Engineering and Management. Air Force Institute of Technology (AU),, Wright-Patterson AFB OH.

Bosse U, Frenzel P (1998) Methane emissions from rice microcosms: The balance of production, accumulation and oxidation. Biogeochemistry 41(3): 199-214

Bouwer EJ, Zehnder AJB (1993) Bioremediation of Organic-Compounds - Putting Microbial-Metabolism to Work. Trends in Biotechnology 11(8): 360-367

Bradley PM (2000) Microbial degradation of chloroethenes in groundwater systems. Hydrogeology Journal 8(1): 104-111

Bradley PM, Chapelle FH (1998) Effect of contaminant concentration on aerobic microbial mineralization of DCE and VC in stream-bed sediments. Environmental Science & Technology 32(5): 553-557

Bradley PM, Chapelle FH (2000) Aerobic microbial mineralization of dichloroethene as sole carbon substrate. Environmental Science & Technology 34(1): 221-223

Broholm K, Ludvigsen L, Jensen TF, Ostergaard H (2005) Aerobic biodegradation of vinyl chloride and cis-1,2-dichloroethylene in aquifer sediments. Chemosphere 60(11): 1555-1564

Brune A, Frenzel P, Cypionka H (2000) Life at the oxic-anoxic interface: microbial activities and adaptations. Fems Microbiology Reviews 24(5): 691-710

Bugg B (2002) An Anion Characterization of a Constructed Wetland used for Chlorinated Ethene Remediation. In: AFIT/GEE/ENV/03M-03 Graduate School of Engineering and Management

Air Force Institute of Technology (AU), Wright-Patterson AFB OH.

Calhoun A, King GM (1997) Regulation of root-associated methanotrophy by oxygen availability in the rhizosphere of two aquatic macrophytes. Appl. Environ. Microbiol. 63(8): 3051-3058

Chang HL, Alvarez-Cohen L (1995) Transformation Capacities of Chlorinated Organics by Mixed Cultures Enriched on Methane, Propane, Toluene, or Phenol. Biotechnology and Bioengineering 45(5): 440-449

Chang HL, Alvarez-Cohen L (1996) Biodegradation of individual and multiple chlorinated aliphatic hydrocarbons by methane-oxidizing cultures. Appl. Environ. Microbiol. 62(9): 3371-3377

Chen WM, Chang JS, Wu CH, Chang SC (2004) Characterization of phenol and trichloroethene degradation by the rhizobium Ralstonia taiwanensis. Research in Microbiology 155(8): 672-680

Clemmer N (2003) Characterization of Chlorinated Solvent Degradation in a Constructed Wetland. In: AFIT/GEE/ENV/03-03. Graduate School of Engineering and Management,. Air Force Institute of Technology (AU), Wright-Patterson AFB OH.

Colby J, Dalton H (1979) Characterization of the 2nd Prosthetic Group of the Flavoenzyme Nadh-Acceptor Reductase (Component-C) of the Methane Mono-Oxygenase from Methylococcus-Capsulatus (Bath). Biochemical Journal 177(3): 903-908

Colby J, Stirling DI, Dalton H (1977) Soluble Methane Mono-Oxygenase of Methylococcus-Capsulatus-(Bath) - Ability to Oxygenate Normal-Alkanes,

Normal-Alkenes, Ethers, and Alicyclic, Aromatic and Heterocyclic-Compounds. Biochemical Journal 165(2): 395-402

Coleman NV, Mattes TE, Gossett JM, Spain JC (2002a) Biodegradation of cis-dichloroethene as the sole carbon source by a beta-proteobacterium. Appl. Environ. Microbiol. 68(6): 2726-2730

Coleman NV, Mattes TE, Gossett JM, Spain JC (2002b) Phylogenetic and kinetic diversity of aerobic vinyl chloride-assimilating bacteria from contaminated sites. Appl. Environ. Microbiol. 68(12): 6162-6171

Colmer TD (2003) Aerenchyma and an inducible barrier to radial oxygen loss facilitate root aeration in upland, paddy and deep-water rice (Oryza sativa L.). Annals of Botany 91(2): 301-309

Conrad R (1999) Contribution of hydrogen to methane production and control of hydrogen concentrations in methanogenic soils and sediments. Fems Microbiology Ecology 28(3): 193-202

Costello AM, Auman AJ, Macalady JL, Scow KM, Lidstrom ME (2002) Estimation of methanotroph abundance in a freshwater lake sediment. Environmental Microbiology 4(8): 443-450

Davis JW, Carpenter CL (1990) Aerobic Biodegradation of Vinyl-Chloride in Groundwater Samples. Appl. Environ. Microbiol. 56(12): 3878-3880

Debont JAM, Harder W (1978) Metabolism of Ethylene by Mycobacterium-E-20. Fems Microbiology Letters 3(2): 89-93

DeJournett TD, Arnold WA, LaPara TM (2007) The characterization and quantification of methanotrophic bacterial populations in constructed wetland sediments using PCR targeting 16S rRNA gene fragments. Applied Soil Ecology 35(3): 648-659

Ding WX, Cai ZC, Tsuruta H (2005) Plant species effects on methane emissions from freshwater marshes. Atmospheric Environment 39(18): 3199-3207

Dolan ME, McCarthy PL (1995) Methanotrophic Chloroethene Transformation Capacities and 1,1-Dichloroethene Transformation Product Toxicity. Environmental Science & Technology 29(11): 2741-2747

Ely RL, Williamson KJ, Guenther RB, Hyman MR, Arp DJ (1995) A Cometabolic Kinetics Model Incorporating Enzyme-Inhibition, Inactivation, and Recovery .1. Model Development, Analysis, and Testing. Biotechnology and Bioengineering 46(3): 218-231

Ely RL, Williamson KJ, Hyman MR, Arp DJ (1997) Cometabolism of chlorinated solvents by nitrifying bacteria: Kinetics, substrate interactions, toxicity effects, and bacterial response. Biotechnology and Bioengineering 54(6): 520-534

Ensign SA, Hyman MR, Arp DJ (1992) Cometabolic Degradation of Chlorinated Alkenes by Alkene Monooxygenase in a Propylene-Grown Xanthobacter Strain. Appl. Environ. Microbiol. 58(9): 3038-3046

Entingh A (2002) Groundwater Flow Through a Constructed Treatment Wetland. In: AFIT/GEE/ENV/02M-03. Graduate School of Engineering and Management. Air Force Institute of Technology (AU), Wright-Patterson AFB OH.

Ewers J, Freierschroder D, Knackmuss HJ (1990) Selection of Trichloroethene (Tce) Degrading Bacteria That Resist Inactivation by Tce. Archives of Microbiology 154(4): 410-413

Fathepure BZ, Elango VK, Singh H, Bruner MA (2005) Bioaugmentation potential of a vinyl chloride-assimilating Mycobacterium sp., isolated from a chloroethene-contaminated aquifer. Fems Microbiology Letters 248(2): 227-234

Fetzner S, Lingens F (1994) Bacterial Dehalogenases - Biochemistry, Genetics, and Biotechnological Applications. Microbiological Reviews 58(4): 641-685

Flessa H, Fischer WR (1992) Plant-Induced Changes in the Redox Potentials of Rice Rhizospheres. Plant Soil 143(1): 55-60

Fliermans CB, Phelps TJ, Ringelberg D, Mikell AT, White DC (1988) Mineralization of Trichloroethylene by Heterotrophic Enrichment Cultures. Appl. Environ. Microbiol. 54(7): 1709-1714

Fogel MM, Taddeo AR, Fogel S (1986) Biodegradation of Chlorinated Ethenes by a Methane-Utilizing Mixed Culture. Appl. Environ. Microbiol. 51(4): 720-724

Folsom BR, Chapman PJ, Pritchard PH (1990) Phenol and Trichloroethylene Degradation by Pseudomonas-Cepacia G4 - Kinetics and Interactions between Substrates. Appl. Environ. Microbiol. 56(5): 1279-1285

Fox BG, Borneman JG, Wackett LP, Lipscomb JD (1990) Haloalkene Oxidation by the Soluble Methane Monooxygenase from Methylosinus-Trichosporium Ob3b - Mechanistic and Environmental Implications. Biochemistry 29(27): 6419-6427

Fox BG, Froland WA, Dege JE, Lipscomb JD (1989) Methane Monooxygenase from Methylosinus-Trichosporium Ob3b - Purification and Properties of a 3-Component System with High Specific Activity from a Type-Ii Methanotroph. Journal of Biological Chemistry 264(17): 10023-10033

Fox BG, Liu Y, Dege JE, Lipscomb JD (1991) Complex-Formation between the Protein-Components of Methane Monooxygenase from Methylosinus-Trichosporium Ob3b - Identification of Sites of Component Interaction. Journal of Biological Chemistry 266(1): 540-550

Frascari D, Pinelli D, Nocentini M, Zannoni A, Fedi S, Baleani E, Zannoni D, Farneti A, Battistelli A (2006) Long-term aerobic cometabolism of a chlorinated solvent mixture by vinyl chloride-, methane- and propane-utilizing biomasses. Journal of Hazardous Materials 138(1): 29-39

Freedman DL, Gossett JM (1989) Biological Reductive Dechlorination of Tetrachloroethylene and Trichloroethylene to Ethylene under Methanogenic Conditions. Appl. Environ. Microbiol. 55(9): 2144-2151

Freedman DL, Herz SD (1996) Use of ethylene and ethane as primary substrates for aerobic cometabolism of vinyl chloride. Water Environment Research 68(3): 320-328

Frenzel P, Rothfuss F, Conrad R (1992) Oxygen Profiles and Methane Turnover in a Flooded Rice Microcosm. Biology and Fertility of Soils 14(2): 84-89

Fries MR, Forney LJ, Tiedje JM (1997a) Phenol- and toluene-degrading microbial populations from an aquifer in which successful trichloroethene cometabolism occurred. Appl. Environ. Microbiol. 63(4): 1523-1530

Fries MR, Hopkins GD, McCarty PL, Forney LJ, Tiedje JM (1997b) Microbial succession during a field evaluation of phenol and toluene as the primary substrates for trichloroethene cometabolism. Appl. Environ. Microbiol. 63(4): 1515-1522

Futamata H, Harayama S, Hiraishi A, Watanabe K (2003) Functional and structural analyses of trichloroethylene-degrading bacterial communities under different phenol-feeding conditions: laboratory experiments. Applied Microbiology and Biotechnology 60(5): 594-600

Futamata H, Harayama S, Watanabe K (2001) Diversity in kinetics of trichloroethylene-degrading activities exhibited by phenol-degrading bacteria. Applied Microbiology and Biotechnology 55(2): 248-253

Gilbert B, Frenzel P (1998) Rice roots and CH4 oxidation: The activity of bacteria, their distribution and the microenvironment. Soil Biology & Biochemistry 30(14): 1903-1916

Green J, Dalton H (1989) Substrate-Specificity of Soluble Methane Monooxygenase - Mechanistic Implications. Journal of Biological Chemistry 264(30): 17698-17703

Guengerich FP, Crawford WM, Watanabe PG (1979) Activation of Vinyl-Chloride to Covalently Bound Metabolites - Roles of 2-Chloroethylene Oxide and 2-Chloroacetaldehyde. Biochemistry 18(23): 5177-5182

Hage JC, Hartmans S (1999) Monooxygenase-mediated 1,2-dichloroetbane degradation by Pseudomonas sp Strain DCA1. Appl. Environ. Microbiol. 65(6): 2466-2470

Hage JC, Kiestra FDG, Hartmans S (2001) Co-metabolic degradation of chlorinated hydrocarbons by Pseudomonas sp strain DCA1. Applied Microbiology and Biotechnology 57(4): 548-554

Hanson RS, Hanson TE (1996) Methanotrophic bacteria. Microbiological Reviews 60(2): 439-471

Harker AR, Kim Y (1990) Trichloroethylene Degradation by 2 Independent Aromatic-Degrading Pathways in Alcaligenes-Eutrophus Jmp134. Appl. Environ. Microbiol. 56(4): 1179-1181

Hartmans S, Debont JAM (1992) Aerobic Vinyl-Chloride Metabolism in Mycobacterium-Aurum L1. Appl. Environ. Microbiol. 58(4): 1220-1226

Hartmans S, Weber FJ, Somhorst DPM, Debont JAM (1991) Alkene Monooxygenase from Mycobacterium - a Multicomponent Enzyme. Journal of General Microbiology 137: 2555-2560

Henry SM, Grbicgalic D (1991) Influence of Endogenous and Exogenous Electron-Donors and Trichloroethylene Oxidation Toxicity on Trichloroethylene Oxidation by Methanotrophic Cultures from a Groundwater Aquifer. Appl. Environ. Microbiol. 57(1): 236-244

Henson JM, Yates MV, Cochran JW (1989) Metabolism of Chlorinated Methanes, Ethanes, and Ethylenes by a Mixed Bacterial Culture Growing on Methane. Journal of Industrial Microbiology 4(1): 29-35

Henson JM, Yates MV, Cochran JW, Shackleford DL (1988) Microbial Removal of Halogenated Methanes, Ethanes, and Ethylenes in an Aerobic Soil Exposed to Methane. Fems Microbiology Ecology 53(3-4): 193-201

Hinsinger P, Plassard C, Jaillard B (2006) Rhizosphere: A new frontier for soil biogeochemistry. Journal of Geochemical Exploration 88(1-3): 210-213

Hirschorn SK, Dinglasan-Panlilio MJ, Edwards EA, Lacrampe-Couloume G, Lollar BS (2007) Isotope analysis as a natural reaction probe to determine mechanisms of biodegradation of 1,2-dichloroethane. Environmental Microbiology 9(7): 1651-1657

Hommes NG, Russell SA, Bottomley PJ, Arp DJ (1998) Effects of soil on ammonia, ethylene, chloroethane, and 1,1,1-trichloroethane oxidation by Nitrosomonas europaea. Appl. Environ. Microbiol. 64(4): 1372-1378

Hopkins GD, Munakata J, Semprini L, McCarty PL (1993a) Trichloroethylene Concentration Effects on Pilot Field-Scale in-Situ Groundwater Bioremediation by Phenol-Oxidizing Microorganisms. Environmental Science & Technology 27(12): 2542-2547

Hopkins GD, Semprini L, McCarty PL (1993b) Microcosm and in-Situ Field Studies of Enhanced Biotransformation of Trichloroethylene by Phenol-Utilizing Microorganisms. Appl. Environ. Microbiol. 59(7): 2277-2285

Horz HP, Raghubanshi AS, Heyer E, Kammann C, Conrad R, Dunfield PF (2002) Activity and community structure of methane-oxidising bacteria in a wet meadow soil. Fems Microbiology Ecology 41(3): 247-257

http://en.wikipedia.org/wiki/Main_Page

Hyman MR, Murton IB, Arp DJ (1988) Interaction of Ammonia Monooxygenase from Nitrosomonas-Europaea with Alkanes, Alkenes, and Alkynes. Appl. Environ. Microbiol. 54(12): 3187-3190

Hyman MR, Russell SA, Ely RL, Williamson KJ, Arp DJ (1995) Inhibition, Inactivation, and Recovery of Ammonia-Oxidizing Activity in Cometabolism of Trichloroethylene by Nitrosomonas-Europaea. Appl. Environ. Microbiol. 61(4): 1480-1487

Ishida H, Nakamura K (2000) Trichloroethylene degradation by Ralstonia sp KN1-10A constitutively expressing phenol hydroxylase: Transformation products, NADH limitation, and product toxicity. Journal of Bioscience and Bioengineering 89(5): 438-445

Janssen DB, Dekoning W (1995) Development and Application of Bacterial Cultures for the Removal of Chlorinated Aliphatics. Water Science and Technology 31(1): 237-247

Janssen DB, Grobben G, Hoekstra R, Oldenhuis R, Witholt B (1988) Degradation of Trans-1,2-Dichloroethene by Mixed and Pure Cultures of Methanotrophic Bacteria. Applied Microbiology and Biotechnology 29(4): 392-399

Janssen DB, Scheper A, Dijkhuizen L, Witholt B (1985) Degradation of Halogenated Aliphatic-Compounds by Xanthobacter-Autotrophicus Gj10. Appl. Environ. Microbiol. 49(3): 673-677

Janssen DB, van der Ploeg JR, Pries F (1995) Genetic adaptation of bacteria to halogenated aliphatic compounds. Environmental Health Perspectives 103: 29-32

Jones V, M.A., Lorah, M.M (2004) Effect of Fe(III) on 1,1,2,2-Tetrachloroethane Degradation and Vinyl Chloride Accumulation in Wetland Sediments of Aberdeen Proving Ground. Bioremed. 8: 31-45

Justin S, Armstrong W (1987) The Anatomical Characteristics of Roots and Plant-Response to Soil Flooding. New Phytologist 106(3): 465-495

Kao CM, Lei SE (2000) Using a peat biobarrier to remediate PCE/TCE contaminated aquifers. Water Res. 34(3): 835-845

Kassenga G, Pardue JH, Moe WM, Bowman KS (2004) Hydrogen thresholds as indicators of dehalorespiration in constructed treatment wetlands. Environmental Science & Technology 38(4): 1024-1030

Kassenga GR, Pardue JH (2006) Effect of competitive terminal electron acceptor processes on dechlorination of cis-1,2-dichloroethene and 1,2-dichloroethane in constructed wetland soils. Fems Microbiology Ecology 57(2): 311-323

King GM (1996) In situ analyses of methane oxidation associated with the roots and rhizomes of a bur reed, Sparganium eurycarpum, in a Maine wetland. Appl. Environ. Microbiol. 62(12): 4548-4555

Klecka GM, Carpenter CL, Gonsior SJ (1998) Biological transformations of 1,2-dichloroethane in subsurface soils and groundwater. Journal of Contaminant Hydrology 34(1-2): 139-154

Klier NJ, West RJ, Donberg PA (1999) Aerobic biodegradation of dichloroethylenes in surface and subsurface soils. Chemosphere 38(5): 1175-1188

Kocamemi BA, Cecen F (2005) Cometabolic degradation of TCE in enriched nitrifying batch systems. Journal of Hazardous Materials 125(1-3): 260-265

Kocamemi BA, Cecen F (2007) Kinetic analysis of the inhibitory effect of trichloroethylene (TCE) on nitrification in cometabolic degradation. Biodegradation 18(1): 71-81

Koops HP, Pommerening-Roser A (2001) Distribution and ecophysiology of the nitrifying bacteria emphasizing cultured species. Fems Microbiology Ecology 37(1): 1-9

Kovacic J (2003) Analysis of anion distributions in the developing strata of a constructed wetland used for chlorinated ethane remediation,. In: AFIT/GEE/ENV/03-03. Graduate School of Engineering and Management. Air Force Institute of Technology (AU), Wright-Patterson AFB OH.

Koziollek P, Bryniok D, Knackmuss HJ (1999) Ethene as an auxiliary substrate for the cooxidation of cis-1,2-dichloroethene and vinyl chloride. Archives of Microbiology 172(4): 240-246

Kristensen E, Alongi DM (2006) Control by fiddler crabs (Uca vocans) and plant roots (Avicennia marina) on carbon, iron, and sulfur biogeochemistry in mangrove sediment. Limnology and Oceanography 51(4): 1557-1571

Lach JD (2004) Treatment of Contaminated Grondwater in a Constructed Wetland: A Biogeochemical Analysis. In. Wright State University, Dayton, OH.

Lauritsen FR, Gylling S (1995) Online Monitoring of Biological Reactions at Low Parts-Per-Trillion Levels by Membrane Inlet Mass-Spectrometry. Analytical Chemistry 67(8): 1418-1420

Lee SW, Keeney DR, Lim DH, Dispirito AA, Semrau JD (2006) Mixed pollutant degradation by Methylosinus trichosporium OB3b expressing either soluble or particulate methane monooxygenase: Can the tortoise beat the hare? Appl. Environ. Microbiol. 72(12): 7503-7509

Liesack W, Schnell S, Revsbech NP (2000) Microbiology of flooded rice paddies. Fems Microbiology Reviews 24(5): 625-645

Little CD, Palumbo AV, Herbes SE, Lidstrom ME, Tyndall RL, Gilmer PJ (1988) Trichloroethylene Biodegradation by a Methane-Oxidizing Bacterium. Appl. Environ. Microbiol. 54(4): 951-956

Lontoh S, Semrau JD (1998) Methane and trichloroethylene degradation by Methylosinus trichosporium OB3b expressing particulate methane monooxygenase. Appl. Environ. Microbiol. 64(3): 1106-1114

Lorah M, Olsen, L. (1999) Degradation of 1,1,2,2-Tetrachloroethane in a Freshwater Tidal Wetland: Field and Laboratory Evidence. . Environ. Sci. Technol 33: 227-234

Lorah MM, Olsen LD (1999) Natural attenuation of chlorinated volatile organic compounds in a freshwater tidal wetland: Field evidence of anaerobic biodegradation. Water Resources Research 35(12): 3811-3827

Lorah MM, Voytek MA (2004) Degradation of 1,1,2,2-tetrachloro ethane and accumulation of vinyl chloride in wetland sediment microcosms and in situ porewater: biogeochemical controls and associations with microbial communities. Journal of Contaminant Hydrology 70(1-2): 117-145

Malachowsky KJ, Phelps TJ, Teboli AB, Minnikin DE, White DC (1994) Aerobic Mineralization of Trichloroethylene, Vinyl-Chloride, and Aromatic-Compounds by Rhodococcus Species. Appl. Environ. Microbiol. 60(2): 542-548

Miller RE, Guengerich FP (1982) Oxidation of Trichloroethylene by Liver Microsomal Cytochrome-P-450 - Evidence for Chlorine Migration in a Transition-State Not Involving Trichloroethylene Oxide. Biochemistry 21(5): 1090-1097

Mitsch WJ, Gosselink JG (2000) The value of wetlands: importance of scale and landscape setting. Ecological Economics 35(1): 25-33

Mohamud Y (2007) Seasonal Variation in the Redox Zones and Biogeochemical Processes within the Constructed Wetland. In. Wright State University, Dayton, OH.

Moran BN, Hickey WJ (1997) Trichloroethylene biodegradation by mesophilic and psychrophilic ammonia oxidizers and methanotrophs in groundwater microcosms. Appl. Environ. Microbiol. 63(10): 3866-3871

Nakajima T, Uchiyama H, Yagi O, Nakahara T (1992) Novel Metabolite of Trichloroethylene in a Methanotrophic Bacterium, Methylocystis Sp M, and Hypothetical Degradation Pathway. Bioscience Biotechnology and Biochemistry 56(3): 486-489

Nelson MJK, Montgomery SO, Mahaffey WR, Pritchard PH (1987) Biodegradation of Trichloroethylene and Involvement of an Aromatic Biodegradative Pathway. Appl. Environ. Microbiol. 53(5): 949-954

Oldenhuis R, Oedzes JY, Vanderwaarde JJ, Janssen DB (1991) Kinetics of Chlorinated-Hydrocarbon Degradation by Methylosinus-Trichosporium Ob3b and Toxicity of Trichloroethylene. Appl. Environ. Microbiol. 57(1): 7-14

Oldenhuis R, Vink R, Janssen DB, Witholt B (1989) Degradation of Chlorinated Aliphatic-Hydrocarbons by Methylosinus-Trichosporium Ob3b Expressing Soluble Methane Monooxygenase. Appl. Environ. Microbiol. 55(11): 2819-2826

Opperman B (2002) Determination of Chlorinated Solvent Contamination in an Upward Flow Constructed Wetland. In: AFIT/GEE/ENV/02M-07. Graduate School of Engineering and Management. Air Force Institute of Technology (AU), Wright-Patterson AFB OH.

Pankow JF, Cherry JA (1996) Dense Chlorinated Solvents and other DNAPLs in Groundwater. Waterloo Press, Portland, OR

Patel RN, Hou CT, Laskin AI, Felix A (1982) Microbial Oxidation of Hydrocarbons - Properties of a Soluble Methane Mono-Oxygenase from a Facultative Methane-Utilizing Organism, Methylobacterium Sp Strain Crl-26. Appl. Environ. Microbiol. 44(5): 1130-1137

Phelps PA, Agarwal SK, Speitel GE, Georgiou G (1992) Methylosinus-Trichosporium Ob3b Mutants Having Constitutive Expression of Soluble Methane

Monooxygenase in the Presence of High-Levels of Copper. Appl. Environ. Microbiol. 58(11): 3701-3708

Phelps TJ, Niedzielski JJ, Malachowsky KJ, Schram RM, Herbes SE, White DC (1991) Biodegradation of Mixed-Organic Wastes by Microbial Consortia in Continuous-Recycle Expanded-Bed Bioreactors. Environmental Science & Technology 25(8): 1461-1465

Popp TJ, Chanton JP, Whiting GJ, Grant N (2000) Evaluation of methane oxidation in the rhizosphere of a Carex dominated fen in north central Alberta, Canada. Biogeochemistry 51(3): 259-281

Rasche ME, Hicks RE, Hyman MR, Arp DJ (1990) Oxidation of Monohalogenated Ethanes and N-Chlorinated Alkanes by Whole Cells of Nitrosomonas-Europaea. Journal of Bacteriology 172(9): 5368-5373

Rasche ME, Hyman MR, Arp DJ (1991) Factors Limiting Aliphatic Chlorocarbon Degradation by Nitrosomonas-Europaea - Cometabolic Inactivation of Ammonia Monooxygenase and Substrate-Specificity. Appl. Environ. Microbiol. 57(10): 2986-2994

Reddy KR, Patrick WH, Lindau CW (1989) Nitrification-Denitrification at the Plant Root-Sediment Interface in Wetlands. Limnology and Oceanography 34(6): 1004-1013

Richard DR, Berns, J.J., Bankston, J.L., Connell, D. (2004) Restored wetland remediation of a chlorinated solvent plume. In: Proceedings of the Seventh International In Situ and On-Site Bioremediation Symposium. Orlando, FL, USA.

Ryoo D, Shim H, Canada K, Barbieri P, Wood TK (2000) Aerobic degradation of tetrachloroethylene by toluene-o-xylene monooxygenase of Pseudomonas stutzeri OX1. Nature Biotechnology 18(7): 775-778

Shannon RD, White JR, Lawson JE, Gilmour BS (1996) Methane efflux from emergent vegetation in peatlands. Journal of Ecology 84(2): 239-246

Shields MS, Montgomery SO, Chapman PJ, Cuskey SM, Pritchard PH (1989a) Novel Pathway of Toluene Catabolism in the Trichloroethylene-Degrading Bacterium-G4. Appl. Environ. Microbiol. 55(6): 1624-1629

Shields MS, Montgomery SO, Cuskey SM, Chapman PJ (1989b) Toluene Degradation and Trichloroethylene Mineralization by an Environmental Isolate. Abstracts of Papers of the American Chemical Society 197: 19-MBTD

Shigematsu T, Hanada S, Eguchi M, Kamagata Y, Kanagawa T, Kurane R (1999) Soluble methane monooxygenase gene clusters from trichloroethylene-degrading Methylomonas sp strains and detection of methanotrophs during in situ bioremediation. Appl. Environ. Microbiol. 65(12): 5198-5206

Shim H, Ryoo D, Barbieri P, Wood TK (2001) Aerobic degradation of mixtures of tetrachloroethylene, trichloroethylene, dichloroethylenes, and vinyl chloride by toluene-o-xylene monooxygenase of *Pseudomonas stutzeri* OX1. Applied Microbiology and Biotechnology 56(1-2): 265-269

Singh H, Loffler FE, Fathepure BZ (2004) Aerobic biodegradation of vinyl chloride by a highly enriched mixed culture. Biodegradation 15(3): 197-204

Slusser TJ (2001) A Wetland Microbial Consortium Capable of Reductively Dechlorinating Perchloroethylene to cis-1,2 Dichloroethylene. In. Wright State University, Dayton, OH.

Sobolewski T (2004) Characterization of Chlorinated Solvent Degradation Profiles Due to Microbial and Chemical Processes in a Constructed Wetland. In: AFIT/GEM/ENV/04M-17. Graduate School of Engineering and Management. Air Force Institute of Technology (AU), Wright-Patterson AFB OH.

Strand SE, Bjelland MD, Stensel HD (1990) Kinetics of Chlorinated-Hydrocarbon Degradation by Suspended Cultures of Methane-Oxidizing Bacteria. Research Journal of the Water Pollution Control Federation 62(2): 124-129

Strandberg GW, Donaldson TL, Farr LL (1989) Degradation of Trichloroethylene and Trans-1,2-Dichloroethylene by a Methanotrophic Consortium in a Fixed-Film, Packed-Bed Bioreactor. Environmental Science & Technology 23(11): 1422-1425

Stucki G, Krebser U, Leisinger T (1983) Bacterial-Growth on 1,2-Dichloroethane. Experientia 39(11): 1271-1273

Sullivan JP, Dickinson D, Chase HA (1998) Methanotrophs, Methylosinus trichosporium OB3b, sMMO, and their application to bioremediation. Critical Reviews in Microbiology 24(4): 335-373

Tsien HC, Brusseau GA, Hanson RS, Wackett LP (1989) Biodegradation of Trichloroethylene by Methylosinus-Trichosporium Ob3b. Appl. Environ. Microbiol. 55(12): 3155-3161

van Bodegom P, Stams F, Mollema L, Boeke S, Leffelaar P (2001) Methane oxidation and the competition for oxygen in the rice rhizosphere. Appl. Environ. Microbiol. 67(8): 3586-3597

Vandenbergh PA, Kunka BS (1988) Metabolism of Volatile Chlorinated Aliphatic-Hydrocarbons by Pseudomonas-Fluorescens. Appl. Environ. Microbiol. 54(10): 2578-2579

Vandenwijngaard AJ, Vanderkamp K, Vanderploeg J, Pries F, Kazemier B, Janssen DB (1992) Degradation of 1,2-Dichloroethane by Ancylobacter-Aquaticus and Other Facultative Methylotrophs. Appl. Environ. Microbiol. 58(3): 976-983

Vannelli T, Logan M, Arciero DM, Hooper AB (1990) Degradation of Halogenated Aliphatic-Compounds by the Ammonia-Oxidizing Bacterium Nitrosomonas-Europaea. Appl. Environ. Microbiol. 56(4): 1169-1171

Verce MF, Gunsch CK, Danko AS, Freedman DL (2002) Cometabolism of cis-1,2-dichloroethene by aerobic cultures grown on vinyl chloride as the primary substrate. Environmental Science & Technology 36(10): 2171-2177

Verce MF, Ulrich RL, Freedman DL (2000) Characterization of an isolate that uses vinyl chloride as a growth substrate under aerobic conditions. Appl. Environ. Microbiol. 66(8): 3535-3542

Verce MF, Ulrich RL, Freedman DL (2001) Transition from cometabolic to growth-linked biodegradation of vinyl chloride by a Pseudomonas sp isolated on ethene. Environmental Science & Technology 35(21): 4242-4251

Vlieg J, Janssen DB (2001) Formation and detoxification of reactive intermediates in the metabolism of chlorinated ethenes. Journal of Biotechnology 85(2): 81-102

Vogel TM, Criddle CS, McCarty PL (1987) Transformations of Halogenated Aliphatic-Compounds. Environmental Science & Technology 21(8): 722-736

Wackett LP, Brusseau GA, Householder SR, Hanson RS (1989) Survey of Microbial Oxygenases - Trichloroethylene Degradation by Propane-Oxidizing Bacteria. Appl. Environ. Microbiol. 55(11): 2960-2964

Wackett LP, Gibson DT (1988) Degradation of Trichloroethylene by Toluene Dioxygenase in Whole-Cell Studies with Pseudomonas-Putida F1. Appl. Environ. Microbiol. 54(7): 1703-1708

Weber FJ, Vanberkel WJH, Hartmans S, Debont JAM (1992) Purification and Properties of the Nadh Reductase Component of Alkene Monooxygenase from Mycobacterium Strain-E3. Journal of Bacteriology 174(10): 3275-3281

Westermann P (1994) The Effect of Incubation-Temperature on Steady-State Concentrations of Hydrogen and Volatile Fatty-Acids During Anaerobic Degradation in Slurries from Wetland Sediments. Fems Microbiology Ecology 13(4): 295-302

Whalen SC (2005) Biogeochemistry of methane exchange between natural wetlands and the atmosphere. Environmental Engineering Science 22(1): 73-94

Wilson JT, Wilson BH (1985) Biotransformation of Trichloroethylene in Soil. Appl. Environ. Microbiol. 49(1): 242-243

Woodland MP, Dalton H (1984) Purification and Characterization of Component-a of the Methane Monooxygenase from Methylococcus-Capsulatus (Bath). Journal of Biological Chemistry 259(1): 53-59

Yang L, Chang YF, Chou MS (1999) Feasibility of bioremediation of trichloroethylene contaminated sites by nitrifying bacteria through cometabolism with ammonia. Journal of Hazardous Materials 69(1): 111-126

Zylstra GJ, Wackett LP, Gibson DT (1989) Trichloroethylene Degradation by Escherichia-Coli Containing the Cloned Pseudomonas-Putida F1 Toluene Dioxygenase Genes. Appl. Environ. Microbiol. 55(12): 3162-3166

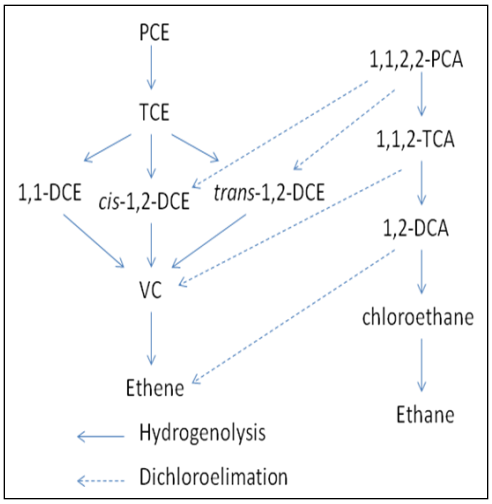

Figure 1.1 Microbial reductive dechlorination pathways for CAHs

Microbial reductive dechlorination pathways for CAHs modified from Lorah et al. (1999) and Aulenta et al. (2006). Reductive biodegradation of oxidized organic compounds can occur via hydrogenolysis, in which the chlorinated compound is sequentially reduced to daughter products by removal of single chlorine in each step. Chlorinated ethanes can also be dechlorinated by dichloroelimination pathway where two chlorines are removed and a double bond is formed between the two carbon atoms with a net input of two electrons.

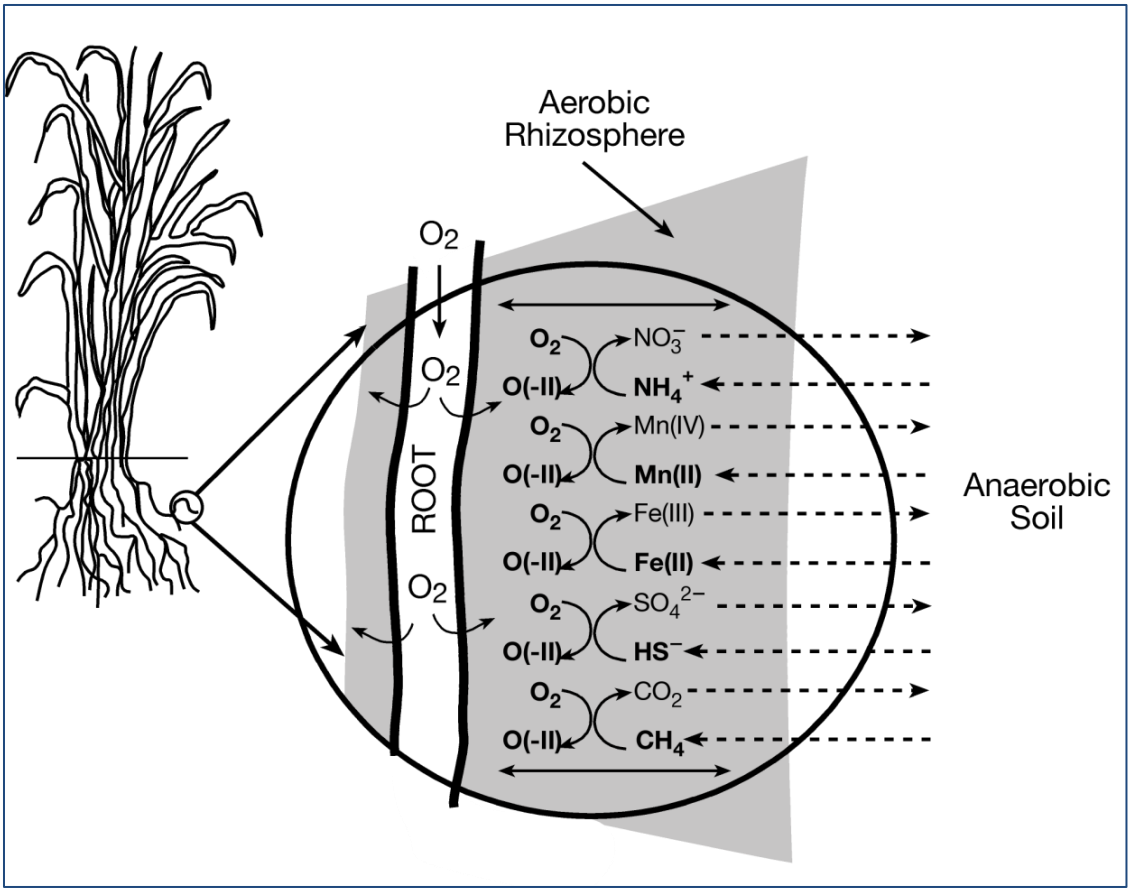

Figure 1.2 Redox processes in the root zone of wetland plants

Oxidation and reduction processes that can occur in the root zone of wetland plants as (modified after Liesack et al. 2000). Oxygen transported into the roots for plant respiration can leak into the surrounding soil and react with reduced geochemical constituents (methane, HS^-, Fe^{2+}, Mn^{2+}, NH_4^+, etc., as shown); the oxidized products (CO_2, SO_4^{2-}, Fe^{3+}, Mn^{4+}, NO_3^-, etc.) can migrate to the anaerobic soil adjacent to the root and get reduced again. This process represents biogeochemical cycling of redox-sensitive species in plant roots.

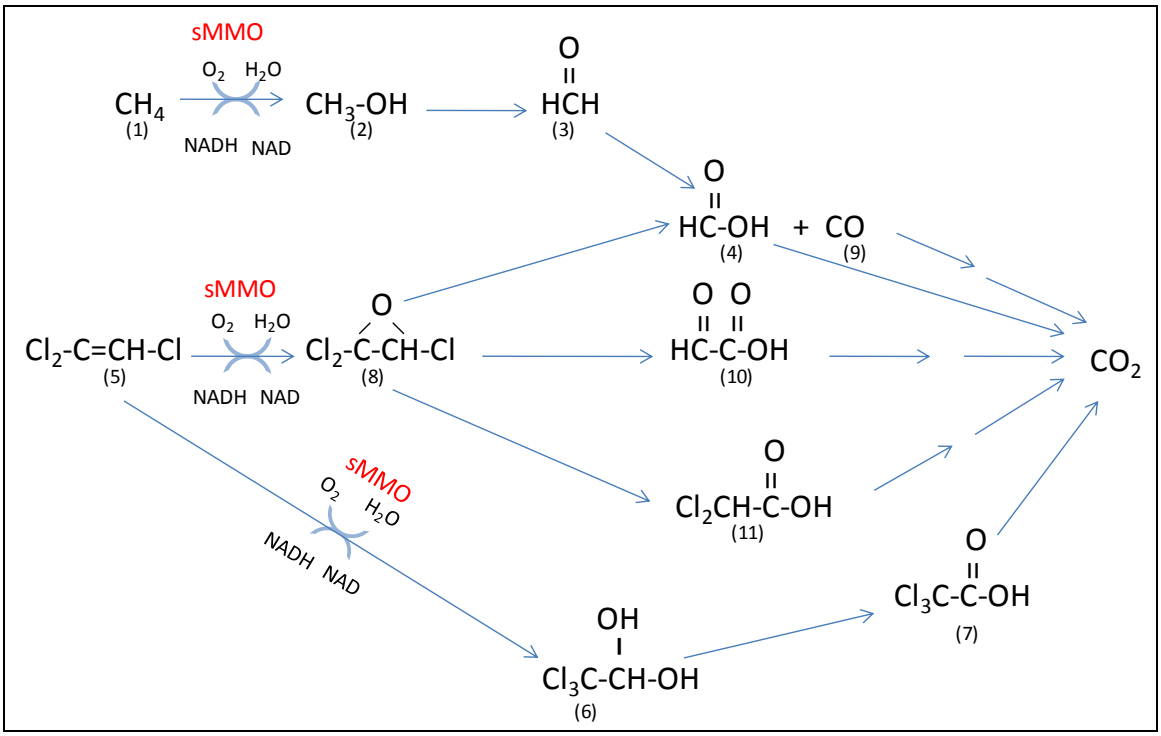

Figure 1.3 Cometabolic oxidation pathways for TCE with methane

Cometabolic oxidation pathways for TCE with methane as the growth substrate modified from Little et al. (1988), Fetzner and Lingens et al. (1994), and Arp (2001). The oxidation of methane (1) by sMMO yields methanol (2), which can subsequently be oxidized to formaldehyde (3), then formic acid (4), and finally CO_2 (Sullivan et al. 1998). TCE (5) is cometabolically oxidized by sMMO either by a pathway with intermediates such as chloral hydrate (6) and then trichloroacetic acid (7); alternatively, TCE is oxidized to TCE epoxide (8), which can spontaneously break down in water to form formic acid (4) and carbon monoxide (9), glyoxylic acid (10), or dichloroacetic acid (11). These products can then be easily mineralized by the heterotrophic or methanotrophic bacteria to CO_2.

Table 1.1 Descriptive information for CAHs

Abbreviation, chemical formula, and chemical structure of common CAHs. Molecular structure (http://en.wikipedia.org/wiki/Main_Page ; Ryoo et al. 2000)

Compound	Abbreviation	Chemical Formula	Chemical Structure
Tetrachloroethene	PCE	C_2Cl_4	
Trichloroethene	TCE	C_2HCl_3	
Dichloroethene isomers	DCEs	$C_2H_2Cl_2$	
	1,1-DCE		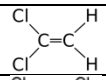
	cis-1,2-DCE		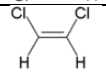
	trans-1,2-DCE		
Chloroethene (Vinyl Chloride)	VC	C_2H_3Cl	
Tetrachloroethane Isomers	TeCAs	$C_2H_2Cl_4$	
	1,1,1,2-PCA		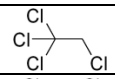
	1,1,2,2-PCA		
Trichloroethane Isomers	TCAs	$C_2H_3Cl_3$	
	1,1,1-TCA		
	1,1,2-TCA		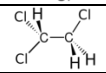
Dichloroethane Isomers	DCAs	$C_2H_4Cl_2$	
	1,1-DCA		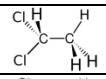
	1,2-DCA		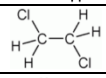
Chloroethane		C_2H_5Cl	

Table 1.2 Gibbs free energy values for aerobic mineralization of CEs and CAs

Gibbs free energy values for aerobic mineralization of CEs and CAs modified from Janssen and De Koning (1995) and Vlieg et al. (2001).

Compound	Reaction	$\Delta G^{o\prime}$(kJ/mole)
PCE	$C_2Cl_4 + 2H_2O + O_2 \rightarrow 2CO_2 + 4HCl$	-1006
TCE	$C_2HCl_3 + H_2O + {}^3/_2O_2 \rightarrow 2CO_2 + 3HCl$	-1072
1,1-DCE	$C_2H_2Cl_2 + 2O_2 \rightarrow 2CO_2 + 2HCl$	-1143
cis-1,2-DCE	$C_2H_2Cl_2 + 2O_2 \rightarrow 2CO_2 + 2HCl$	-1143
trans-1,2-DCE	$C_2H_2Cl_2 + 2O_2 \rightarrow 2CO_2 + 2HCl$	-1145
VC	$C_2H_3Cl + {}^5/_2O_2 \rightarrow 2CO_2 + HCl + H_2O$	-1237
1,1,1,2-PCA	$C_2H_2Cl_4 + H_2O + {}^3/_2O_2 \rightarrow 2CO_2 + 4HCl$	-1142
1,1,1-TCA	$C_2H_3Cl_3 + 2O_2 \rightarrow 2CO_2 + 3HCl$	-1217
1,1-DCA	$C_2H_4Cl_2 + {}^5/_2O_2 \rightarrow 2CO_2 + 2HCl + H_2O$	-1283
1,2-DCA	$C_2H_4Cl_2 + {}^5/_2O_2 \rightarrow 2CO_2 + 2HCl + H_2O$	-1279
chloroethane	$C_2H_5Cl + 3O_2 \rightarrow 2CO_2 + HCl + 2H_2O$	-1381

2 NATURAL ATTENUATION OF CHLORINATED ETHENES IN AN UPWARD-FLOW TREATMENT WETLAND: HIGH-RESOLUTION VERTICAL GEOCHEMICAL CHARACTERIZATION BY NOVEL PORE WATER SAMPLERS

2.1 INTRODUCTION

Chlorinated solvents are groundwater contaminants of major concern due to the threat they pose to human health as known or suspected carcinogens. As such it is important to understand their natural attenuation processes in the environment, which includes sorption, dilution, volatilization, and chemical and microbiological transformations. Of these, an in-depth understanding of the microbiological transformation or biodegradation processes is especially important because they can be applied as a natural, cost-effective remediation practice. Recent studies have demonstrated that natural wetlands can be effective in treating groundwater contaminated with chlorinated solvents through biodegradation (Lorah 1999; Lorah & Olsen 1999; Lorah & Voytek 2004). Wetlands promote biological activity and provide unique environments for both oxidative and reductive biodegradation (Amon et al. 2007; Imfeld et al. 2009), which together can allow for complete removal of chlorinated solvents from groundwater. Based on the potential for pollutant destruction, constructed wetlands have been proposed as a technology for the treatment of groundwater contaminated with chlorinated solvents (Kassenga et al. 2004; Kassenga & Pardue 2006; Amon et al. 2007).

Wetland environments have abundant supply of natural organic carbon that can provide electron donors such as hydrogen and volatile fatty acids (Westermann 1994; Conrad 1999; Kao & Lei 2000; Kassenga et al. 2004; Kassenga & Pardue 2006). These electron donors can support metabolic microbial reduction by the process known as

halorespiration where the chlorinated compounds act as the terminal electron acceptors (Kassenga et al. 2004). CAHs can also be reduced cometabolically in Fe(III)-reducing (Aulenta et al. 2006), sulfate-reducing, methanogenic, or acetogenic conditions (Bradley 2000; Kassenga et al. 2004). Of these, methanogenic conditions have been found to result in more complete degradation of CAHs to non-toxic end products, such as ethane and ethene (Freedman & Gossett 1989). Reductive biodegradation of oxidized organic compounds, such as tetrachloroethene (PCE), can occur via hydrogenolysis (Aulenta et al. 2006), in which PCE is sequentially reduced to daughter products such as trichloroethene (TCE), dichloroethene isomers (DCEs), vinyl chloride (VC), and ethene (Aulenta et al. 2006) by removal of single chlorine in each step. Chlorinated ethanes can also be dechlorinated by dichloroelimination pathway where two chlorines are removed and a double bond is formed between the two carbon atoms with a net input of two electrons (Aulenta et al. 2006). This pathway allows tetrachloroethane (TeCA) to be reduced to DCE isomers (Lorah & Olsen 1999; Lorah & Voytek 2004).

If complete degradation of CAHs does not occur through reductive dechlorination, less chlorinated daughter CAHs, such as DCEs and VC, can accumulate in the anaerobic zones of wetland environments (Lorah & Olsen 1999; Lorah & Voytek 2004). However, less chlorinated aliphatic hydrocarbons compounds have the potential to undergo oxidative biodegradation. This can occur in the anaerobic soil coupled to Fe(III) reduction (Bradley & Chapelle 1996; Bradley & Chapelle 1997; Bradley & Chapelle 1998b), sulfate reduction (Bradley & Chapelle 1998b), humic acid reduction (Bradley et al. 1998), and CO_2 reduction or methanogenesis (Bradley & Chapelle 1999). Oxidative degradation of less chlorinated aliphatic hydrocarbons can also occur in the presence of

oxygen in the near-surface environments of the wetland as well as in the root zone, particularly the rhizosphere, of wetland plants (Anderson et al. 1993; Anderson & Walton 1995; Bankston et al. 2002). Plants growing in waterlogged, anaerobic wetland environments must themselves provide oxygen to their roots because of the slow diffusivity of oxygen in water compared to air. This is accomplished via a high-porosity continuous gas space within the plant tissue called the *aerenchyma*, a specialized tissue that supports enhanced longitudinal transport of oxygen from plant shoots to their roots (Justin & Armstrong 1987; Armstrong et al. 2000; Colmer 2003). In the process, some of this oxygen can leak into the immediate soil environment surrounding the roots, referred to as *radial oxygen loss* (ROL) (Hinsinger et al. 2006). ROL can provide aerobic microenvironment surrounding the plant roots in an otherwise anaerobic soil in shallow vegetated wetlands, and facilitate oxidative degradation of less-chlorinated aliphatic hydrocarbons by metabolic and cometabolic processes in plant roots. Only two less-chlorinated ethenes, DCE isomers (Klier et al. 1999; Bradley & Chapelle 1998a; Bradley 2000; Bradley & Chapelle 2000; Coleman et al. 2002a; Broholm et al. 2005) and VC (Davis & Carpenter 1990; Coleman et al. 2002b; Fathepure et al. 2005), and a chlorinated ethane, 1,2,-DCA (Stucki et al. 1983; Janssen et al. 1985; Vandenbergh & Kunka 1988; Vandenwijngaard et al. 1992; Janssen et al. 1995; Janssen & Dekoning 1995; Klecka et al. 1998; Hage & Hartmans 1999; Hage et al. 2001), have been reported as the sole carbon source for microbial metabolism.

When chlorinated solvents are degraded cometabolically, a primary substrate is needed to initiate the production of suitable oxygenases (Bradley 2000). These substances provide an energy source and induce production of the oxygenase-expressing

cometabolic enzymes (Alvarez-Cohen & Speitel 2001). Numerous growth substrates have been identified, including methane (CH_4) (Fogel et al. 1986; Little et al. 1988; Chang & Alvarez-Cohen 1996; Broholm et al. 2005), toluene (Wackett & Gibson 1988; Shields et al. 1989a; Shields et al. 1989b; Zylstra et al. 1989) phenol (Folsom et al. 1990; Harker & Kim 1990; Hopkins et al. 1993), ethene (Debont & Harder 1978; Hartmans et al. 1991; Weber et al. 1992; Freedman & Herz 1996; Koziollek et al. 1999; Verce et al. 2001) , and ammonia (Arciero et al. 1989; Rasche et al. 1991; Vannelli et al. 1990; Arcangeli et al. 1996). Many of these substrates are found in wetland environments, making them available to the appropriate microorganisms as growth and energy sources; in particular, CH_4 and ammonia can be readily available due to the high soil organic matter content and its breakdown by fermentation (Whalen 2005)and ammonification processes (Jackson et al. 2008). Plants also secrete organic compounds, such as phenols, which can be used as substrates (Chen et al. 2004).

2.1.1 Biogeochemical Processes in the Experimental Wetland

The chlorinated solvent degradation in wetlands is influenced by the availability of electron donors and acceptors and the associated microbial activities. The availability of oxygen in the shallow subsurface in the wetland may depend on the influx of oxygen by diffusion and the consumption of oxygen by the soil organisms and by chemical oxidation (Bedford et al. 1991; Ratering & Schnell 2000). Redox gradient can result as the oxygen gets depleted by the different physiological groups of microorganisms. When a subsurface environment become anaerobic after being aerobic, the electron acceptors are reduced sequentially in the following order by their corresponding bacteria: nitrate, Mn (IV), Fe(III), sulfate, and CO_2 (Ratering & Schnell 2000). If the subsurface

environment gets fresh influx of oxygen and becomes aerobic again, reduced species, such as Fe(II), sulfide, and ammonium, can be re-oxidized creating a cycling effect. Such a change in redox environment can result from periodic flooding or fluctuations in the water table in the wetlands.

2.1.1.1 Nitrogen cycling in shallow, vegetated wetlands

A nitrogen cycle can exist in vegetated wetlands, which involves both nitrification and denitrification processes (Jackson et al. 2008). The process of nitrification is the microbiological oxidation of ammonia to nitrite, and nitrite to nitrate. Denitrification (also called nitrate respiration) can occur via dissimilatory means by two pathways (Atlas 1993). In the first pathway, under anaerobic condition the nitrate-reducing bacteria can transform nitrate to nitrite coupled to electron transport phosphorylation that generates energy, or it can be reduced further via hydrolylamine to ammonia, called nitrate ammonification (Atlas 1993; Megonigal 2004). The second pathway of microbial nitrate reduction to nitrogen also occurs in the anaerobic environment, and it proceeds via the conversion of nitrate through nitrite to nitric oxide (N_2O), and nitrous oxide (NO), to then finally to nitrogen gas (N_2) (Atlas 1993; Megonigal 2004). In wetlands environments, this pathway of nitrate reduction to gaseous nitrogen products (N_2O and N_2) has been linked with the nitrification process in the plant rhizosphere (Reddy et al. 1989; Arth et al. 1998). The nitrogen cycle in the shallow vegetated wetland settings is initiated by the diffusion of dissolved ammonia from the surrounding anaerobic soil into the plant rhizosphere. The ammonia is then oxidized in the rhizosphere to form nitrate (Reddy et al. 1989; Arth et al. 1998), which can be taken up either by the plant roots or it can diffuse into the adjacent anaerobic soil where it undergoes denitrification microbially and

transforms into gaseous N_2O and N_2, which then can diffuse through the roots and into the atmosphere (Jackson et al. 2008).

2.1.1.2 Iron cycling in shallow, vegetated wetlands

Iron in wetland environments can be found in the reduced, more soluble and mobile form as Fe(II) or in the oxidized, less soluble and solid/immobile form as Fe(III). In the Fe(III) form, iron exists as oxides, hydroxides or oxyhydroxides, which are commonly found on the roots of wetland plants (Bacha & Hossner 1977; Chen et al. 1980; Taylor et al. 1984; Hansel et al. 2001; Weiss et al. 2004), often referred to as 'iron plaque'. The formation of iron plaque can lead to biogeochemical cycling of iron, involving both Fe(II) and Fe(III) forms in alternating oxidation and reduction processes, respectively, both of which can be microbially mediated (the overall phenomenon sometimes referred to as "ferrous wheel"). As microbially-produced Fe(II) encounters an anaerobic-aerobic interface (in the sediment or in plant rhizosphere), this creates a potential habitat for iron-oxidizing bacteria (FeOB) and the aqueous Fe(II) is converted into solid Fe(III) oxyhydroxide phases. In producing solid (amorphous, or poorly crystalline) Fe(III) oxyhydroxides (Weiss et al. 2004; Weiss et al. 2005), the FeOB create an excellent substrate for Fe(III)-reducing bacteria (FeRB) to be utilized in the anaerobic zones of the shallow wetlands. The microbial reduction of Fe(III) oxides as part of the iron cycling has important biogeochemical implications; (a) microbial Fe(III) reduction can suppress both sulfate reduction (Kostka et al. 2002a; Kostka et al. 2002b), and CH_4 production (Roden & Zachara 1996; van der Nat & Middelburg 1998; Frenzel et al. 1999; King & Garey 1999; Neubauer et al. 2005) as FeRB can outcompete sulfate reducing bacteria (SRBs) and methanogens for substrate (Lovley & Phillips 1987). FeRB are also

capable of coupling Fe(III)-reduction with oxidation of organic pollutants (Bradley & Chapelle 1996; Bradley & Chapelle 1997; Bradley & Chapelle 1998b).

2.1.1.3 Sulfur cycling in shallow, vegetated wetlands

Sulfur is cycled in the wetland between sulfide (HS^-), its most reduced form, and sulfate, its most oxidized form, but sulfur can exist in a number of intermediate redox forms (Megonigal 2004). In anaerobic conditions, sulfate can undergo reduction to hydrogen sulfide (H_2S) by the activity of SRBs. However, reduced sulfur as H_2S can be chemically or microbially oxidized to thiosulfate, or get incorporated into iron sulfides (Rickard & Luther 2007) or organic matter (Blodau et al. 2007; Brown 1985; Brown 1986). Thiosulfate can also undergo disproportionation into sulfate, elemental sulfur (S^0) and H_2S, which is facilitated by the SRBs (Jorgensen 1990; Jorgensen & Bak 1991). The wetland plants can support sulfur cycling through microbial oxidation of sulfide to sulfate in the plant rhizosphere due to O_2 availability from the roots by ROL (Wind & Conrad 1997; Liesack et al. 2000). The sulfate thus formed is then either taken up by the plants or diffuse away into the adjacent anaerobic soil where it can get reduced microbially back to sulfide (Wind & Conrad 1997). Microcosm studies with rice plants has shown greater sulfate reduction in the soil adjacent to the root surface (Wind & Conrad 1997). Further details on sulfur cycling in the vegetated wetland is summarized elsewhere (Evans et al. 1997).

2.1.1.4 Methane in shallow, vegetated wetlands

Wetlands are a major source of atmospheric CH_4 by the activity of methanogenic bacteria due to the abundance of labile organic material within the wetland soil. The

production of CH_4 in the wetland soil is fueled by the decay of organic matter in the anaerobic portions of the wetland, where electron acceptors, such as nitrate, Fe(III), and sulfate, have been depleted. CH_4 can be produced in the wetland by methanogenic microorganisms through a series of steps, involving two main substrates hydrogen (H_2) and acetate, derived from hydrolytic and fermenting bacteria that decompose complex organic matter (Megonigal 2004; Whalen 2005). Acetotrophic methanogens produce CH_4 through fermentation of acetate, while hydrogenotrophic methanogens produce CH_4 by utilizing H_2 as an electron donor for the reduction of CO_2 (Megonigal 2004; Whalen 2005). In vegetated wetlands, CH_4 oxidation in the presence of O_2 occurs either shallow aerobic soil just above the water table, at the sediment-water interface in flooded wetlands, or in plant rhizosphere by O_2 from the roots of emergent plants (Armstrong & Armstrong 1991; Frenzel et al. 1992; Popp et al. 2000; Broholm et al. 2005). In vegetated wetalnds, as CH_4 diffuses from the bulk reducing soil into plant rhizosphere, the methane-oxidizing (also called methanotrophic) bacteria inhabiting the surface of the plant roots can facilitate CH_4 oxidation in the presence of O_2 (Shannon et al. 1996; Bosse & Frenzel 1998; Brune et al. 2000; Ding et al. 2005). The methanotrophic bacteria in the plant rhizosphere can oxidize a substantial portion of CH_4 produced in the bulk wetland soil (King 1996; Calhoun & King 1997; Bosse & Frenzel 1998; Gilbert & Frenzel 1998).

2.1.2 Measurement of pore water chemistry in wetlands

A detailed characterization of the pore water chemistry is critical for determining the ambient geochemical parameters and redox conditions of the subsurface, including shallow and deep soil zones. This can be accomplished by several approaches and methods originally developed for measuring trace metal and ion concentrations in pore

water from a wide variety of environments. Conventional methods rely on either *in situ* or *ex situ* techniques for obtaining pore water samples (Bufflap & Allen 1995); *ex situ* techniques are the older of the two methods, and they include approaches to extract the pore-water by squeezing and centrifuging the sediments. (Bufflap & Allen 1995). The *ex situ* techniques of pore water extraction require removal of sediments from their natural environments, thereby potentially introducing sampling artifacts, caused by changes in temperature and pressure, contamination due to exposure to oxygen, etc., which can introduce error in analytical results. The *in situ* pore water sampling techniques have been developed to minimize sampling artifacts, and they utilize the following field devices: suction filtration (Makemson 1972; Nayar et al. 2006), rhizon extraction (Seeberg-Elverfeldt et al. 2005), and equilibrium dialysis (Hesslein 1976; Mayer 1976); among these, dialysis samplers have been proven to be effective sampling devices (Hesslein 1976; Mayer 1976) that consist of discrete chambers, each with one or two opening(s) covered with dialysis membranes. The dialysis sampler (each with numerous chambers) is manually placed in the subsurface where the pore water is in contact with the membrane; prior to their placement, the sample chambers are filled with distilled and de-ionized water that slowly come to equilibrium with the sediment pore-water after passing through a dialysis membrane (Hesslein 1976). The water contained in each chamber after equilibration is then removed for geochemical analysis. These samplers can discriminate against various large size molecules in aqueous phase by using a dialysis membrane of a desired size, and the membranes also exclude the particulate matter, thus eliminating the need for filtration (Hesslein 1976).

The application of dialysis samplers for pore-water geochemical characterization originated with Mayan (1976) and Hesslein (1976). Mayan (1976) used dialysis bags that consisted of a perforated Plexiglas tube separated into chambers by rubber washers fitted over an inserted Plexiglas rod. Each chamber consisted of one dialysis bag wrapped around the Plexiglas rod. Hesslein's sampler, also called a '*peeper*', was fabricated using a similar concept but a different design: two clear Plexiglas sheets of a thinner (0.32 cm) and thicker (1.27 cm) thickness, where the thicker sheet had compartments to house 4mL water samples. Hesslein's sampler was prepared by filling the compartments with distilled water and carefully laying a piece of dialysis membrane over the full compartments so that any air bubbles were excluded. The thinner acrylic sheet was laid over the membrane and the sheets were screwed together with nylon screws. The whole sampler was then placed in a closed bath of degassed distilled water and allowed to lose most of its dissolved gasses by equilibration. The sampler was then pushed vertically into the soft, estuarine sediments, and allowed to equilibrate with pore-water for two weeks.

Hesslein's sampler design has been replicated with modifications in numerous geochemical studies (Bottomley & Bayly 1984; Carignan 1984; Carignan et al. 1985; Apte et al. 1989; Magaritz et al. 1989; Kaplan et al. 1991; Carignan et al. 1994; Teasdale et al. 1995), and the device has been applied to characterize groundwater contaminated with volatile organic compounds (VOCs) (Lorah & Olsen 1999; Laor 2003; Alvarez et al. 2004; Jackson et al. 2005). Recently, dialysis samplers were developed and employed in a phytoremediation field study to characterize the degradation of VOCs in the rhizosphere of trees (Jackson et al. 2005). The design of the dialysis chambers was

adapted from the original design of the 'peepers' (Hesslein 1976); samplers were constructed from 1.2 m long, solid Plexiglas tubes approximately 5 cm in diameter. Multiple cells were cut into the Plexiglas, spaced approximately 7.5 cm on center and each able to hold approximately 20 ml of water. One side of the cells was covered with two membranes (0.2μm inner membrane and 0.8μm nylon outer membrane) that would allow dissolved constituents to equilibrate between the groundwater and the deionized water placed in the sampler prior to deployment. The samplers remained in the field for a two-week equilibration period. The equilibrated water was removed from each cell by insertion of a sterile needle into the cell through the membrane and withdrawing the water with a syringe. The water was analyzed for chlorinated VOCs, organic acids, chloride ion, and dissolved gases.

The chemicals profiles of gaseous VOC levels in the unsaturated zone was measured by a device called multilayer sampler (MLS) at a vertical resolution of less than 3 cm (Laor 2003). The MLS consisted of individual units with chambers connected together, and separated with flexible Viton seals placed in between units. Each unit had a stainless steel frame in which stainless steel dialysis cells of 150 mL were inserted at right angles to each other. The concentration-depth profiles of the pore-water constituents including gases in the unsaturated zone were obtained (Laor 2003) by first filling the MLS chambers with distilled water, closing them with a dialysis membrane, and crimped in a PVC hoop with a Viton O-ring. The MLS assembly was then placed in an observation well and equilibrated with the surrounding pore-water for several weeks.

In the present study, a new field device, called pore water sampler (PWS), was developed for a high-resolution geochemical characterization of the experimental wetland

receiving VOC-contaminated groundwater. The design of the PWS is inspired by the samplers described above (Laor 2003; Jackson et al. 2005), but with a simpler, more rugged construction and closely-spaced vertical resolution; PWS units were employed in the present study successfully to reconstruct depth-concentration profiles of redox sensitive species (nitrate, ferrous iron, sulfate, methane) as well as chlorinated ethenes at shallow depths of the vegetated wetland. The PWS units were deployed in the field for characterizing the pore water chemistry once a month during the summer of 2008.

2.2 MATERIALS AND METHODS

2.2.1 Experimental Wetland

A pilot-scale, experimental wetland was constructed in the year 2000 at the Wright-Patterson Air Force Base or WPAFB (Dayton, OH), to investigate the natural attenuation of chlorinated ethenes in the groundwater passing through the wetland (see Figure 2.1). The pilot-scale wetland was constructed in an excavated-pit (37m x 18m, and 1.5m depth), lined with a ~30 cm thick clay layer and PVC geomembrane for hydraulic isolation from the underlying soil/aquifer (Amon et al., 2007). The excavated pit was then filled with a gravel layer at the bottom, and three layers of hydric soil (Figure 2.1) brought in from a drained wetland nearby. The PCE-contaminated groundwater was extracted from the underlying aquifer ([PCE] ~35 µg L^{-1}), and pumped into the experimental wetland at the bottom; the groundwater flowed upward through the hydric soil layers, emerged at the wetland surface, and then flowed into a sewer. The residence time of the groundwater passing through the treatment wetland was typically ~4 days. The WPAFB experimental wetland has 66 clusters of piezometers, installed in a 6x11 grid (Figure 2.2), with each cluster having 3 stainless-steel drive-point piezometers

(Solinst Model 615S) screened at different depths for groundwater sampling. The depths of the piezometer screens (114, 69 and 23 cm below ground surface; Figure 2.1b) correspond to the layers C, B and A of the wetland. The site was planted with multiple species of indigenous species of vegetation, and some plant roots may extend the full depth of the wetland (Amon et al. 2007).

Biogeochemical investigations of the wetland field site were carried out during 2000-'08 (Lach 2004; Amon et al. 2007) to characterize the variations in redox-active and other dissolved species with the help of water samples collected from the 3-D network of piezometers in the soil layers C, B and A (at depths of 114, 69 and 23 cm below ground surface). The above approach involving multi-level sampling has provided an insight into the ambient geochemical processes at the site.

High resolution sampling can provide support for the application of constructed wetlands as a treatment technology as it can reveal trends and degradation patterns not obvious from the data provided by piezometers alone. In 2008, PCE and its daughter products were analyzed in addition to water chemistry parameters to characterize PCE biodegradation in the wetland. Three 5.08 cm diameter wells were installed in the wetlands (Figure 2.2: PWS wells 3, 4, and 8) for deployment of newly designed PWS to gather geochemical data from depths between approximately 20 and 80 cm below the ground surface, a zone suspected of increased root activity. The retractable and reusable PWS units provided the variation in water chemistry at 9.21 cm vertical interval, a resolution that could not achieved by sampling with piezometers alone. The results from PWS units were combined with measurements from piezometers and from the influent to construct the depth-

concentration profiles of geochemical parameters at three PWS locations (PW3, PW4, and PW8).

2.2.2 Pore Water Sampler Design

The passive samplers were made of a solid PVC rod of 4.45 cm diameter machined to a length of 11.11 cm with a cylindrical 3.18 cm diameter (internal volume: 19.5 mL) cavity bored into the PVC rod from one side to create the sample cavity. The cylindrical cavity had a rounded bottom to maximize the volume of the cavity. For a water-tight seal, a 3.8 cm square, 5µm thick porous stainless steel plate (Mott Corporation, Farmington, CT) was fastened with four #4-40 screws under which is a 0.16 cm thick viton O-ring (3.18 cm inside diameter x 3.49 cm outside diameter). The pore-water sampler had sampling ports on both ends with septa material covering the ports being held in place with 0.64 cm 20 vented screws and washers. The vented screws allowed access to the sample collection cavity by a sampling syringe and needle. A 5.08 cm outer diameter, 0.32 cm thick Viton washer is placed between each sampler to provide a tight fit against the well casing and therefore prevent vertical migration of the wetland water within the monitoring well. The Viton washer isolates each pore-water sampler and ensures that only the water within each targeted interval has contact with the respective pore-water sampler. Typically, a set of 6-8 PWS units were attached together, using 0.64 cm 20 screws, for installation into PW wells, enabling a pore-water sample to be obtained approximately every 9.21 cm. Figure 2.3 provides design drawings and photographs of the pore-water sampler prototype.

2.2.3 Predicted vs. Measured Solute Concentration in PWS chamber

The time required for pore water to diffuse through the PWS faceplates and sample cavity and reach equilibrium in the field was estimated by calculations and laboratory evaluation. Fick's Second Law of Diffusion (Equation (1)) was used to find the diffusion rates:

$$\frac{dC}{dt} = D\frac{d^2C}{dx^2} \quad (1)$$

where C is the concentration of the diffusing substance, x is the space coordinate, D is the diffusion coefficient, and t is time.

Calculations showed that the diffusion time through the 5µm thick porous stainless steel faceplate used in the prototype PWS was expected to be an order of magnitude less than the diffusion time within the sampling cavity (Waldron 2007). Ignoring the porous plate, the diffusion within the sampling cavity was modeled as diffusion through a single plane sheet of a homogeneous medium (i.e. water) of thickness l. The PWS cavity is 2.9 cm deep with a diameter of 3.2 cm and volume of 19.5 ml. Considering these dimensions, a thickness l of 2.45 cm was used to approximate the average distance a solute molecule would diffuse in the water before reaching the no-flow boundary at the edge of the sampling cavity. Assuming no solute is initially in the sampling cavity, and that there's a constant concentration of solute, C_0, at the opening (faceplate) of the cavity, the following boundary (Equations 2a and 2b) and initial (Equation 2c) conditions are applicable:

$$C = C_0,\ x = 0,\ t \geq 0 \quad (2a)$$

$$\frac{dC}{dx} = 0,\ x = l = 2.45\ cm,\ t \geq 0 \quad (2b)$$

$$C = 0,\ 0 < x < l,\ t = 0 \quad (2c)$$

The solution to Equation (1) with initial/boundary conditions (2) is an infinite series of complementary error functions (Crank 1975); the series converges rapidly except for large values of Dt/l^2 (Crank 1975):

$$C = C_o \sum_{n=0}^{\infty}(-1)^n erfc\frac{(2n+1)l-x}{2\sqrt{Dt}} + C_o \sum_{n=0}^{\infty}(-1)^n erfc\frac{(2n+1)l+x}{2\sqrt{Dt}} \quad (3)$$

Calculated equilibrium concentrations were determined using equation 3 and diffusion coefficients, D (cm^2/s), taken from the literature (D=1.06x10^{-5} for sulfate, D=2.03x10^{-5} for chloride, and D=1.90x10^{-5} for nitrate (Cussler 1984)). These were compared to diffusion rates observed during the bench scale evaluations of the PWS to determine a minimum time the PWS units need to be deployed in the field to reach equilibrium with the surrounding pore water. A reservoir solution of known concentrations of anions was prepared with anions of interest (chloride, nitrate, and sulfate) to conduct the bench scale measurement of the diffusion coefficient in the PWS. Samples were taken from the PWS several times over a period of 9 days and analyzed on the IC.

A plot of normalized anion concentration (C/C_0) over time from both measurements and modeled values are shown in Figure 2.4. The modeled values provide a good fit to the data. Based on the smallest D, for sulfate, equation (3) was used to show that even for the slowest diffusing anion, after 14 days, the concentration measured in the PWS cavity would be 97% of C_0. Thus, leaving the PWS in place for at least 14 days gives confidence that the measured anion concentration in the PWS cavity represents the anion concentration in the pore water.

2.2.4 Sampling Procedures

2.2.4.1 PWS Assembly Field Installation and Retrieval

Prior to field deployment, the individual PWS units were assembled and their reservoirs filled with filtered deionized water. The PWS units were placed in the dessicator and vacuumed overnight. After which, all the PWS units for a given well were assembled together and the entire unit deoxygenated by N_2 purging for approximately 5 days. The assembled PWS units in their N_2-purged container were transported to the field. Prior to installation, the assembled PWS units were attached to an extension rod. After purging of the well, the entire assembly was placed in the well and the PWS units were allowed to equilibrate with the surrounding pore-water for at least two weeks as determined by the laboratory studies above (Figure 2.4) After which, the PWS units were retrieved, the extension rods removed, and they were prepared for transport back to the laboratory. Each stainless steel plate was wrapped with parafilm and tape and labeled. The PWS units were detached from each other and the individual units were placed in a N_2-purged glove bag. Each PWS well was sampled once a month for five months. The middle and lower layers of two adjacent piezometers were sampled in conjunction with the PWS units. The number of piezometers for each well, their corresponding depths below ground, adjacent piezometer numbers, sampling dates, and number of days in the field are listed in Table 2.1.

2.2.4.2 Sample Preparations and Analysis

The PWS assembly was removed from the N_2-filled polyethelene glove bag, and then immediately transferred into the reducing environment of an anaerobic chamber in

preparation for withdrawing water samples from individual PWS chambers. Approximately 4 ml of water was withdrawn from the PWS units at a slow speed using a gas-tight glass syringe. This sample volume was divided for analysis of organic parameters by gas chromatography compounds (chlorinated ethenes and CH_4) by HP GC6890 with Tekmar Velocity XPT purge-and-trap with FID and ECD; 3ml was reserved for CH_4 analysis by headspace injection and the remaining 1ml was used for chlorinated ethene analysis by purge and trap. A second syringe, a 20ml polypropylene syringe, was used to withdraw the remaining sample. This sample volume was divided for analysis of the inorganic parameters: 1ml each was reserved for 10x dilution of ammonia and iron analysis by Perkin Elmer's Lambda 45 UV spectrophotometer; 1ml was used for 5x diluted duplicate analysis of anions (chloride, nitrate, nitrite, sulfate) by Dionex ion chromatograph model 2500; 200µl for alkalinity analysis by spectrophotometer techniques, and the remaining volume was used for pH by a handheld Denver Instrument AP10 pH/mV meter. See Appendix A for details on sampling and analysis procedures.

2.3 RESULTS AND DISCUSSION

2.3.1 Variations in pH, alkalinity and chloride

The profiles in Figure 2.5 show chloride concentrations, pH, and alkalinity. The profiles mostly show consistency between sample locations in space, particularly for chloride concentrations and pH. Chloride ion is a conservative tracer and its consistent trend between locations and lack of variation with depth suggest homogeneous conditions and good flow in the wetland. If there was mixing with freshwater, decreasing concentrations would be evident and if evapotranspiration was occurring, there would be

increasing concentrations. The concentrations are about 2.5 mM throughout the profile, which suggests neither phenomenon is occurring significantly.

The pH of the pore water in the wetland does not vary significantly (ranges between 6.5 to 7.5), which is similar to a natural, sedge-dominated fen at the nearby location, that is fed by near-neutral pH groundwater, similar to the groundwater supplying the treatment wetland, and the two soils are quite similar (Amon et al. 2007). The variations in the pH with depth at the 3 PWS sites (Figure 2.5b) is less than 1 unit yet it is systematic; it decreases along the water flow-path (through layers C and B) from the bottom of the wetland up through the upper middle, possibly due to release of organic acids and carbon dioxide due to fermentative and oxidative breakdown of the soil organic matter by microbial processes.

The variations in alkalinity from the bottom of the wetland up to about 76 cm below the surface and then decreases to the surface. The sharp increase in alkalinity along water flow-path (lower half) may be caused by dissolution of soil minerals (i.e., $CaCO_{3(s)} + H^{+} = Ca^{2+} + HCO_3^{-}$). The decrease in the middle layer up to the top may be due to the minerals taken up by plants and microorganisms (Mitsch & Gosselink 2000). This could be especially true being that it is summer and the plants are undergoing active growth. Alkalinity can also be generated from dissimilatory sulfate reduction and the reduction of ferric oxyhydroxides to Fe(II) (see redox characteristics below). These are biologically mediated processes, resulting in either proton consumption or bicarbonate formation, which are both chemically equivalent to alkalinity generation (Anderson & Schiff 1987).

2.3.2 Variations in redox-sensitive species in the wetland

2.3.2.1 Ammonia

The profiles in Figure 2.6 also show the vertical distributions of ammonia. Ammonia is being produced in the bottom of the wetland due to ammonification processes of organic nitrogen in the wetland soil (Jackson et al. 2008). The profiles show ammonium being decreased in the middle of the wetland up to the surface, possibly due to plant uptake or nitrification processes from oxygen that leaks from the plant roots. Ammonia that accumulates in the anaerobic areas of the wetland can diffuse into the root zone as a result of concentration gradients (Reddy et al. 1989). Once in the root zone, nitrification can occur with ammonia being oxidized to nitrite and nitrite being oxidized to nitrate (Atlas 1993). There is not a corresponding increase in nitrate (see Figure 2.7 below), which may mean that nitrate is being reduced or depleted by plant uptake where nitrate uptake can be comparable to ammonia uptake (Kirk & Kronzucker 2005) or greater due to the attraction of ammonia to the negatively charged soil (Jackson et al. 2008).

2.3.2.2 Nitrate, Iron, Sulfate, and Methane

Nitrate, ferrous iron, sulfate, and methane profiles are show in Figure 2.7. Overall these profiles show reducing conditions near the bottom of the wetland up through the middle and then more oxidizing conditions in the middle and up towards the surface. Nitrate profiles are mostly consistent between PWS locations. Concentrations disappear from the bottom of the wetland up to the top, possibly due to plant uptake or nitrate reduction occurring in the bottom reducing part of the wetland as nitrate is the TEA. Nitrate reduction, also called denitrification or nitrate respiration, can occur via

dissimilatory means by two pathways (Atlas 1993). In the first pathway, nitrate-reducing bacteria reduce nitrate to nitrite under anaerobic conditions. Nitrite can be excreted by the reducing bacteria or reduced further via hydroxylamine to ammonia, called nitrate ammonification (Atlas 1993). The second pathway is more complete and proceeds microbially via the conversion of nitrate through nitrite to nitrous oxide and nitrous oxide to nitrogen gas (Atlas 1993). Nitrite was not detected in the wetland.

The iron profiles are mostly consistent between locations. It is possible that iron reduction may be occurring in the lower and middle layer as evidenced by increased Fe (II) concentrations. The decrease in concentrations in the upper middle and surface layers may be due to oxidation to Fe(III), due to rhizospheric activities possibly creating an iron cycle. The iron cycle in the rhizosphere consists of the microbial oxidation of Fe(II) to Fe(III) as oxygen is leaked from the roots into the rhizosphere. This provides a substantial pool of Fe(III) which can form Fe(III) oxides on the surface of the wetland roots as represented. It is possible that these Fe(III) oxides can be transported to the nearby anaerobic soil where microbial reduction to Fe(II) can occur, which can then be oxidized back to Fe(III) as more oxygen is transported into the roots. More amorphous Fe(III) oxides have been found in the rhizosphere compared to the non-rhizospheric soil because of the activity of iron-oxidizing bacteria FeOB (Weiss et al. 2004). Amorphous Fe(III) oxides are more reactive in that they are subject to near or complete dissolution (Thamdrup 2000), allowing more rapid reduction in the rhizosphere compared to the non-rhizosphere. Iron cycling in the root zone may be more obvious in PW3 and PW8 as there is a larger zone of stable ferrous iron (cycling of oxidation and reduction processes, keeping concentrations stable) as compared to PW4.

The sulfate profiles are consistent between locations. It appears as if sulfate is being reduced in the bottom of the wetland in conjunction with nitrate and iron reduction. Sulfate concentrations are reduced to mostly zero. The rhizosphere of wetland plants can sustain the sulfur cycle starting with microbial aerobic oxidation of hydrogen sulfide to sulfate by the leakage of O_2 from the roots (Wind & Conrad 1997; Liesack et al. 2000). Sulfate was not detected at the top of the wetland possibly due to root uptake or its reduction in the nearby anaerobic soil.

Methanogenesis is evident in the lower layer, followed by oxidation near the upper middle and surface layers. It is possible that the methane-producing bacteria (also called methanogens) are using the organic material for CH_4 production in the anaerobic portions of the wetland where alternative electron acceptors (nitrate, Fe(III), and sulfate) have been reduced. This provides a growth substrate for methane oxidizers for methane-oxidizing bacteria inhabiting the surface of the plant roots that can facilitate CH_4 oxidation in the presence of oxygen (Shannon et al. 1996; Bosse & Frenzel 1998; Brune et al. 2000; Ding et al. 2005)Other studies have found that methanotrophic bacteria in the rhizosphere can consume a substantial portion of the CH_4 produced in the bulk wetland soil (King 1996; Calhoun & King 1997; Bosse & Frenzel 1998; Gilbert & Frenzel 1998)

2.3.3 Natural Attenuation of VOCs in the Wetland

VOC concentrations are displayed in Figure 2.8. Although the levels have significantly declined since the construction of the wetland in 2000, it is still evident that PCE is being reduced in the lower part as the concentrations go from ~0.04 µM to near zero in the middle and top. Other studies have found that wetland environments are favorable for reductive biodegradation via halorespiration (Kassenga et al. 2004) as well

as co-metabolically in Fe(III)-reducing (Aulenta et al. 2006), sulfate-reducing, methanogenic, or acetogenic conditions (Bradley 2000; Kassenga et al. 2004). PCE reduction is occurring in conjunction with the formation of TCE, which is possible evidence of hydrogenolysis because TCE is the first daughter product formed in this process. In hydrogenolysis, PCE is sequentially reduced to TCE, DCEs, VC, and ethene by removal of a single chlorine in each step (Aulenta et al. 2006). TCE production is mostly followed by its disappearance, which may also be due to reduction or it could be the result of oxidative cometabolic processes as it is near the oxidative conditions in the root zone.

Support for continued reduction is the formation of VC. Without detection of the DCE isomers, TCE could be reduced by abiotic pathways or though hydrogenolysis (Lorah & Olsen 1999; Lorah & Voytek 2004) with DCE isomers being produced without detection because it is immediately reduced to form VC. The disappearance of TCE and reduced DCE and VC concentrations may also be due to oxidative degradation processes.

Oxidative degradation may be occurring in the near-surface environments of the wetland and root zone of wetland plants via ROL (Anderson et al. 1993; Anderson & Walton 1995; Bankston et al. 2002). Oxidation may be via metabolic or cometabolic pathways. VC has been found to be metabolically degraded; microorganisms have been identified that can use these compounds as an energy source (Hartmans et al. 1985; Hartmans & Debont 1992; Verce et al. 2000; Verce et al. 2001; Coleman et al. 2002b; Singh et al. 2004; Fathepure et al. 2005) . For both TCE and VC, several studies have found that cometabolic degradation can occur by growth substrates found in the wetland. In this study the decrease in CH_4 (Figure 2.7) and ammonia (Figure 2.6) correspond with the decrease in VC (Figure 2.8), possibly supporting aerobic cometabolism.

2.3.4 Conclusions

The profiles obtained from the PWS units help reveal the chemistry in the constructed wetland at WPAFB. The consistency between locations and the agreement with results obtained from sampling the piezometers (i.e., the PWS readings in the first 80cm are comparable to the piezometer readings in the 80-140 cm interval) gives support for using PWS units. The fine resolution provides details, especially in the root zone, that cannot be determined sampling with piezometers alone. From the profiles, it is evident that reducing conditions are at the bottom of the wetland with overlapping zones of nitrate, iron, and sulfate reduction and methanogenesis. The wetlands become more oxidizing the closer to the surface and in the root zone showing methane and ammonia oxidation, which can aid in VC cometabolism. The vertical resolution provided by the PWS units, allows the differences in the depths to be determined.

2.4 REFERENCES

Alvarez-Cohen L, Speitel GE (2001) Kinetics of aerobic cometabolism of chlorinated solvents. Biodegradation 12(2): 105-126

Alvarez D, Petty, J., Huckins, J., Lones-Lepp, T., Getting, D., Goddard, J., Manahan, S. (2004) Development of a Passive, In Situ, Integrative Sampler for Hydrophilic Organic Contaminants in Aquatic Environments. Environ. Tox. Chem. 23(7): 1640-1648

Amon JP, Agrawal A, Shelley ML, Opperman BC, Enright MP, Clemmer ND, Slusser T, Lach J, Sobolewski T, Gruner W, Entingh AC (2007) Development of a wetland

constructed for the treatment of groundwater contaminated by chlorinated ethenes. Ecol. Eng. 30(1): 51-66

Anderson RF, Schiff SL (1987) Alkalinity Generation and the fate of sulfure in Lake-Sediments. Can. J. Fish. Aquat. Sci. 44: 188-193

Anderson TA, Guthrie EA, Walton BT (1993) Bioremediation in the Rhizosphere. Environmental Science & Technology 27(13): 2630-2636

Anderson TA, Walton BT (1995) Comparative Fate of [C-14] Trichloroethylene in the Root-Zone of Plants from a Former Solvent Disposal Site. Environmental Toxicology and Chemistry 14(12): 2041-2047

Apte SC, Gardner MJ, Hunt DTE (1989) An Evaluation of Dialysis as a Size-Based Separation Method for the Study of Trace-Metal Speciation in Natural-Waters. Environmental Technology Letters 10(2): 201-212

Arcangeli JP, Arvin E, Mejlhede M, Lauritsen FR (1996) Biodegradation of cis-1,2-dichloro-ethylene at low concentrations with methane-oxidizing bacteria in a biofilm reactor. Water Res. 30(8): 1885-1893

Arciero D, Vannelli T, Logan M, Hooper AB (1989) Degradation of Trichloroethylene by the Ammonia-Oxidizing Bacterium Nitrosomonas-Europaea. Biochemical and Biophysical Research Communications 159(2): 640-643

Armstrong J, Armstrong W (1991) A Convective through-Flow of Gases in Phragmites-Australis (Cav) Trin Ex Steud. Aquat. Bot. 39(1-2): 75-88

Armstrong W, Cousins D, Armstrong J, Turner DW, Beckett PM (2000) Oxygen distribution in wetland plant roots and permeability barriers to gas-exchange with

the rhizosphere: a microelectrode and modelling study with Phragmites australis. Annals of Botany 86(3): 687-703

Arth I, Frenzel P, Conrad R (1998) Denitrification coupled to nitrification in the rhizosphere of rice. Soil Biology & Biochemistry 30(4): 509-515

Atlas RaB, R. (1993) Microbial Ecology. The Benjamin Cummings Publishing Company, Redwood City

Aulenta F, Majone M, Tandoi V (2006) Enhanced anaerobic bioremediation of chlorinated solvents: environmental factors influencing microbial activity and their relevance under field conditions. Journal of Chemical Technology and Biotechnology 81(9): 1463-1474

Bacha RE, Hossner LR (1977) Characteristics of Coatings Formed on Rice Roots as Affected by Iron and Manganese Additions. Soil Science Society of America Journal 41(5): 931-935

Bankston JL, Sola DL, Komor AT, Dwyer DF (2002) Degradation of trichloroethylene in wetland microcosms containing broad-leaved cattail and eastern cottonwood. Water Res. 36(6): 1539-1546

Bedford BL, Bouldin DR, Beliveau BD (1991) Net Oxygen and Carbon-Dioxide Balances in Solutions Bathing Roots of Wetland Plants. Journal of Ecology 79(4): 943-959

Blodau C, Mayer B, Peiffer S, Moore TR (2007) Support for an anaerobic sulfur cycle in two Canadian peatland soils. Journal of Geophysical Research-Biogeosciences 112(G2):

Bosse U, Frenzel P (1998) Methane emissions from rice microcosms: The balance of production, accumulation and oxidation. Biogeochemistry 41(3): 199-214

Bottomley EZ, Bayly IL (1984) A Sediment Porewater Sampler Used in Root Zone Studies of the Submerged Macrophyte, Myriophyllum-Spicatum. Limnology and Oceanography 29(3): 671-673

Bradley PM (2000) Microbial degradation of chloroethenes in groundwater systems. Hydrogeology Journal 8(1): 104-111

Bradley PM, Chapelle FH (1996) Anaerobic mineralization of vinyl chloride in Fe(III)-reducing, aquifer sediments. Environmental Science & Technology 30(6): 2084-2086

Bradley PM, Chapelle FH (1997) Kinetics of DCE and VC mineralization under methanogenic and Fe(III)-reducing conditions. Environmental Science & Technology 31(9): 2692-2696

Bradley PM, Chapelle FH (1998a) Effect of contaminant concentration on aerobic microbial mineralization of DCE and VC in stream-bed sediments. Environmental Science & Technology 32(5): 553-557

Bradley PM, Chapelle FH (1998b) Microbial mineralization of VC and DCE under different terminal electron accepting conditions. Anaerobe 4(2): 81-87

Bradley PM, Chapelle FH (1999) Role for acetotrophic methanogens in methanogenic biodegradation of vinyl chloride. Environmental Science & Technology 33(19): 3473-3476

Bradley PM, Chapelle FH (2000) Aerobic microbial mineralization of dichloroethene as sole carbon substrate. Environmental Science & Technology 34(1): 221-223

Bradley PM, Chapelle FH, Lovley DR (1998) Humic acids as electron acceptors for anaerobic microbial oxidation of vinyl chloride and dichloroethene. Appl. Environ. Microbiol. 64(8): 3102-3105

Broholm K, Ludvigsen L, Jensen TF, Ostergaard H (2005) Aerobic biodegradation of vinyl chloride and cis-1,2-dichloroethylene in aquifer sediments. Chemosphere 60(11): 1555-1564

Brown KA (1985) Sulfur Distribution and Metabolism in Waterlogged Peat. Soil Biology & Biochemistry 17(1): 39-45

Brown KA (1986) Formation of Organic Sulfur in Anaerobic Peat. Soil Biology & Biochemistry 18(2): 131-140

Brune A, Frenzel P, Cypionka H (2000) Life at the oxic-anoxic interface: microbial activities and adaptations. Fems Microbiology Reviews 24(5): 691-710

Bufflap SE, Allen HE (1995) Sediment Pore-Water Collection Methods for Trace-Metal Analysis - a Review. Water Research 29(1): 165-177

Burris DR, Delcomyn CA, Smith MH, Roberts AL (1996) Reductive dechlorination of tetrachloroethylene and trichloroethylene catalyzed by vitamin B-12 in homogeneous and heterogeneous systems. Environmental Science & Technology 30(10): 3047-3052

Calhoun A, King GM (1997) Regulation of root-associated methanotrophy by oxygen availability in the rhizosphere of two aquatic macrophytes. Appl. Environ. Microbiol. 63(8): 3051-3058

Carignan R (1984) Interstitial Water Sampling by Dialysis - Methodological Notes. Limnology and Oceanography 29(3): 667-670

Carignan R, Rapin F, Tessier A (1985) Sediment Porewater Sampling for Metal Analysis - a Comparison of Techniques. Geochimica Et Cosmochimica Acta 49(11): 2493-2497

Carignan R, Stpierre S, Gachter R (1994) Use of Diffusion Samplers in Oligotrophic Lake-Sediments - Effects of Free Oxygen in Sampler Material. Limnology and Oceanography 39(2): 468-474

Chang HL, Alvarez-Cohen L (1996) Biodegradation of individual and multiple chlorinated aliphatic hydrocarbons by methane-oxidizing cultures. Appl. Environ. Microbiol. 62(9): 3371-3377

Chen CC, Dixon JB, Turner FT (1980) Iron Coatings on Rice Roots - Morphology and Models of Development. Soil Science Society of America Journal 44(5): 1113-1119

Chen WM, Chang JS, Wu CH, Chang SC (2004) Characterization of phenol and trichloroethene degradation by the rhizobium Ralstonia taiwanensis. Research in Microbiology 155(8): 672-680

Coleman NV, Mattes TE, Gossett JM, Spain JC (2002a) Biodegradation of cis-dichloroethene as the sole carbon source by a beta-proteobacterium. Appl. Environ. Microbiol. 68(6): 2726-2730

Coleman NV, Mattes TE, Gossett JM, Spain JC (2002b) Phylogenetic and kinetic diversity of aerobic vinyl chloride-assimilating bacteria from contaminated sites. Appl. Environ. Microbiol. 68(12): 6162-6171

Colmer TD (2003) Aerenchyma and an inducible barrier to radial oxygen loss facilitate root aeration in upland, paddy and deep-water rice (Oryza sativa L.). Annals of Botany 91(2): 301-309

Conrad R (1999) Contribution of hydrogen to methane production and control of hydrogen concentrations in methanogenic soils and sediments. Fems Microbiology Ecology 28(3): 193-202

Crank J (1975) The Mathematics of Diffusion. Oxford University Press, Oxford New York

Cussler EL (1984) Diffusion Mass transfer in fluid systems. Cambridge University Press, Cambridge

Davis JW, Carpenter CL (1990) Aerobic Biodegradation of Vinyl-Chloride in Groundwater Samples. Appl. Environ. Microbiol. 56(12): 3878-3880

Debont JAM, Harder W (1978) Metabolism of Ethylene by Mycobacterium-E-20. Fems Microbiology Letters 3(2): 89-93

Ding WX, Cai ZC, Tsuruta H (2005) Plant species effects on methane emissions from freshwater marshes. Atmospheric Environment 39(18): 3199-3207

Emerson D, Revsbech NP (1994a) Investigation of an Iron-Oxidizing Microbial Mat Community Located near Aarhus, Denmark - Field Studies. Appl. Environ. Microbiol. 60(11): 4022-4031

Emerson D, Revsbech NP (1994b) Investigation of an Iron-Oxidizing Microbial Mat Community Located near Aarhus, Denmark - Laboratory Studies. Appl. Environ. Microbiol. 60(11): 4032-4038

Evans HE, Dillon PJ, Molot LA (1997) The use of mass balance investigations in the study of the biogeochemical cycle of sulfur. Hydrol. Process. 11(7): 765-782

Fathepure BZ, Elango VK, Singh H, Bruner MA (2005) Bioaugmentation potential of a vinyl chloride-assimilating Mycobacterium sp., isolated from a chloroethene-contaminated aquifer. Fems Microbiology Letters 248(2): 227-234

Fogel MM, Taddeo AR, Fogel S (1986) Biodegradation of Chlorinated Ethenes by a Methane-Utilizing Mixed Culture. Appl. Environ. Microbiol. 51(4): 720-724

Folsom BR, Chapman PJ, Pritchard PH (1990) Phenol and Trichloroethylene Degradation by Pseudomonas-Cepacia G4 - Kinetics and Interactions between Substrates. Appl. Environ. Microbiol. 56(5): 1279-1285

Freedman DL, Gossett JM (1989) Biological Reductive Dechlorination of Tetrachloroethylene and Trichloroethylene to Ethylene under Methanogenic Conditions. Appl. Environ. Microbiol. 55(9): 2144-2151

Freedman DL, Herz SD (1996) Use of ethylene and ethane as primary substrates for aerobic cometabolism of vinyl chloride. Water Environment Research 68(3): 320-328

Frenzel P, Bosse U, Janssen PH (1999) Rice roots and methanogenesis in a paddy soil: ferric iron as an alternative electron acceptor in the rooted soil. Soil Biology & Biochemistry 31(3): 421-430

Frenzel P, Rothfuss F, Conrad R (1992) Oxygen Profiles and Methane Turnover in a Flooded Rice Microcosm. Biology and Fertility of Soils 14(2): 84-89

Gilbert B, Frenzel P (1998) Rice roots and CH4 oxidation: The activity of bacteria, their distribution and the microenvironment. Soil Biology & Biochemistry 30(14): 1903-1916

Gossett JM (1987) Measurement of Henrys Law Constants for C1 and C2 Chlorinated Hydrocarbons. Environmental Science & Technology 21(2): 202-208

Hage JC, Hartmans S (1999) Monooxygenase-mediated 1,2-dichloroetbane degradation by Pseudomonas sp Strain DCA1. Appl. Environ. Microbiol. 65(6): 2466-2470

Hage JC, Kiestra FDG, Hartmans S (2001) Co-metabolic degradation of chlorinated hydrocarbons by Pseudomonas sp strain DCA1. Applied Microbiology and Biotechnology 57(4): 548-554

Hansel CM, Fendorf S, Sutton S, Newville M (2001) Characterization of Fe plaque and associated metals on the roots of mine-waste impacted aquatic plants. Environmental Science & Technology 35(19): 3863-3868

Harker AR, Kim Y (1990) Trichloroethylene Degradation by 2 Independent Aromatic-Degrading Pathways in Alcaligenes-Eutrophus Jmp134. Appl. Environ. Microbiol. 56(4): 1179-1181

Hartmans S, Debont JAM (1992) Aerobic Vinyl-Chloride Metabolism in Mycobacterium-Aurum L1. Appl. Environ. Microbiol. 58(4): 1220-1226

Hartmans S, Debont JAM, Tramper J, Luyben K (1985) Bacterial-Degradation of Vinyl-Chloride. Biotechnology Letters 7(6): 383-388

Hartmans S, Weber FJ, Somhorst DPM, Debont JAM (1991) Alkene Monooxygenase from Mycobacterium - a Multicomponent Enzyme. Journal of General Microbiology 137: 2555-2560

Hesslein RH (1976) Insitu Sampler for Close Interval Pore Water Studies. Limnology and Oceanography 21(6): 912-914

Hinsinger P, Plassard C, Jaillard B (2006) Rhizosphere: A new frontier for soil biogeochemistry. Journal of Geochemical Exploration 88(1-3): 210-213

Hopkins GD, Munakata J, Semprini L, McCarty PL (1993) Trichloroethylene Concentration Effects on Pilot Field-Scale in-Situ Groundwater Bioremediation by Phenol-Oxidizing Microorganisms. Environmental Science & Technology 27(12): 2542-2547

Imfeld G, Braeckevelt M, Kuschk P, Richnow HH (2009) Monitoring and assessing processes of organic chemicals removal in constructed wetland. Chemosphere 74: 349-362

Jackson LE, Burger M, Cavagnaro TR (2008) Roots nitrogen transformations, and ecosystem services. Annu. Rev. Plant Biol. 59: 341-363

Jackson WA, Martino L, Hirsh S, Wrobel J, Pardue JH (2005) Application of a dialysis sampler to monitor phytoremediation processes. Environmental Monitoring and Assessment 107(1-3): 155-171

Janssen DB, Dekoning W (1995) Development and Application of Bacterial Cultures for the Removal of Chlorinated Aliphatics. Water Science and Technology 31(1): 237-247

Janssen DB, Scheper A, Dijkhuizen L, Witholt B (1985) Degradation of Halogenated Aliphatic-Compounds by Xanthobacter-Autotrophicus Gj10. Appl. Environ. Microbiol. 49(3): 673-677

Janssen DB, van der Ploeg JR, Pries F (1995) Genetic adaptation of bacteria to halogenated aliphatic compounds. Environmental Health Perspectives 103: 29-32

Jorgensen BB (1990) A Thiosulfate Shunt in the Sulfur Cycle of Marine-Sediments. Science 249(4965): 152-154

Jorgensen BB, Bak F (1991) Pathways and Microbiology of Thiosulfate Transformations and Sulfate Reduction in a Marine Sediment (Kattegat, Denmark). Appl. Environ. Microbiol. 57(3): 847-856

Justin S, Armstrong W (1987) The Anatomical Characteristics of Roots and Plant-Response to Soil Flooding. New Phytologist 106(3): 465-495

Kao CM, Lei SE (2000) Using a peat biobarrier to remediate PCE/TCE contaminated aquifers. Water Res. 34(3): 835-845

Kaplan E, Banerjee S, Ronen D, Magaritz M, Machlin A, Sosnow M, Koglin E (1991) Multilayer Sampling in the Water-Table Region of a Sandy Aquifer. Ground Water 29(2): 191-198

Kassenga G, Pardue JH, Moe WM, Bowman KS (2004) Hydrogen thresholds as indicators of dehalorespiration in constructed treatment wetlands. Environmental Science & Technology 38(4): 1024-1030

Kassenga GR, Pardue JH (2006) Effect of competitive terminal electron acceptor processes on dechlorination of cis-1,2-dichloroethene and 1,2-dichloroethane in constructed wetland soils. Fems Microbiology Ecology 57(2): 311-323

King GM (1996) In situ analyses of methane oxidation associated with the roots and rhizomes of a bur reed, Sparganium eurycarpum, in a Maine wetland. Appl. Environ. Microbiol. 62(12): 4548-4555

King GM, Garey MA (1999) Ferric tron reduction by bacteria associated with the roots of freshwater and marine macrophytes. Appl. Environ. Microbiol. 65(10): 4393-4398

Kirk GJD, Kronzucker HJ (2005) The potential for nitrification and nitrate uptake in the rhizosphere of wetland plants: A modelling study. Annals of Botany 96(4): 639-646

Klecka GM, Carpenter CL, Gonsior SJ (1998) Biological transformations of 1,2-dichloroethane in subsurface soils and groundwater. Journal of Contaminant Hydrology 34(1-2): 139-154

Klier NJ, West RJ, Donberg PA (1999) Aerobic biodegradation of dichloroethylenes in surface and subsurface soils. Chemosphere 38(5): 1175-1188

Kostka JE, Gribsholt B, Petrie E, Dalton D, Skelton H, Kristensen E (2002a) The rates and pathways of carbon oxidation in bioturbated saltmarsh sediments. Limnology and Oceanography 47(1): 230-240

Kostka JE, Roychoudhury A, Van Cappellen P (2002b) Rates and controls of anaerobic microbial respiration across spatial and temporal gradients in saltmarsh sediments. Biogeochemistry 60(1): 49-76

Koziollek P, Bryniok D, Knackmuss HJ (1999) Ethene as an auxiliary substrate for the cooxidation of cis-1,2-dichloroethene and vinyl chloride. Archives of Microbiology 172(4): 240-246

Lach JD (2004) Treatment of Contaminated Grondwater in a Constructed Wetland: A Biogeochemical Analysis. In. Wright State University, Dayton, OH.

Laor Y, Ronen, D., Ellen, G. (2003) Using a Passive Multilayer Sampler for Measuring Detaild Profiles of Gas-Phase VOCs in the Unsaturated Zone. Environ. Sci. Technol. 37: 352-360

Lide DR, Frederikse HPR (1995) CRC Handbook of Chemistry and Physics, 76th Edition. CRC Press, Inc., Boca Raton, FL

Liesack W, Schnell S, Revsbech NP (2000) Microbiology of flooded rice paddies. Fems Microbiology Reviews 24(5): 625-645

Little CD, Palumbo AV, Herbes SE, Lidstrom ME, Tyndall RL, Gilmer PJ (1988) Trichloroethylene Biodegradation by a Methane-Oxidizing Bacterium. Appl. Environ. Microbiol. 54(4): 951-956

Lorah M, Olsen, L. (1999) Degradation of 1,1,2,2-Tetrachloroethane in a Freshwater Tidal Wetland: Field and Laboratory Evidence. . Environ. Sci. Technol 33: 227-234

Lorah MM, Olsen LD (1999) Natural attenuation of chlorinated volatile organic compounds in a freshwater tidal wetland: Field evidence of anaerobic biodegradation. Water Resources Research 35(12): 3811-3827

Lorah MM, Voytek MA (2004) Degradation of 1,1,2,2-tetrachloro ethane and accumulation of vinyl chloride in wetland sediment microcosms and in situ porewater: biogeochemical controls and associations with microbial communities. Journal of Contaminant Hydrology 70(1-2): 117-145

Lovley DR, Phillips EJP (1987) Competitive Mechanisms for Inhibition of Sulfate Reduction and Methane Production in the Zone of Ferric Iron Reduction in Sediments. Appl. Environ. Microbiol. 53(11): 2636-2641

Magaritz M, Wells M, Amiel AJ, Ronen D (1989) Application of a Multilayer Sampler Based on the Dialysis Cell Technique for the Study of Trace-Metals in Groundwater. Applied Geochemistry 4(6): 617-624

Makemson JC (1972) Interstitial Water Sampler for Sandy Beaches. Limnology and Oceanography 17(4): 626-&

Mayer LM (1976) Chemical Water Sampling in Lakes and Sediments with Dialysis Bags. Limnology and Oceanography 21(6): 909-912

Megonigal J, Hines, ME, Visscher, PT (2004) Anaerobic Metabolism: Linkages to Trace Gases and Aerobic Processes. Elsevier-Pergamon, Oxford, UK

Mitsch WJ, Gosselink JG (2000) Wetlands, 3rd ed. John Wiley and Sons, New York, USA

Nayar S, Miller D, Bryars S, Cheshire AC (2006) A simple, inexpensive and large volume pore water sampler for sandy and muddy substrates. Estuarine Coastal and Shelf Science 66(1-2): 298-302

Neubauer SC, Givler K, Valentine SK, Megonigal JP (2005) Seasonal patterns and plant-mediated controls of subsurface wetland biogeochemistry. Ecology 86(12): 3334-3344

Pankow JF (1991) Aquatic Chemistry Concepts. CRC Press, Inc., Boca Raton, FL

Popp TJ, Chanton JP, Whiting GJ, Grant N (2000) Evaluation of methane oxidation in the rhizosphere of a Carex dominated fen in north central Alberta, Canada. Biogeochemistry 51(3): 259-281

Rasche ME, Hyman MR, Arp DJ (1991) Factors Limiting Aliphatic Chlorocarbon Degradation by Nitrosomonas-Europaea - Cometabolic Inactivation of Ammonia Monooxygenase and Substrate-Specificity. Appl. Environ. Microbiol. 57(10): 2986-2994

Ratering S, Schnell S (2000) Localization of iron-reducing activity in paddy soil by profile studies. Biogeochemistry 48(3): 341-365

Reddy KR, Patrick WH, Lindau CW (1989) Nitrification-Denitrification at the Plant Root-Sediment Interface in Wetlands. Limnology and Oceanography 34(6): 1004-1013

Rickard D, Luther GW (2007) Chemistry of iron sulfides. Chem. Rev. 107(2): 514-562

Roden EE, Zachara JM (1996) Microbial reduction of crystalline iron(III) oxides: Influence of oxide surface area and potential for cell growth. Environmental Science & Technology 30(5): 1618-1628

Schwarzenbach RP, Gschwend PM, Imboden DM (1995) Environmental organic chemistry illustrative examples, problems, and case studies. John Wiley and Sons, Inc., New York

Seeberg-Elverfeldt J, Schluter M, Feseker T, Kolling M (2005) Rhizon sampling of porewaters near the sediment-water interface of aquatic systems. Limnology and Oceanography-Methods 3: 361-371

Shannon RD, White JR, Lawson JE, Gilmour BS (1996) Methane efflux from emergent vegetation in peatlands. Journal of Ecology 84(2): 239-246

Shields MS, Montgomery SO, Chapman PJ, Cuskey SM, Pritchard PH (1989a) Novel Pathway of Toluene Catabolism in the Trichloroethylene-Degrading Bacterium-G4. Appl. Environ. Microbiol. 55(6): 1624-1629

Shields MS, Montgomery SO, Cuskey SM, Chapman PJ (1989b) Toluene Degradation and Trichloroethylene Mineralization by an Environmental Isolate. Abstracts of Papers of the American Chemical Society 197: 19-MBTD

Singh H, Loffler FE, Fathepure BZ (2004) Aerobic biodegradation of vinyl chloride by a highly enriched mixed culture. Biodegradation 15(3): 197-204

Stucki G, Krebser U, Leisinger T (1983) Bacterial-Growth on 1,2-Dichloroethane. Experientia 39(11): 1271-1273

Taylor GJ, Crowder AA, Rodden R (1984) Formation and Morphology of an Iron Plaque on the Roots of Typha-Latifolia L Grown in Solution Culture. American Journal of Botany 71(5): 666-675

Teasdale PR, Batley GE, Apte SC, Webster IT (1995) Pore-Water Sampling with Sediment Peepers. Trac-Trends in Analytical Chemistry 14(6): 250-256

Thamdrup B (2000) Bacterial manganese and iron reduction in aquatic sediments. In: Advances in Microbial Ecology, Vol 16. Advances in Microbial Ecology. p 41-84

van der Nat F, Middelburg JJ (1998) Seasonal variation in methane oxidation by the rhizosphere of Phragmites australis and Scirpus lacustris. Aquat. Bot. 61(2): 95-110

Vandenbergh PA, Kunka BS (1988) Metabolism of Volatile Chlorinated Aliphatic-Hydrocarbons by Pseudomonas-Fluorescens. Appl. Environ. Microbiol. 54(10): 2578-2579

Vandenwijngaard AJ, Vanderkamp K, Vanderploeg J, Pries F, Kazemier B, Janssen DB (1992) Degradation of 1,2-Dichloroethane by Ancylobacter-Aquaticus and Other Facultative Methylotrophs. Appl. Environ. Microbiol. 58(3): 976-983

Vannelli T, Logan M, Arciero DM, Hooper AB (1990) Degradation of Halogenated Aliphatic-Compounds by the Ammonia-Oxidizing Bacterium Nitrosomonas-Europaea. Appl. Environ. Microbiol. 56(4): 1169-1171

Verce MF, Ulrich RL, Freedman DL (2000) Characterization of an isolate that uses vinyl chloride as a growth substrate under aerobic conditions. Appl. Environ. Microbiol. 66(8): 3535-3542

Verce MF, Ulrich RL, Freedman DL (2001) Transition from cometabolic to growth-linked biodegradation of vinyl chloride by a Pseudomonas sp isolated on ethene. Environmental Science & Technology 35(21): 4242-4251

Wackett LP, Gibson DT (1988) Degradation of Trichloroethylene by Toluene Dioxygenase in Whole-Cell Studies with Pseudomonas-Putida F1. Appl. Environ. Microbiol. 54(7): 1703-1708

Waldron JM (2007) Characterization of Chlorinated ethene Degradation in a Vertical Flow Constructed Wetlands. In: AFIT/GEM/ENV/07-M17. Graduate School of Engineering and Management. Air Force Institute of Technology (AU), Wright Patterson AFB OH.

Weber FJ, Vanberkel WJH, Hartmans S, Debont JAM (1992) Purification and Properties of the Nadh Reductase Component of Alkene Monooxygenase from Mycobacterium Strain-E3. Journal of Bacteriology 174(10): 3275-3281

Weiss JV, Emerson D, Megonigal JP (2004) Geochemical control of microbial Fe(III) reduction potential in wetlands: comparison of the rhizosphere to non-rhizosphere soil. Fems Microbiology Ecology 48(1): 89-100

Weiss JV, Emerson D, Megonigal JP (2005) Rhizosphere iron(III) deposition and reduction in a Juncus effusus L.-dominated wetland. Soil Science Society of America Journal 69(6): 1861-1870

Westermann P (1994) The Effect of Incubation-Temperature on Steady-State Concentrations of Hydrogen and Volatile Fatty-Acids During Anaerobic Degradation in Slurries from Wetland Sediments. Fems Microbiology Ecology 13(4): 295-302

Whalen SC (2005) Biogeochemistry of methane exchange between natural wetlands and the atmosphere. Environmental Engineering Science 22(1): 73-94

Wind T, Conrad R (1997) Localization of sulfate reduction in planted and unplanted rice field soil. Biogeochemistry 37(3): 253-278

Zylstra GJ, Wackett LP, Gibson DT (1989) Trichloroethylene Degradation by Escherichia-Coli Containing the Cloned Pseudomonas-Putida F1 Toluene Dioxygenase Genes. Appl. Environ. Microbiol. 55(12): 3162-3166

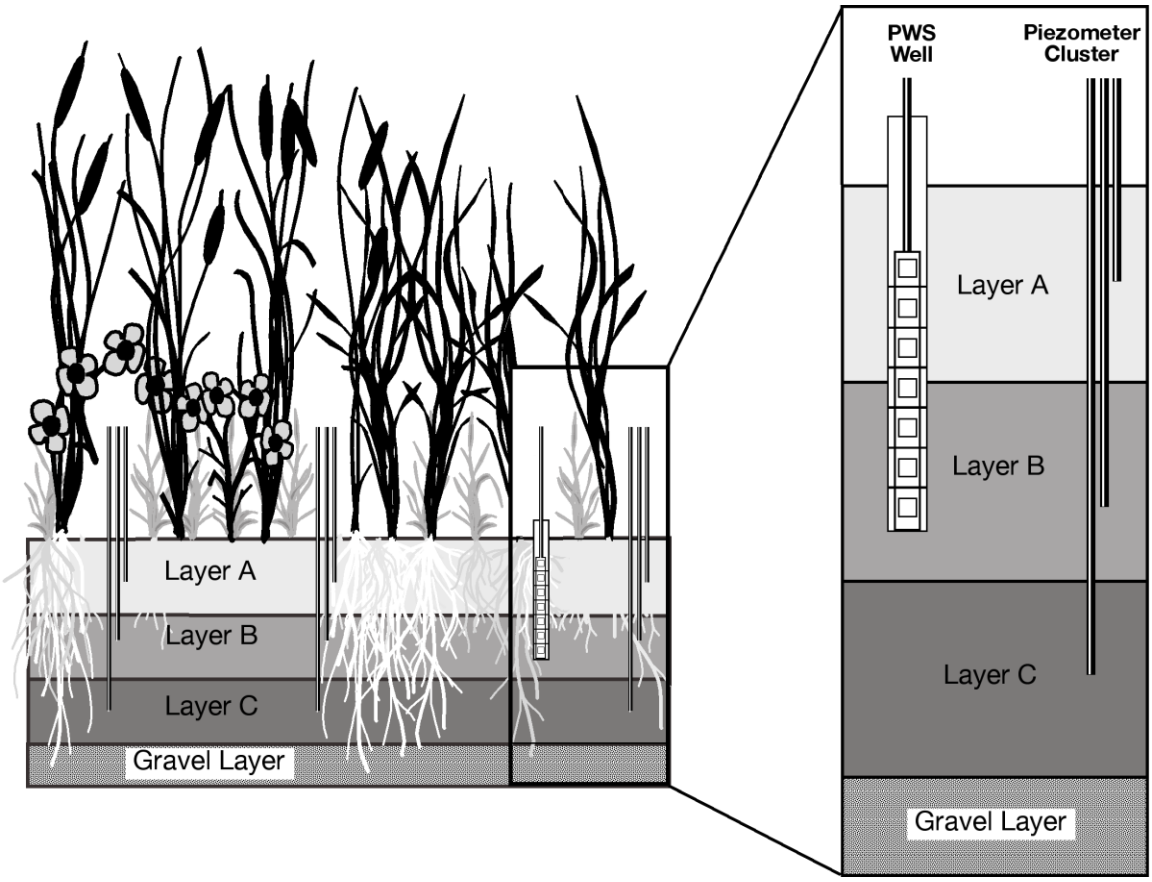

Figure 2.1 Cross-section view of the experimental wetland at WPAFB

Cross-section view of the vertical-flow experimental wetland at the Wright-Patterson Air Force Base, Ohio. The excavated pit was filled with a gravel layer (23 cm thick) at the bottom, and three layers of hydric soil, each 46 cm thick. The design details including its hydraulics is described elsewhere (Amon et al. 2007). The piezometer screens are positioned in each of the three layers, whereas the PWS assembly extends from ~80 to 20 cm below ground surface. Additional details are provided in section 2.2.1.

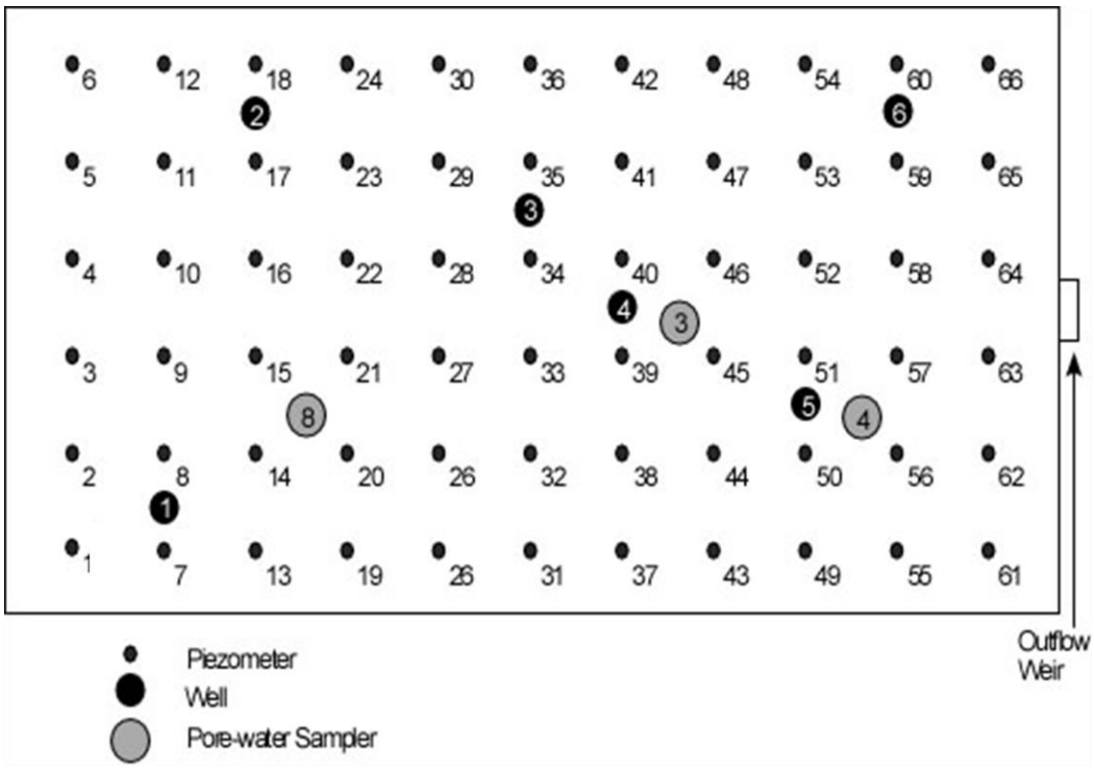

Figure 2.2 Schematic of pore water sampler locations at the WPAFB experimental wetland

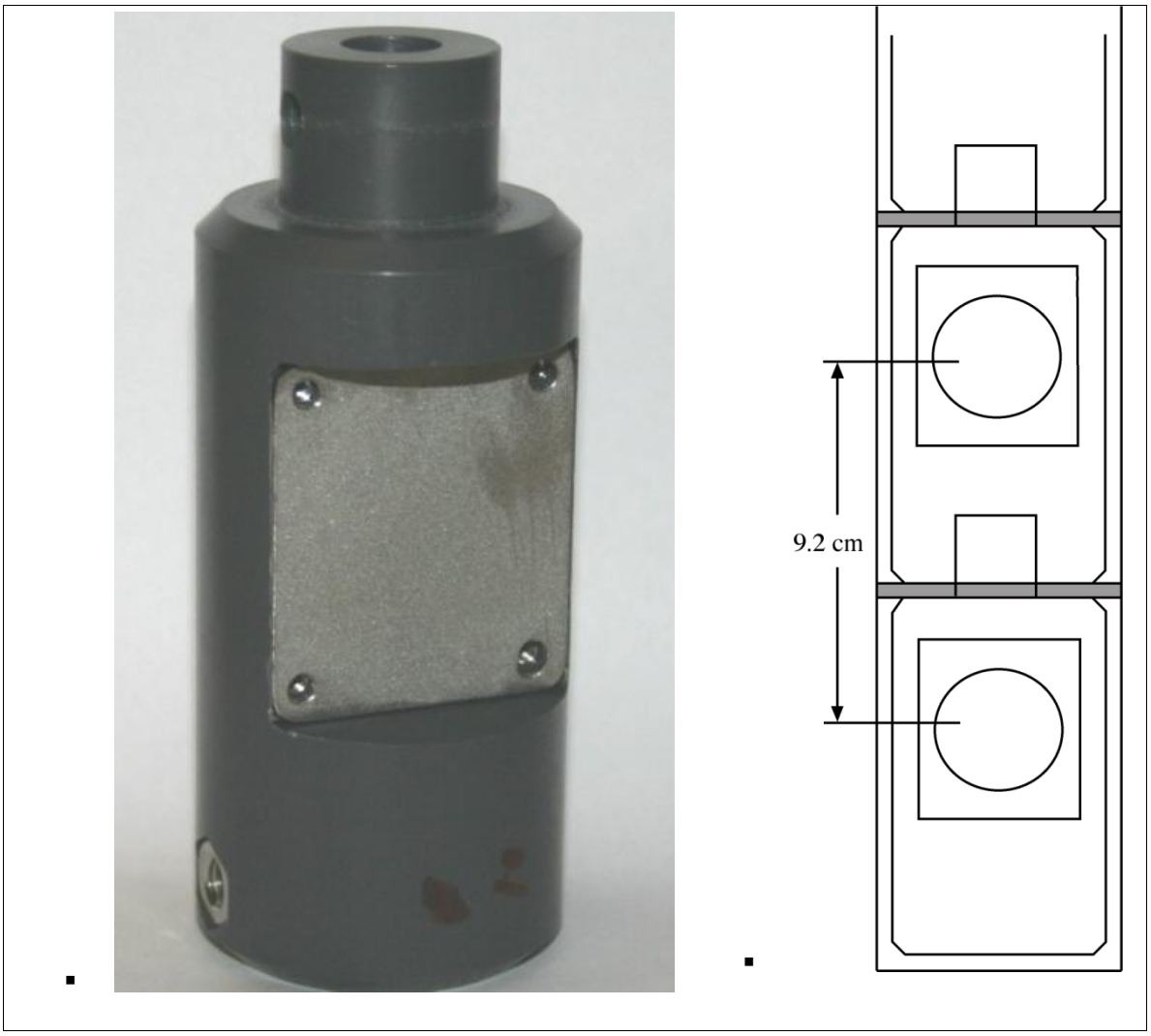

Figure 2.3 Pore water sampler schematic and photograph

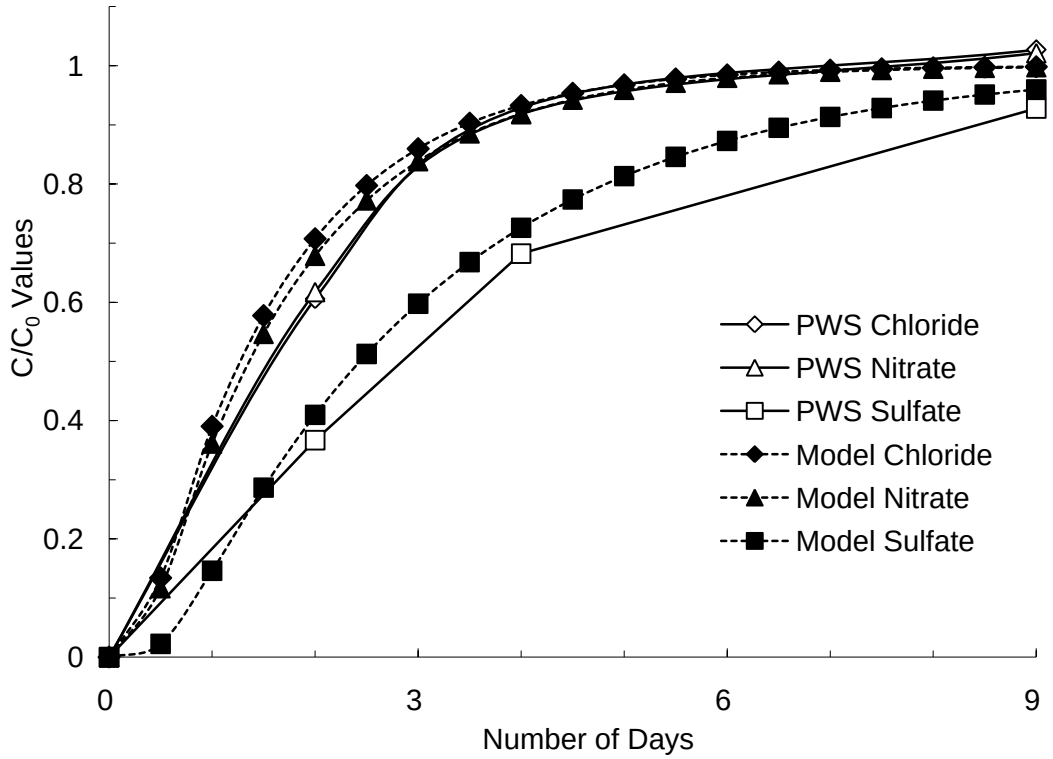

Figure 2.4 Predicted and measured normalized anion concentration for PWS.

Predicted (model) and measured normalized anion concentration (C/C_0) over time from both measurements and modeled values for PWS units. Modeled values were determined using D (cm^2/s), taken from the literature (D=1.06x10^{-5} for sulfate, D=2.03x10^{-5} for chloride, and D=1.90x10^{-5} for nitrate (Cussler 1984)). Measured values were determined using known concentrations of chloride, nitrate, and sulfate prepared in triplicate and samples taken from the PWS units several times over a period of 9 days.

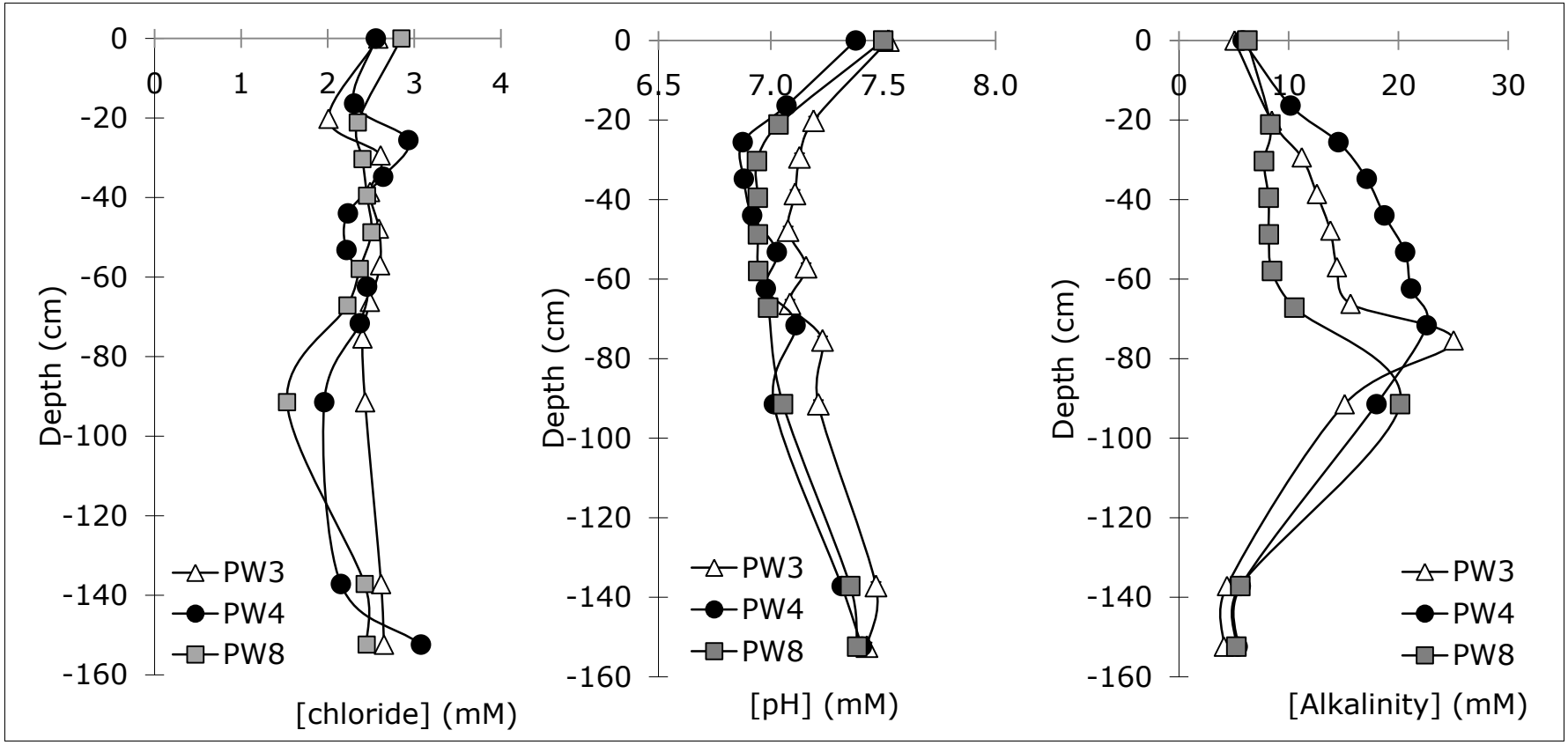

Figure 2.5 Variations in alkalinity, pH, and chloride ion at the WPAFB experimental wetland

Variations in alkalinity, pH, and chloride ion with depth in the treatment wetland averaged over the months May to September 2008 for three locations in the wetland (PW3, PW4, and PW8). The water samples for the analysis were collected as follows: (a) for 0-80 cm depth interval from pore-water samplers (#3, #4 and #8); and (b) for 80-140 cm depth interval, from piezometers (39, 46, 51, 57, 15, and 20). The reported values at lowest depth represent the water entering the wetland cell that was sampled at the pump house.

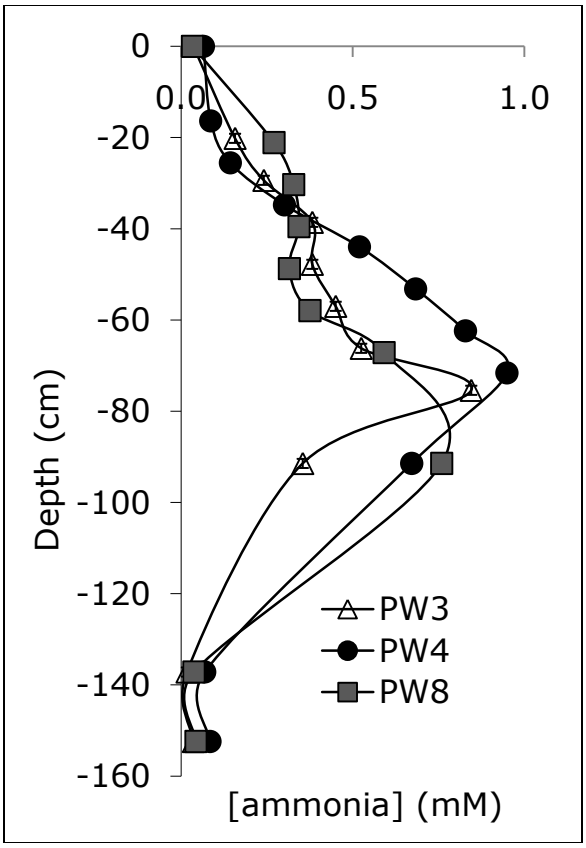

Figure 2.6 Variations in ammonia at the WPAFB experimental wetland

Variations in ammonia with depth in the treatment wetland averaged over the months May to September 2008 for three locations in the wetland (PW3, PW4, and PW8). The water samples for the analysis were collected as follows: (a) for 0-80 cm depth interval from pore-water samplers (#3, #4 and #8); and (b) for 80-140 cm depth interval, from piezometers (39, 46, 51, 57, 15, and 20). The reported values at lowest depth represent the water entering the wetland cell that was sampled at the pump house.

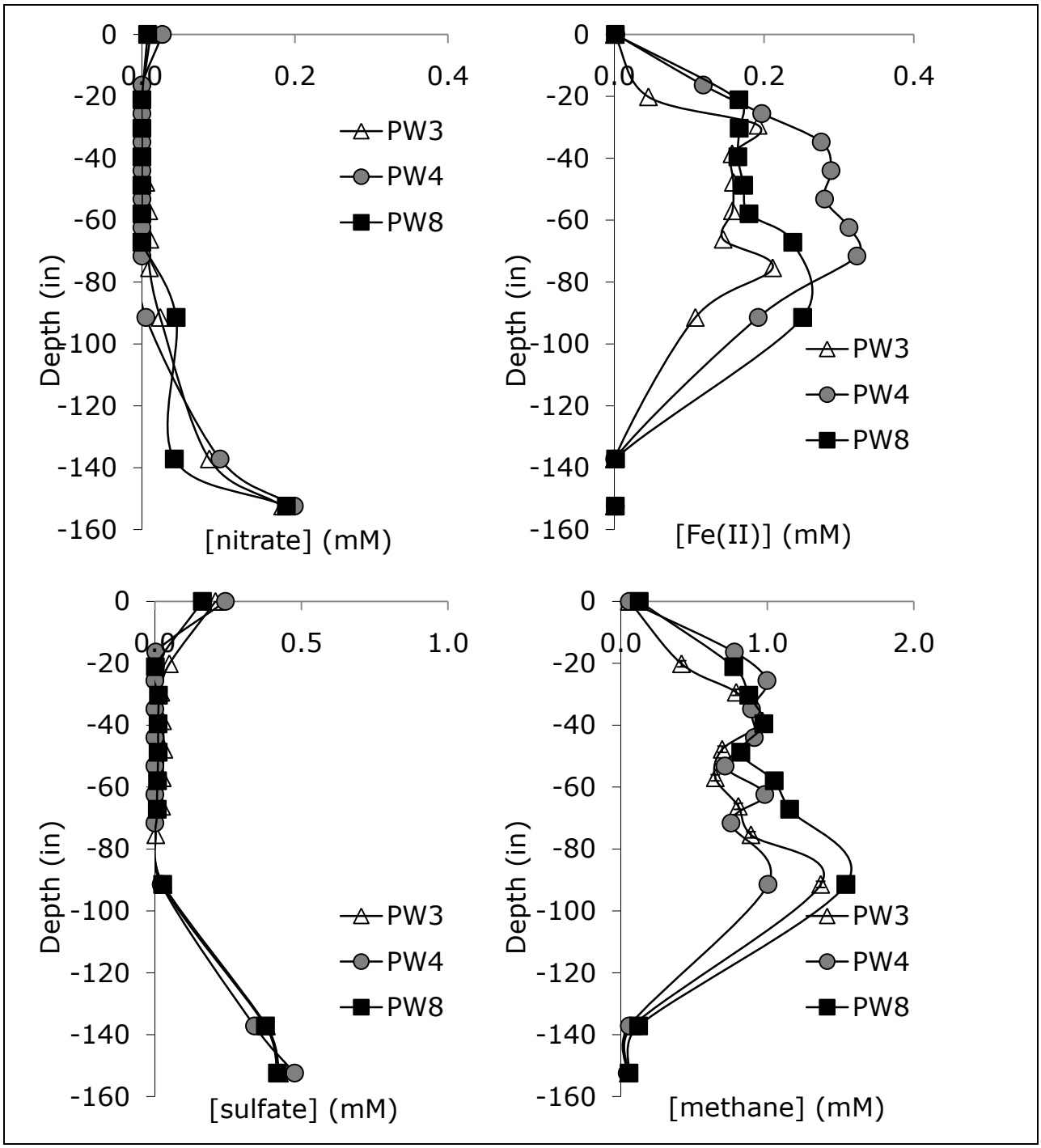

Figure 2.7 Variations in redox /TEAP species at the WPAFB experimental wetland

Variations in redox /TEAP species (mM) at 3 locations in the wetlands averaged over the months May to September 2008 for three locations in the wetland (PW3, PW4, and PW8). The water samples for the analysis were collected as follows: (a) for 0-80 cm depth interval from pore-water samplers (#3, #4 and #8); and (b) for 80-140 cm depth interval, from piezometers (39, 46, 51, 57, 15, and 20). The reported values at lowest depth represent the water entering the wetland cell that was sampled at the pump house.

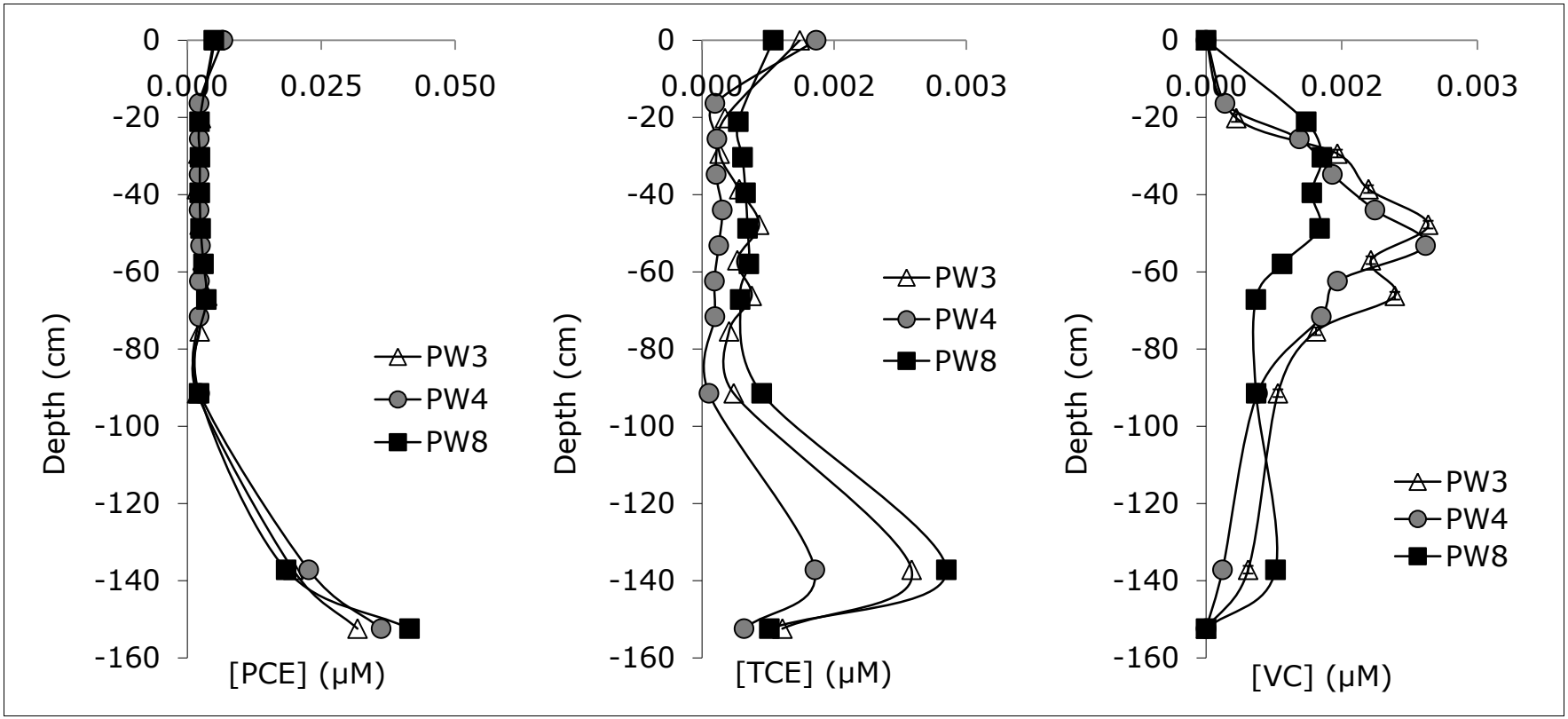

Figure 2.8 Variations in PCE, TCE, and VC at the WPAFB experimental wetland

Variations in perchloroethene (PCE) and its degradation products, trichloroethene (TCE) and vinyl chloride (VC) species (uM) at 3 locations (PW3, PW4, and PW8) in the treatment wetland showing sequential reductive dechlorination. The water samples for the analysis were collected as follows: (a) for 0-80 cm depth interval from pore-water samplers (#3, #4 and #8); and (b) for 80-140 cm depth interval, from piezometers (39, 46, 51, 57, 15, and 20). The reported values at lowest depth represent the water entering the wetland cell that was sampled at the pump house.

Table 2.1 PWS wells and sampling events.

PWS well information and sampling events for vertical profiles PW3, PW4, and PW8 For piezometer and PWS well locations see Figure 2.2

Well #	# PWS units	Range of Depths Below ground (cm)	Adjacent Peizmeter #s	Dates Sampled in 2008 (days in field)
3	7	20.2-75.4	39, 46	5/7 (27), 6/11 (33), 7/07 (21), 8/11 (31), 9/4 (14)
4	7	16.4-71.6	51, 57	5/13 (21), 6/23 (14), 7/14 (20), 8/13 (26), 9/11 (24)
8	6	21.1-67.2	15, 20	5/29 (27), 6/30 (20), 7/23 (24), 8/25 (24), 9/25 (27)

3 AEROBIC COMETABOLIC DEGRADATION OF TRICHLOROETHENE BY METHANE AND AMMONIA OXIDIZING MICROORGANISMS NATURALLY ASSOCIATED WITH *CAREX COMOSA* ROOTS

3.1 INTRODUCTION

Trichloroethene (TCE) is one of the most common groundwater contaminants, and it poses a threat to human health as a suspected carcinogen (ATSDR 1997). Natural attenuation of TCE has been examined as a possible remediation practice as it is more advantageous, both economically and environmentally, than conventional options such as pump-and-treat that are time and money intensive (Powers 1996; NRC 2000). However, natural attenuation of TCE is not always effective. In reducing environments, TCE biodegradation often leads to accumulation of less-chlorinated, more-toxic intermediate compounds, such as vinyl chloride. In comparison, oxidative biodegradation of TCE is more desirable because it allows for TCE mineralization to carbon dioxide (CO_2), a nontoxic end-product. For this to occur, environmental conditions favoring TCE cometabolism are required, including aerobic conditions as well as suitable microorganisms, and access to their growth substrates.

TCE can be degraded cometabolically by aerobic microorganisms that utilize a wide range of growth substrates, such as methane (Fogel et al. 1986; Little et al. 1988), toluene (Shim et al. 2001), phenol (Chen et al. 2004), ammonia (Kocamemi & Cecen 2007), and several others. In particular, methane as a growth substrate has been successfully studied in a number of systems using both mixed (Fogel et al. 1986) and pure cultures (Little et al. 1988). In cometabolic degradation of TCE with methane, the methane-oxidizing microorganism produce a non-specific enzyme, (methane

monooxygenase or MMO), that oxidizes methane as its substrate and can also fortuitously degrade TCE (Sullivan et al. 1998). In this process, TCE oxidation is initiated as an epoxidation reaction catalyzed by the MMO, with NADH as an immediate energy source (Chang & Alvarez-Cohen 1995). Similarly, ammonia can also serve as a growth substrate for cometabolic TCE degradation (Rasche et al. 1991; Moran & Hickey 1997; Yang et al. 1999), although it has not been studied as extensively as methane and such research has focused on laboratory studies mostly with pure cultures of *Nitrosomonas europaea*. The enzyme produced during ammonia oxidation, ammonia monooxygenase (AMO), can also degrade TCE cometabolically, but with limited success due possibly to inhibitory effects of TCE on ammonia oxidizers (Rasche et al. 1991; Yang et al. 1999).

The oxidative biodegradation of chlorinated ethenes with plant roots has been investigated at bench scale (Bankston et al. 2002; Tawney et al. 2008). Further, TCE biodegradation by the oxidative pathway has been suggested at the shallow depths of an experimental wetland, particularly due to the presence of wetland plant roots (Amon et al. 2007). The root zone of wetland plants can provide the appropriate conditions to support certain oxidizing microorganisms (King 1996). Oxygen is transported from the shoot to the root tissues of wetland plants for metabolic purposes, and a portion of that can diffuse out into the plant rhizosphere and the immediate soil environments (Armstrong et al. 2000; Colmer 2003). The specific aerobic microbial communities that inhabit the microaerobic environment in plant rhizosphere can oxidize methane (King 1996) and ammonia (Reddy et al. 1989), which are produced in the surrounding anaerobic soil and migrate toward plant roots (Bosse & Frenzel 1997). In microcosms planted with rice,

approximately 90% of methane oxidation has been reported at a depth where roots were the only source of oxygen (Bosse and Frenzel 1997), and a significantly greater number of methane-oxidizing microorganisms in the soil immediately around roots (within 0.1 to 0.2 mm) than in the soil farther away from the roots. Similarly, the nitrification activities (i.e., ammonia oxidation) in rice plants decreased with increasing distance from the root zone, and they were positively correlated with the ammonia-oxidizing bacteria abundance (Li et al. 2007).

The main objective of this investigation was to provide a proof-of-concept that oxidative TCE degradation can be facilitated by the methane- and ammonia-oxidizing microorganisms that are naturally associated with wetland plant roots by cometabolic pathways. Recent studies have indicated that microbial processes can facilitate removal of chlorinated hydrocarbons in vegetated wetland settings (Amon et al. 2007; Imfeld et al. 2008). Prior to this, studies of chlorinated hydrocarbon degradation with wetland soils by reductive dehalogenation processes have been studied (Lorah & Olsen 1999; Kassenga et al. 2004; Lorah & Voytek 2004). Other studies have examined degradation of chlorinated hydrocarbons in soil/aquatic systems assisted by plants, including by rhizodegradation (Nzengung & Jeffers 2001; James et al. 2009), phytovolatilization (Bankston et al. 2002; Imfeld et al. 2009), and uptake and biotransformation, i.e., metabolic degradation within plant tissues (Newman et al. 1997; Nzengung & Jeffers 2001; Wang et al. 2004). While the studies describing the role of microbial processes in plant rhizosphere in chlorinated hydrocarbon degradation are limited (Bankston et al. 2002; Tawney et al. 2008), the synergistic activity of the plant-microbe system in the

wetland in the removal of organic chemical removal has increasingly been recognized (Imfeld et al. 2009).

In the present study, the role of naturally occurring methane- and ammonia-oxidizing microbes associated with plant roots in oxidative cometabolic TCE degradation has been examined. This is the first study to our knowledge that provides direct evidence for a mechanism of microbial TCE degradation with plant roots by studying the roots themselves. Bench-scale microcosm experiments were performed using soil-free roots from the wetland plant species *Carex comosa* (longhaired sedge). Live plants were not used to eliminate plant effects, such as uptake and volatilization, and to study the activity of bacteria directly associated with the roots. Methane and ammonia were evaluated as growth substrates for their role in TCE degradation by aerobic cometabolism since these compounds are often abundantly produced in anaerobic wetland soil. We expected to investigate the activities of root-associated methane- and ammonia-oxidizing microorganisms by measuring substrate and product concentrations over time when growth media was added to the microcosms. After the enrichment period, we also expected that the root-associated methane and ammonia oxidizers will demonstrate the ability to degrade TCE though aerobic cometabolism in the presence of methane and ammonia substrates, respectively. This approach enabled us to evaluate the potential of cometabolic TCE degradation by methane and ammonia oxidizers associated with wetland plant roots.

3.2 MATERIALS AND METHODS

3.2.1 Collection of wetland plants

Wetland plants (*Carex comosa)* were collected from a natural wetland located in Dayton, OH (USA) in September 2008. After collection, the plants were placed in individual pots containing a 50:50 mix of peat moss and wetland soil, and maintained in a university greenhouse until use (~25-40 weeks). In order to prepare for the bench-scale microcosm experiments described below, the roots from individual *Carex comosa* specimens were clipped, separated from the plant shoot, and washed with de-ionized water thoroughly to remove attached soil. The entire root was used so as to include the root tip, lateral root and primary root.

3.2.2 Growth media

Mineral media were prepared separately for methane and ammonia oxidizers for their optimal growth. The methane-oxidizing microorganisms associated naturally with plant roots were enriched with growth medium 'A' (Fogel et al. 1986) containing 200 mg $MgSO_4 \cdot 7H_2O$, 20 mg $CaCl_2 \cdot 2H_2O$, 1,000 mg $NaNO_3$, 3 mg $FeSO_4 \cdot 7H_2O$, 40 mg KCl, 160 mg KH_2PO_4, 184 mg Na_2HPO_4, 0.07 mg $ZnSO_4 \cdot 7H_2O$, 0.02 mg $MnCl_2 \cdot 4H_2O$, 0.02 mg H_3BO_4, 0.1 mg $CoCl_2 \cdot 6H_2O$, 0.01 mg $CuC1_2$, 0.02 mg $NiCl_2 \cdot 6H_2O$ and 0.03 mg $Na_2MoO_4 \cdot 2H_2O$ dissolved in 1 L of de-ionized water (final pH 6.8) (addition of methane described below). Ammonia-oxidizing microorganisms naturally-associated with plant roots were enriched with growth medium 'B' containing 94 mg $(NH_4)_2SO_4$, 400 mg $NaHCO_3$, 100 mg $MgSO_4$, 50 mg KH_2PO_4, 445 mg $Na_2HPO_4 \cdot 12H_2O$, 30 mg KCl, 50 mg $CaCl_2 \cdot 2H_2O$, 3 mg $FeSO_4 \cdot 7H_2O$, 0.02 mg $MnCl_2$, 0.7 mg $ZnSO_4 \cdot H_2O$, 0.02 mg H_3BO_4,

0.01 mg $CuCl_2$, 0.03 mg $Na_2MoO_4 \cdot 2H_2O$, 0.02 mg $NiCl_2 \cdot 6H_2O$, 0.1 mg $CoCl_2 \cdot 6H_2O$ dissolved in 1 L of de-ionized water (final pH 7.8).

3.2.3 Experimental design

3.2.3.1 Microbial enrichment with methane and ammonia (in absence of TCE)

Six microcosms (160 mL borosilcate glass serum bottles; Wheaton, Millville, NJ) were used for the subset of experiments with methane as a substrate. Three bottles were prepared as live microcosms with 1 g of fresh roots and 100 mL of growth medium A, and the three remaining bottles were prepared as killed controls with 1 g of fresh roots, 100 mL of growth medium A, and 6.24 mg L^{-1} of sodium azide to inhibit gram-negative bacterial growth, including the growth of methane-oxidizing bacteria (Ginestet et al. 1998). After these additions, a headspace of 60 mL remained in each microcosm. All microcosms were bubbled with air for ~30 min to start the experiment with enough dissolved oxygen to maintain aerobic conditions. The microcosms were then capped with Teflon-lined grey butyl rubber stoppers (20 mm dia.; Wheaton, Millville, NJ) and sealed with aluminum crimps (Wheaton, Millville, NJ). Pure gaseous methane (CH_4) (5.25 mL, equivalent to 1.9 mg L^{-1} aqueous CH_4) were injected into each bottle using a gas-tight glass syringe (Hamilton, Reno, NV). The bottles were then wrapped in aluminum foil and placed on a rotary shaker (Glas-Col, Terre Haute, IN) at 30 rpm for gentle horizontal mixing in an upside down position at 22±1 °C.

There were four cycles of microbial enrichment with methane (called, EM1 through EM4) as a substrate over an 18-day period, where each cycle corresponding to a period during which methane degraded nearly completely in the live microcosms, and

needed to be replenished. At the end of each cycle, all microcosms were opened to carefully discard the aqueous growth medium without removing the roots and replaced with 100 mL of fresh growth medium (killed controls were amended with 6.24 mg L^{-1} of sodium azide), bubbled with air, sealed and wrapped in aluminium foil as described earlier. The new cycle began by amending the microcosms with gaseous CH_4 (aqueous CH_4 = 1.9 mg L^{-1}), followed by their incubation on the rotary shaker. Six additional microcosms were set up (3 live and 3 killed controls) with ammonia as substrate with an experimental design similar to the microcosms set up with methane as the substrate (described above), but with the following variations: (a) growth medium 'B' was used, containing 20 mg L^{-1} of N-ammonium (NH_4^+), (b) CH_4 was not added, (c) 10 mg L^{-1} of allylthiourea was used in the killed control microcosms (instead of sodium azide) to inhibit the growth of ammonia-oxidizers, and (d) 3 microbial enrichment cycles (called, AE1 through AE3) were completed during a 32-day period.

3.2.3.2 Cometabolic TCE degradation with methane and ammonia substrates

Following the 4 cycles of microbial enrichment with methane (described above), 4 additional cycles (TM1 through TM4) were completed in the triplicate microcosms with methane under identical experimental conditions, but with 150 µg L^{-1} of TCE added. Similarly, following the 3 cycles of microbial enrichment with ammonia (described above), 2 additional cycles (TA1 and TA2) were completed in the triplicate microcosms with ammonia under identical experimental conditions, but with 150 µg L^{-1} of TCE added. A number of cycles equal to both sets of live microcosms were completed for the killed control microcosms.

3.2.4 Analysis

The following analyses were performed to determine the activity of methane- and ammonia-oxidizing microorganisms associated with roots in the microcosms. In microcosms with methane and TCE amendments, concentrations of CH_4, dissolved oxygen (DO), dissolved inorganic carbon (DIC), and TCE were measured daily in each cycle. Similarly, in the microcosms with ammonia and TCE amendments, [NH_4^+], [NO_2^-], [NO_3^-], DO, and [TCE] were measured daily in each cycle. Aqueous samples were processed through 0.22 µm, 25 mm dia. syringe filters (Restek, Bellefonte, PA) before analysis; NO_2^- and NO_3^- were quantified by ion chromatography (IC) (DX2500, Dionex Corporation, Sunnyvale, CA), and NH_4^+ was quantified by the salicylate method (Hach Company, Loveland, Co) using a spectrophometer (Lambda 45 UV/Vis, Perkin Elmer; Waltham, MA). The measurements of NO_2^- and NO_3^- were combined and it is referred henceforth as NOx. The pH measurements were made using a meter (AP10 pH/mV/temp, Denver Instrument, Bohemia, NY) by collecting 2-2.5 mL aqueous samples from each of the methane and ammonia microcosms, after gas sampling on day 1 and day 5 of each cycle. Headspace samples from the microcosms were analyzed by gas chromatography to estimate aqueous phase [CH_4], DO, and [DIC] and [TCE] in each microcosm. CH_4 and TCE were analyzed by a HP 6890 series GC system with flame ionization (FID) and electron capture (ECD) detectors; CH_4 was separated on a capillary column (GS GasPro, 30m x 0.32mm; J&W Scientific) connected to an FID, and TCE was separated on a capillary column (HP-624, 30m x 0.32mm; Agilent Technologies), connected to an ECD. O_2 and CO_2 were analyzed by a HP 5890 series GC system with a thermal conductivity

detector (TCD), and separated on a packed column (Shin Carbon 100/120, 2m x 1mm; Restek, Belefonte, PA) (see Appendix B.2).

The aqueous [CH_4] and [TCE] at equilibrium were calculated by the Gas law and Henry's law using a published approach (Burris et al. 1996). Based on measured partial pressures of O_2 and CO_2 in the microcosm headspace, the dissolved [O_2] or DO was calculated using Henry's Law (Lide & Frederikse 1995), and [dissolved inorganic carbon] or DIC was calculated using Henry's Law and carbonate system equilibrium relationships at the measured pH (Pankow 1991). Detailed calculation approaches are available in the Appendix B.2.

3.2.5 Data treatment and statistical analysis

For each of the TCE cycles for methane and ammonia microcosms, the initial TCE degradation rates and consumption/production rates of solutes (i.e., CH_4, DO, DIC, NH_4^+, and NOx) were calculated using the difference between their respective measured values on day 2 subtracted from their measured values on day 1 for each treatment (with the exception of the second TCE cycle with ammonia, which was from day 0 to day 5). The initial rates were taken as day 1 to day 2, rather than day 0 to day 1, to avoid the data analysis during transient conditions caused by microcosm reset prior to each cycle. Similarly, TCE was not analyzed on the day it was injected in the microcosms, (i.e., day 0), to allow for a 24 hr equilibration of TCE between the liquid and headspace. Transformation yield (T_y) was calculated for the 4 TCE cycles with methane by subtracting the average loss in TCE and methane found in the killed controls from the live microcosm and then dividing TCE mass degraded by methane mass degraded.

For the methane- or ammonia-oxidizing microorganisms, the statistical differences in their treatments (i.e., control vs. live microcosms) were determined for each solute using a one-way repeated analysis of variance (RM ANOVA) with time as the repeated factor. If the differences between the live and control microcosms were found to be statistically significant, the Tukey post hoc tests were performed to determine the differences between control and live treatments for each time point. For the solute consumption/production rates of each cycle, the effects of treatments were examined using a one-way RM ANOVA and Tukey post hoc tests. As necessary, the data were log-transformed before statistical analysis to fit the assumption of homoscedasticity. Statistical analyses were performed using Statistica 9^{TM} (Statsoft, Tulsa, OK, USA).

3.3 RESULTS AND DISCUSSION

3.3.1 Association of methane and ammonia oxidizers with Carex comosa roots

Comparisons of live and killed microcosms amended with soil-free roots indicates that the increase in substrate metabolism was likely due to increase in population size of methane and ammonia oxidizers associated with the plant roots in their respective enrichment cycles. During the four enrichment cycles with methane (ME1 through ME4), [CH_4] and [DO] were significantly lower and [DIC] was significantly higher in the live microcosms compared to the controls through time (one-way RM ANOVAs, treatment effect, time effect, P<0.05, Figure 3.1). Likewise, during the three cycles of microbial enrichment with ammonia (AE1 through AE3), [NH_4^+] were significantly lower in the live microcosm compared to the controls through time (one-way RM ANOVAs, treatment effect, time effect, P<0.01, Figure 3.2). Further, [DO] were significantly lower and [NOx] were significantly higher in the live microcosms in

comparison to the controls for the ammonia system, but their statistical significance was not consistent between the cycles (See the Appendix B.2). The approach to replace the growth medium at the end of each cycle discarded the microorganisms growing in suspended form and favored the enrichment of microorganisms that were growing on the root surface and perhaps also inhabiting the interior of root tissues (Bosse & Frenzel 1997).

Comparison of results during enrichment cycles after initial set-up (ME1 vs. AE1) indicate that significant methane oxidation was observed quicker in comparison to ammonia oxidation in the live microcosms. This may be due to higher initial population of methane oxidizers associated with the roots that allowed them to become dominant over heterotrophic microorganisms more quickly, in comparison to ammonia oxidizers. Methane oxidizers are generally adaptable to a wide range of environmental conditions (Hanson & Hanson 1996). In ME1, oxygen and methane levels concomitantly decreased in the microcosms on day 4, indicating activity of methane oxidizers. By comparison, in AE1, the initial decrease in oxygen occurred without concomitant ammonia degradation in both control and live microcosms until day 14, suggesting initial oxygen uptake may have been due to heterotrophic activity. It appears that either the initial population of ammonia oxidizers in the root samples was low, or the ammonia oxidizers had physiological limitations requiring a longer enrichment period compared to methane oxidizers. Indeed, ammonia oxidizers are relatively slow growing organisms (Vaccari et al. 2006) and methane oxidizers are ubiquitous with consumption rates depending on ambient methane concentration (Rogers & Williams 1991).

During enrichment cycles, the initial methane degradation and oxygen consumption rates ($d[CH_4]/dt$ and $d[DO]/dt$) increased from cycle ME1 to cycle ME3,

and then decreased slightly or stabilized in cycle ME4, whereas initial DIC production rates (d[DIC]/dt) were significantly different between treatments but not with time (one-way RM ANOVAs, treatment effect, $P<0.001$, and cycle effect, $P>0.05$; Table S1 in Appendix B.2). In comparison, the initial ammonia degradation and NOx production rates ($d[NH_4^+]/dt$ and d[NOx]/dt) increased rapidly from cycle AE1 to AE3, whereas initial oxygen consumption rates did not show the same trend (one-way RM ANOVAs, treatment effect, cycle effect, $P<0.01$; Table B.1 in Appendix B.2).

The investigation demonstrated quite clearly that methane and ammonia oxidizers are associated with the roots of *Carex comosa*, a phenomenon that may be common among various wetland plants, which is consistent with the similar observations in other plant species (Bosse & Frenzel 1997; Li et al. 2007). A sustained degradation of methane and ammonia through the enrichment cycles in this study showed that wetland plant roots can provide a favorable environment for the growth of methane- and ammonia-oxidizing microorganisms. Wetland plants can overcome anaerobic environments by transporting oxygen from the atmosphere to their roots via the aerenchyma tissue (Armstrong et al. 2000; Colmer 2003). During this process, some oxygen typically leaks from the roots into the surrounding soil (i.e. rhizosphere), an otherwise anaerobic environment, creating a microaerobic niche suitable for growth of methane and ammonia oxidizers (Vaccari et al. 2006). The primary electron donors (methane and ammonia) for these organisms are produced in the anaerobic zone of wetland soils (Neill 1995; Chanton et al. 1997) and diffuse into the rhizosphere (Reddy et al. 1989; King 1996), and the juxtaposition of anaerobic and microaerobic environments can create an ideal niche for microorganisms that can cometabolize TCE.

3.3.2 TCE degradation potential by root-associated methane and ammonia oxidizers

The main objective of this study was to evaluate the TCE degradation potential of methane and ammonia oxidizers associated with *Carex comosa* roots. In experiments with methane, [TCE] were significantly lower in the live microcosms compared to the killed controls through time in four TCE cycles with methane, TM1 through TM4 (one-way RM ANOVAs, treatment effect, time effect, $P<0.05$, Figure 3.3). Also, during these cycles, [CH_4] and [DO] were significantly lower and [DIC] significantly higher in the live microcosms compared to the controls through time (one-way RM ANOVAs, treatment effect, time effect, $P<0.05$, Figure 3.3). Further, in experiments with ammonia, [TCE], [NH_4^+], and [DO] were significantly lower and [NOx] were significantly higher in the live microcosms compared to the killed controls through time in cycle TA1 (one-way RM ANOVAs, treatment effect, time effect, $P<0.05$, Figure 3.4). In cycle TA2, [TCE] were not significantly different in the live microcosms compared to the controls (one-way RM ANOVA, treatment effect, time effect, $P>0.05$, Figure 3.4). However, for other analytes, significant differences were observed in [NH_4^+] between time and treatments (one-way RM ANOVA, treatment effect, time effect, $P<0.01$, Figure 3.4), [NOx] between treatments (one-way RM ANOVA, treatment effect, $P<0.05$, Figure 3.4) on two days (day 13 and day 17), and [DO] with time (one-way RM ANOVAs, time effect, $P<0.01$, Figure 3.4). The DO did not exhibit a treatment effect (i.e., no significant differences between live microcosms and killed controls).

The results presented here have partially validated our initial hypothesis that root-associated methane and ammonia oxidizers have the ability to degrade TCE though aerobic cometabolic processes. Methane oxidizers were found to significantly

cometabolize TCE, whereas the activity of ammonia oxidizers stalled soon after their exposure to TCE. This result is consistent with an earlier study (Bankston et al. 2002) that showed simultaneous TCE and methane degradation in microcosms containing soil from broad-leaf cattail roots. By using soil-free roots, this study provided a better understanding of the role of root-associated microorganisms in TCE degradation.

In this study, the average net TCE loss between live and control microcosms was ~40% for each TCE cycle of methane experiment. This is consistent with previous studies that demonstrated cometabolic TCE degradation with methane in bench-scale systems (Fogel et al. 1986; Little et al. 1988; Shukla et al. 2009). In a comparable study, a mixed culture obtained from sediment enriched for several weeks with 18% methane headspace demonstrated TCE degradation was 90% at initial [TCE] at 80 μg L^{-1} (Fogel et al. 1986). Another study with higher initial [TCE] and less methane (400 μg L^{-1} TCE, and 8% headspace, respectively) found 40% loss in TCE due to degradation after 10 days using a pure culture enriched from well water (Little et al. 1988). A direct comparison of our TCE removal rates with other studies is not particularly informative because rates depend on experimental parameters such as initial [TCE] and [CH_4], and microbial biomass. In the present study, d[CH_4]/dt shows a declining trend on days 2-4 of cycles TM3 and TM4 and pseudo first-order like kinetics, thus suggesting methane oxidation to become somewhat limited in later part of the cycles.

The average T_y for TM1 through TM4 cycles were 2.8, 3.6, 2.9 and 2.1 TCE (μg) CH_4^{-1} (mg) respectively. This is less than those reported for a variety of cultures, ranging from 15 to 50 μg TCE mg CH_4^{-1} (Alvarez-Cohen & Speitel 2001), possibly due to lower initial [TCE] in this study, and the potential for less efficient methane utilization at lower

[TCE] (Chang & Criddle 1997). However, with an initial [TCE] of 150 μg L^{-1} and methane at 9% headspace used in the present study, a significant amount of TCE was degraded in the system with soil-free roots. Initial rates for CH_4, TCE and DO loss, and DIC production (d[C]/dt) were significantly different between treatments (one-way RM ANOVAs, treatment effect, $P<0.05$, see Table 3.1) during all four TM cycles. CH_4 and TCE degradation rates were also significantly different between cycles (one-way RM ANOVAs, cycle effect, $P<0.05$, Table 3.1) with the rates increasing from cycle TM1 to cycle TM3, and then remaining constant from cycle TM3 to cycle TM4, which suggests a lack of significant epoxide toxicity development during TM cycles (Ely et al. 1995; Hyman et al. 1995; Kocamemi & Cecen 2007).

The potential for cometabolic oxidation of TCE by ammonia oxidizers was not statistically significant because initial degradation was followed quickly by inhibition of both ammonia and TCE degradation under the experimental conditions. Several investigations have shown oxidative cometabolic TCE degradation using mixed nitrifying cultures (Yang et al. 1999; Kocamemi & Cecen 2005). In the present study, approximately 15% of initial [TCE] (150 μg L^{-1}) degraded in 2 days in live microcosms compared to the killed controls before complete inhibition of the system. In comparison, Yang et al. (1999) showed TCE cometabolism by a nitrifying culture enriched from a sewage treatment plant at initial [TCE] were between 125 and 200 μg L^{-1}, while higher initial TCE levels (>200 μg L^{-1}) induced inhibition of ammonium oxidation. Kocamemi and Cecen (2005) provided evidence for ammonia oxidation at a high initial [TCE] (4500 μg L^{-1}), and showed 68% ammonia removal in comparison to controls. The differences between the results of the

present investigation and those of Yang et al. (1999) and Kocamemi and Cecen (2005) may be attributed to differences in nitrifying strains.

The initial TCE degradation rates (d[TCE]/dt) during cycles TA1 and TA2 provide evidence of toxicity as no TCE degradation was observed in cycle TA2. The initial rates of [TCE], [NH_4^+] and [DO] loss, and [NOx] production were not significantly different between treatments or with cycles (one-way RM ANOVAs, treatment effect, cycle effect, $P>0.05$, Table 3.1). The inhibitory effect of TCE on ammonia oxidation has been attributed to two potential mechanisms: (a) AMO affinity for TCE may be equivalent (Hyman et al. 1995) or greater (Ely et al. 1995) in comparison to its affinity for ammonia, and (b) exposure of ammonia oxidizers to TCE (Kocamemi & Cecen 2005) or TCE epoxide (a cometabolism byproduct) (Rasche et al. 1991) may cause substantial cellular injury and AMO inhibition. The specific mechanism of AMO inhibition in the present study is unclear, yet there was evidence of toxicity in the precipitous decrease in ammonia oxidation rate that immediately followed TCE addition (compare d[NH_4^+]/dt in cycle AE2 vs. cycle TA1). It is possible that toxic TCE epoxide induced significant damages to the enzyme system. After exposure to TCE, nitrifying cells are often slow to recover and show low rates of ammonia-oxidizing activity (Hyman et al. 1995). In this study, the root-associated ammonia oxidation did not recover or regained their activity. A longer enrichment period with greater initial [NH_4^+] may have been helpful in developing larger biomass in withstanding toxic exposure. In summary, TCE cometabolism by methane oxidizers was clearly more effective than by ammonia oxidizers within the same initial root-associated microbial community under similar experimental conditions.

3.3.3 Conclusions

This bench-scale investigation clearly demonstrated that methane and ammonia oxidation can be facilitated by the naturally-occurring microorganisms that are associated with wetland plant (*Carex comosa*) roots. Methane oxidation developed faster than ammonia oxidation during the enrichment period, possibly due to greater initial population of methane oxidizers with the roots or their ability to better compete with other (heterotrophic) microorganisms. Methane oxidizers demonstrated significant TCE degradation reproducibly. For a shorter enrichment period (2 weeks), methane oxidizers were effective in TCE degradation at bench scale without an inhibitory effect due to TCE degradation on methane oxidation. However, a rapid and complete inhibition of ammonia oxidation was observed under similar experimental conditions in the nitrifying system. Such inhibition of ammonia oxidation may be attributed to a greater sensitivity of ammonia oxidizers towards TCE or its degradation product (TCE epoxide). Follow-up studies may include the role of TCE and substrate levels (methane and ammonia) on TCE degradation and toxicity will be determined. The results presented here provides key evidence for oxidative cometabolic TCE degradation in vegetated wetlands that has direct implications for the natural attenuation of TCE in impacted aquatic environments.

3.4 REFERENCES

Alvarez-Cohen L, Speitel GE (2001) Kinetics of aerobic cometabolism of chlorinated solvents. Biodegradation 12(2): 105-126

Amon JP, Agrawal A, Shelley ML, Opperman BC, Enright MP, Clemmer ND, Slusser T, Lach J, Sobolewski T, Gruner W, Entingh AC (2007) Development of a wetland

constructed for the treatment of groundwater contaminated by chlorinated ethenes. Ecol. Eng. 30(1): 51-66

Armstrong W, Cousins D, Armstrong J, Turner DW, Beckett PM (2000) Oxygen distribution in wetland plant roots and permeability barriers to gas-exchange with the rhizosphere: a microelectrode and modelling study with Phragmites australis. Annals of Botany 86(3): 687-703

ATSDR AfTSaDR (1997) Toxicological Profile for Trichloroethylene (Update). Atlanta, GA.

Bankston JL, Sola DL, Komor AT, Dwyer DF (2002) Degradation of trichloroethylene in wetland microcosms containing broad-leaved cattail and eastern cottonwood. Water Res. 36(6): 1539-1546

Bosse U, Frenzel P (1997) Activity and distribution of methane-oxidizing bacteria in flooded rice soil microcosms and in rice plants (Oryza sativa). Appl. Environ. Microbiol. 63(4): 1199-1207

Burris DR, Delcomyn CA, Smith MH, Roberts AL (1996) Reductive dechlorination of tetrachloroethylene and trichloroethylene catalyzed by vitamin B-12 in homogeneous and heterogeneous systems. Environmental Science & Technology 30(10): 3047-3052

Chang HL, Alvarez-Cohen L (1995) Transformation Capacities of Chlorinated Organics by Mixed Cultures Enriched on Methane, Propane, Toluene, or Phenol. Biotechnology and Bioengineering 45(5): 440-449

Chang WK, Criddle CS (1997) Experimental evaluation of a model for cometabolism: Prediction of simultaneous degradation of trichloroethylene and methane by a methanotrophic mixed culture. Biotechnology and Bioengineering 56(5): 492-501

Chanton J, Whiting G, Blair N, Lindau C, Bollich P (1997) Methane Emission from Rice; Stable Isotopes, Diurnal Variations, and CO2 Exchange. Global Biogeochem. Cy. 11: 15-27

Chen WM, Chang JS, Wu CH, Chang SC (2004) Characterization of phenol and trichloroethene degradation by the rhizobium Ralstonia taiwanensis. Research in Microbiology 155(8): 672-680

Colmer TD (2003) Aerenchyma and an inducible barrier to radial oxygen loss facilitate root aeration in upland, paddy and deep-water rice (Oryza sativa L.). Annals of Botany 91(2): 301-309

Ely RL, Williamson KJ, Guenther RB, Hyman MR, Arp DJ (1995) A Cometabolic Kinetics Model Incorporating Enzyme-Inhibition, Inactivation, and Recovery .1. Model Development, Analysis, and Testing. Biotechnology and Bioengineering 46(3): 218-231

Fogel MM, Taddeo AR, Fogel S (1986) Biodegradation of Chlorinated Ethenes by a Methane-Utilizing Mixed Culture. Appl. Environ. Microbiol. 51(4): 720-724

Ginestet P, Audic J-M, Urbain V, Block J-C (1998) Estimation of Nitrifying Bacterial Activities by Measuring Oxygen Uptake in the Presence of the Metabolic Inhibitors Allylthiourea and Azide. Applied and Environmental Microbiology 64(6): 2266–2268

Hanson RS, Hanson TE (1996) Methanotrophic bacteria. Microbiological Reviews 60(2): 439-471

Hyman MR, Russell SA, Ely RL, Williamson KJ, Arp DJ (1995) Inhibition, Inactivation, and Recovery of Ammonia-Oxidizing Activity in Cometabolism of Trichloroethylene by Nitrosomonas-Europaea. Appl. Environ. Microbiol. 61(4): 1480-1487

Imfeld G, Aragones CE, Zeiger S, Von Eckstadt CV, Paschke h, R. T, Weiss H, Richnow HH (2008) Tracking in situ Biodegradation of 1,2-Dichloroethenes in a Model Wetland. Environmental Sciences and Technology 42: 7924-7930

Imfeld G, Braeckevelt M, Kuschk P, Richnow HH (2009) Monitoring and assessing processes of organic chemicals removal in constructed wetland. Chemosphere 74: 349-362

James CA, Xin G, Doty SL, Muiznieks I, Newman L, Strand SE (2009) A mass balance study of phytoremediation of perchloroethylene-contaminated groundwater. Environmental Pollution 157: 2564-2569

Kassenga G, Pardue JH, Moe WM, Bowman KS (2004) Hydrogen thresholds as indicators of dehalorespiration in constructed treatment wetlands. Environmental Science & Technology 38(4): 1024-1030

King GM (1996) In situ analyses of methane oxidation associated with the roots and rhizomes of a bur reed, Sparganium eurycarpum, in a Maine wetland. Appl. Environ. Microbiol. 62(12): 4548-4555

Kocamemi BA, Cecen F (2005) Cometabolic degradation of TCE in enriched nitrifying batch systems. Journal of Hazardous Materials 125(1-3): 260-265

Kocamemi BA, Cecen F (2007) Kinetic analysis of the inhibitory effect of trichloroethylene (TCE) on nitrification in cometabolic degradation. Biodegradation 18(1): 71-81

Li YL, Zhang YL, Hu J, Shen QR (2007) Contribution of nitrification happened in rhizospheric soil growing with different rice cultivars to N nutrition. Biology and Fertility of Soils 43(4): 417-425

Lide DR, Frederikse HPR (1995) CRC Handbook of Chemistry and Physics, 76th Edition. CRC Press, Inc., Boca Raton, FL

Little CD, Palumbo AV, Herbes SE, Lidstrom ME, Tyndall RL, Gilmer PJ (1988) Trichloroethylene Biodegradation by a Methane-Oxidizing Bacterium. Appl. Environ. Microbiol. 54(4): 951-956

Lorah MM, Olsen LD (1999) Natural attenuation of chlorinated volatile organic compounds in a freshwater tidal wetland: Field evidence of anaerobic biodegradation. Water Resources Research 35(12): 3811-3827

Lorah MM, Voytek MA (2004) Degradation of 1,1,2,2-tetrachloro ethane and accumulation of vinyl chloride in wetland sediment microcosms and in situ porewater: biogeochemical controls and associations with microbial communities. Journal of Contaminant Hydrology 70(1-2): 117-145

Moran BN, Hickey WJ (1997) Trichloroethylene biodegradation by mesophilic and psychrophilic ammonia oxidizers and methanotrophs in groundwater microcosms. Appl. Environ. Microbiol. 63(10): 3866-3871

Neill C (1995) Seasonal Flooding, Nitrogen Mineralization and Nitrogen-Utilization in a Prairie Marsh. Biogeochemistry 30(3): 171-189

Newman LA, Strand SE, Choe N, Duffy J, Ekuan J, Ruszaj M, Shurtleff BB, Wilmoth J, Heilman P, Gordon MP (1997) Uptake and biotransformation of trichloroethylene by hybrid poplars. Environmental Sciences and Technology 31: 1062-1067

NRC NRC (2000) Natural Attenuation for Groundwater Remediation Washington, D.C.

Nzengung VA, Jeffers P (2001) Sequestration, phytoreduction, and phytooxidation of halogenated organic chemicals by aquatic and terrestrial plants. International Journal of Phytoremediation 3: 13-40

Pankow JF (1991) Aquatic Chemistry Concepts. CRC Press, Inc., Boca Raton, FL

Powers MB, and D. K. Rubin (1996) Doing what comes naturally—Nothing. Engineering News-Record October 14: 16-28

Rasche ME, Hyman MR, Arp DJ (1991) Factors Limiting Aliphatic Chlorocarbon Degradation by Nitrosomonas-Europaea - Cometabolic Inactivation of Ammonia Monooxygenase and Substrate-Specificity. Appl. Environ. Microbiol. 57(10): 2986-2994

Reddy KR, Patrick WH, Lindau CW (1989) Nitrification-Denitrification at the Plant Root-Sediment Interface in Wetlands. Limnology and Oceanography 34(6): 1004-1013

Rogers JE, Williams BW (1991) Microbial Production and Consumption of Greenhouse Gases: Methane, Nitorgen Oxides, and Halomethanes. American Society for Microbiology, Washington, D.C.

Shim H, Ryoo D, Barbieri P, Wood TK (2001) Aerobic degradation of mixtures of tetrachloroethylene, trichloroethylene, dichloroethylenes, and vinyl chloride by toluene-o-xylene monooxygenase of *Pseudomonas stutzeri* OX1. Applied Microbiology and Biotechnology 56(1-2): 265-269

Shukla AK, Vishwakarma P, Upadhyay SN, Tripathi AK, Prasana HC, Dubey SK (2009) Biodegradation of trichloroethylene (TCE) by methanotrophic community. Bioresource Technology 100(9): 2469-2474

Sullivan JP, Dickinson D, Chase HA (1998) Methanotrophs, Methylosinus trichosporium OB3b, sMMO, and their application to bioremediation. Critical Reviews in Microbiology 24(4): 335-373

Tawney I, Becker JG, Baldwin AH (2008) A Novel Dual-Compartment, Continuous-Flow Wetland Microcosm to Assess cis-Dichloroethene removal from the Rhizosphere. International Journal of Phytoremediation 10: 455-471

Vaccari DA, Strom PF, Alleman JE (2006) Environmental Biology for Engineers and Scientists. Wiley-Interscience, Hoboken, NJ

Wang X, Dossett MP, Gordon MP, Strand SE (2004) Fate of carbon tetrachloride during phytoremediation with poplar under controlled field conditions.. Environmental Sciences and Technology 38: 305-322

Yang L, Chang YF, Chou MS (1999) Feasibility of bioremediation of trichloroethylene contaminated sites by nitrifying bacteria through cometabolism with ammonia. Journal of Hazardous Materials 69(1): 111-126

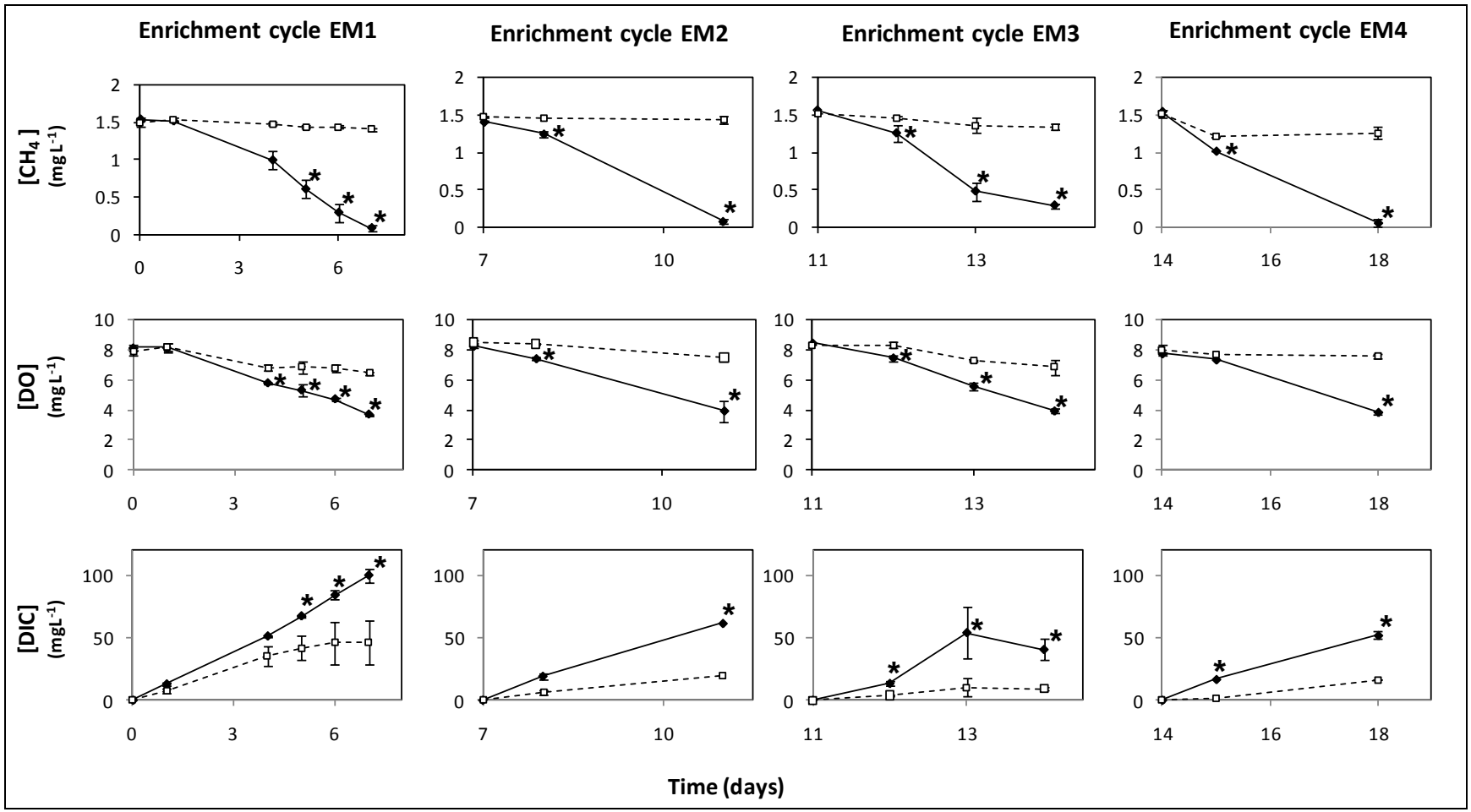

Figure 3.1 Enrichment cycles during methane experiment

Aqueous [CH_4], [DO], and [DIC] in the control (white squares) and the live (black diamonds) microcosms for the four enrichment cycles of the methane experiment (mean ± 1 SD, n=3 per treatment). Asterisk (*) indicates a significant difference between control and live microcosms (Tukey HSD post hoc tests, $p<0.05$)

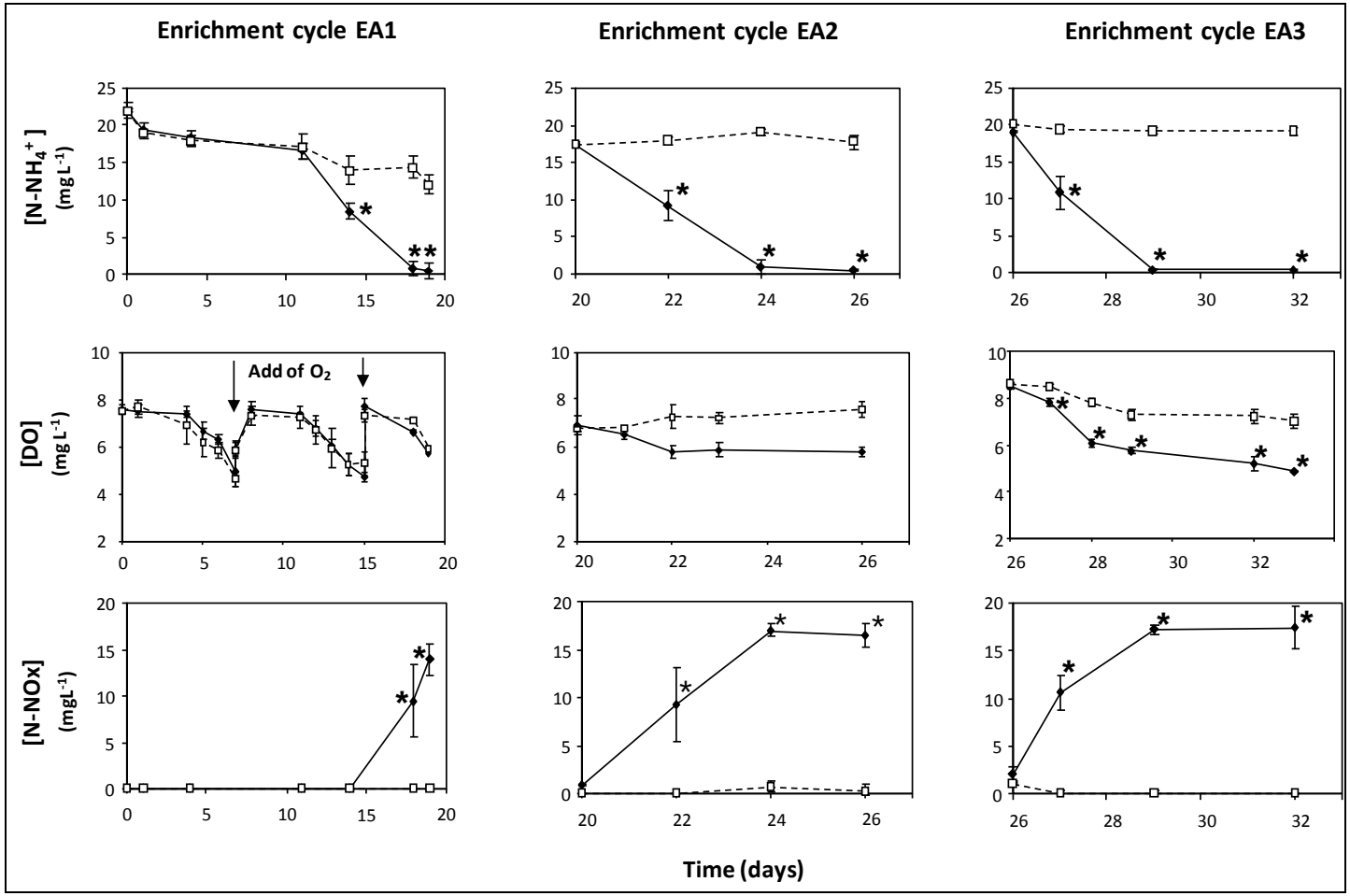

Figure 3.2 Enrichment cycles during ammonia experiment

Aqueous [N-NH_4^+], [DO], and [N-NOx] in the control (white squares) and the live (black diamonds) microcosms for the three enrichment cycles of the ammonia experiment (mean ± 1 SD, n=3 per treatment). Asterisk (*) indicates a significant difference between control and live microcosms (Tukey HSD post hoc tests, $p<0.05$)

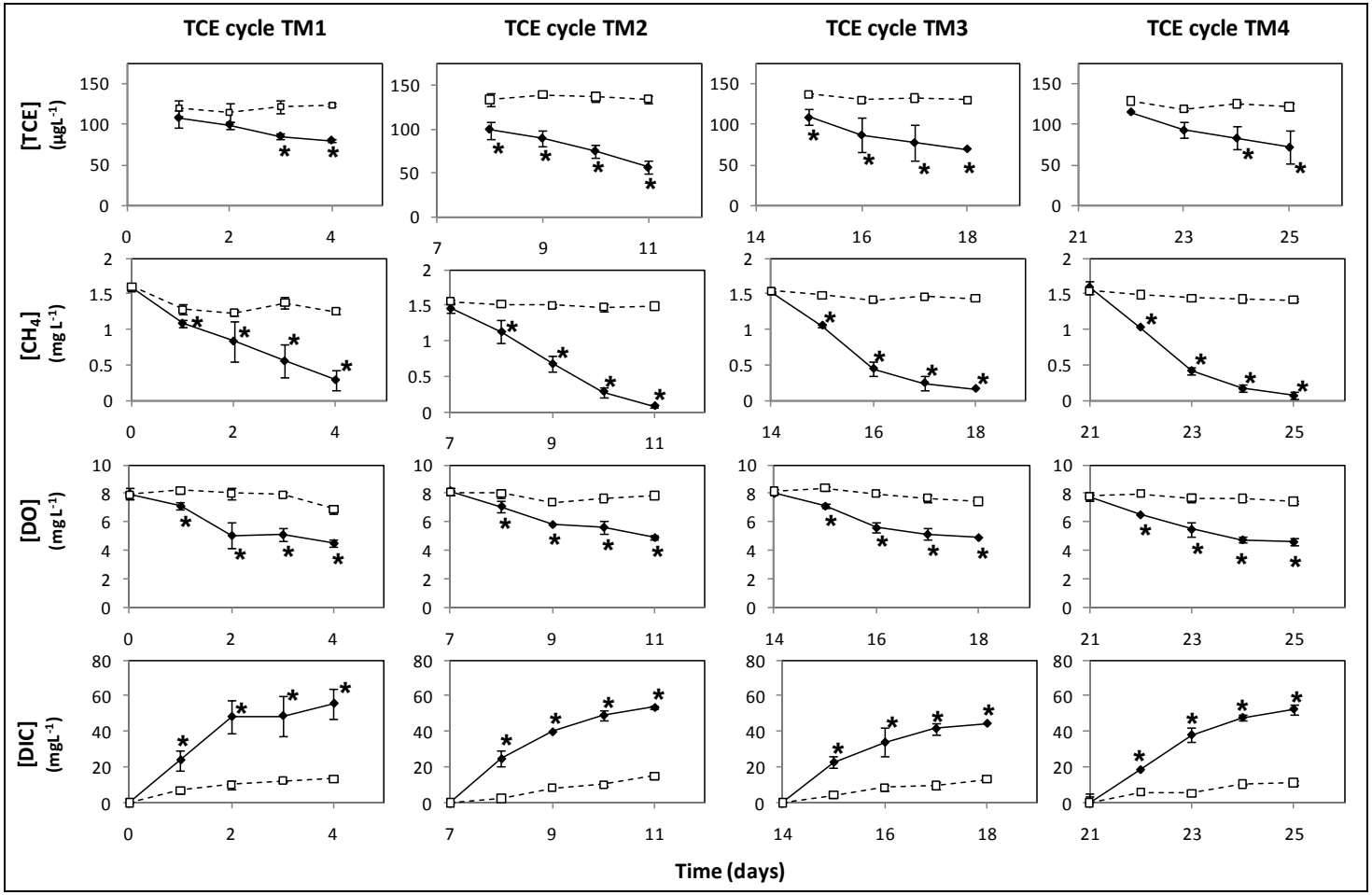

Figure 3.3 TCE cycles during methane experiment

Aqueous [TCE], [CH_4], [DO], and [DIC] in the control (white squares) and the live (black diamonds) microcosms for the four TCE cycles of the methane experiment (mean ± 1 SD, n=3 per treatment). Asterisk (*) indicates a significant difference between control and live microcosms (Tukey HSD post hoc tests, $p<0.05$)

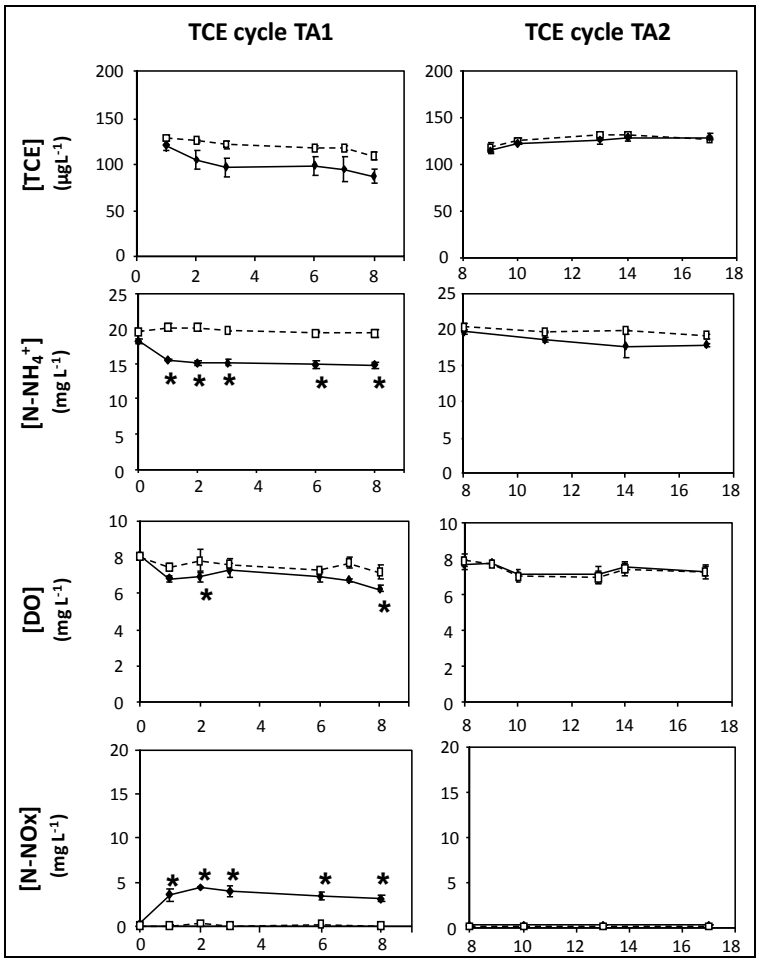

Figure 3.4 TCE cycles during ammonia experiment

Aqueous [TCE], [N-NH_4^+], [DO], and [N-NOx] in the control (white squares) and the live (black diamonds) microcosms for the two TCE cycles of the ammonia experiment (mean ± 1 SD, n=3 per treatment). Asterisk (*) indicates a significant difference between control and live microcosms (Tukey HSD post hoc tests, $p<0.05$)

Table 3.1 Initial rates during the TCE cycles of the methane and ammonia experiments

Initial loss/production rates (d[C]/dt) of solutes (CH_4, NH_4^+, DO, NOx, and DIC) in control and live microcosms for each cycle of TCE amendment (mean ± SD, n = 3) calculated over a 24 h period except for the cycle 2 of the ammonia experiment (96 hr period)

Initial Rate d[C]/dt	**TCE Cycles with Methane (TM)**				**TCE Cycles with Ammonia (TA)**	
	Cycle TM 1	**Cycle TM 2**	**Cycle TM 3**	**Cycle TM 4**	**Cycle TA 1**	**Cycle TA 2***
TCE loss rate (μg L^{-1} d^{-1})						
Control	5.67 ± 5.32	-5.37 ± 4.78	6.97 ± 1.16	10.3 ± 2.04	3.92 ± 2.32	0.00 ± 0.00
Live	8.16 ± 6.35	10.1 ± 2.40	22.1 ± 11.9	22.3 ± 5.40	7.68 ± 1.94	0.00 ± 0.00
CH_4 loss rate (mg L^{-1} d^{-1})						
Control	0.04 ± 0.04	0.01 ± 0.02	0.07 ± 0.01	0.04 ± 0.02	--	--
Live	0.24 ± 0.24	0.45 ± 0.12	0.61 ± 0.08	0.61 ± 0.08	--	--
NH_4^+ loss rate (mg L^{-1} d^{-1})						
Control	--	--	--	--	0.05 ± 0.54	0.00 ± 0.00
Live	--	--	--	--	0.36 ± 0.19	0.22 ± 0.39
DO loss rate (mg L^{-1} d^{-1})						
Control	0.19 ± 0.55	0.62 ± 0.15	0.39 ± 0.20	0.28 ± 0.20	0.00 ± 0.00	0.15 ± 0.10
Live	2.04 ± 0.98	1.28 ± 0.29	1.52 ± 0.26	1.01 ± 0.30	0.00 ± 0.00	0.16 ± 0.03
DIC production rate (mg L^{-1} d^{-1})						
Control	3.24 ± 2.19	5.76 ± 1.38	4.31 ± 0.74	0.00 ± 0.05	--	--
Live	24.1 ± 8.06	15.1 ± 1.59	11.1 ± 7.11	19.5 ± 4.03	--	--

NOx production rate (mg L^{-1} d^{-1})						
Control	--	--	--	--	0.18 ± 0.04	0.00 ± 0.00
Live	--	--	--	--	0.56 ± 0.86	0.00 ± 0.00

* Rates calculated over a 96h period.

4 COMETABOLIC BIODEGRADATION OF TRICHLOROETHENE BY METHANE OXIDIZERS NATURALLY ASSOCIATED WITH WETLAND PLANT ROOTS: INVESTIGATIONS WITH *CAREX COMOSA* AND *SCIRPUS ATROVIRENS*

4.1 INTRODUCTION

TCE is a common groundwater contaminant that poses a threat to human health as a suspected carcinogen (ATSDR 1997). However, TCE can be naturally attenuated in the environment through aerobic and anaerobic microbial degradation processes. In particular, TCE biodegradation by cometabolic oxidative pathways can lead to its mineralization, facilitated by aerobic microorganisms that utilize a wide range of growth substrates, such as methane (Fogel et al. 1986; Little et al. 1988), toluene (Shim et al. 2001), phenol (Chen et al. 2004) ammonia (Kocamemi and Cecen 2007), and several others. Methane as a growth substrate has been successfully studied in a number of systems using both mixed (Fogel et al. 1986) and pure cultures (Little et al. 1988). During cometabolic degradation of TCE with methane, the methane-oxidizing bacteria (or methanotrophs) produce a non-specific enzyme, methane monooxygenase (MMO), that oxidizes methane as its substrate and can also fortuitously degrade TCE (Sullivan et al. 1998). In this process, TCE degradation is initiated as an epoxidation reaction catalyzed by the MMO, with NADH as an immediate energy source (Chang and Alvarez-Cohen 1995).

Microbial methane production (methanogenesis) is ubiquitous in the anaerobic wetland sediment (Neill 1995; Chanton et al. 1997); however, methane can readily degrade by microbial processes in the oxygenated parts of the wetland, such as near the sediment-water interface and in the rhizosphere of wetland plants. Studies have found

that 15–90% of methane produced in various water-logged environments (rice fields, freshwater marshes and swamps) gets oxidized in the rhizosphere of wetland plants by the methanotrophs within the wetland before entering the atmosphere (Holzapfelpschorn et al. 1986; Epp and Chanton 1993; Bosse and Frenzel 1997; Lombardi et al. 1997; Bosse and Frenzel 1998; van der Nat and Middelburg 1998; Popp et al. 2000; Megonigal 2002). Methane-oxidizers may not only colonize the root exterior but can also grow within the root itself, possibly in response to oxygen limitation (Calhoun and King 1997). Further, the activity level of the methanotrophs associated with wetland plant roots may vary seasonally and among plant species (King 1994). Methanotrophs associated with the plant rhizosphere have been reported as being relatively sensitive to oxygen, and their activity may be limited to a greater extent by availability of oxygen than by methane (King 1994). Oxygen availability in the rhizosphere can vary among wetland plants, with proportional changes in methane-oxidizer activity (Calhoun and King 1997). The phenomenon of oxygen leakage from plant roots into the surrounding rhizosphere is called radial oxygen loss (ROL), and it may vary significantly among plant species, even among the members of the same genus that show similarities in root morphology (Inoue and Tsuchiya 2008).

Past research on chlorinated ethene (CE) degradation in wetland sediments has focused on reductive (Lorah and Olsen 1999; Kassenga et al. 2003; Kassenga et al. 2004; Kassenga and Pardue 2006; Amon et al. 2007) and oxidative transformation processes (Bankston et al. 2002; Tawney et al. 2008), though a greater emphasis has been made on CE transformation pathways in reducing conditions. Despite limited number of studies examining CE degradation in wetland plant roots (Bankston et al. 2002; Tawney et al.

2008), there may be significant potential for such degradation in vegetated wetlands by the root-associated methane-oxidizers. However, cometabolic TCE removal within roots may vary among wetland plant species resulting from variations in root characteristics themselves affecting methane oxidation. The aim of the current investigation was to evaluate TCE degradation potential by methane-oxidizers that may be naturally associated with the roots of two common wetland plants, *Carex comosa* and *Scirpus atrovirens* (commonly called 'longhaired sedge' and 'green bulrush', respectively), both of which are found in North America, and they show modest differences in their respective root characteristics. Above plants species were selected for the laboratory investigation as they are among the species utilized at the experimental wetland constructed for the pilot-scale treatment of groundwater contaminated with chlorinated ethenes (Amon et al. 2007). In the present study, the activities of root-associated methane-oxidizing bacteria were evaluated for the above plant species, and the influences of the methane oxidation activity of these bacteria on TCE degradation were investigated. This approach enabled us to evaluate the potential role of rhizospheric processes in two common wetland plants, which can influence TCE degradation by natural attenuation processes distributed in shallow zones of vegetated wetlands.

4.2 MATERIALS AND METHODS

4.2.1 Root Characterization

Two wetland plant species (*Carex comosa* Boott. and *Scirpus atrovirens* Willd., both from the family *Cyperaceae,* referred to henceforth as *CC* and *SA* respectively) were collected from a natural fen located near Dayton, OH (USA) in September 2008. After collection, the plants were maintained in the university greenhouse until use (~40 weeks)

in individual tree pots (2 gal, 15 x 15 cm opening, and 41 cm) containing a 50/50 mix of peat moss and local fen soil. The light cycle in the greenhouse was ambient during the long days of the year, and augmented with fluorescent lights that maintain light at no less than 13.5 hours during the short winter days. The bench-scale experiments (described below) were conducted with *CC* or *SA* roots that were separated from plant shoot by clipping, washed with de-ionized water thoroughly to remove attached soil, and then dried in air before weighing. The physical attributes of representative root samples of *CC* and *SA* plants of similar age were characterized, including their dimensions and dry weight. A modest number of representative samples of root from *CC* and *SA* plants were obtained and characterized in terms of their average length per unit mass (n= 40), and the average diameter of root (n = 120), based on which the nominal surface area per mass ($cm^2\ g^{-1}$) and nominal volume per mass ($cm^3\ g^{-1}$) for both species were estimated.

4.2.2 Microcosm Design

Batch experiments were set-up using 2.4 L microcosms, each made of white Teflon material (18.2 cm tall x 13.8 cm inner dia, and 3.5 cm wall thickness). Each microcosm had a stir bar at the bottom, and a porous shelf made of PEEK mesh-cloth located at 6.5 cm height from the microcosm base, to support root materials. There were two ports in the lid of microcosms, each fitted with Teflon pipe adapters and 0.625 cm OD Teflon tubing; one port was for gas bubbling/liquid sampling and the other port is for venting or liquid amendments. A third opening in the microcosm lid, customized to fit a 20 mm dia. rubber stopper and an aluminum crimp, was used for collecting gas samples from the microcosm headspace using gastight syringes (Hamilton, Reno, NV); this port

was closed with a Teflon-lined grey butyl rubber stopper and sealed with an aluminum crimp (both from Wheaton, Milliville, NJ).

4.2.3 TCE Experiments

Six microcosms (2.4 L Teflon microcosms, as above) were set up as follows: three were prepared as 'live' microcosms with 15 g of fresh roots, either from *CC* or *SA*, and 1440 mL of growth medium (Fogel et al. 1986) and the remaining three microcosms were prepared as 'killed' controls in the same manner, but with 6.24 mg L^{-1} of sodium azide to inhibit the growth of gram-negative bacteria, including the methane-oxidizing bacteria (Ginestet et al. 1998). After these additions, a headspace of 960 mL remained in each microcosm. Prior to sealing the microcosms with Teflon-lined grey butyl rubber stoppers and aluminum crimps, all microcosms were bubbled with air for ~30 min to start the experiment, with a dissolved oxygen (DO) at ~8 mg L^{-1} and its headspace filled with air. Pure gaseous methane (CH_4) was added into each microcosm (90 mL, equivalent to 3.68 mmoles mass, or 0.13 mM or 2.1 mg L^{-1} aqueous [CH_4]) using a gas-tight glass syringe (Hamilton, Reno, NV), and the microcosms were continuously mixed at 60 rpm on individual stir plates at ambient temperature (22±1 °C). For microcosms either with *CC* or *SA* roots, there were three cycles of microbial enrichment with CH_4 as a substrate (cycles EC1 through EC3, with no TCE added), where each cycle corresponded to a period during which CH_4 degraded nearly completely in the microcosms, and needed to be replenished. Following the 3 enrichment cycles without TCE, 6 additional cycles (TC1 through TC6) were completed with variations in TCE amendments as follows: 4 cycles of 150 μg L^{-1}, 1 cycle of 600 μg L^{-1}, and 1 cycle of 900 μg L^{-1}. In between TCE cycles, there were short inter-cycle periods, where the microcosms were bubbled with air

for 30 minutes to remove volatiles from the preceding TCE cycle and to oxygenate the system. After bubbling, the microcosms were sealed, amended with CH_4 only, and incubated for 2 days.

4.2.4 Chemicals and Analysis

TCE stock solution was prepared by adding 20 µL of TCE (99+% ACS grade, Aldrich Chemicals Co., Milwaukee, WI) to a 160 mL borosilicate glass serum bottle containing organic-free Milli-Q water, and sealed with a Teflon-lined rubber stopper and aluminum crimp without headspace, and then the bottle was placed on a rotary shaker for 48 hr to allow TCE to dissolve completely. Headspace samples from the microcosms were analyzed by gas chromatography to estimate aqueous phase mass and total mass of CH_4, TCE, oxygen (O_2), and inorganic carbon in each microcosm. CH_4 and TCE were analyzed by a HP 6890 series GC system with flame ionization (FID) and electron capture (ECD) detectors, where CH_4 was separated on a capillary column (GS GasPro, 30m x 0.32mm; J&W Scientific) connected to the FID, and TCE was separated on a capillary column (HP-624, 30m x 0.32mm; Agilent Technologies) connected to the ECD. O_2 and carbon dioxide (CO_2) were analyzed by a HP 5890 series GC system with a thermal conductivity detector and a packed column (Shin Carbon 100/120, 2m x 1mm; Restek, Bellefonte, PA). Peak area values for TCE from GC analysis were transformed into aqueous concentrations at equilibrium using laboratory calibration curves and a published method (Burris et al. 1996). The aqueous CH_4 concentration at equilibrium were calculated by the application of Gas law and Henry's law (Burris et al. 1996) and its dimensionless Henry's constant (K'_H for CH_4 at 25°C = 28.5; (Gossett 1987)). Based on measured partial pressures of O_2 in the microcosm headspace, the DO concentration and

total oxygen (TO) mass were calculated using Henry's Law (K'_H for O_2 gas at 25 ºC = 3.8 x 10^{-2}; (Lide and Frederikse 1995)). Similarly the dissolved inorganic carbon (DIC) concentration and total inorganic carbon (TIC) mass were calculated using Henry's Law (K'_H for CO_2 gas at 25 ºC = 0.83) and carbonate system equilibrium relationships at measured pH (Pankow 1991). The pH measurements were made using a handheld meter (model AP10 pH/mV/temp, Denver Instrument, Bohemia, NY) by collecting 2.5 ml aqueous samples from each microcosm after gas sampling (see section III in Appendix A, for calculation procedure).

4.2.5 Data Treatment and Statistical Analysis

For each cycle during enrichment and TCE addition, the initial rate of mass loss/production of solutes (i.e., CH_4, TO, TIC and TCE) were calculated using the difference between their measured values on day 1 and day 2 (with the exception that the last enrichment cycle, which was from day 0 to day 3) (Anderson and McCarty 1997). The initial rates were taken as mass difference between day 1 and day 2, as opposed to day 0 and day 1, in order to avoid the transient conditions imposed by microcosm reset in between cycles. Above initial mass loss/production rates were then normalized to reactor fluid volume (1.44 L), and reported in mmoles d^{-1} L^{-1}; TCE loss rate is reported in μmoles d^{-1} L^{-1}. Transformation yield (T_y) was calculated by subtracting the average losses in TCE and CH_4 in the killed controls from the live microcosms, and then dividing total TCE mass degraded by total CH_4 mass degraded (including CH_4 loss in the enrichment cycles, and inter-cycles methane amendments without TCE; Anderson and McCarty 1997).

For the enrichment cycles EC1 through EC3, and cycles TC1 through TC4 with TCE, the effects of treatment (i.e., control vs. live microcosms), plant species (i.e., *CC* vs. *SA*) and cycle number on the initial loss/production rates of solute (CH_4, TO, TIC, and TCE) were measured using a three-way factorial analysis of variance (ANOVA) with treatment, species, and cycles being the independent factors. This approach was considered appropriate instead of repeated measures ANOVA with cycle as the repeat factor because each cycle was considered independent of the previous cycles due to inter-cycle reset of microcosms. For cycles TC5 and TC6 (higher TCE concentration treatment), a two-factorial ANOVA was employed to test the effects of species and treatment on initial loss/production rates with treatment and species as the independent factors. A *t*-test was used to compare root characteristics and stiochiometric ratios between root species. Statistical analyses were performed using Statistica 9TM (Statsoft, Tulsa, OK, USA).

4.3 RESULTS AND DISCUSSION

4.3.1 Root Attributes

CC and *SA* root samples showed differences in terms of their dimensional attributes and their appearance (Figure 4.1). The *SA* roots were more fibrous and had a significantly greater length per unit mass in comparison to *CC* roots; 107.30 ± 42.99 cm g^{-1} for *SA* versus 57.99 ± 14.28 cm g^{-1} for *CC* (n = 40) *(t*-test, $P<0.0001$*)*. Further, the average diameter of *CC* root was significantly greater than *SA* roots; 0.13 ±0.02 cm for *CC* versus 0.07 ± 0.02 cm for *SA* (n=120) *(t*-test, $P<0.0001$*)*. Based on above diameter measurements, and assuming a cylindrical shape for all roots, the nominal root surface area per unit root mass was nearly twice as much for *CC* in comparison to *SA*; 0.72 $cm^2 g^{-1}$ for *CC* versus 0.33 $cm^2 g^{-1}$ for *SA*. However, using a similar approach, the nominal root

volume per unit root mass was similar for the two species; 21.8 $cm^3 g^{-1}$ for *CC* versus 20.3 $cm^3 g^{-1}$ for *SA*.

In addition, there were visual differences between the *CC* and *SA* roots at the time these plants were removed from pots maintained in the greenhouse (Figure 4.1); the *CC* roots exhibited an orange tint, whereas the *SA* roots were mostly coated with a thin film of fine-grained black solid. The orange tint of *CC* roots may indicate a coating of iron oxyhydroxide, and as such it suggests a more oxidizing rhizospheric condition leading to oxidation of porewater Fe(II), presumably caused by greater ROL (Van der Nat and Middelburg 1998; Weiss et al. 2005). This is consistent with thicker *CC* roots that may exhibit greater ROL, and a greater CH_4 loss during enrichment cycles with *CC* roots (see discussion in *Microbial Enrichment*) suggesting a more favorable habitat for aerobic microbes (e.g., iron oxidizing bacteria and methane oxidizers). The black coating on *SA* roots, on the other hand, may indicate possible iron monosulfide (FeS) formation due to microbial reduction of sulfate available in the pore water. Sulfate reducing bacteria can often be associated with emergent plant roots (Wind and Conrad 1997), and FeS formation (through sulfate reduction) on *SA* roots suggests a geochemical condition that may have been strongly reducing. Further, a sulfate reducing condition may have developed in *SA* roots perhaps due to excess DOC released from *SA* roots (Figure C.5, in Appendix B.3).

4.3.2 Microbial Enrichment

Our results demonstrated that both plants species, *CC* and *SA*, had methane-oxidizing activity associated with their roots, expressed as simultaneous loss in O_2 and CH_4 levels. The initial loss rates for CH_4 and TO and initial production rate for TIC were

significantly different between live and control microcosms (three-way factorial ANOVA, treatment effect, $P<0.05$; Table 4.1, and Table C.1 in Appendix B.3), and between enrichment cycles (three-way factorial ANOVA, cycle effect, $P<0.001$; Table 4.1, and Table B.3.1 in Appendix B.3). The variations in initial rates of CH_4 and TO due to the effects of species and treatment depended on the cycle (three-way factorial ANOVA, treatment x species x cycle, $P<0.05$; Table 4.1, and Table B.3.1 in Appendix B.3). Initial rates of CH_4 degradation were also significantly different between species (three-way factorial ANOVA, species effect, $P<0.00001$; Table 4.1, and Table B.3.1 in Appendix B.3). The average mass of CH_4 oxidized was considerably greater during enrichment cycles for *CC* roots compared to *SA* roots (Figures B.3.1, B.3.2 and B.3.5 in Appendix B.3), which may suggest that a greater number of methane-oxidizers were initially present with *CC* roots, and *CC* may have provided a favorable habitat for greater CH_4 oxidation; this is consistent with the orange tint of *CC* roots indicative of its greater oxidizing characteristics in comparison to *SA* roots. The average mass of TIC formed was significantly larger than mass of CH_4 oxidized during each cycle for both roots (see *Stoichiometry and Mass Balance*), suggesting mineralization of DOC leached from roots as a significant process. Further, the TIC mass from DOC mineralization was considerably greater for *SA* roots compared to *CC* roots in enrichment cycles (Figures B.3.1, B.3.2 and B.3.5 in Appendix B.3).

4.3.3 TCE Degradation

During the first four cycles with TCE (TC1 through TC4), the initial loss rates for CH_4 and TO and initial production rate for TIC were significantly different between live and control microcosms (three-way factorial ANOVA, treatment effect, $P<0.05$; Table

4.1, and Table B.3.1 in Appendix B.3) as well as for CH_4 and TO during the last two cycles (TC5 and TC6) (two-way factorial ANOVA, treatment effect, $P<0.01$; Table 4.1, and Table B.3.1 in Appendix B.3). During the first 4 cycles, the effects of treatment and species on TO variations depended on the cycle (three-way factorial ANOVA, species x treatment x cycle, $P<0.05$; Table 4.1, and Table B.3.1 in Appendix B.3). However, the differences in methane-oxidizing activity between *CC* and *SA* roots observed during the enrichment cycles were not significant during TC cycles; the CH_4 oxidation was similar for the two species (with the exception of cycle TC1), and the initial rates of methane loss were comparable through cycles TC2 through TC6 (three-way factorial ANOVA, species effect, $P<0.05$ for TC1-TC4 and two-way factorial ANOVA, species effect, $P>0.05$; Table 4.1). Further, the decrease in initial rate of CH_4 degradation in TC cycles in comparison to EC cycles is consistent with earlier reports that methane utilization becomes partially inhibited by TCE transformation (Anderson and McCarty 1997; Chang and Criddle 1997). However, MMO deactivation due to TCE epoxide toxicity was not evident as the initial rate for CH_4 degradation remained nearly steady through cycles TC1 through TC6, and did not progressively decline as would be expected in case of toxicity.

Degradation of TCE with both *CC* and *SA* roots in all 6 TC cycles was observed, including for initial dissolved TCE concentrations at 600 and 900 μg L^{-1} (cycles TC5 and TC6). The study showed TCE loss in live microcosms compared to killed controls (Figure B.3.4, in Appendix B.3) corresponded with CH_4 degradation, suggesting that TCE loss can be attributed to cometabolic oxidation by methane-oxidizers in live microcosms. For both plant roots, initial TCE degradation rates significantly differed between treatments (i.e., live vs. control microcosms) (three-way factorial ANOVA for TC1-TC4

and two-way factorial ANOVA for TC5-TC6, treatment effect, $P<0.05$; Table 4.1, and Table B.3.1 in Appendix B.3), yet they were fairly consistent between the species in cycles TC1 through TC4 (three-way factorial ANOVA, species effect, P>0.05; Table 4.1, and Table B.3.1 in Appendix B.3), but rates increased in cycles TC5 and TC6 as more TCE was added (Table 4.1, and Table B.3.1 in Appendix B.3). The increase in initial TCE degradation rates was similar for the two plant roots in TCE cycle 5 (two-way factorial ANOVA, species effect, P>0.05; Table 4.1, and Table B.3.1 in Appendix B.3), but the initial rate was significantly greater for CC roots in cycle TC6 (two-way factorial ANOVA, species effect, P<0.05; see Table 4.1, and Table B.3.1 in Appendix B.3), which may be attributed to greater methane oxidation supported by the larger root surface area.

Further, the average net TCE mass losses for the two roots in TC1 through TC6 cycles were similar (24% with *CC* roots and 32% with *SA* roots) at the experimental conditions (150-900 μg L^{-1} TCE and 2.1 mg L^{-1} of aqueous CH_4). The average net T_y was 0.0004 ± 0.0001 mmol TCE/mmol CH_4 for both *CC* and *SA*, which is lower than reported literature values by a factor of 2 (Alvarez-Cohen and Speitel 2001) presumably due to less efficient TCE oxidation at low TCE concentration, where CH_4 has a greater chance to occupy/bind with active MMO sites than TCE (Chang and Alvarez-Cohen 1995; Chang and Criddle 1997). A significantly higher T_y (0.0019 mmol TCE/mmol CH_4) was reported in batch system for a methane-oxidizing mixed culture in soil at an initial TCE concentration of 1710 μg L^{-1} (Anderson and McCarty 1997), due presumably to a much lower initial TCE concentration in this study. A significantly greater values of T_y has been predicted by the methane-oxidizing bacteria at higher TCE concentrations (Chang and Criddle 1997), and it was attributed to a more efficient CH_4 utilization in TCE transformation.

4.3.4 Stoichiometry and Mass Balance

Mass balance analysis indicates that the TIC produced in individual cycles throughout the study with either root was significantly greater than available carbon from CH_4 (stoichiometrically, the TIC to CH_4 ratio should be ~1 if all CH_4 gets oxidized), which suggests that excess TIC was produced by heterotrophic oxidation of dissolved organic carbon (DOC) released from the roots (Figure B.3.5 in Appendix B.3). In other words, the analysis has shown that DOC oxidation (by heterotrophs) was an important process that was active in parallel to methanotrophic activity in enrichment cycles, and it also persisted through TCE cycles. Stoichiometric analysis further indicates that during enrichment cycles the ratios of average TIC formed to CH_4 degraded were significantly greater for *SA* (2.82±0.42) in comparison to *CC* (1.46±0.10) (*t*-test, $P<0.05$) roots, suggesting that greater amount of labile carbons was released from the *SA* roots leading to greater TIC production in EC1 through EC3 cycles. The suggestion of a greater DOC release from *SA* roots, in comparison to *CC* roots in enrichment cycles, is significant, and it is consistent with formation of FeS on *SA* roots under reducing condition discussed earlier (see *Root Attributes*). The analysis further suggests that greater availability of labile organic carbon from plant roots may stimulate the heterotrophic microorganisms leading to oxygen depletion and reducing conditions in the plant rhizosphere. While water table depth in a wetland is generally considered to be an important regulating factor in methane-oxidation processes in shallow subsurface, the availability of excess labile organic matter from plant roots can be a secondary factor affecting methane oxidation (and TCE cometabolism) in the rhizosphere.

4.3.5 Implications

Our recent field study has shown a near complete removal of chlorinated ethenes in the groundwater passing through the constructed wetland (Amon et al. 2007). The present bench-scale study provides a validation of simultaneous degradation of methane and chlorinated ethene in the shallow, vegetated zone of the wetland (Amon et al. 2007), and offers a mechanism for destruction of chlorinated ethenes through aerobic cometabolism. The study concludes that the overall potential for TCE degradation may be similar for *Carex comosa* and *Scirpus atrovirens* roots despite certain differences in their morphology, which suggests that TCE degradation can also occur with other emergent plants expressing methanotrophic activity, such as *Oryza sativa, Carex aquatilis, Carex rostrata, Phragmites australis, Scirpus lacustris, Pontederia cordata, Sparganium eurycarpu,* and *Sagittaria latifolia* (Holzapfelpschorn et al. 1986; Bosse and Frenzel 1997; Calhoun and King 1997; Bosse and Frenzel 1998; Calhoun and King 1998; van der Nat and Middelburg 1998; Popp et al. 2000). The present study offers important insight about the role of wetland plants in the natural attenuation of TCE in contaminated aquatic environments, such as urban wetlands, or wetlands impacted by industrial solvents. The results may also be helpful for application of constructed or restored wetlands in pollutant mitigation and site management.

Our future study includes investigating chlorinated hydrocarbon degradation in flow-through mesocosms with several species of live (whole) wetland plants, and examining the effect of methane and TCE concentrations on degradation kinetics by root-associated methane oxidizers. In addition, root-associated methane-oxidizing microbial community in TCE degrading systems will be characterized using molecular techniques.

4.4 REFERENCES

Alvarez-Cohen L, Speitel GE (2001) Kinetics of aerobic cometabolism of chlorinated solvents. Biodegradation 12(2): 105-126

Amon JP, Agrawal A, Shelley ML, Opperman BC, Enright MP, Clemmer ND, Slusser T, Lach J, Sobolewski T, Gruner W, Entingh AC (2007) Development of a wetland constructed for the treatment of groundwater contaminated by chlorinated ethenes. Ecol. Eng. 30(1): 51-66

Anderson JE, McCarty PL (1997) Transformation yields of chlorinated ethenes by a methanotrophic mixed culture expressing particulate methane monooxygenase. Appl. Environ. Microbiol. 63(2): 687-693

ATSDR AfTSaDR (1997) Toxicological Profile for Trichloroethylene (Update). Atlanta, GA.

Bankston JL, Sola DL, Komor AT, Dwyer DF (2002) Degradation of trichloroethylene in wetland microcosms containing broad-leaved cattail and eastern cottonwood. Water Res. 36(6): 1539-1546

Bosse U, Frenzel P (1997) Activity and distribution of methane-oxidizing bacteria in flooded rice soil microcosms and in rice plants (Oryza sativa). Appl. Environ. Microbiol. 63(4): 1199-1207

Bosse U, Frenzel P (1998) Methane emissions from rice microcosms: The balance of production, accumulation and oxidation. Biogeochemistry 41(3): 199-214

Burris DR, Delcomyn CA, Smith MH, Roberts AL (1996) Reductive dechlorination of tetrachloroethylene and trichloroethylene catalyzed by vitamin B-12 in

homogeneous and heterogeneous systems. Environmental Science & Technology 30(10): 3047-3052

Calhoun A, King GM (1997) Regulation of root-associated methanotrophy by oxygen availability in the rhizosphere of two aquatic macrophytes. Appl. Environ. Microbiol. 63(8): 3051-3058

Calhoun A, King GM (1998) Characterization of root-associated methanotrophs from three freshwater macrophytes: Pontederia cordata, Sparganium eurycarpum, and Sagittaria latifolia. Appl. Environ. Microbiol. 64(3): 1099-1105

Chang HL, Alvarez-Cohen L (1995) Transformation Capacities of Chlorinated Organics by Mixed Cultures Enriched on Methane, Propane, Toluene, or Phenol. Biotechnology and Bioengineering 45(5): 440-449

Chang WK, Criddle CS (1997) Experimental evaluation of a model for cometabolism: Prediction of simultaneous degradation of trichloroethylene and methane by a methanotrophic mixed culture. Biotechnology and Bioengineering 56(5): 492-501

Chanton J, Whiting G, Blair N, Lindau C, Bollich P (1997) Methane Emission from Rice; Stable Isotopes, Diurnal Variations, and CO2 Exchange. Global Biogeochem. Cy. 11: 15-27

Chen WM, Chang JS, Wu CH, Chang SC (2004) Characterization of phenol and trichloroethene degradation by the rhizobium Ralstonia taiwanensis. Research in Microbiology 155(8): 672-680

Epp MA, Chanton JP (1993) Rhizospheric Methane Oxidation Determined Via the Methyl-Fluoride Inhibition Technique. Journal of Geophysical Research-Atmospheres 98(D10): 18413-18422

Fogel MM, Taddeo AR, Fogel S (1986) Biodegradation of Chlorinated Ethenes by a Methane-Utilizing Mixed Culture. Appl. Environ. Microbiol. 51(4): 720-724

Ginestet P, Audic J-M, Urbain V, Block J-C (1998) Estimation of Nitrifying Bacterial Activities by Measuring Oxygen Uptake in the Presence of the Metabolic Inhibitors Allylthiourea and Azide. Applied and Environmental Microbiology 64(6): 2266–2268

Gossett JM (1987) Measurement of Henrys Law Constants for C1 and C2 Chlorinated Hydrocarbons. Environmental Science & Technology 21(2): 202-208

Holzapfelpschorn A, Conrad R, Seiler W (1986) Effects of vegetation on the emission of methane from submerged paddy soil. Plant Soil 92(2): 223-233

Inoue TM, Tsuchiya T (2008) Interspecific differences in radial oxygen loss from the roots of three Typha species. Limnology 9(3): 207-211

Kassenga G, Pardue JH, Moe WM, Bowman KS (2004) Hydrogen thresholds as indicators of dehalorespiration in constructed treatment wetlands. Environmental Science & Technology 38(4): 1024-1030

Kassenga GR, Pardue JH (2006) Effect of competitive terminal electron acceptor processes on dechlorination of cis-1,2-dichloroethene and 1,2-dichloroethane in constructed wetland soils. Fems Microbiology Ecology 57(2): 311-323

Kassenga GR, Pardue JH, Blair S, Ferraro T (2003) Treatment of chlorinated volatile organic compounds in upflow wetland mesocosms. Ecol. Eng. 19(5): 305-323

King GM (1994) Associations of methanotrophs with the roots and rhizomes of aquatic vegetation. Appl. Environ. Microbiol. 60(9): 3220-3227

Kocamemi BA, Cecen F (2007) Kinetic analysis of the inhibitory effect of trichloroethylene (TCE) on nitrification in cometabolic degradation. Biodegradation 18(1): 71-81

Lide DR, Frederikse HPR (1995) CRC Handbook of Chemistry and Physics, 76th Edition. CRC Press, Inc., Boca Raton, FL

Little CD, Palumbo AV, Herbes SE, Lidstrom ME, Tyndall RL, Gilmer PJ (1988) Trichloroethylene Biodegradation by a Methane-Oxidizing Bacterium. Appl. Environ. Microbiol. 54(4): 951-956

Lombardi JE, Epp MA, Chanton JP (1997) Investigation of the methyl fluoride technique for determining rhizospheric methane oxidation. Biogeochemistry 36(2): 153-172

Lorah MM, Olsen LD (1999) Natural attenuation of chlorinated volatile organic compounds in a freshwater tidal wetland: Field evidence of anaerobic biodegradation. Water Resources Research 35(12): 3811-3827

Megonigal J, Schlesinger, W. (2002) Methane-Limited Methanotrophy in Tidal Freshwater Swamps. Global Biogeochem. Cy. 16: 1088-1098

Neill C (1995) Seasonal Flooding, Nitrogen Mineralization and Nitrogen-Utilization in a Prairie Marsh. Biogeochemistry 30(3): 171-189

Pankow JF (1991) Aquatic Chemistry Concepts. CRC Press, Inc., Boca Raton, FL

Popp TJ, Chanton JP, Whiting GJ, Grant N (2000) Evaluation of methane oxidation in the rhizosphere of a Carex dominated fen in north central Alberta, Canada. Biogeochemistry 51(3): 259-281

Shim H, Ryoo D, Barbieri P, Wood TK (2001) Aerobic degradation of mixtures of tetrachloroethylene, trichloroethylene, dichloroethylenes, and vinyl chloride by toluene-o-xylene monooxygenase of *Pseudomonas stutzeri* OX1. Applied Microbiology and Biotechnology 56(1-2): 265-269

Sullivan JP, Dickinson D, Chase HA (1998) Methanotrophs, Methylosinus trichosporium OB3b, sMMO, and their application to bioremediation. Critical Reviews in Microbiology 24(4): 335-373

Tawney I, Becker JG, Baldwin AH (2008) A Novel Dual-Compartment, Continuous-Flow Wetland Microcosm to Assess cis-Dichloroethene removal from the Rhizosphere. International Journal of Phytoremediation 10: 455-471

Van der Nat F, Middelburg JJ (1998a) Effects of two common macrophytes on methane dynamics in freshwater sediments. Biogeochemistry 43(1): 79-104

van der Nat F, Middelburg JJ (1998b) Seasonal variation in methane oxidation by the rhizosphere of Phragmites australis and Scirpus lacustris. Aquat. Bot. 61(2): 95-110

Weiss JV, Emerson D, Megonigal JP (2005) Rhizosphere iron(III) deposition and reduction in a Juncus effusus L.-dominated wetland. Soil Science Society of America Journal 69(6): 1861-1870

Wind T, Conrad R (1997) Localization of sulfate reduction in planted and unplanted rice field soil. Biogeochemistry 37(3): 253-278

Figure 4.1 ***Carex comosa*** **and** ***Scirpus atrovirens*** **Roots**

Roots of *Carex comosa* (top) and *Scirpus atrovirens* (bottom). Visual differences were observed between the *CC* and *SA* roots at the time of removal from the greenhouse; the *CC* roots exhibited an orange tint, whereas the *SA* roots were mostly coated with a thin film of fine-grained black solid.

Table 4.1 Initial loss/production Rates

Initial loss/production rates of solute mass (CH_4, TO, and TIC) in control and live microcosms for the *CC* and *SA* experiments (mean ± SD, n = 3). The initial mass loss/production rates are normalized to reactor fluid volume, and reported in mmoles d^{-1} L^{-1}; TCE loss rate is reported in μmoles d^{-1} L^{-1}. The initial rates of solute loss or production are calculated between day 1 and day 2 (~24 hr period) for all cycles reported below (except for cycle 4 during enrichment, which was averaged over the first 3 days).

Initial Rate	**Enrichment Cycles**			**TCE Cycles**					
	Cycle EC1	**Cycle EC2**	**Cycle EC3**	**Cycle TC1**	**Cycle TC2**	**Cycle TC3**	**Cycle TC4**	**Cycle TC5**	**Cycle TC6**
Initial [CH_4] ($mg\ L^{-1}$)	*2.1*	*2.1*	*2.1*	*2.1*	*2.1*	*2.1*	*2.1*	*2.1*	*2.1*
Initial [TCE] ($\mu g\ L^{-1}$)	--	--	--	*150*	*150*	*150*	*150*	*600*	*900*
TCE loss rate									
CC- Live	--	--	--	0.16 ± 0.06	0.11 ± 0.05	0.08 ± 0.01	0.15 ± 0.01	0.74 ± 0.28	1.15 ± 0.15
CC-Control	--	--	--	0.08 ± 0.11	0.01 ± 0.03	0.00 ± 0.03	0.07 ± 0.03	0.25 ± 0.36	0.00 ± 0.13
SA – Live	--	--	--	0.07 ± 0.04	0.18 ± 0.12	0.19 ± 0.02	0.14± 0.12	0.68 ± 0.11	0.72 ± 0.18
SA - Control	--	--	--	0.00 ± 0.05	0.10 ± 0.07	0.13 ± 0.05	0.00 ± 0.04	0.41 ± 0.02	0.00 ± 0.12
CH_4 loss rate									
CC- Live	0.05 ± 0.04	0.89 ± 0.27	0.68 ± 0.14	0.30 ± 0.10	0.22 ± 0.04	0.21 ± 0.06	0.25 ± 0.11	0.22 ± 0.09	0.29 ± 0.09
CC-Control	0.08 ± 0.07	0.12 ± 0.09	0.07 ± 0.03	0.04 ± 0.02	0.00 ± 0.10	0.06 ± 0.05	0.06 ± 0.06	0.04 ± 0.08	0.00 ± 0.01
SA – Live	0.04 ± 0.04	0.35 ± 0.16	0.26 ± 0.04	0.14 ± 0.04	0.25 ± 0.03	0.20 ± 0.10	0.21 ± 0.06	0.20 ± 0.03	0.20 ± 0.10
SA - Control	0.00 ± 0.04	0.04 ± 0.18	0.00 ± 0.02	0.01 ± 0.02	0.01 ± 0.06	0.00 ± 0.11	0.00 ± 0.09	0.01 ± 0.03	0.02 ± 0.06
TO loss rate									
CC- Live	0.06 ± 0.03	0.85 ± 0.21	0.74 ± 0.09	0.68 ± 0.07	0.65 ± 0.02	0.32 ± 0.22	0.30 ± 0.05	0.33 ± 0.09	0.38 ± 0.05

CC-Control	0.13 ± 0.19	0.14 ± 0.05	0.18 ± 0.07	0.13 ± 0.15	0.26 ± 0.16	0.00 ± 0.07	0.04 ± 0.07	0.03 ± 0.09	0.01 ± 0.05
SA – Live	0.36 ± 0.19	0.57 ± 0.30	0.43 ± 0.15	0.41 ± 0.03	0.35 ± 0.11	0.28 ± 0.10	0.55 ± 0.17	0.47 ± 0.07	0.41 ± 0.09
SA - Control	0.17 ± 0.06	0.11 ± 0.19	0.23 ± 0.05	0.20 ± 0.15	0.36 ± 0.06	0.07 ± 0.18	0.08 ± 0.16	0.13 ± 0.09	0.13 ± 0.10
TIC production rate									
CC- Live	0.50 ± 0.25	0.39 ± 0.27	0.94 ± 0.24	0.44 ± 0.17	0.74 ± 0.23	0.48 ± 0.11	0.54± 0.06	0.31 ± 0.17	0.82 ± 0.07
CC-Control	0.65 ± 0.19	0.35 ± 0.33	0.37 ± 0.10	0.18 ± 0.18	0.30 ± 0.90	0.56 ± 0.20	0.15 ± 0.12	0.07 ± 0.06	0.61 ± 0.32
SA – Live	0.45 ± 0.12	0.25 ± 0.29	0.87 ± 0.10	0.54 ± 0.01	1.11 ± 0.23	0.59 ± 0.22	0.62 ± 0.34	0.23 ± 0.18	0.31 ± 0.02
SA - Control	0.33 ± 0.18	0.04± 0.07	0.61 ± 0.17	0.78 ± 0.63	0.69 ± 0.50	0.60 ± 0.35	0.40 ± 0.26	0.18 ± 0.14	0.19 ± 0.08

5 DEGRADATION KINETICS OF CHLORINATED ALIPHATIC HYDROCARBONS BY COMETABOLIZING METHANE OXIDIZERS NATURALLY ASSOCIATED WITH WETLAND PLANT ROOTS

5.1 INTRODUCTION

Chlorinated aliphatic hydrocarbons (CAHs) are common groundwater contaminants that pose threats to human health, as known or suspected carcinogens (ATSDR 1997). As such, there is a need to understand both natural and engineered processes that can remove CAHs from the environment. Natural attenuation of CAHs has been examined as a potential site remediation approach as it is advantageous economically and environmentally compared to conventional options that are resource intensive. Natural attenuation by biodegradation is especially important because it can occur for a wide range of CAHs by both oxidative and reductive means. Highly-chlorinated CAHs, such as tetrachloroethene, can undergo biodegradation under strongly reducing conditions, whereas less-chlorinated CAHs, such as vinyl chloride, are preferentially biodegraded under oxidizing conditions (Vogel et al. 1987; Bradley 2000).

Wetlands can provide unique environments for oxidative and reductive transformations of CAHs (Amon et al. 2007; Tawney et al. 2008). Reductive transformation of CAHs can be facilitated by the abundant natural organic matter in the wetland soil that can provide electron donors, such as hydrogen (H_2) and volatile fatty acids (Conrad 1999), and support processes such as halorespiration, where the CAHs act as the terminal electron acceptors (Kassenga et al. 2004; Amon et al. 2007). If complete degradation is not achieved through reductive dechlorination, less-chlorinated daughter

CAHs may accumulate in the anaerobic zones of wetland environments. However, daughter CAHs can degrade further and get mineralized under oxidizing conditions in the near-surface environments of the wetland, such as near the sediment-water interface, and in the root zone of wetland plants, by serving as electron donors for microbial metabolism or by cometabolic processes in the presence of numerous growth substrates (Anderson & Walton 1995; Bankston et al. 2002). Oxygen transported from plant shoot to root tissues for metabolic functions can diffuse out into the rhizosphere and the immediate soil environment (Justin & Armstrong 1987; Colmer 2003), which may create favorable conditions for oxidation of CAHs.

Few researchers have examined CAH degradation by oxidative processes in shallow wetland settings with a focus on root zone processes (Bankston et al. 2002; Tawney et al. 2008). Tawney et al. (2008) reported that *cis*DCE degradation can be accomplished by native microorganisms associated with *Phragmites australis* roots, perhaps through cometabolic processes that were facilitated by the release of oxygen and exudates by the roots. Aerobic cometabolism of TCE by methane oxidizing microorganisms that are naturally associated with roots of wetland plants, *Carex comosa* (Powell et al. 2010) and *Scirpus atroviren* roots (Powell et al. 2010; Powell & Agrawal in review), has been reported at bench-scale (see Figure 5.1 for schematic of TCE degradation with wetland plants). The above results suggest that *cis*DCE and other CAHs may potentially degrade similarly by methane oxidizers that are naturally associated with wetland plants (King 1996), particularly since methane is readily available in wetland soils due to the abundance of soil organic matter and the ability of methanogenic microorganisms to breakdown the organic matter for methane production.

The aim of the current investigation was to evaluate the degradation potential and reaction kinetics of three CAHs (*cis*DCE, TCE and 1,1,1TCA) by methane oxidizing microorganisms naturally associated with wetland plant roots of *Carex comosa* Boott. (long hair sedge) at bench-scale. The degradation potential of TCE by naturally occurring methane oxidizers in a similar system (with wetland plant roots of *Carex comosa*) has already been reported (Powell et al. 2010; Powell & Agrawal in review). We expected that the root-associated methane oxidizers had the ability to degrade *cis*DCE, TCE, and 1,1,1TCA via aerobic cometabolism in the presence of methane as a primary substrate. This approach enabled us to evaluate the degradation potential of the above CAHs by naturally occurring methane oxidizers associated with wetland plant roots, and obtain parameters describing degradation kinetics.

5.2 MATERIALS AND METHODS

5.2.1 Plant collection

Wetland plants (*Carex comosa)* were collected from a natural wetland site located in Dayton, OH (USA) in September 2008. After collection, the live plants were maintained in the university greenhouse for approximately 8 months in individual pots containing a 50/50 mix of peat moss and soil from a natural wetland nearby. The plant roots were separated from the plant shoot by clipping, and were thoroughly washed with de-ionized water to remove attached soil in order to prepare for the bench-scale experiments described below.

5.2.2 Experimental set-up

Six microcosms (160 mL borosilcate glass serum bottles; Wheaton, Milliville, NJ) were prepared, where each microcosm had 1 g of fresh roots and 100 mL of growth medium (Fogel et al. 1986) with 60 mL headspace remaining. Three bottles were prepared as live, and the remaining three bottles as killed controls, amended with 6.24 mg L^{-1} of sodium azide to inhibit gram-negative bacterial growth, including the growth of methane-oxidizing bacteria (Ginestet et al. 1998). All microcosms were bubbled with air for ~30 min to start the experiment with dissolved oxygen sufficient to maintain aerobic conditions. The microcosms were then capped with Teflon-lined grey butyl rubber stoppers (20 mm dia.) and sealed with aluminum crimps (both from Wheaton, Milliville, NJ). Pure gaseous methane (CH_4) (5.25 mL equivalent to 1.9 mg L^{-1} aqueous CH_4) was injected into each bottle using a gas-tight glass syringe (Hamilton, Reno, NV) before the bottles were wrapped in aluminum foil, and placed on a rotary shaker (Glas-Col, Terre Haute, IN) set at 30 rpm in an upside down position for gentle horizontal mixing at room temp (22±1 °C). Four cycles of microbial enrichment with CH_4 only were completed followed by 4 cycles with CH_4 and a CAH (~150 μg L^{-1} of *cis*DCE, TCE, or 1,1,1TCA). In experiments with 1,1,1TCA, the microcosms were amended with ~150 μg L^{-1} of TCE as well in the last two cycles (in cycles 5 and 6). Each cycle was 4 days long, and corresponded to a period during which CH_4 degraded nearly completely in the microcosms, and needed to be replenished. At the end of each cycle, all microcosms were opened to carefully discard the aqueous growth medium without removing the roots and replaced with 100 mL of fresh growth medium and amendments, and then incubated at the conditions described earlier.

5.2.3 Chemicals

Stock solutions were prepared separately for each CAH by adding 20 µl of TCE, 25 µl of *cis*DCE, and 25 µl of 1,1,1TCA (99+% ACS grade, Aldrich Chemicals Co., Milwaukee, WI) to a 160 ml glass serum bottle containing Milli-Q water and sealed with a Teflon-lined rubber stopper and aluminum crimp without headspace, and then the bottle was placed on a rotary shaker for 48 hr, to allow the CAH to dissolve completely.

5.2.4 Analysis

Headspace samples from the microcosms were analyzed by gas chromatography to quantify the aqueous concentrations and the total mass of CH_4, CAHs, oxygen (O_2), and inorganic carbon in each microcosm. CH_4 and CAHs were analyzed by a HP 6890 series GC system with flame ionization (FID) and electron capture (ECD) detectors. O_2 and carbon dioxide (CO_2) were analyzed by a HP 5890 series GC system with a thermal conductivity detector. Peak area values from GC analysis were transformed into aqueous concentrations using laboratory calibration curves and a published method (Burris et al. 1996). The aqueous concentrations of CH_4 and CAHs at equilibrium were calculated by the Gas law and Henry's law using a published approach (Burris et al. 1996). Based on measured partial pressures of O_2 and CO_2 in the microcosm headspace, the aqueous [O_2] (DO) and total oxygen mass (TO) were calculated using Henry's Law (Lide & Frederikse 1995), and [dissolved inorganic carbon] (DIC) and total inorganic carbon mass (TIC) were calculated using Henry's Law and carbonate system equilibrium relationships at the measured pH (Pankow 1991). The pH measurements were made using a handheld meter (model AP10 pH/mV/temp, Denver Instrument, Bohemia, NY) by collecting 2-2.5 ml

aqueous samples from each microcosm after gas sampling. See Appendix A, for calculation approaches.

5.2.5 Biomass estimation

The microbial biomass in the microcosms was expected to be attached to the root surface or embedded within the plant roots. The microbial biomass in each cycle was estimated using the stoichiometry of O_2 and CH_4 utilization/loss (Jenal-Wanner & McCarty 1997), which were obtained by subtracting the total O_2 and CH_4 loss in the controls from the live microcosms. The mass loss in the control microcosms was subtracted from the live microcosms to account for mass loss due to the presence of the plant roots. The theoretical O_2 loss was determined using mass balance (Eq. 1, below), in which a fraction of CH_4 lost is oxidized to CO_2 and used for energy (Eq. 1a) and the remaining fraction of CH_4 is assimilated into biomass ($C_5H_7O_2N$) (Eq. 1b):

$$f_e CH_4 + 2f_e O_2 \rightarrow 2f_e H_2O + f_e CO_2 \quad (1a)$$

$$f_s CH_4 + {}^3/_5 f_s O_2 + {}^1/_5 f_s(H^+ + NO_3^-) \rightarrow {}^1/_5 f_s C_5H_7O_2N + {}^7/_5 f_s H_2O \quad (1b)$$

where f_e represents the fraction of CH_4 oxidized for energy, and f_s is the fraction of CH_4 assimilated as biomass (i.e., $f_s + f_e = 1$). The sum of above equations (1a and 1b) is represented in Eq. 1 below:

$$CH_4 + ({}^3/_5 + {}^7/_5 f_e)\, O_2 + {}^1/_5 f_s(H^+ + NO_3^-) \rightarrow {}^1/_5 f_s C_5H_7O_2N + ({}^7/_5 f_s + 2f_e)H_2O + f_e CO_2 \quad (1)$$

In order to calculate f_e (and f_s), the measured ratio of CH_4 mass to O_2 mass utilized was set equal to the stoichiometric ratio expressed in Eq. 1 (i.e., ${}^3/_5 + {}^7/_5 f_e$ = CH_4 mass loss/TO loss); f_s was then utilized to calculate the biomass yield from CH_4 assimilation, Y, as biomass (mmol) per methane (mmol). The biomass concentration, $[X]$ (mmol L^{-1}), was calculated by normalizing the biomass yield, Y, for the liquid volume in the

microcosm (100 mL). Active biomass concentration, $[X_a]$ (mmol L^{-1}), was then estimated based on the biomass growth-and-decay relationship, shown in Eq. 2 (Jenal-Wanner & McCarty 1997):

$$\frac{dX_a}{dt} = Y\left(-\frac{dS}{dt}\right) - bX_a \quad (2)$$

where $-dS/dt$ (mmol L^{-1} d^{-1}) is the rate of CH_4 utilization, and b (d^{-1}) is the organism decay rate. After the enrichment period, it was assumed that $[X_a]$ should reach a steady state value, $[X_{ss}]$ (mmol L^{-1}), due to balance between biomass growth and decay, as in Eq. 3 below:

$$X_{ss} = \frac{YS_T}{VTb} \quad (3)$$

where S_T (mmol) is the total CH_4 loss during a cycle, V (mL) is volume of liquid (100 mL), T (d) is the total cycle length in days; and b taken to be 0.549 d^{-1} (Chang & Criddle 1997).

5.2.6 Data treatment and degradation kinetics

The relative masses, M/M_o, of CH_4 and CAH were calculated for each sampling event, with M_o being their average mass in the control microcosms, and M being their average mass in the live microcosms (Anderson & McCarty 1997). Transformation yield (T_y) was calculated by subtracting the average mass loss in CAH and in CH_4 found in control microcosms from the average mass loss in the live microcosms, and then dividing CAH mass (μmol) degraded by CH_4 mass (mmol) degraded (Anderson & McCarty 1997). Since the aqueous medium in each microcosm was discarded after each cycle, T_y was calculated for each cycle individually. Assuming pseudo first-order kinetics, CAH

degradation rate-constants, $k_{obs\text{-}CAH}$ (d^{-1}), were obtained as fitting parameters (Suarez & Rifai 1999), using Eq. 4 below:

$$[CAH]_i = [CAH]_o e^{-k_{obs-CAH} t_i} \quad (4)$$

where $[CAH]_i$ (μmol L^{-1}) is the CAH concentration at any time, t_i (days), and $[CAH]_o$ (μmol L^{-1}) is the initial CAH concentration; in Eq. 4 above, $k_{obs\text{-}CAH}$ (d^{-1}) can be further defined in terms of $k_{1\text{-}CAH}$ (L $mmol^{-1}$ d^{-1}), the pseudo first-order degradation rate-constant for CAH that is normalized with respect to active biomass, $[X_{ss}]$ (mmol L^{-1}) using Eq 5 below:

$$k_{obs\text{-}CAH}/[X_{ss}] = k_{1\text{-}CAH} \quad (5)$$

A similar approach was used to obtain the degradation rate-constants for CH_4, $k_{obs\text{-}CH4}$ (d^{-1}) assuming pseudo first-order kinetics in Eq. 6 below:

$$[CH_4]_i = [CH_4]_o e^{-k_{obs-CH4} t_i} \quad (6)$$

where $[CH_4]_i$ (μmol L^{-1}) is the CH_4 concentration at any time, t_i (days), and $[CH_4]_o$ (μmol L^{-1}) is the initial CH_4 concentration. As above, $k_{obs\text{-}CH4}$ (d^{-1}) can be further defined in terms of $k_{1\text{-}CH4}$ (L $mmol^{-1}$ d^{-1}), the pseudo first-order degradation rate-constant for CH_4 that is normalized with respect to active biomass, $[X_{ss}]$ (mmol L^{-1}) using Eq 7 below:

$$k_{obs\text{-}CH4}/[X_{ss}] = k_{1\text{-}CH4} \quad (7)$$

The values for $k_{1\text{-}CH4}$ (L $mmol^{-1}$ d^{-1}) and $k_{1\text{-}CAH}$ (L $mmol^{-1}$ d^{-1}) obtained as described above are compared to similar studies (Arvin 1991; Oldenhuis et al. 1991; Arcangeli et al. 1996; Chang & Criddle 1997; Lontoh & Semrau 1998) (Table 5.1).

5.2.7 Statistical analysis.

The effects of methane-oxidizing bacteria treatment (i.e., control vs. live microcosms) were measured on each measurement of CH_4 and CAH mass using a one-way repeated analysis of variance (RM ANOVA) with time as the repeated factor. Statistical analyses were performed using Statistica 9^{TM} (Statsoft, Tulsa, OK, USA).

5.3 RESULTS AND DISCUSSION

5.3.1 CAH degradation with roots

In experiments with *cis*DCE, significant differences in [*cis*DCE] were observed between the live and control microcosms through time in 4 cycles with CH_4 (one-way RM ANOVAs, treatment effect, time effect, $P<0.001$, Figure 5.2a). *cis*DCE can undergo metabolic oxidative degradation in the environment (Coleman et al. 2002; Broholm et al. 2005); however, in this study, *cis*DCE degradation was attributed to cometabolism by the activity of methane-oxidizing bacteria as its loss corresponded to loss in CH_4 and TO, and production of TIC (Figures 5.3, B.4.1 and B.4.7). With initial [*cis*DCE] at 150 ug L^{-1}, the percent loss in *cis*DCE mass in each cycle averaged around 90% and the degradation rate constants for CH_4 and *cis*DCE were comparable through 4 cycles (see Figure 5.3, and k_{obs} in Table B.4.1), which suggest lack of significant toxicity development due to the production of epoxides (Arcangeli et al. 1996). This is in contrast to a previous study (Arcangeli et al. 1996), in which *cis*DCE and methane removal was less efficient at initial [*cis*DCE] above 100 ugL^{-1}. The average net T_y for cycles 1-4 were 0.95 ± 0.04, 1.57 ± 0.50, 1.69 ± 0.60, and 1.18 ± 0.04 *cis*DCE (µmol) CH_4^{-1} (mmol), which is 2-5 times less than reported values (Arvin 1991; Anderson & McCarty 1997), possibly due to the

differences in experimental conditions, including [*cis*DCE]. The initial [*cis*DCE] of 1.14 µM in this study was much less compared to other studies (28 µM (Arvin 1991), and 86 µM (Anderson & McCarty 1997)), which may limit efficient *cis*DCE degradation, in comparison to higher [*cis*DCE]. Chang and Criddle (1997) found greater values of T_y at high [TCE], and attributed that to a more efficient CH_4 utilization for TCE transformation.

In experiments with TCE, significant differences in [TCE] were observed between the live and control microcosms through time in the four cycles with methane (one-way RM ANOVAs, treatment effect, time effect, $P<0.05$, Figure 5.2b). As with the *cis*DCE system, TCE degradation also corresponded to loss in CH_4 and TO, and production of TIC (Figures 5.3, B.4.2 and B.4.7). Such simultaneous TCE and CH_4 loss may indicate cometabolic TCE oxidation by methane oxidizers in the live microcosms, similar to a study with soil from broad-leaf cattail roots (Bankston et al. 2002). In using soil-free roots, this study provides clear evidence that root-associated microorganisms are responsible for the degradation. With initial [TCE] at 150 ug L^{-1}, the average loss in TCE mass was 46 ± 10 % for the 4 cycles, and the degradation rate-constants for CH_4 and TCE (Figure 5.3, and k_{obs} in Table B.4.1) increased in cycles 1 through 4, which suggests that significant epoxide toxicity did not develop (Alvarez-Cohen & McCarty 1991a; Alvarez-Cohen & McCarty 1991b; Henry & Grbicgalic 1991; Chang & Criddle 1997; Han et al. 1999). The average net T_y for cycles 1-4 were from 0.34 ± 0.05, 0.44 ± 0.04, to 0.35 ± 0.11, and 0.26 ± 0.11 TCE (µmol) CH_4^{-1} (mmol), which are considerably less than the reported T_y range 1.5-7.5 TCE (µmol) CH_4^{-1} (mmol) in similar studies (Anderson & McCarty 1997). This may be attributed to a lower initial [TCE] used in this study as methane is used more

efficiently at higher [TCE] (Chang & Criddle 1997), and CH_4 has a greater chance to occupy/bind with active MMO sites than TCE (Chang & Alvarez-Cohen 1995; Chang & Criddle 1997). The ratio of initial [CH_4] to initial [TCE] in the study was ~104, in comparison to 0.34-12 found in previous studies [20].

In experiments with 1,1,1,TCA, the [1,1,1TCA] were not significantly different between the live microcosms and killed controls for any of the four cycles with CH_4 (one-way RM ANOVAs, treatment effect, time effect, $P>0.05$, Figure 5.2c). However, significant changes were observed through time in CH_4 and TO loss, and TIC production in the live microcosms in comparison to the controls (one-way RM ANOVAs, treatment effect, time effect, $P<0.01$, Figures 5.3, B.4.3 and B.4.7). Recent studies have indicated conflicting evidence concerning cometabolic 1,1,1TCA degradation by methane oxidizers; a few studies reported no 1,1,1TCA degradation (Broholm et al. 1990; Henson et al. 1989) while others indicated potential for 1,1,1TCA degradation (Strand et al. 1990; Chang & Alvarez-Cohen 1996). The results of the present study are consistent with Broholm et al. (1990) in which 1,1,1TCA degradation was not observed, and CH_4 degradation wasn't influenced by the presence of 1,1,1TCA up to an initial [1,1,1TCA] of 103 mg L^{-1}. However, Strand et al. (1990) found 1,1,1TCA degradation due to the activity of methane oxidizers at initial [1,1,1TCA] up to 4.47 mg L^{-1}, and yet an increase in initial [CH_4] in excess of 0.25 mg L^{-1} negatively influenced 1,1,1TCA degradation. In the present study, aqueous [CH_4] was maintained at ~1.9 mg L^{-1}, which may have been too high for 1,1,1TCA degradation to occur.

The TCE amendments in the last two cycles (#5 and #6) showed significant differences in [TCE] between the live and control microcosms over time (one-way RM

ANOVAs, treatment effect, time effect, $P<0.01$, Figure 5.2c). In a similar study, the observed TCE degradation rates were lower with both TCE and 1,1,1TCA present than with TCE only and 1,1,1TCA degradation was inhibited in the presence of TCE (Strand et al. 1990). The observed rates for CH_4 and TCE degradation in the current experiment with 1,1,1TCA and TCE were similar to the current TCE only experiment (see Figure 5.3, and k_{obs} in Table B.4.1). The average TCE loss was ~40%. And the average net T_y was 0.31 ± 0.11 and 0.36 ± 0.03 TCE (μmol) CH_4^{-1} (mmol) in the last two cycles, respectively, which is similar to T_y reported above for TCE only experiments.

5.3.2 Degradation parameters

Using the mass balance in Eq. 1, Y, $[X]$, and $[X_{ss}]$ were estimated (Table 5.1), where $[X]$ represents the total biomass concentration, and $[X_{ss}]$ represents the steady-state active biomass concentration resulting from continuous growth-and-decay, such that $[X_{ss}]$ is less than $[X]$. The biomass yield, Y, reported here (Table 5.1) is slightly greater than literature values possibly due to the method used by Jenal-Wanner and McCarty (1997) to estimate biomass; their method compares the ratio of stoichiometric oxygen to methane loss with actual values in the experiment. Jenal-Wanner and McCarty (1997) indicated that the biomass estimate by their method can be higher because of losses in both soluble and particulate biomolecules, which in this study may have occurred as the supernatant was discarded after each cycle (Jenal-Wanner & McCarty 1997). However, actual microbial [biomass] present can still be underestimated in any given cycle due to the possibility that biomass can remain attached to the roots and persist through cycles.

Methane degradation exhibited pseudo first-order kinetics with average observed rate-constant, $k_{1\text{-}CH4}X_{ss}$ (d^{-1}), of 0.49 ± 0.29, 0.52 ± 0.26, and 0.64 ± 0.15 L d^{-1} for *cis*DCE,

1,1,1TCA, and TCE experiments, respectively. Both TCE and *cis*DCE also exhibited pseudo first-order degradation kinetics with average observed degradation rate-constants; $k_{1\text{-}CAH}X_{ss}$ (d^{-1}), of 0.15 ± 0.02 and 0.59 ± 0.07, respectively (Table B.4.1). In comparison, the pseudo first-order degradation rate constants reported in the literature for bench-scale studies are summarized in Suarez and Rifai (1999) with median values of 0.26 (d^{-1}) for TCE and 0.434 (d^{-1}) for DCE isomers. The degradation of *cis*DCE was faster than TCE in the present study, which is consistent with literature reports. Arvin (1991) found the transformation rate of *cis*DCE to be 50% higher than that for TCE.

The $k_{1\text{-}CAH}$ values in this study were less than the literature values obtained from pure culture studies by three orders of magnitude for *cis*DCE, and one to three orders of magnitude for TCE (Table 5.1), which may be attributed to factors such as differences in the experimental design (e.g., temperature; mixed vs. pure cultures; addition of formate, etc.), and the approach to estimate active biomass. Further, the smaller $k_{1\text{-}CAH}$ values obtained in this study may be attributed to mass-transfer effects, since the microbial biomass was presumably localized on or within the roots and not dispersed throughout the batch reactors. While the $k_{1\text{-}CAH}$ values in this study were significantly different than pure-culture studies (Chang & Criddle 1997; Lontoh & Semrau 1998; Aziz et al. 1999; Oldenhuis et al. 1991), they were comparable to values reported for biofilm systems (Table 5.1). It can be argued that similar $k_{1\text{-}CAH}$ values may be due to the similarity of the microbial systems, where the active biomass may be considered a biofilm growing on the root surface. This study suggests that the removal of CAHs within wetland plant roots may be mechanistically comparable to processes within the biofilms (Arvin 1991; Arcangeli et al. 1996), and this insight can be helpful in determining realistic estimates of its performance.

5.4 REFERENCES

Alvarez-Cohen L, McCarty PL (1991a) Effects of Toxicity, Aeration, and Reductant Supply on Trichloroethylene Transformation by a Mixed Methanotrophic Culture. Applied and Environmental Microbiology 57(1): 228-235

Alvarez-Cohen L, McCarty PL (1991b) Product Toxicity and Cometabolic Competitive-Inhibition Modeling of Chloroform and Trichloroethylene Transformation by Methanotrophic Resting Cells. Applied and Environmental Microbiology 57(4): 1031-1037

Amon JP, Agrawal A, Shelley ML, Opperman BC, Enright MP, Clemmer ND, Slusser T, Lach J, Sobolewski T, Gruner W, Entingh AC (2007) Development of a wetland constructed for the treatment of groundwater contaminated by chlorinated ethenes. Ecol. Eng. 30(1): 51-66

Anderson JE, McCarty PL (1997) Transformation yields of chlorinated ethenes by a methanotrophic mixed culture expressing particulate methane monooxygenase. Appl. Environ. Microbiol. 63(2): 687-693

Anderson TA, Walton BT (1995) Comparative Fate of [C-14] Trichloroethylene in the Root-Zone of Plants from a Former Solvent Disposal Site. Environmental Toxicology and Chemistry 14(12): 2041-2047

Arcangeli JP, Arvin E, Mejlhede M, Lauritsen FR (1996) Biodegradation of cis-1,2-dichloro-ethylene at low concentrations with methane-oxidizing bacteria in a biofilm reactor. Water Res. 30(8): 1885-1893

Arvin E (1991) Biodegradation Kinetics of Chlorinated Aliphatic-Hydrocarbons with Methane Oxidizing Bacteria in an Aerobic Fixed Biofilm Reactor. Water Res. 25(7): 873-881

ATSDR AfTSaDR (1997) Toxicological Profile for Trichloroethylene (Update). Atlanta, GA.

Aziz CE, Georgiou G, Speitel GE (1999) Cometabolism of chlorinated solvents and binary chlorinated solvent mixtures using M-trichosporium OB3b PP358. Biotechnology and Bioengineering 65(1): 100-107

Bankston JL, Sola DL, Komor AT, Dwyer DF (2002) Degradation of trichloroethylene in wetland microcosms containing broad-leaved cattail and eastern cottonwood. Water Res. 36(6): 1539-1546

Bradley PM (2000) Microbial degradation of chloroethenes in groundwater systems. Hydrogeology Journal 8(1): 104-111

Broholm K, Jensen BK, Christensen TH, Olsen L (1990) Toxicity of 1,1,1-Trichloroethane and Trichloroethene on a Mixed Culture of Methane-Oxidizing Bacteria. Appl. Environ. Microbiol. 56(8): 2488-2493

Broholm K, Ludvigsen L, Jensen TF, Ostergaard H (2005) Aerobic biodegradation of vinyl chloride and cis-1,2-dichloroethylene in aquifer sediments. Chemosphere 60(11): 1555-1564

Burris DR, Delcomyn CA, Smith MH, Roberts AL (1996) Reductive dechlorination of tetrachloroethylene and trichloroethylene catalyzed by vitamin B-12 in

homogeneous and heterogeneous systems. Environmental Science & Technology 30(10): 3047-3052

Chang HL, Alvarez-Cohen L (1995) Transformation Capacities of Chlorinated Organics by Mixed Cultures Enriched on Methane, Propane, Toluene, or Phenol. Biotechnology and Bioengineering 45(5): 440-449

Chang HL, Alvarez-Cohen L (1996) Biodegradation of individual and multiple chlorinated aliphatic hydrocarbons by methane-oxidizing cultures. Appl. Environ. Microbiol. 62(9): 3371-3377

Chang WK, Criddle CS (1997) Experimental evaluation of a model for cometabolism: Prediction of simultaneous degradation of trichloroethylene and methane by a methanotrophic mixed culture. Biotechnology and Bioengineering 56(5): 492-501

Coleman NV, Mattes TE, Gossett JM, Spain JC (2002) Biodegradation of cis-dichloroethene as the sole carbon source by a beta-proteobacterium. Appl. Environ. Microbiol. 68(6): 2726-2730

Colmer TD (2003) Aerenchyma and an inducible barrier to radial oxygen loss facilitate root aeration in upland, paddy and deep-water rice (Oryza sativa L.). Annals of Botany 91(2): 301-309

Conrad R (1999) Contribution of hydrogen to methane production and control of hydrogen concentrations in methanogenic soils and sediments. Fems Microbiology Ecology 28(3): 193-202

Fogel MM, Taddeo AR, Fogel S (1986) Biodegradation of Chlorinated Ethenes by a Methane-Utilizing Mixed Culture. Appl. Environ. Microbiol. 51(4): 720-724

Ginestet P, Audic J-M, Urbain V, Block J-C (1998) Estimation of Nitrifying Bacterial Activities by Measuring Oxygen Uptake in the Presence of the Metabolic Inhibitors Allylthiourea and Azide. Applied and Environmental Microbiology 64(6): 2266–2268

Han JI, Lontoh S, Semrau JD (1999) Degradation of chlorinated and brominated hydrocarbons by Methylomicrobium album BG8. Archives of Microbiology 172(6): 393-400

Henry SM, Grbicgalic D (1991) Influence of Endogenous and Exogenous Electron-Donors and Trichloroethylene Oxidation Toxicity on Trichloroethylene Oxidation by Methanotrophic Cultures from a Groundwater Aquifer. Appl. Environ. Microbiol. 57(1): 236-244

Henson JM, Yates MV, Cochran JW (1989) Metabolism of Chlorinated Methanes, Ethanes, and Ethylenes by a Mixed Bacterial Culture Growing on Methane. Journal of Industrial Microbiology 4(1): 29-35

Jenal-Wanner U, McCarty PL (1997) Development and Evaluation of Semicontinuous Slurry Microcosms to Simulate *in Situ* Biodegradation of Trichloroethylene in Contaminated Aquifers. Environmental Sciences and Technology 31: 2915-2922

Justin S, Armstrong W (1987) The Anatomical Characteristics of Roots and Plant-Response to Soil Flooding. New Phytologist 106(3): 465-495

Kassenga G, Pardue JH, Moe WM, Bowman KS (2004) Hydrogen thresholds as indicators of dehalorespiration in constructed treatment wetlands. Environmental Science & Technology 38(4): 1024-1030

King GM (1996) In situ analyses of methane oxidation associated with the roots and rhizomes of a bur reed, Sparganium eurycarpum, in a Maine wetland. Appl. Environ. Microbiol. 62(12): 4548-4555

Lide DR, Frederikse HPR (1995) CRC Handbook of Chemistry and Physics, 76th Edition. CRC Press, Inc., Boca Raton, FL

Lontoh S, Semrau JD (1998) Methane and trichloroethylene degradation by Methylosinus trichosporium OB3b expressing particulate methane monooxygenase. Appl. Environ. Microbiol. 64(3): 1106-1114

Oldenhuis R, Oedzes JY, Vanderwaarde JJ, Janssen DB (1991) Kinetics of Chlorinated-Hydrocarbon Degradation by Methylosinus-Trichosporium Ob3b and Toxicity of Trichloroethylene. Appl. Environ. Microbiol. 57(1): 7-14

Pankow JF (1991) Aquatic Chemistry Concepts. CRC Press, Inc., Boca Raton, FL

Powell CL, Agrawal A (in review) Cometabolic biodegradation of trichloroethene by methane oxidizers naturally associated with wetland plant roots: Investigations with Carex comosa and Scirpus atrovirens. Wetlands:

Powell CL, Nogaro G, Agrawal A (2010) Aerobic cometabolic degradation of trichloroethene by methane and ammonia oxidizing microorganisms naturally associated with Carex comosa roots. Biodegradation:

Strand SE, Bjelland MD, Stensel HD (1990) Kinetics of Chlorinated-Hydrocarbon Degradation by Suspended Cultures of Methane-Oxidizing Bacteria. Research Journal of the Water Pollution Control Federation 62(2): 124-129

Suarez MP, Rifai HS (1999) Biodegradation Rates for Fuel Hydrocarbons and Chlorinated Solvents in Groundwater. Bioremediation Journal 3(4): 337-362

Tawney I, Becker JG, Baldwin AH (2008) A Novel Dual-Compartment, Continuous-Flow Wetland Microcosm to Assess cis-Dichloroethene removal from the Rhizosphere. International Journal of Phytoremediation 10: 455-471

Vogel TM, Criddle CS, McCarty PL (1987) Transformations of Halogenated Aliphatic-Compounds. Environmental Science & Technology 21(8): 722-736

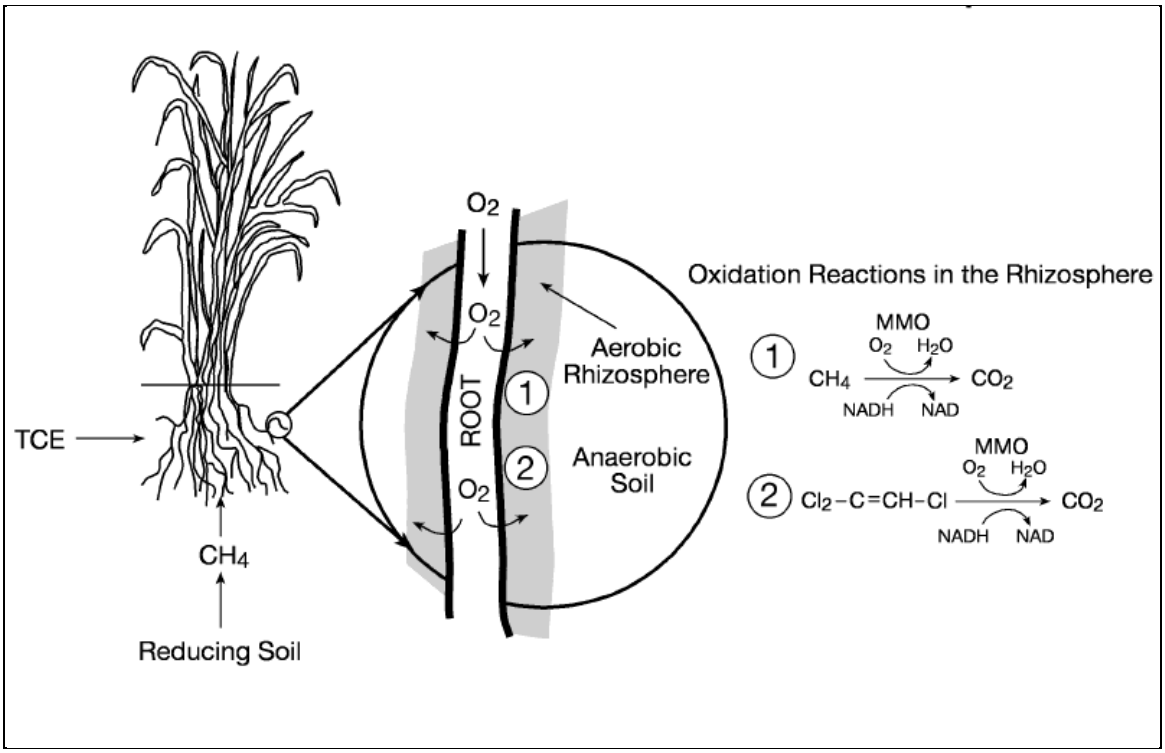

Figure 5.1 TCE cometabolism by methane-oxidizers in the root zone of wetland plants.

A schematic of aerobic TCE cometabolism by methane-oxidizers in the root zone of wetland plants.

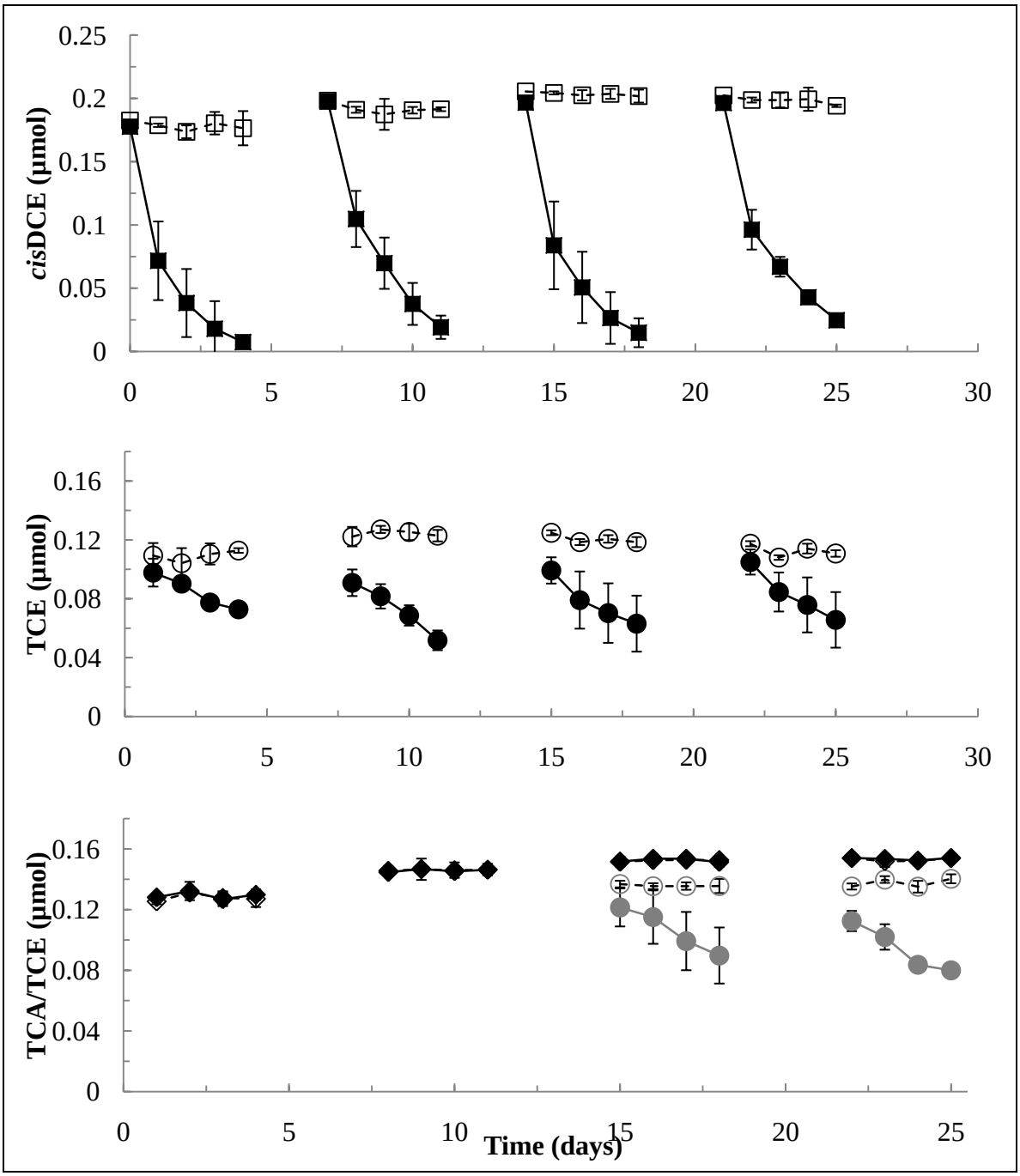

Figure 5.2. Variations in total mass of *cis*DCE, TCE, and 1,1,1TCA

Variations in total mass of *cis*DCE, TCE, and 1,1,1TCA iin live (black symbols) and control (white symbols) microcosms with CH_4 (mean ± SD, n=3 per treatment). The gray symbols in the bottom chart in cycles 3 and 4 represent TCE in live (gray circles) and control (white circles) microcosms.

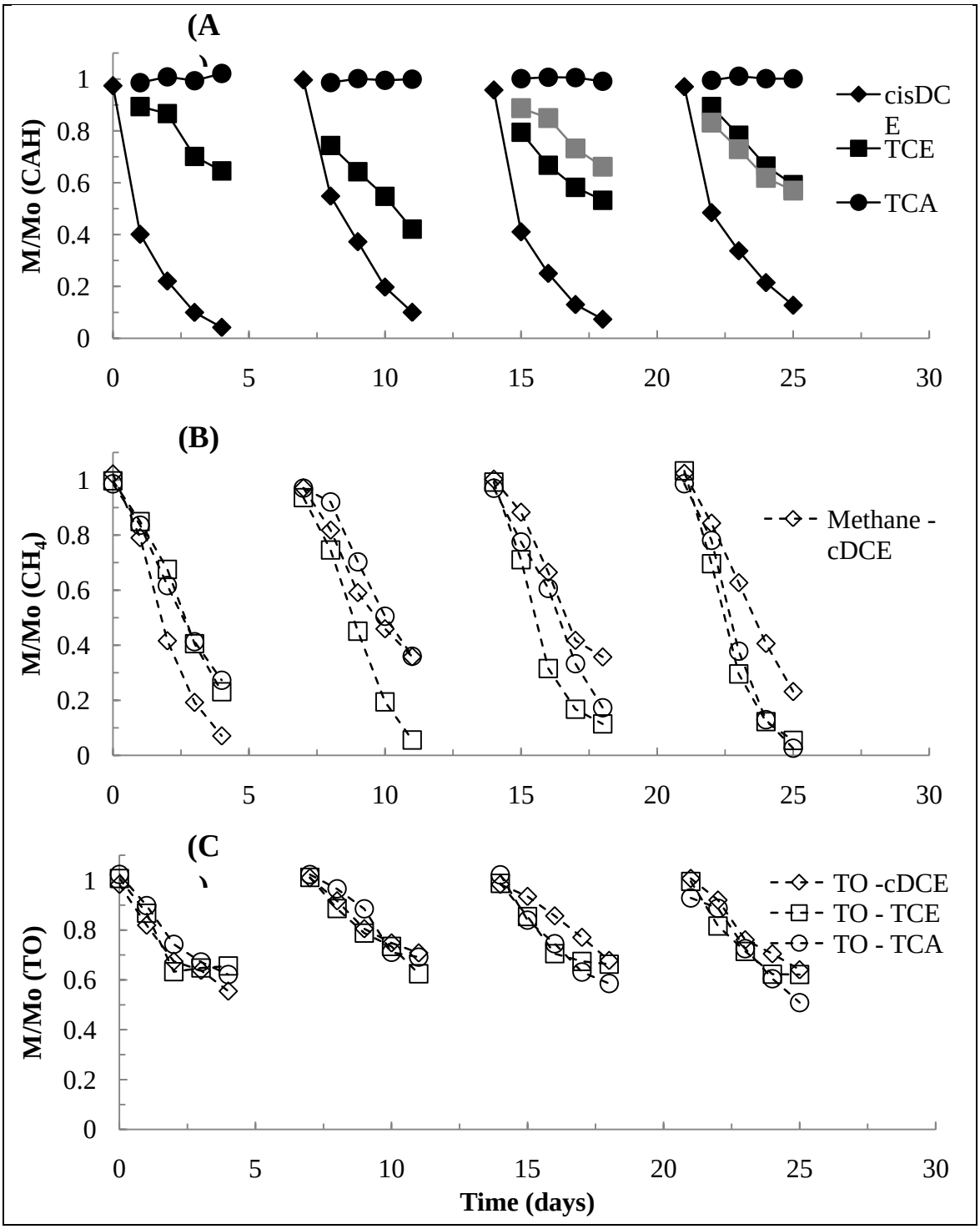

Figure 5.3. Mean relative changes in mass

Mean relative changes in mass of (A) CAH, (B) methane, and (C) oxygen (TO) in the microcosms during the experiments with *cis*DCE, TCE, and 1,1,1TCA (n=3 per treatment). The gray symbols in chart (A) above in cycles 3 and 4 show TCE amendments in microcosms originally with TCA.

Table 5.1. Average Kinetic Parameters

Average Kinetic Parameters for *cis*DCE andTCE. See Table B.4.1 for $k_{obs\text{-}CAH}$ and X_{ss} values for each cycle

	*cis*DCE	TCE	TCE (TCA exp)
TO/CH_4 (mmol $mmol^{-1}$) measured	1.19 ± 0.04	1.09 ± 0.14	1.42 ± 0.13
TO/CH_4 (mmol $mmol^{-1}$) theoretical	$({}^3/_5 + {}^7/_5 f_e)$		
f_e	0.42 ± 0.03	0.35 ± 0.10	0.59 ± 0.09
f_e literature values	0.44 (Chang & Criddle 1997)		
Y (mmol $mmol^{-1}$)*	0.12 ± 0.01	0.13 ± 0.02	0.08 ± 0.02
Y (mmol $mmol^{-1}$)* literature values	0.05-0.07 (Alvarez-Cohen & McCarty 1991; Chang & Criddle 1997; Strand et al. 1990)		
X (mmol L^{-1})*	1.58 ± 0.36	2.03 ± 0.55	1.12 ± 0.43
X_{ss} (mmol L^{-1})*	0.72 ± 0.17	0.92 ± 0.25	0.51± 0.19
$k_{1\text{-}CAH} X_{ss}$ (d^{-1}) measured	0.59 ± 0.07	0.15 ± 0.02	0.12 ± 0.01
$k_{1\text{-}CAH}$ (L $mmol^{-1}$ d^{-1}) * measured	0.83 ± 0.14	0.17 ± 0.04	0.19 ± 0.03
$k_{1\text{-}CAH}$ (L $mmol^{-1}$ d^{-1}) * literature values-cultures	994.4 (Oldenhuis et al. 1991), 971.8. (Aziz et al. 1999) (*M. trichosporium* OB3b)	8.81 (Chang & Criddle 1997) (mixed), 5.65 (Lontoh & Semrau 1998), 327.7 (Oldenhuis et al. 1991) (*M. trichospoium* OB3b)	
$k_{1\text{-}CAH}$ (L $mmol^{-1}$ d^{-1}) * literature values-biofilm	0.963 (Arcangeli et al. 1996) (mixed)	0.33 (Arvin 1991) (mixed)	

*Unit conversions assumed the formula weight for microbial biomass to be ~113 g mol^{-1}

6 SUMMARY

The goal of this research was to evaluate the potential for naturally-occurring microorganisms associated with the roots of selected wetland plants to degrade chlorinated aliphatic hydrocarbons (CAHs). The doctoral research project was divided into the following parts, involving field and laboratory (bench-scale) studies: (1) The field investigation was completed in 2007, and consisted of using newly designed passive devices (pore water samplers) to construct a biogeochemical characterization of an experimental wetland, built at the Wright-Patterson Air Force Base, OH, for evaluation of CAH degradation processes in the shallow vegetated zone; (2) The laboratory (bench-scale) investigation was accomplished during 2008 and 2009 using microcosms containing soil-free, washed roots of two wetland plants, *Carex comosa* and *Scirpus atrovirens*. Laboratory studies of CAH degradation were completed with clipped roots (in comparison to studies with whole/live plants) in order to avoid effects from live plants, such as transpiration, volatilization, and uptake, and influences from soil bacteria. The laboratory investigation was separated into the following objectives: (1) Investigation of TCE degradation potential by methane and ammonia-oxidizing microorganisms that are naturally associated with the roots of *Carex comosa* plant, (2) Investigation of TCE degradation potential by methane-oxidizing microorganisms that are naturally associated with two wetland plant species, *Carex comosa* and *Scirpus atrovirens* roots, and (3) Modeling the degradation kinetics of three different CAHs (*cis*DCE, 1,1,1TCA, and TCE) by methane-oxidizing microorganisms naturally associated with the roots of *Carex comosa*

6.1 A BIOGEOCHEMICAL CHARACTERIZATION OF THE EXPERIMENTAL WPAFB WETLAND, SHOWING CE DEGRADATION IN THE SHALLOW VEGETATED ZONE

The goal of this study was to use newly designed pore water samplers (PWSs) to provide a high-resolution biogeochemical characterization of the pore water parameters in an upward flow constructed wetland formerly receiving chlorinated ethene-contaminated groundwater. The retractable and reusable PWSs were placed in the field at three different locations during the summer months for monthly pore water collection and analysis of redox sensitive species (sulfate, nitrate, ferrous iron, methane) as well as chlorinated ethenes. Pore water was collected at depths between approximately 20 and 80 cm below the ground surface, a suspected zone of increased root activity. The PWSs were designed to study the variation in water chemistry at 9.21 cm vertical resolution; a resolution that could not be obtained by sampling with piezometers alone. The results were used in conjunction with the adjacent piezometers in the middle and lower layers (80 to 140 cm) and measurement from the influent to create vertical profiles.

- The profiles for chloride concentrations, pH, and alkalinity showed consistency between sample locations in space. The pH of the pore water in the wetland did not vary significantly (range between 6.5 to 7.5), yet it decreased along the water flow-path from the bottom of the wetland up through the upper middle. The alkalinity increased from the bottom of the wetland up to about 76 cm below the surface and then decreased to the surface.
- The profiles for ammonium, iron (II), and methane showed consistency between sample locations in space. The concentrations increased from the lower part of the

wetland up to the middle and then decreased in upper part corresponding with the root zone.

- The profiles for nitrate and sulfate showed consistency between sample locations in space. The concentrations decreased from the bottom of the wetland to nearly zero in the middle portion.
- The profiles for the chlorinated ethenes show possible degradation processes. PCE concentrations decreased from the bottom of the wetland to zero in the lower portion. TCE concentrations increased in the lower portion and then decreased in the middle portion and VC formed in the lower to middle portion of the wetland and then decreased in the middle to the surface.

The following conclusions may be drawn in this study:

A. The consistency between PWS locations and comparison with results from piezometers gives support for using PWSs. The fine resolution of the PWSs provides details that could not be determined by sampling with piezometers alone.
B. The pH decrease along water flow-path could possibly be due to release of organic acids and carbon dioxide due to fermentative and oxidative breakdown of the soil organic matter by microbial processes. The sharp increase in alkalinity along water flow-path may be caused by dissolution of soil minerals and the decrease in the middle layer up to the top may be due to the minerals taken up by plants and microorganisms.
C. PCE loss in the bottom of the wetland suggests reductive dechlorination (hydrogenolysis) to TCE and further to VC as both are detected along the water flow-path.

D. Reducing conditions were found at the bottom of the wetland with overlapping zones of nitrate, iron, and sulfate reduction and methanogenesis. The wetlands become more oxidizing near the middle (root zone) and upper layers showing methane and ammonia oxidation, which can aid in VC cometabolism.

6.2 INVESTIGATION OF TCE DEGRADATION POTENTIAL BY METHANE AND AMMONIA-OXIDIZING MICROORGANISMS NATURALLY ASSOCIATED WITH THE ROOTS OF *CAREX COMOSA*

The goal of this study was to examine the degradation potential of trichloroethene (TCE) by the aerobic methane- and ammonia-oxidizing microorganisms naturally associated with wetland plant (*Carex comosa*) roots. The activity and TCE degradation potential of root-associated methane-and ammonia-oxidizing microorganisms naturally present on the root surface and/or embedded within the roots was investigated in 160 mL glass bottle microcosms (in triplicate), each with 1 g of washed, soil-free roots and amended with gaseous methane and oxygen (initial aqueous concentrations were 1.9 mg/L methane and 8 mg/L oxygen) or ammonia and oxygen (initial aqueous concentrations were 20 mg/L of NH_4^+-N and 8 mg/L oxygen). The experimental set-up for the methane experiments included 4 enrichment cycles with methane (no TCE added), followed by 4 cycles with TCE amendments at 150 μg/L. The experimental set-up for the ammonia experiment included 3 enrichment cycles with ammonia (no TCE added), followed by 2 cycles with TCE amendments at 150 μg/L.

- Significant methane and ammonia oxidation were observed reproducibly in batch reactors with washed roots incubated in growth media, where methane oxidation developed faster (2 weeks) compared to ammonia oxidation (4 weeks) in live microcosms.

- After enrichment, the methane oxidizers demonstrated their ability to degrade 150 μg L^{-1} TCE effectively at 1.9 mg L^{-1} of aqueous CH_4. In contrast, ammonia oxidizers showed a rapid and complete inhibition of ammonia oxidation with 150 μg L^{-1} TCE at 20 mg L^{-1} of NH_4^+-N.
- No inhibitory effect of TCE degradation was detected on methane oxidation at above experimental conditions. The average TCE mass removal was ~ 40% and the average T_y for the TCE cycles were 2.8, 3.6, 2.9 and 2.1 μg TCE/ mg CH_4 respectively.

The following conclusions may be drawn in this study:

A. This bench-scale investigation clearly demonstrated that methane and ammonia oxidation can be facilitated by the naturally-occurring microorganisms that are associated with wetland plant (*Carex comosa*) roots. Methane oxidation developed faster than ammonia oxidation during the enrichment period, possibly due to greater initial population of methane oxidizers with the roots or their ability to better compete with other (heterotrophic) microorganisms.

B. Methane oxidizers demonstrated significant TCE degradation reproducibly. For a shorter enrichment period, methane oxidizers were effective in TCE degradation at bench scale without an inhibitory effect due to TCE degradation on methane oxidation.

C. A rapid and complete inhibition of ammonia oxidation was observed under similar experimental conditions in the nitrifying system. Such inhibition of ammonia oxidation may be attributed to a greater sensitivity of ammonia oxidizers towards TCE or its degradation product (TCE epoxide).

D. This study provides key evidence for oxidative cometabolic TCE degradation in vegetated wetlands that has direct implications for the natural attenuation of TCE in impacted aquatic environments.

6.3 INVESTIGATION OF TCE DEGRADATION POTENTIAL BY METHANE OXIDIZING MICROORGANISMS THAT ARE NATURALLY-ASSOCIATED WITH ROOTS OF *CAREX COMOSA* AND *SCIRPUS ATROVIRENS* PLANTS

The goal of this study was to evaluate the degradation potential of TCE through aerobic cometabolism by the methane-oxidizing microorganisms associated with the roots of two wetland plant species, *Carex comosa* and *Scirpus atrovirens*. The aerobic cometabolic degradation of TCE was investigated in 2.4 L Teflon microcosms (in triplicate), each with 15 g of washed, soil-free roots and amended with gaseous methane and oxygen (initial aqueous concentrations were 2.1 mg/L methane and 8 mg/L oxygen) in 9 cycles, to examine the role of root-associated methane-oxidizers. The experimental set-up included 3 enrichment cycles with methane (no TCE added), followed by 6 cycles with variations in TCE amendments (4 cycles at 150 μg/L, 1 cycle at 600 μg/L, and 1 cycle at 900 μg/L).

- The results indicate that methane-oxidizers, which could cometabolically degrade TCE, are naturally associated with the roots of common wetland plants, *Carex comosa* and *Scirpus atrovirens*. The activity of methane-oxidizers and TCE degradation potential were quite comparable for plant species investigated, and the process was reproducible, efficient and rapid.
- The initial rates of methane degradation in 6 cycles with TCE amendments varied between 0.21 and 0.30 mg/L/day for *Carex comosa*, and between 0.14 and 0.25 mg/L/day for *Scirpus atrovirens*. Further, the initial rates of TCE degradation in 4 cycles

amended with aqueous TCE at 150 μg/L varied between 0.08 and 0.16 μg/L/day for *Carex comosa*, and between 0.07 and 0.19 μg/L/day for *Scirpus atrovirens*.

- The average TCE mass removal varied between 24 and 32%, and the overall transformation yield (T_y) was calculated as 0.0004 mmol TCE/mmol CH_4 for both plant species.

The following conclusions may be drawn in this study:

A. *Carex comosa* and *Scirpus Atrovirens* roots have differing morphology. The thinker roots of *Carex comosa* may provide greater oxygen loss, and thus support more oxidizing conditions (for Fe(II) and methane-oxidizing microbes) in its rhizosphere.

B. Greater CH_4 loss with *Carex comosa* roots during enrichment may indicate greater initial number of methane oxidizers in the roots possibly due to the roots offering a more favorable habitat for aerobic microbes (e.g., iron oxidizing and methane oxidizing bacteria).

C. Both *Carex comosa* and *Scirpus atrovirens* roots may provide suitable habitat for methane-oxidizing activities. Following enrichment, methane oxidation and TCE degradation was similar for both plant species.

D. TCE degradation potential observed with *Carex comosa* and *Scirpus atrovirens* roots may occur with other emergent plants expressing methanotrophic activity, and wetland plants can play an important role in natural attenuation of TCE in contaminated aquatic environments.

6.4 MODELING OF DEGRADATION KINETICS OF CIS-DCE, 1,1,1-TCA, AND TCE BY METHANE OXIDIZING MICROORGANISMS NATURALLY ASSOCIATED WITH *CAREX COMOSA* ROOTS.

The goal of this study was to evaluate the cometabolic degradation kinetics of cis-1,2-dichloroethene (*cis*DCE), TCE, and 1,1,1-trichloroethane (1,1,1TCA) by methane oxidizers associated with the roots of the wetland plant species *Carex comosa*. Laboratory microcosms (160 ml glass bottles) were created with 1 g of washed roots to study the activity and CAH degradation potential of the root-associated methane oxidizers at initial aqueous methane concentrations of ~1.9 mg L^{-1}, and initial aqueous CAH concentrations of ~150 μg L^{-1}. The experimental set-up included 4 enrichment cycles with methane (no TCE added), followed by 4 cycles with CAH amendments. Microbial biomass in each CAH cycle was estimated using the stoichiometry of O_2 and CH_4 utilization/loss, which were obtained by subtracting the total O_2 and CH_4 loss in the controls from the live microcosms.

- The results indicate that methane-oxidizers could significantly degraded *cis*DCE and TCE through cometabolic pathways, with a relative degradation efficiency of approximately 90% and 46%, respectively. 1,1,1TCA degradation was not observed in the presence of active methane oxidizers.
- Both TCE and *cis*DCE degradation could be described by first-order kinetics, with pseudo first-order degradation rate-constants of 0.15 ± 0.02 and 0.59 ± 0.07 d^{-1}, respectively.
- Normalized degradation rate constants (**$k_{1\text{-}CAH}$**) in this study were less than the literature values obtained from pure culture studies by three orders of magnitude for *cis*DCE, and one to three orders of magnitude for TCE.

The following conclusions may be drawn in this study:

A. TCE and 1,2-*cis*DCE degradation was possible by methane oxidizers naturally associated *Carex comosa* roots. 1,1,1-TCA degradation was not observed under the experimental conditions.

B. $k_{1\text{-CAH}}$ values for TCE and *cis*DCE were much less than the values obtained for systems with pure-cultures which may be attributed to several factors relating to experimental design or biomass approximation.

C. $k_{1\text{-CAH}}$ values were comparable to values reported for biofilm systems, possibly due to the similarity of the microbial systems, where the active biomass in this study may be considered a biofilm growing on the root surface.

D. The removal of CAHs within wetland plant roots may be mechanistically comparable to processes within the biofilms, and this insight can be helpful in determining realistic estimates of its performance.

APPENDIX A ANALYSIS AND CALCULATIONS

A.1 FIELD SAMPLE ANALYSIS AND CALCULATIONS

A.1.1 Methane and Chlorinated Ethenes

The GC procedures of purge and trap and headspace injection were used to detect chlorinated ethenes such as Perchloroethene (PCE), Trichloroethene (TCE), isomers of Dichloroethene (cis and trans DCE) and Vinyl chloride (VC) as well as nonchlorinated methane. Samples were divided for purge and trap and headspace injection: 7.5ml stored in 15ml Teflon sealed and capped bottles for next-day analysis by direct headspace injection and 5ml stored in a luer-locked syringe for same-day analysis by purge and trap. For headspace injection, the 15ml bottles were rotated upside down for approximately 3 hours and are stored in the refrigerator overnight. The next day, the bottles were brought to room temperature and analyzed on the GC in triplicate by headspace injection. Data in the form of peak areas were obtained from each chromatograph and converted into concentration units (parts per billion (ppb)) based on the value of slope obtained from analysis of VOC standards. Concentrations were divided by the respective molecular weights of the compounds to get millimolar concentrations (mM).

Liquid standard preparations were for PCE, TCE, cis-DCE, and trans-DCE. 160ml bottles were filled with DI water, sealed and capped without head space. A known amount of VOC was injected into the bottle to give a concentration of 20ppm. For dissolution to occur, the bottles were placed on a rotator for approximately 48 hrs for PCE and TCE and 24 hrs for cis-DCE and trans-DCE. Serum bottles were filled with DI water, sealed and capped without head space. Dilutions were prepared for a range of

concentrations (Table A.1) by taking out a known volume of water and adding the same volume of stock. The standards were placed on a rotator for approximately 1 hr after which, the analysis were by purge and trap method.

Table A.1 VOC Liquid Standards

Data used to calculate VOC Liquid Standards.

PCE			
Density		1.6	g/cc
Vol. bottle for stock sol		160	Ml
Vol. PCE injected into stock bottle *(99.9+%, HPLC grade, Sigma Aldrich)*		2.0	Ml
Mass PCE in stock bottle.		3.2	mg PCE
Concentration of stock sol.		20	mg/l (ppm)
Serum bottle.		72	Ml
No.	**Vol. of stock solution to be injected (µl)**	**Concentration in 72ml serum bottle (µg/L)**	
1	36	10	
2	72	20	
3	108	30	
4	180	50	
5	360	100	
TCE			
Density		1.47	g/cc
Vol. bottle for stock sol;		160	Ml
Vol. TCE injected into stock bottle *(99%, Sigma Aldrich)*		2.2	Ml
Mass TCE in stock bottle.		3.2	mg TCE
Concentration of stock sol.		20.2	mg/l (ppm)
Serum bottle.		72	Ml
No.	**Vol. of stock solution to be injected (µl)**	**Concentration in 72ml serum bottle (µg/L)**	
1	36	10	
2	71	20	
3	107	30	
4	178	50	
5	356	100	

cis-DCE			
Density		1.26	g/cc
Vol. bottle for stock sol;		160	Ml
Vol. Cis- DCE injected into stock bottle (*99%, Sigma Aldrich)*		2.5	Ml
Mass Cis-DCE in stock bottle.		3.2	mg cis-DCE
Concentration of stock sol.		19.7	mg/l (ppm)
Serum bottle.		72	Ml
No.	**Vol. of stock solution to be injected (µl)**	**Concentration in 72ml serum bottle (µg/L)**	
1	36	10	
2	72	20	
3	108	30	
4	180	50	
5	360	100	
Trans-DCE			
Density		1.28	g/cc
Vol. bottle for stock sol;		160	Ml
Vol. Trans-DCE injected into stock bottle *(99.7%, (GC) Stabilized, Acros Organics)*		2.5	Ml
Mass Trans-DCE in stock bottle.		2.56	mg trans-DCE
Concentration of stock sol.		20	mg/l (ppm)
Serum bottle.		72	Ml
No.	**Vol. of stock solution to be injected (µl)**	**Concentration in 72ml serum bottle (µg/L)**	
1	36	10	
2	72	20	
3	108	30	
4	180	50	
5	360	100	

Gaseous standard preparations were for Methane and VC. Serum bottles were filled with 9 mL of deionized water and then sealed and capped. A different volume of gas was injected into each bottle (30 µl, 100 µl, 300 µl, and 1ml). Analysis was by direct head space injection The procedure was similar for VC except standard samples were

prepared in 72 ml bottles and the analysis were by purge and trap. For methane see Appendix A.3.1 The table below lists the GC parameters.

Table A.2 GC operating parameters

The operating procedures for the 6890 GC.

Hewlett-Packard 6890 GC	
•analytical equipment : GC/FID	•analytical equipment : GC/ECD
•target compounds: •temperature of injector : 200ºC •temperature of detector :250ºC •oven temperature programming : -initial : 50ºC for 2min -rate : 10ºC/min from 50ºC to 160ºC no hold at 100ºC -post tempt: 50 ºC •splitless •column : J&W Scientific. Inc. No. 1134332 GS Gas Pro Capillary (30m*0.32mm* 0.00mm nominal) •H_2 flow : 40 ml/min •Air flow : 450 ml/min •Make up gas flow: N_2, constant flow 45ml/min •Injection volume from the headspace	•target compounds: •temperature of injector : 50ºC •temperature of detector :250ºC •oven temperature programming : -initial : 50ºC for 2min -rate : 10ºC/min from 50ºC to 160ºC no hold at 100ºC -post tempt: 50 ºC •Splitless •column : Agilent 19091V-413 HP-624 Special Analysis Column Capillary (30m*0.32mm*1.8um nominal) •Anode Flow : 6ml/min •make up gas flow : N_2, 60ml/min • Injection volume from the headspace

A.1.2 Ion analysis

The samples (2 mL each) for ion analysis were filtered into a centrifuge tube filled with 8ml of filtered deionized water for a 5 times dilution. Approximately 0.5 ml of the diluted sample was injected into the cuvettes for anion chromatography analysis using Dionex ion chromatograph model 2500; triplicates were prepared for each sample. Data in the form of peak areas were obtained from each chromatograph and converted into concentration units (parts per billion (ppm)) based on the value of slope obtained from

analysis of ion standards (Table A.3). Concentrations were divided by the respective molecular weights of the ions to get millimolar concentrations (mM).

Table A.3 Anion Standards

Data used to calculate Anion Standards.

Analyte	Manufacturer	Concentration of Stock (C1) (ppm)	Volume of Stock Solution (V1) (ml)	Volume of Standard (V2) (ml)	Concentration of Standard Solution (C2) (ppm)
SO_4^{2-}	FisherChemicals	1000	0.1, 0.2, 1	100	1, 2, 10
NO_3^-	FisherChemicals	1000	0.02, 0.1, 0.3	100	0.2, 1, 3
NO_2^-	FisherChemicals	1000	0.02, 0.1, 0.3	100	0.2, 1, 3
Cl^-	FisherChemicals	1000	0.2, 1, 3	100	2, 10, 30

A.1.3 Iron analysis

The reagents needed for iron analysis on the spectrophotometer were Concentrated hydrochloric acid (12N HCl), Acetate buffer solution, Hydroxylamine solution, 1,10-Phenanthroline solution. The samples were stored in syringes with luer-lock tips and placed in a glove box for sample preparation. 0.25ml of 12N HCl was added by pipette to each sample for stabilization. 1ml of sample water was filtered into centrifuge tubes from the syringes using a 0.2μm filter and 9ml of filtered deionized water was added for dilution. The samples were separated into total iron analysis and ferrous iron analysis. For total iron the following reagents were added: 1ml of diluted sample, 1ml of acetate buffer solution, 0.5ml of hydroxylamine solution, 0.5ml of 1,10-Phenanthroline solution. For ferrous iron the following reagents were added: 1ml of diluted sample, 1ml of acetate buffer solution, 1ml of 1,10-Phenanthroline solution. After 10 minutes, the solutions were added to the spectrophotometer cuvettets and analyzed on a Perkin Elmer Lambda

45 UV/VIS spectrophotometer using a wavelength quant method at λ=510. Data in the form of absorbance were obtained from the spectrophotometer and converted into concentration units (parts per million (ppm)) based on the value of slope obtained from analysis of iron standards (Table A.4). Concentrations were divided by the respective molecular weights of the compounds to get millimolar concentrations (mM).

Table A.4 Iron standards

Data used to calculate Iron Standards.

Iron Standards	Concentration of Stock (C1) (ppm)	Volume of Stock Solution (V1) (ml)	Volume of Standard (V2) (ml)	Concentration of Standard Solution (C2) (ppm)
1	50	0	10	0
2	50	0.15	10	0.75
3	50	0.3	10	1.5
4	50	0.6	10	3
5	50	0.9	10	4.5
6	50	1.2	10	6

A.1.4 Ammonia Analysis

The following materials were needed for ammonia analysis by the Hach method on the spectrophotometer: Hach tubes, Ammonia Salicylate reagent pillows, Ammonia Cyanurate reagent pillows. The samples were stored in syringes with luer-lock tips and placed in a glove box for sample preparation. 1ml of sample water was filtered into centrifuge tubes from the syringes using a 0.2μm filter and 9ml of filtered deionized water was added for dilution. 2ml of diluted sample was added to Hach tubes and then an ammonia Salicylate reagent pillow and an ammonia Cyanurate reagent pillow were added to the Hach tubes. After 20 minutes, the solutions were added to the spectrophotometer

cuvette and analyzed on a Perkin Elmer Lambda 45 UV/VIS spectrophotometer using a wavelength quant method at λ=655. Data in the form of absorbance were obtained from the spectrophotometer and converted into concentration units (parts per million (ppm)) based on the value of slope obtained from analysis of ammonia standards (Table A.5). Concentrations were divided by the respective molecular weights of the compounds to get millimolar concentrations (mM).

Table A.5 Ammonia standards

Data used to calculate ammonia standards.

Ammonia Standards	Concentration of Stock (C1) (ppm)	Volume of Stock Solution (V1) (ml)	Volume of Standard (V2) (ml)	Concentration of Standard Solution (C2) (ppm)
1	1	0	5	0
2	1	0.1	5	0.02
3	1	0.3	5	0.06
4	1	0.5	5	0.1
5	1	1	5	0.2
6	1	3	5	0.6
7	1	5	5	1
8	10	0.75	5	1.5
9	10	1.25	5	2.5

A.1.5 Alkalinity Analysis

The following materials were needed for alkalinity analysis (Sarazin et al. 1988) on the spectrophotometer: Alkalinity Reagent (10mM Formic Acid + 50 mg/L Bromophenol Blue) and Sodium Bicarbonate. The samples were stored in syringes with luer-lock tips and placed in a glove box for sample preparation. 200µl of sample water was filtered into centrifuge tubes from the syringes using a 0.2µm filter and 2ml of Alkalinity Reagent was added. After 30 minutes, the solutions were added to the spectrophotometer

cuvette and analyzed on a Perkin Elmer Lambda 45 UV/VIS spectrophotometer using a wavelength quant method at λ=590. Data in the form of absorbance were obtained from the spectrophotometer and converted into concentration units (mM) based on the value of slope obtained from analysis of alkalinity standards (Table A.6).

Table A.6 Alkalinity standards

Data used to calculate alkalinity standards.

Alkalinity Standards	Concentration of Stock (C1) (ppm)	Volume of Stock Solution (V1) (ml)	Volume of Standard (V2) (ml)	Concentration of Standard Solution (C2) (ppm)
1	20	0	50	0
2	20	2.5	50	1
3	20	5	50	2
4	20	12.5	50	5
5	20	25	50	10
6	20	50	50	20

A.2 GAS CHROMATOGRAPHIC ANALYSIS

The headspace samples from the microcosms were analyzed by gas chromatography to estimate aqueous phase CH_4, TCE (0.25 mL), DO, and DIC (0.05 mL) concentrations in each microcosm. CH_4 and TCE were analyzed by a HP 6890 series GC system with flame ionization (FID) and electron capture (ECD) detectors; CH_4 separated on a capillary column (GS GasPro, 30m x 0.32mm; J&W Scientific) connected to FID, and TCE was separated on a capillary column (HP-624, 30m x 0.32mm; Agilent Technologies), connected to ECD, with helium as the carrier gas at constant flow of 2.1 mL min^{-1}. The 6890 GC method settings for both analytes were as follows: inlet and detector temperatures at 200 ºC and 250 ºC, respectively, and oven temperature program was 50 ºC for 2 min, 10 ºC min^{-1} from 50 to 160 ºC, and no hold at 160 ºC (total 13 min).

The make-up gas for the GC was N_2 with a flow rate of 60 mL min^{-1} for ECD, and 45 mL min^{-1} for FID. The flow rate of H_2 and air were 40 mL min^{-1} and 450 mL min^{-1}, respectively. O_2 and CO_2 were analyzed by a HP 5890 series GC system with a thermal conductivity detector (TCD), and a packed column (Shin Carbon 100/120, 2m x 1mm; Restek, Belefonte, PA), with N_2 as carrier gas. The GC method settings for O_2 and CO_2 analysis were as follows: inlet and detector temperatures at 100 ºC and 160 ºC, respectively, and oven temperature program was 30 ºC for 1.5 min, 25 ºC min^{-1} from 30 to 155 ºC, and no hold at 155 ºC (total 6.5 minutes).

A.3 CALCULATIONS FOR ESTIMATING VOLATILE'S MASS

A.3.1 Methane

The number of moles, n, was determined using the ideal gas law;

$$n = \frac{PV}{RT}$$

where R = gas constant (0.0821 atm L mol^{-1} K^{-1}; T = temperature (298 K), P = Pressure (1 atm); V = volume of gas injected.

The number of moles was divided by the aqueous volume (V_w) to give moles per liter before partitioning and then the moles per liter were converted to the concentration (C_w) in mg per liter using the molecular weight of methane (16 g $mole^{-1}$):

$$C_w = \frac{n}{V_w}\ x\ 16\ \frac{g}{mole}$$

The total mass of methane in the microcosm was determined by:

$$m = C_w * V_w$$

where, V_w = volume of water, and m = mass of methane in moles.

A dimensionless Henry's constant ($K_H^{'}$) of 28.5 for Methane at 20°C (Schwarzenbach et al. 1995) was used to determine the fraction in water (f_w):

$$f_w = \frac{1}{(1 + K_H^{'}\left(\frac{V_a}{V_w}\right))}$$

where, V_a = volume of air.

The fraction in water was used to determine the mass in the aqueous phase after partitioning (m_w):

$$m_w = f_w \, x \, m$$

and the mass of methane in the head space (m_a)

$$m_a = m \, x \, (1 - f_w).$$

The concentrations in the aqueous phase (C'_w) and head space were determined using the respective masses and volumes:

$$C_w^{'} = \frac{m_w}{V_w} \text{ and } C_a = \frac{m_a}{V_a}.$$

A.3.2 Oxygen

The aqueous concentration was calculated using Henry's law and a Henrys constant (k_H) of 1.3x 10^{-3} mole L^{-1} atm^{-1} (Lide and Frederikse 1995) and partial pressure

(*Pi*) in the headspace (in atm) and converted to mg L^{-1} using the molecular weight of oxygen (32 g $mole^{-1}$) and after a unit conversion:

$$C_w^{'} = k_H x P_i \; x \; 32 \; \frac{g}{mole} \; x \; 1000 \; \frac{mg}{g}$$

The total mass of oxygen in moles (*m*) was found by calculating the mass in the aqueous phase using the aqueous volume (V_w) and adding it to the mass in the headspace, which was determined using the ideal gas law calculated with the partial pressure and the volume in the headspace (V_a):

$$m = \left(\frac{P_i V_a}{RT} \; x \; 32 \; \frac{g}{mole} \; x \; 1000 \frac{mg}{g}\right) + \; (C_w^{'} \; x \; V_w)$$

where *R* = gas constant (0.0821 atm L mol^{-1} K^{-1}; *T* = temperature (298 K)

A.3.3 Carbon dioxide

The aqueous concentration of CO_2 or dissolved inorganic carbonate (DIC) was calculated using the following relationships (Pankow 1991):

$$[DIC] = \; ([H_2CO_3^*] + \; [HCO_3^-] + \; [CO_3^{2-}]$$

If pH ~7, then

$$[DIC] = \; ([H_2CO_3^*] + \; [HCO_3^-]$$

where

$$[H_2CO_3^*] = \; k_H \; x \; pCO_2$$

and

$$[HCO_3^-] = \frac{k_1 \, x \, k_H x \, pCO_2}{10^{-pH}}$$

where, $k_H = 10^{-1.47}$ and $k_1 = 10^{-6.35}$

Adding the two together and doing a unit conversion:

$$C_w^{'} = ([H_2CO_3^*] + \, [HCO_3^-]) \, x \, 44 \, \frac{g}{mole} \, x \, 1000 \, \frac{mg}{g}$$

The total mass (m) was found by calculating the mass in the aqueous phase using the aqueous volume (V_w) and adding it to the mass in the headspace, which is determined using the ideal gas law calculated with the partial pressure (P_i) and the volume in the headspace (V_a):

$$m = \left(\frac{P_i V_a}{RT} \, x \, 44 \, \frac{g}{mole} \, x \, 1000 \frac{mg}{g}\right) + \, (C_w^{'} \, x \, V_w)$$

where R = gas constant (0.0821 atm L mol^{-1} K^{-1}; T = temperature (298 K)

A.3.4 CAH Calculations

Stock solutions were prepared separately for each CAH by adding 20 µl of TCE (99.5% ACS grade, ACROS Organics Co., Morris Plains, NJ), 25 µl of *cis*DCE (97% ACS grade, Aldrich Chemicals Co., Milwaukee, WI), and 25 µl of 1,1,1TCA (99+% ACS grade, Aldrich Chemicals Co., Milwaukee, WI) to a 160 ml glass serum bottle containing Milli-Q water and sealed with Teflon-lined rubber stopper and aluminum crimp without headspace, and then the bottle was placed on a rotary shaker for 48 hr, to allow the CAH to dissolve completely. The CAH stock solution was removed from the sealed serum bottle using a glass syringe needle pierced through the stopper. The CAH

concentrations in the water and in the serum bottle headspace after partitioning were calculated using a published approach (Burris et al. 1996). The concentration (C_w) in mg per liter before equilibration was determined as follows:

$$C_w = \frac{V}{V_w}\ x\ C$$

The total mass in the microcosm was determined by:

$$m = C_w * V_w$$

where, V_w = volume of water.

A dimensionless Henry's constant ($K_H^{'}$) of 0.299 for TCE, 0.124 for *cis*DCE, and 0.584 for 1,1,1TCA at 20°C (Gossett 1987) was used to determine the fraction in water (f_w):

$$f_w = \frac{1}{(1 + K_H^{'}\left(\frac{V_a}{V_w}\right))}$$

where, V_a = volume of air.

The fraction in water was used to determine the mass in the aqueous phase after partitioning (m_w):

$$m_w = f_w\ x\ m$$

and the mass in head space (m_a)

$$m_a = m\ x\ (1 - f_w).$$

The concentrations in the aqueous phase (C'_w) and head space were determined using the respective masses and volumes:

$$C'_w = \frac{m_w}{V_w} \text{ and } C_a = \frac{m_a}{V_a}$$

A.3.5 References

Schwarzenbach, R. P.; Gschwend, P. M.; Imboden, D. M., *Environmental organic chemistry illustrative examples, problems, and case studies*. John Wiley and Sons, Inc.: New York, 1995; p 392.

Lide, D. R.; Frederikse, H. P. R., *CRC Handbook of Chemistry and Physics, 76th Edition*. 76th Edition ed.; CRC Press, Inc.: Boca Raton, FL, 1995.

Pankow, J. F., *Aquatic Chemistry Concepts*. CRC Press, Inc.: Boca Raton, FL, 1991; p 683.

Burris, D. R.; Delcomyn, C. A.; Smith, M. H.; Roberts, A. L., Reductive dechlorination of tetrachloroethylene and trichloroethylene catalyzed by vitamin B-12 in homogeneous and heterogeneous systems. *Environmental Science & Technology* **1996,** *30*, (10), 3047-3052.

Gossett, J. M., Measurement of Henrys Law Constants for C1 and C2 Chlorinated Hydrocarbons. *Environmental Science & Technology* **1987,** *21*, (2), 202-208.

Jenal-Wanner, U.; McCarty, P. L., Development and Evaluation of Semicontinuous Slurry Microcosms to Simulate *in Situ* Biodegradation of Trichloroethylene in Contaminated Aquifers. *Environmental Sciences and Technology* **1997,** *31*, 2915-2922.

Chang, W. K.; Criddle, C. S., Experimental evaluation of a model for cometabolism: Prediction of simultaneous degradation of trichloroethylene and methane by a methanotrophic mixed culture. *Biotechnology and Bioengineering* **1997,** *56*, (5), 492-501.

APPENDIX B ADDITIONAL INFORMATION

B.1 FIELD EXPERIMENTAL DATA

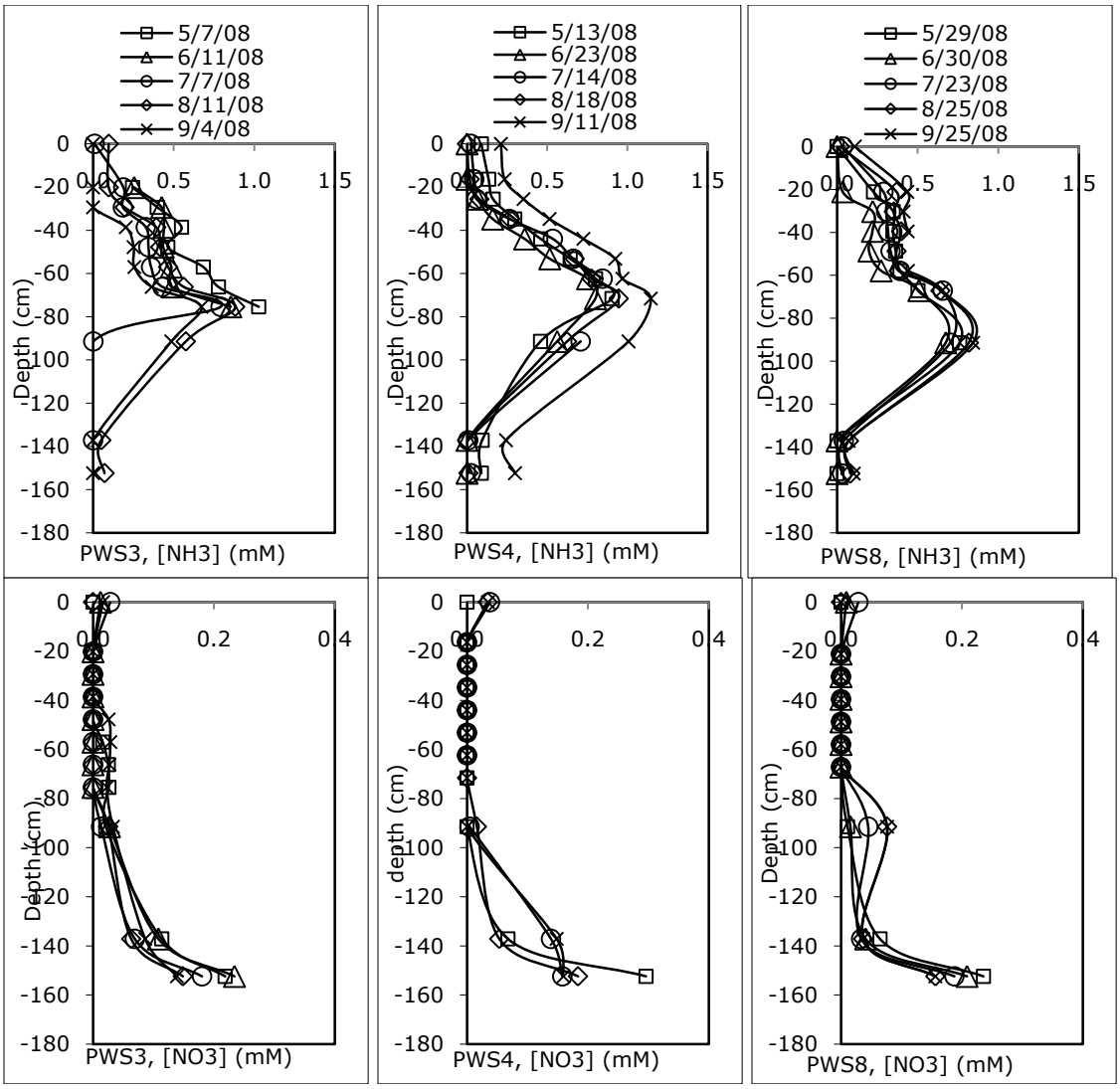

Figure B.1.1 WPAFB wetland profiles of nitrate and ammonia

Nitrate and ammonia (mM) profiles from the PWS units and Piezometers

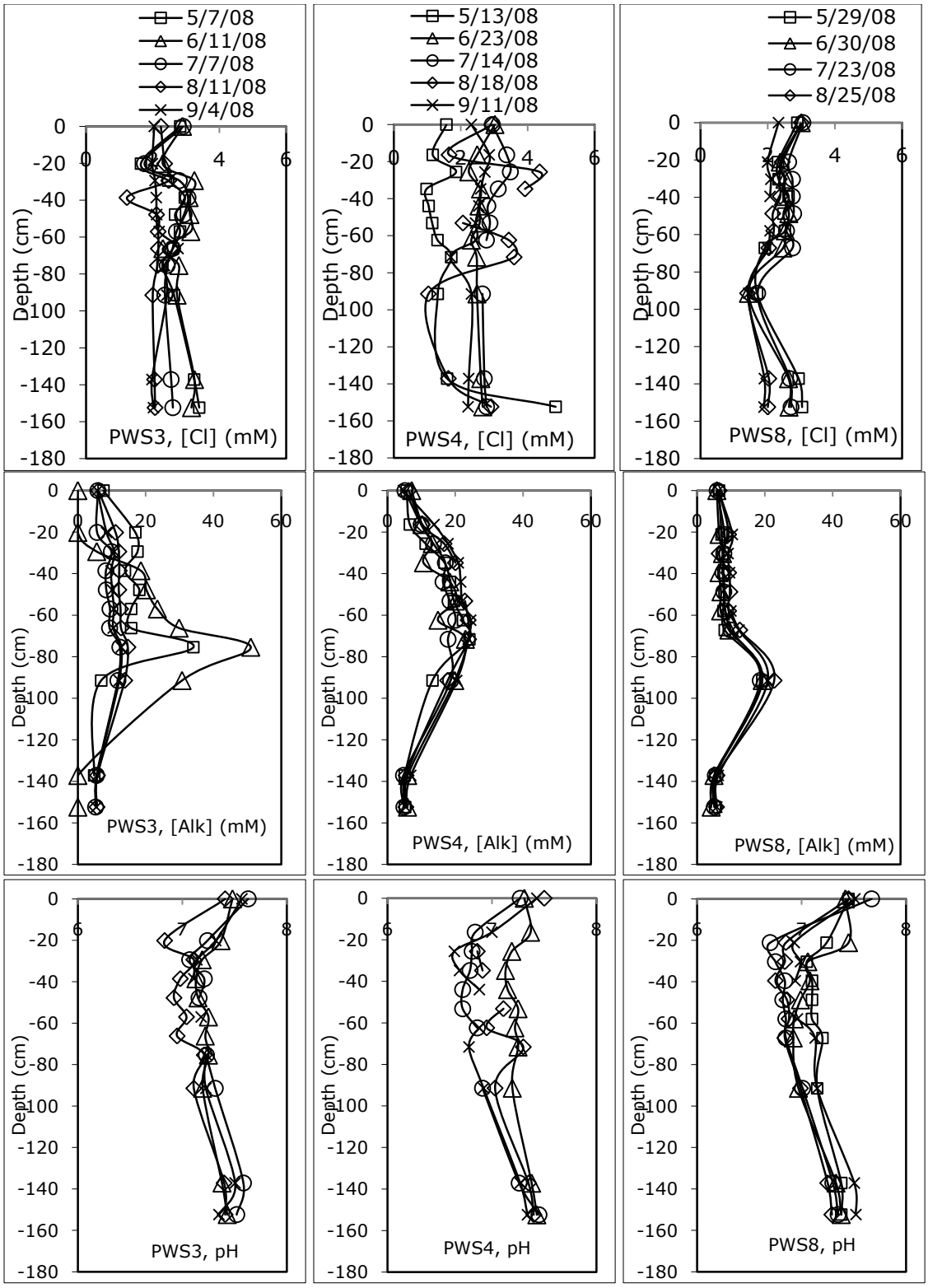

Figure B.1.2 WPAFB wetland profiles of Chloride, pH, and Alkalinity

Chloride (mM), pH, and Alkalinity (mM) profiles from the PWS units and Piezometers

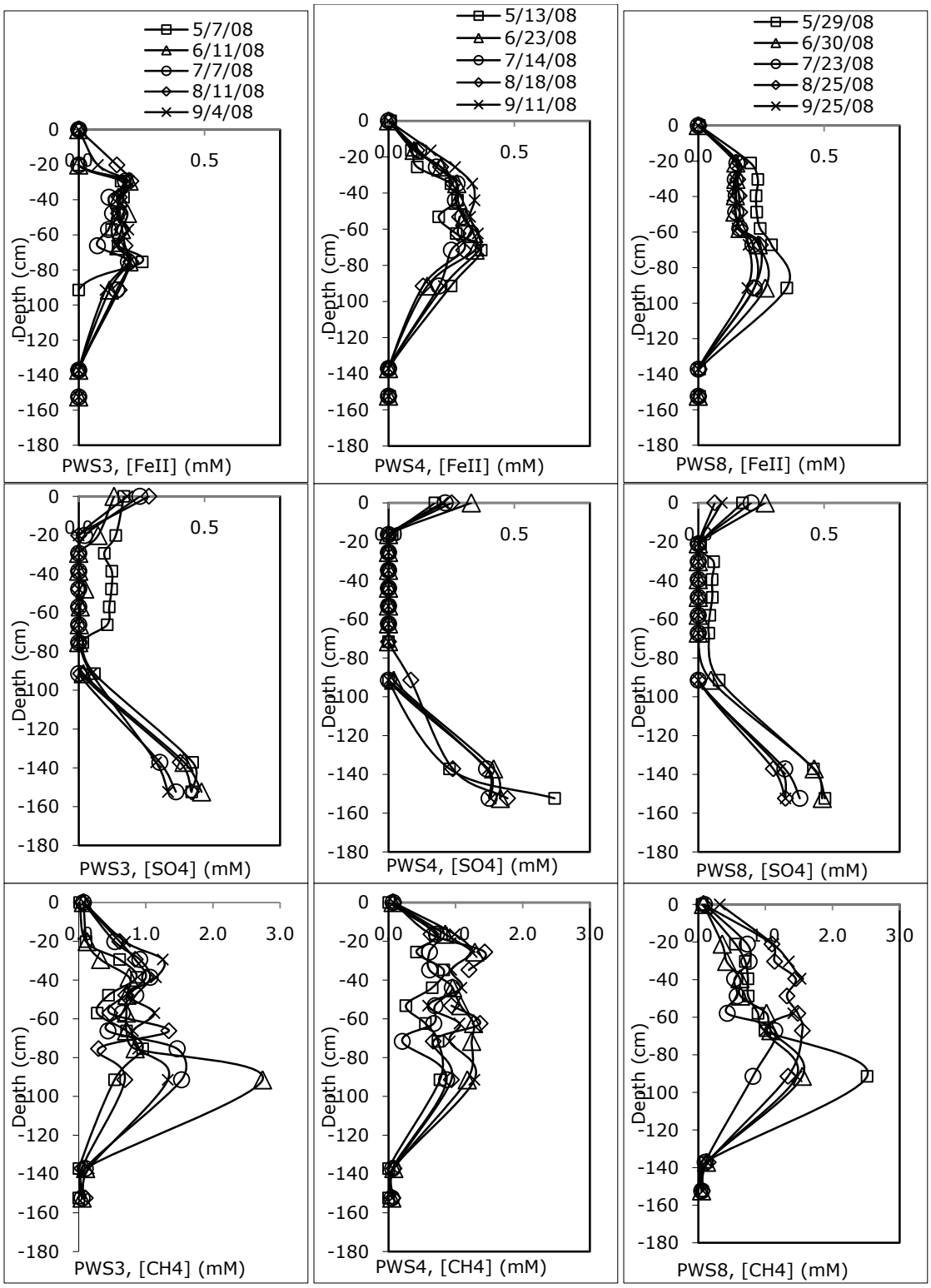

Figure B.1.3 WPAFB wetland profiles of ferrous iron, sulfate, and methane

Fe(II) (mM), SO4, and CH4 (mM) profiles from the PWS units and Piezometers.

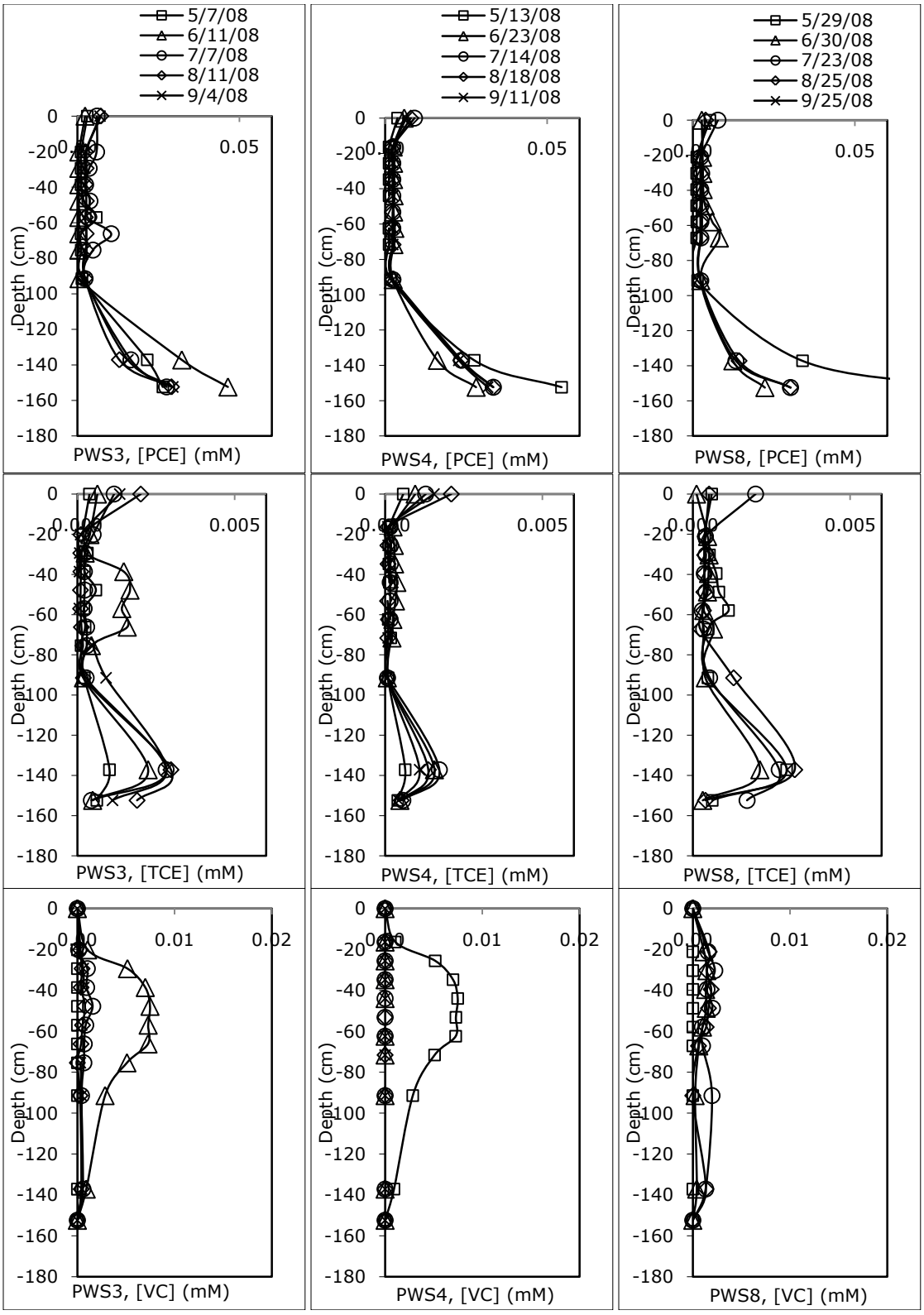

Figure B.1.4 WPAB wetland profiles of PCE, TCE, and VC

PCE (µM), TCE (µM), and VC (µM) profiles from the PWS units and Piezometers

B.2 METHANE AND AMMONIA EXPERIMENTAL DATA

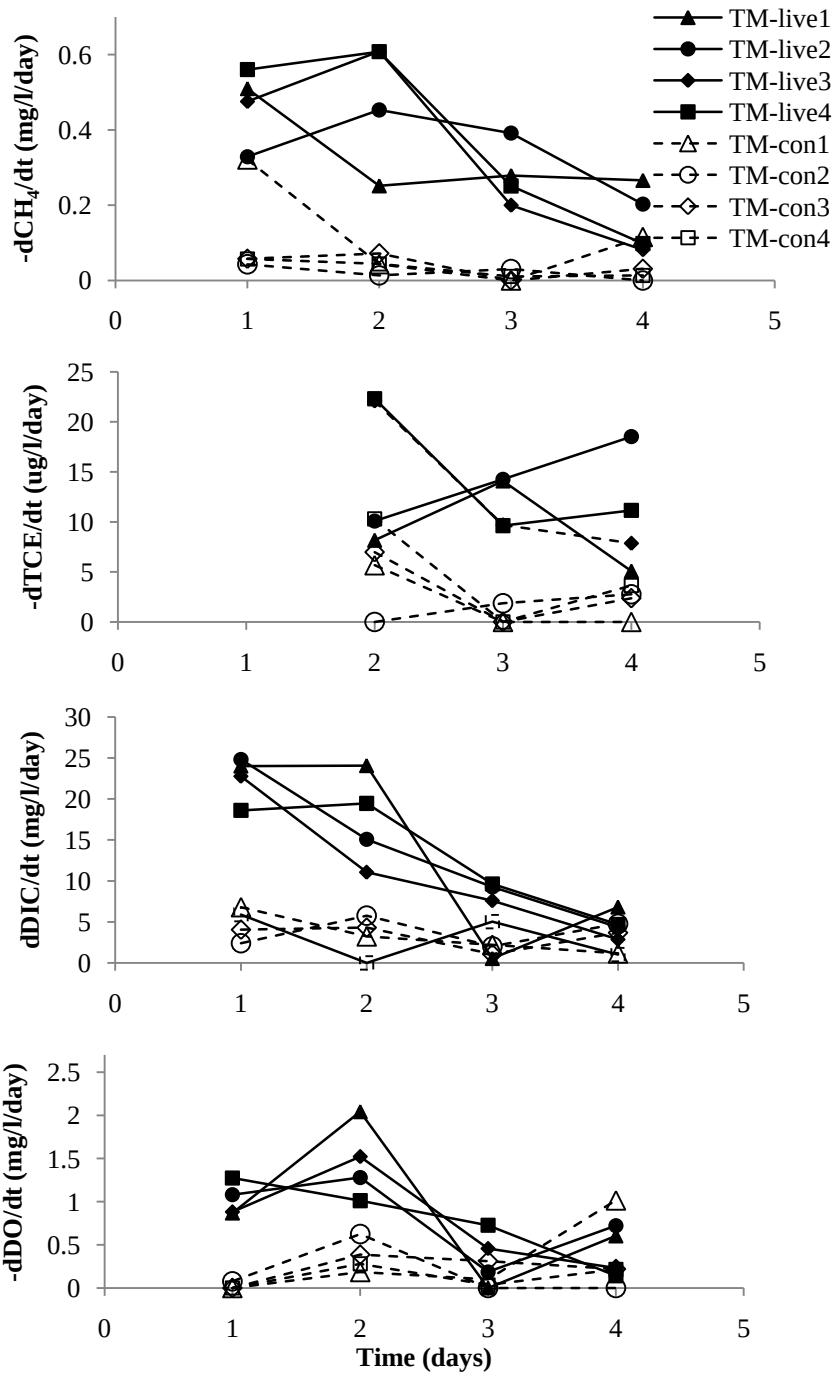

Figure B.2.1 Average rates during TCE cycles of the methane experiment

Average rates of CH_4 and TCE degradation, DO loss, and DIC production rates through the cycles for live and control microcosms

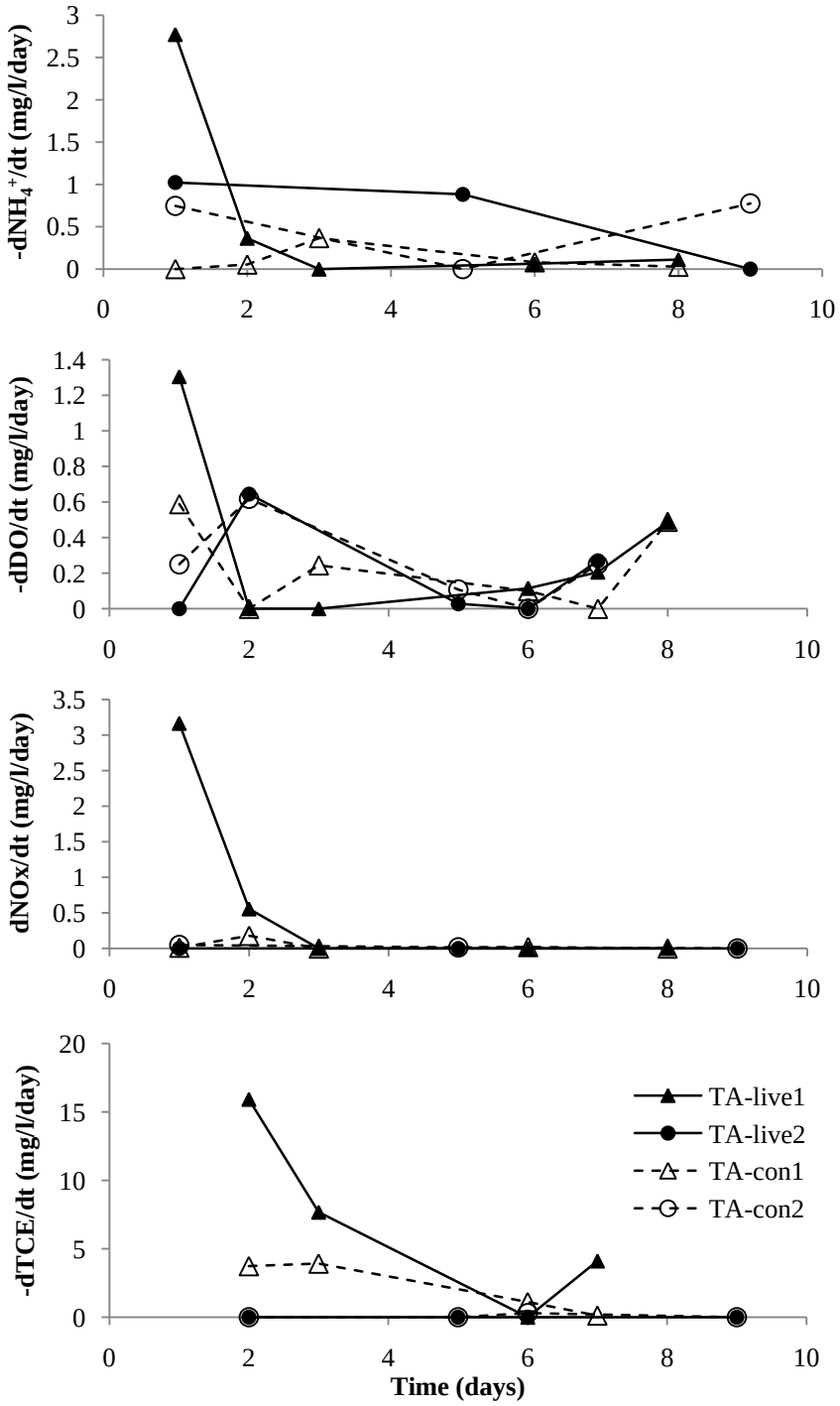

Figure B.2.1 Average rates during TCE cycles of the ammonia experiment

Average rates of NH_4^+ and TCE degradation, DO consumption and NOx production through the cycles for live and controls microcosms

Table B.2.1 Initial rates of solutes during the enrichment cycle of the methane and ammonia experiments

Average loss/production rates of solutes (CH_4, NH_4^+, DO, NOx, and DIC) in control and live microcosms for each cycle of methane and ammonia enrichments (mean ± SD, n = 3).

Average rate d[C]/dt (mg L^{-1} d^{-1})	Enrichment with Methane (EM)				Enrichment with Ammonia (EA)		
	Cycle EM1	Cycle EM2	Cycle EM3	Cycle EM4	Cycle EA1	Cycle EA2	Cycle EA3
CH_4 loss							
Control	0.00 ± 0.01	0.01 ± 0.02	0.06 ± 0.02	0.06 ± 0.02	-	-	-
Live	0.14 ± 0.03	0.33 ± 0.00	0.42 ± 0.01	0.37 ± 0.01	-	-	-
NH_4^+ loss							
Control	-	-	-	-	0.52 ± 0.08	0.04 ± 0.07	0.27 ± 0.12
Live	-	-	-	-	1.12 ± 0.00	2.82 ± 0.05	6.25 ± 0.05
DO loss							
Control	0.27 ± 0.08	0.25 ± 0.06	0.49 ± 0.24	0.13 ± 0.01	0.35 ± 0.01	0.00 ± 0.00	0.45 ± 0.09
Live	0.59 ± 0.02	1.08 ± 0.14	1.51 ± 0.07	1.08 ± 0.10	0.43 ± 0.08	0.19 ± 0.04	0.91 ± 0.07
DIC production							
Control	8.72 ± 2.00	4.79 ± 1.45	3.09 ± 0.50	4.10 ± 0.61	-	-	-
Live	12.7 ± 0.12	15.3 ± 0.56	13.5 ± 2.80	13.0 ± 0.87	-	-	-
NOx production							
Control	-	-	-	-	0.00 ± 0.00	0.06 ± 0.10	0.00 ± 0.00
Live	-	-	-	-	0.73 ± 0.09	2.61 ± 0.18	5.03 ± 0.40

B.3 *CAREX COMOSA* AND *SCIRPUS ATROVIRENS* EXPERIMENTAL DATA

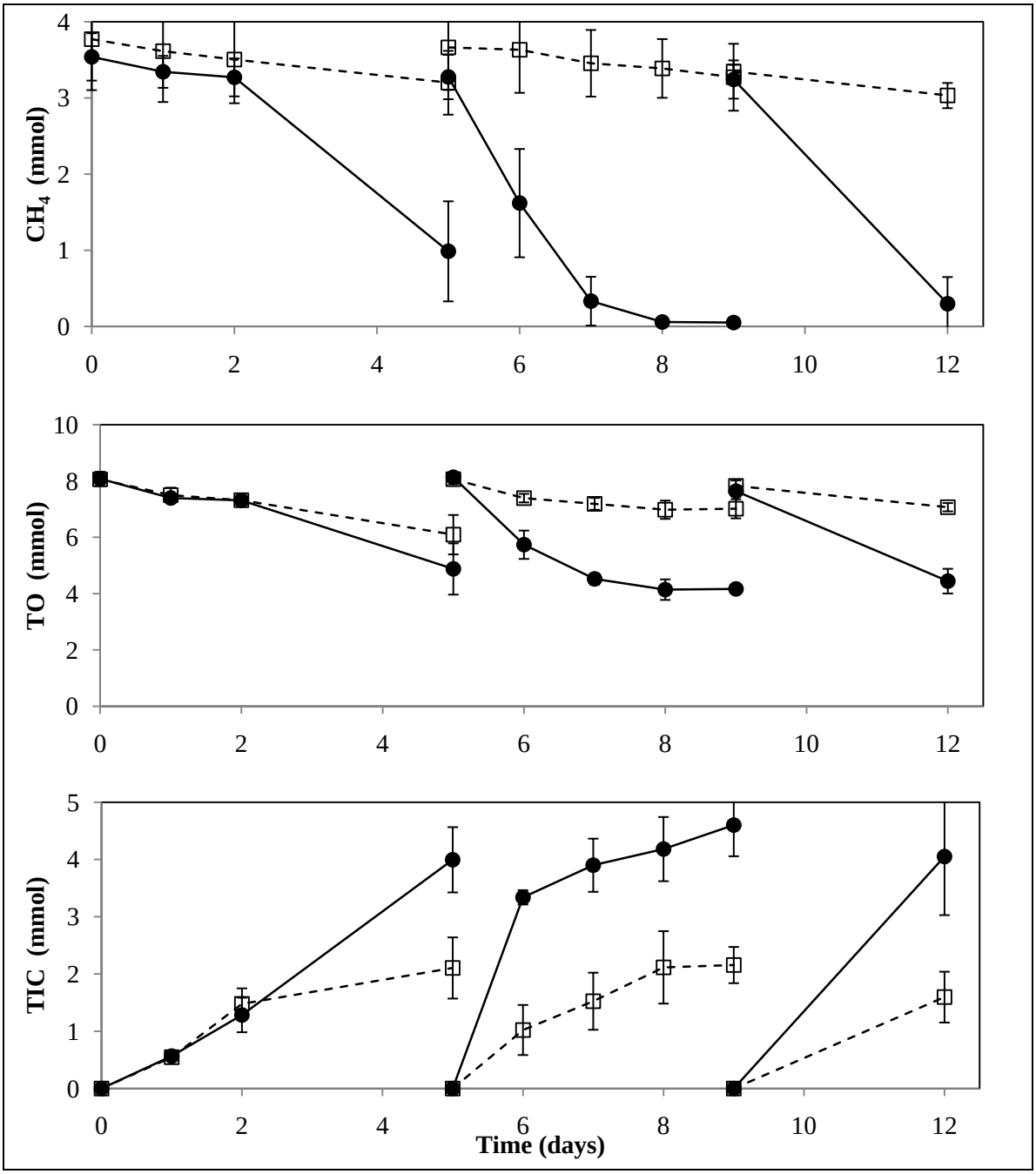

Figure B.3.1 Mass of CH_4, TO, and TIC for the *Carex comosa* enrichment cycles

Mass of CH_4, TO, and TIC in the live (black circles) and control microcosms (white squares) for the enrichment cycles (EC1 through EC3) with *Carex comosa* (mean ± 1 SD, n=3 per treatment).

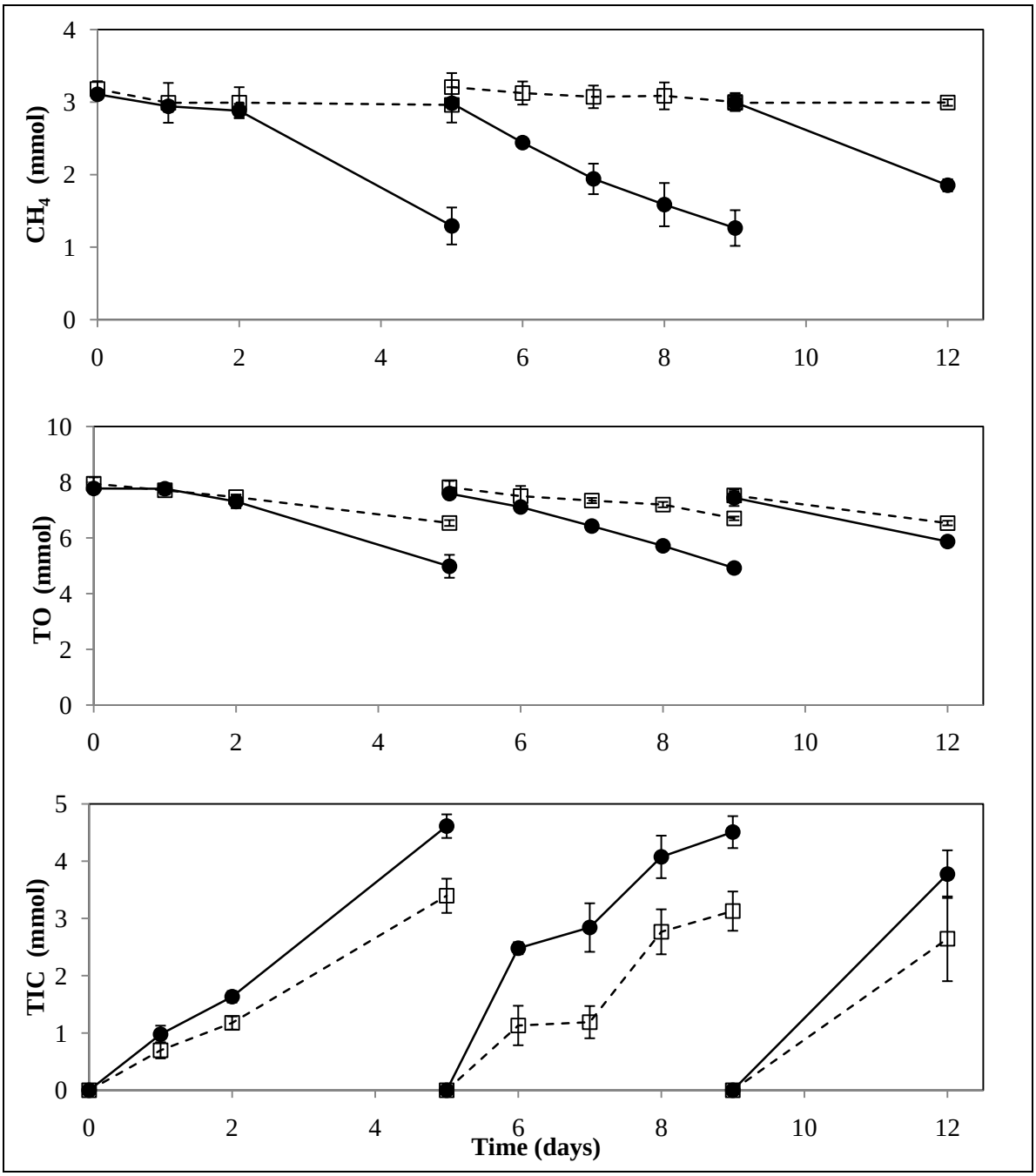

Figure B.3.2 Mass of CH_4, TO, and TIC in the *Scirpus atrovirens* enrichment cycles

Mass of CH_4, TO, and TIC in the live (black circles) and control microcosms (white squares) for the enrichment cycles (EC1 through EC3) with *Scirpus atrovirens* (mean ± 1 SD, n=3 per treatment).

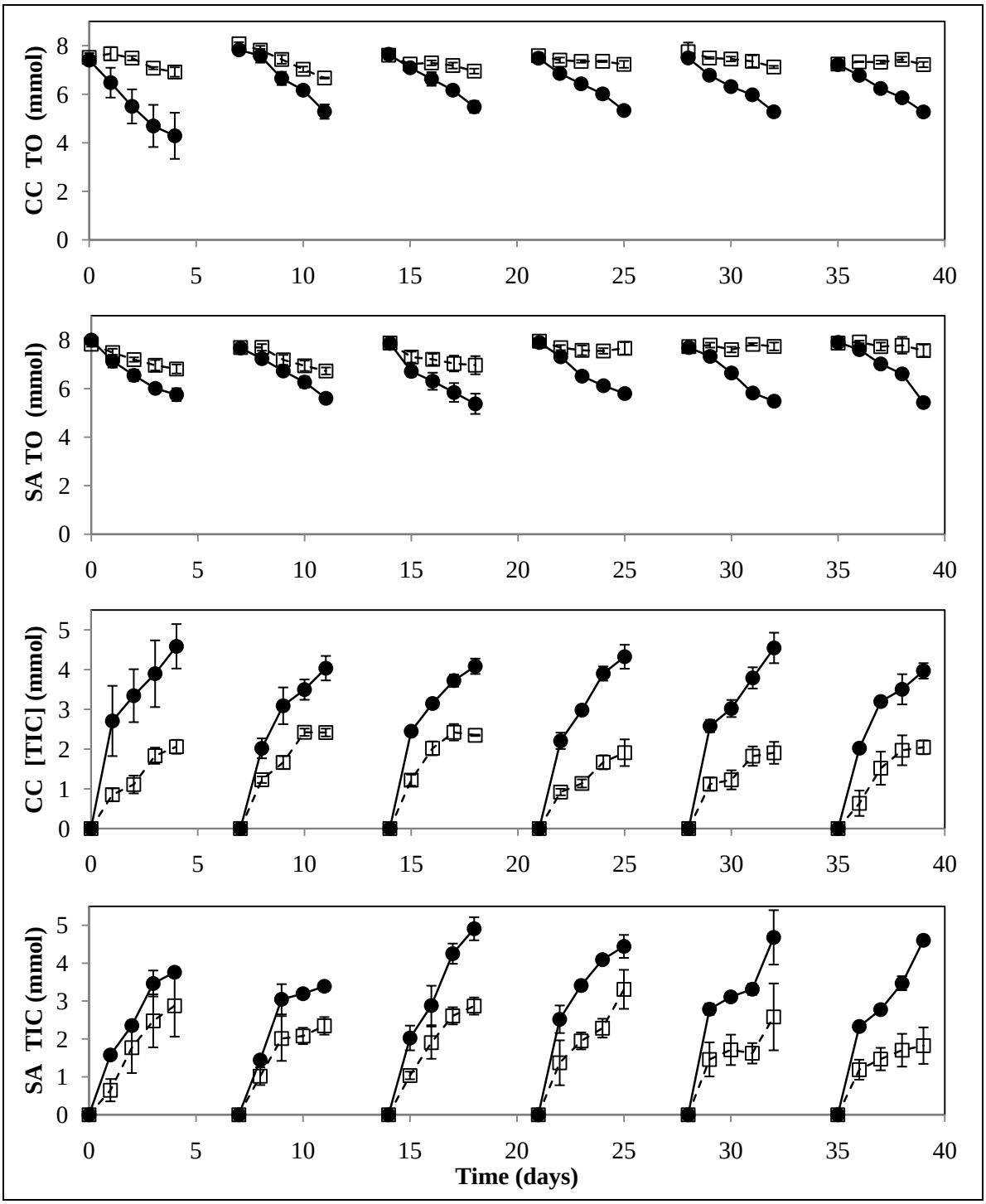

Figure B.3.3 Mass of TO and TIC in *Carex comosa* and *Scirpus atrovirens* TCE cycles

Mass of TO and TIC in the live (black circles) and control microcosms (white squares) for six TCE cycles (TC1 through TC6) with *Carex comosa* and *Scirpus atrovirens* (mean ± 1 SD, n=3 per treatment).

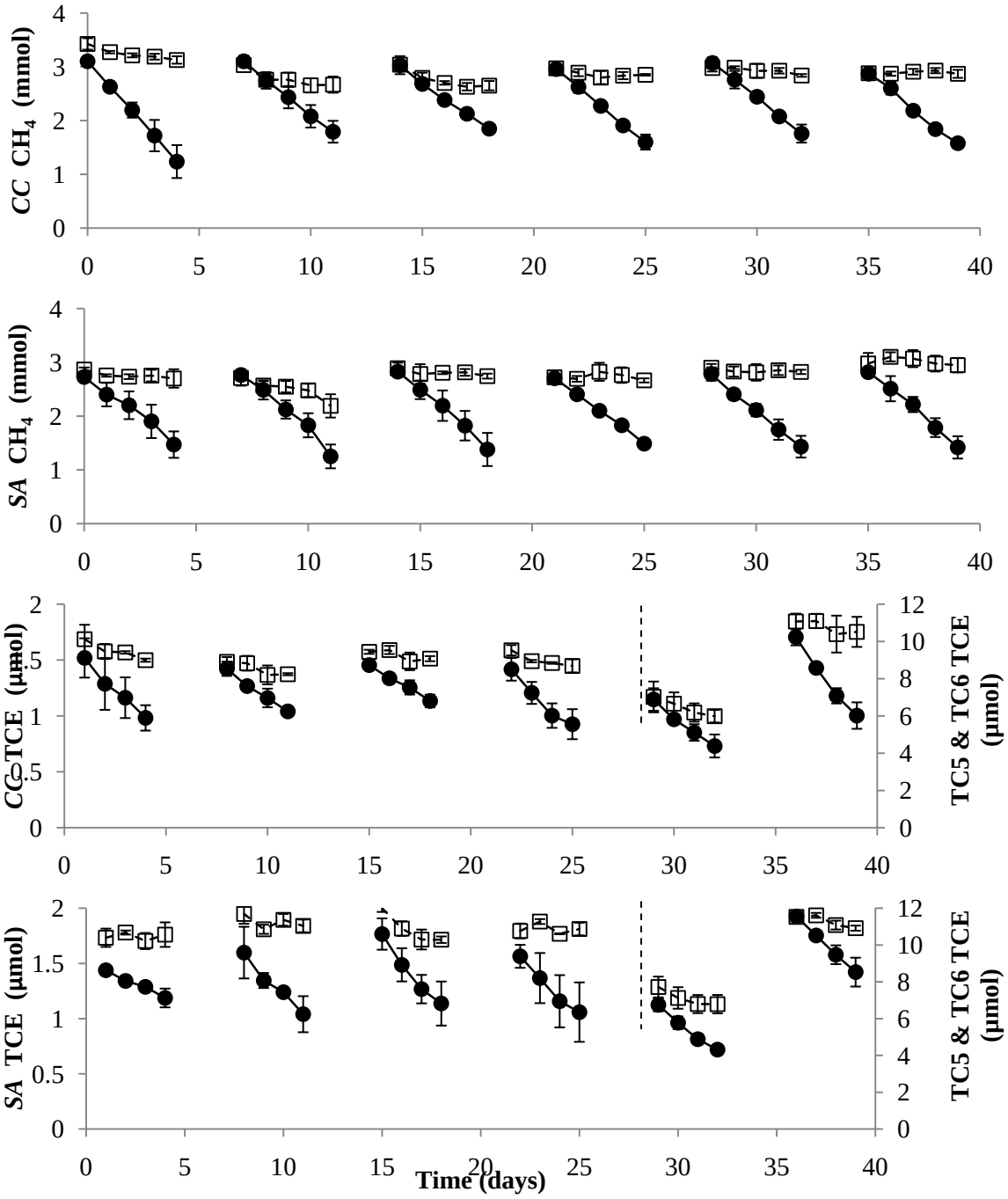

Figure B.3.4 Mass of CH_4 and TCE in *Carex comosa* and *Scirpus atrovirens* TCE cycles

Total mass of TCE and CH_4 in the live (black circles) and control (white squares) microcosms for all six TCE cycles (TC1 through TC6) with *Carex comosa* and *Scirpus atrovirens* (mean ± 1 SD, n=3 per treatment). Cycles 5 and 6 are plotted on the secondary (right) y-axis for TCE.

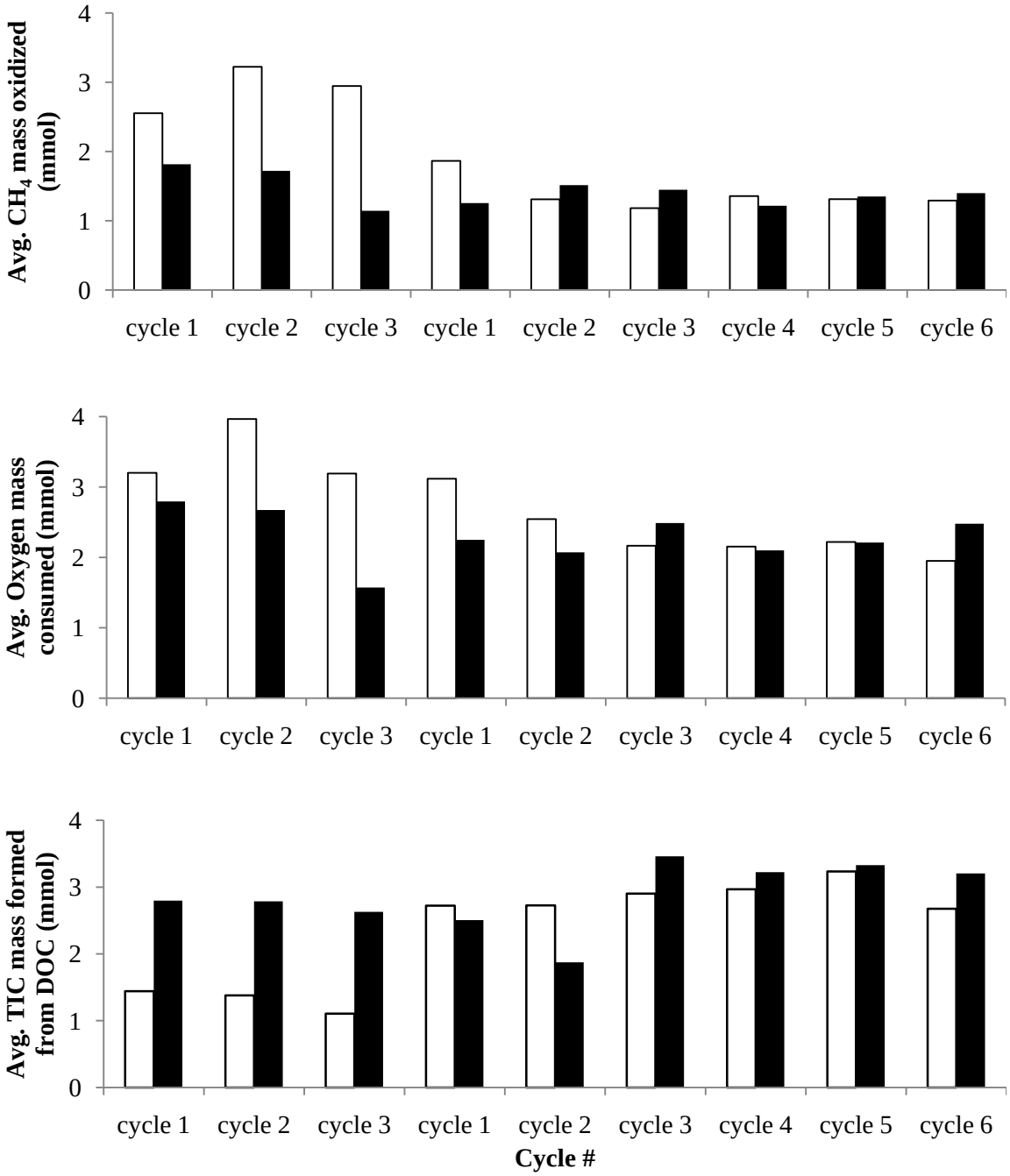

Figure B.3.5 Methane oxidized, oxygen consumed, and TIC formed from DOC

Average molar mass of methane oxidized (top), oxygen consumed (middle), and TIC formed from DOC (= total TIC formed-methane oxidized) (bottom) in live microcosms with *CC* (white bars) and *SA* (black bars) roots. The data for control microcosms are not shown.

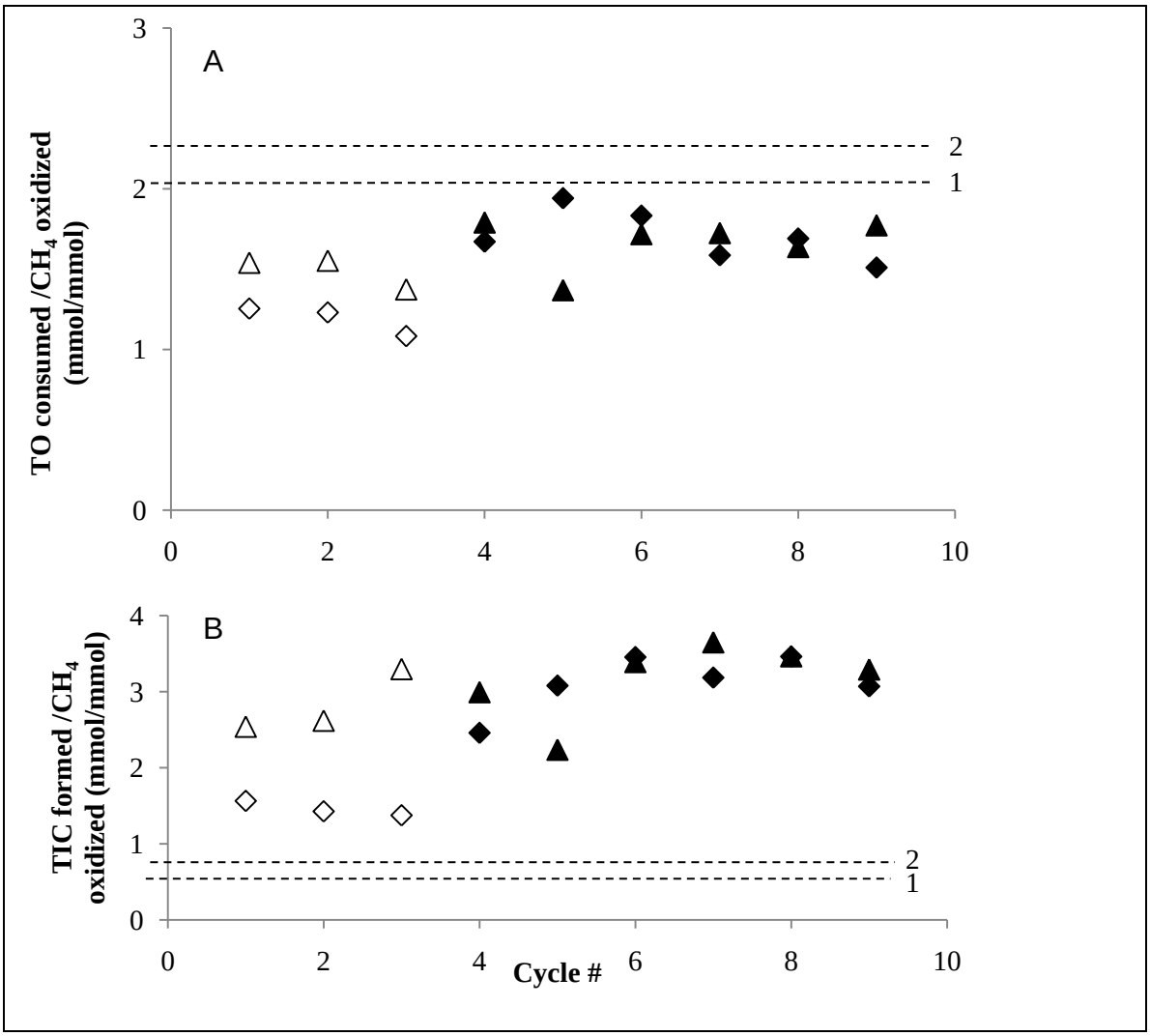

Figure B.3.6 Stiochiometric ratios during the *Carex comosa* and *Scirpus atrovirens* experiment

Ratios for TO consumed to CH_4 oxidized (A) and TIC formed to CH_4 oxidized (B) are displayed with *CC* (diamonds) and *SA* roots (triangles) during enrichment (open symbols) and TCE cycles (closed symbols). On x-axis, cycles 1-3 are for enrichment (EC1 through EC3), and cycles 4-9 are for TCE (TC1 through TC6). The dashed lines '1' and '2' represent TO requirements per mole of methane (plot A above) and TIC production per mole of methane (plot B above), as per equation 1 (includes biomass production): $CH_4 + 1.66O_2 + 0.482H^+ + 0.0482\ NO_3^- \rightarrow 1.85H_2O + 0.76CO_2 + 0.48C_5H_7O_2N$ (biomass), and equation 2 (no biomass production): $CH_4 + 2O_2 \rightarrow CO_2 + 2H_2O$.

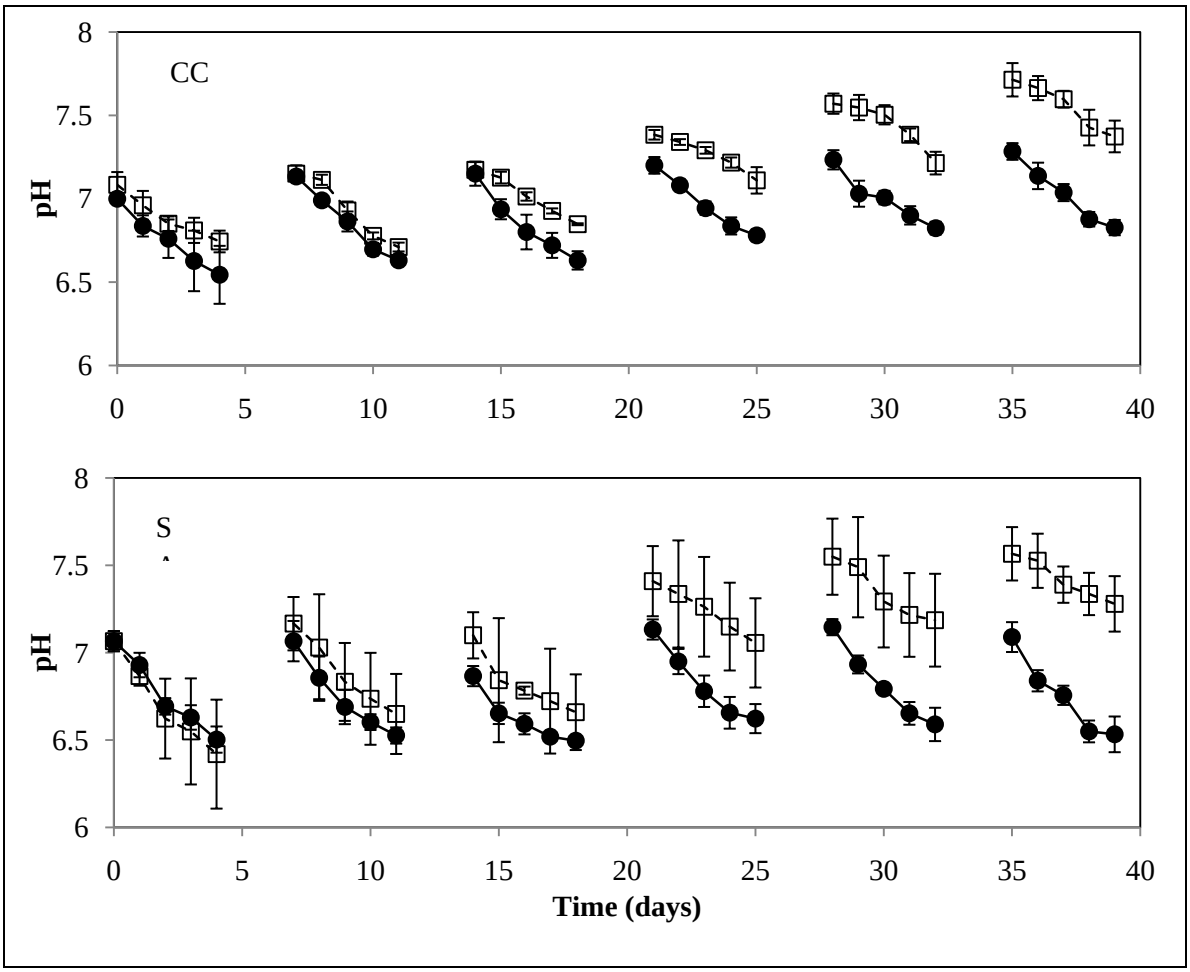

Figure B.3.7 pH during the *Carex comosa* and *Scirpus atrovirens* experiment

Measured pH values for *CC* (top) and *SA* microcosms (bottom) for 6 TCE cycles (TC1 through TC6), shown for live (black circles) and control (open squares) microcosms. The data shows intra-cycle pH decrease in all microcosms in all cycles. The pH decrease in control microcosms may be caused by DIC production (mineralization of DOC leached from roots by heterotrophic microbes); whereas pH decrease in live microcosms may be caused by DIC production (mineralization of DOC leached from roots + mineralization of methane, due to combined heterotrophic and methanotrophic activities). The measurement also shows initial pH increase for successive cycles for both roots, especially for control microcosms. Such inter-cycle increase in initial pH in successive cycles reflects corresponding increase in alkalinity (Figure B below), presumably caused by build-up of soluble cations (for e.g., Ca^{2+}) in the reactors leaching from the roots (Hinsinger 1998, Hinsinger et al. 2005**)**.

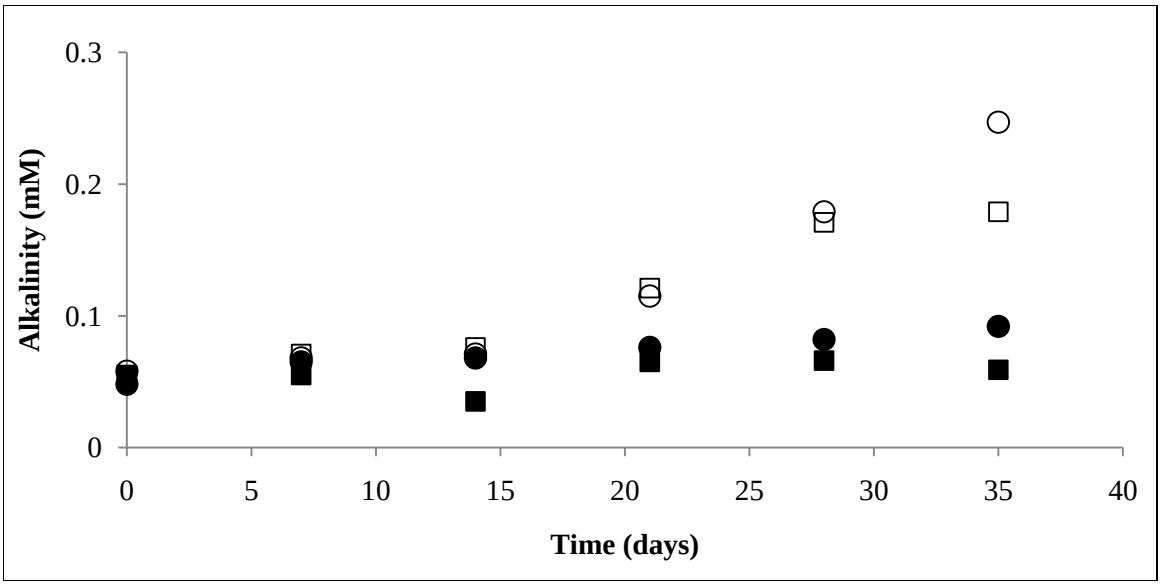

Figure B.3.8 Initial alkalinity during the *Carex comosa* and *Scirpus atrovirens* experiment

Calculated average initial alkalinity values (mM) (Pankow 1991) in live and control microcosms during cycles TC1 through TC6 for *SA* (black squares for live microcosms and open squares for control microcosms) and *CC* roots (black circles for live microcosms, and open circles for control microcosms).

Table B.3.1 Factorial ANOVA Tests

Three-way factorial ANOVA tests measuring the effects of species, treatment, and cycle on normalized initial loss/production rates of solute mass during enrichment cycles (EC1 through EC3) and 4 TCE cycles (TC1 through TC4), and the two-way factorial ANOVA tests measuring the effects of species and treatment on normalized initial loss/production rates of solute mass during cycles TC5 and TC6.

Enrichment																
	TCE				**CH_4**				**TO**				**TIC**			
Source of Variation	***SS***	***df***	***F***	***P***	***SS***	***df***	***F***	***P***	***SS***	***df***	***F***	***P***	***SS***	***df***	***F***	***P***
Species	----	----	----	----	0.37	1	139.2	0.000000	0.04	1	2.5	0.126948	0.10	1	2.3	0.144418
Treatment	----	----	----	----	0.98	1	30.45	0.000011	0.85	1	50.4	0.000000	0.28	1	6.4	0.018232
Cycle	----	----	----	----	0.60	2	24.9	0.000001	0.38	2	11.1	0.000385	1.17	2	13.5	0.00012
Species*Treatment	----	----	----	----	0.13	1	11.2	0.002680	0.08	1	4.4	0.045860	0.00	1	0.1	0.750604
Species*Cycle	----	----	----	----	0.12	2	5.0	0.015062	0.22	2	6.6	0.005073	0.17	2	2.0	0.15884
Treatment*Cycle	----	----	----	----	0.48	2	19.8	0.000008	0.37	2	11.0	0.000397	0.29	2	3.3	0.054306
Species*Treatment*Cycle	----	----	----	----	0.12	2	4.8	0.017606	0.19	2	5.5	0.010653	0.14	2	1.7	0.212703
error					0.29	24			0.41	24			1.04	24		
TCE cycles 1-4																
	TCE				**CH_4**				**TO**				**TIC**			
Source of Variation	***SS***	***df***	***F***	***P***	***SS***	***df***	***F***	***P***	***SS***	***df***	***F***	***P***	***SS***	***df***	***F***	***P***
Species	0.00	1	0.6	0.433058	0.03	1	6.3	0.017407	0.00	1	0.0	0.89737	0.71	1	9.2	0.004858
Treatment	0.13	1	41.1	0.000000	0.53	1	104.7	0.000000	1.13	1	72.7	0.000000	0.38	1	4.8	0.034981
Cycle	0.01	3	0.8	0.509246	0.00	3	0.1	0.947444	0.44	3	9.6	0.000117	0.55	3	2.4	0.088561
Species*Treatment	0.00	1	0.8	0.373008	0.00	1	0.2	0.625773	0.08	1	5.2	0.029962	0.07	1	1.0	0.336298
Species*Cycle	0.10	3	10.7	0.00005	0.03	3	1.9	0.145566	0.13	3	2.8	0.055236	0.19	3	0.8	0.497332
Treatment*Cycle	0.01	3	1.1	0.353004	0.01	3	0.5	0.696911	0.07	3	1.5	0.232972	0.47	3	2.0	0.131579
Species*Treatment*Cycle	0.02	3	1.7	0.192208	0.03	3	1.9	0.155635	0.17	3	3.7	0.022221	0.14	3	0.6	0.615507
error	0.10	32			0.16	32			0.50	32			2.48	32		
TCE cycle 5																
	TCE				**CH4**				**TO**				**TIC**			
Source of Variation	***SS***	***df***	***F***	***P***	***SS***	***df***	***F***	***P***	***SS***	***df***	***F***	***P***	***SS***	***df***	***F***	***P***
Species	0.01	1	0.1	0.719969	0.00	1	0.4	0.557721	0.05	1	6.3	0.035988	0.00	1	0.0	0.897728

Treatment	0.42	1	7.6	0.024647	0.10	1	24.2	0.001172	0.31	1	43.1	0.000175	0.06	1	2.9	0.128277
Species*Treatment	0.04	1	0.7	0.442195	0.00	1	0.0	0.852972	0.00	1	0.3	0.616314	0.02	1	1.1	0.315521
error	0.44	8			0.03	8			0.06	8			0.17	8		
TCE cycle 6																
	TCE				**CH4**				**TO**				**TIC**			
Source of Variation	***SS***	***df***	***F***	***P***	***SS***	***df***	***F***	***P***	***SS***	***df***	***F***	***P***	***SS***	***df***	***F***	***P***
Species	0.16	1	7.7	0.023872	0.00	1	0.2	0.679757	0.02	1	2.9	0.124949	0.64	1	22.9	0.001387
Treatment	2.84	1	133.1	0.000003	0.18	1	34.0	0.00039	0.31	1	51.5	0.000094	0.07	1	2.7	0.14132
Species*Treatment	0.12	1	5.4	0.047954	0.01	1	2.4	0.158455	0.01	1	0.9	0.361293	0.01	1	0.2	0.654263
error	0.17	8			0.04	8			0.06	8			0.17	8		

B.4 KINETICS EXPERIMENTAL DATA

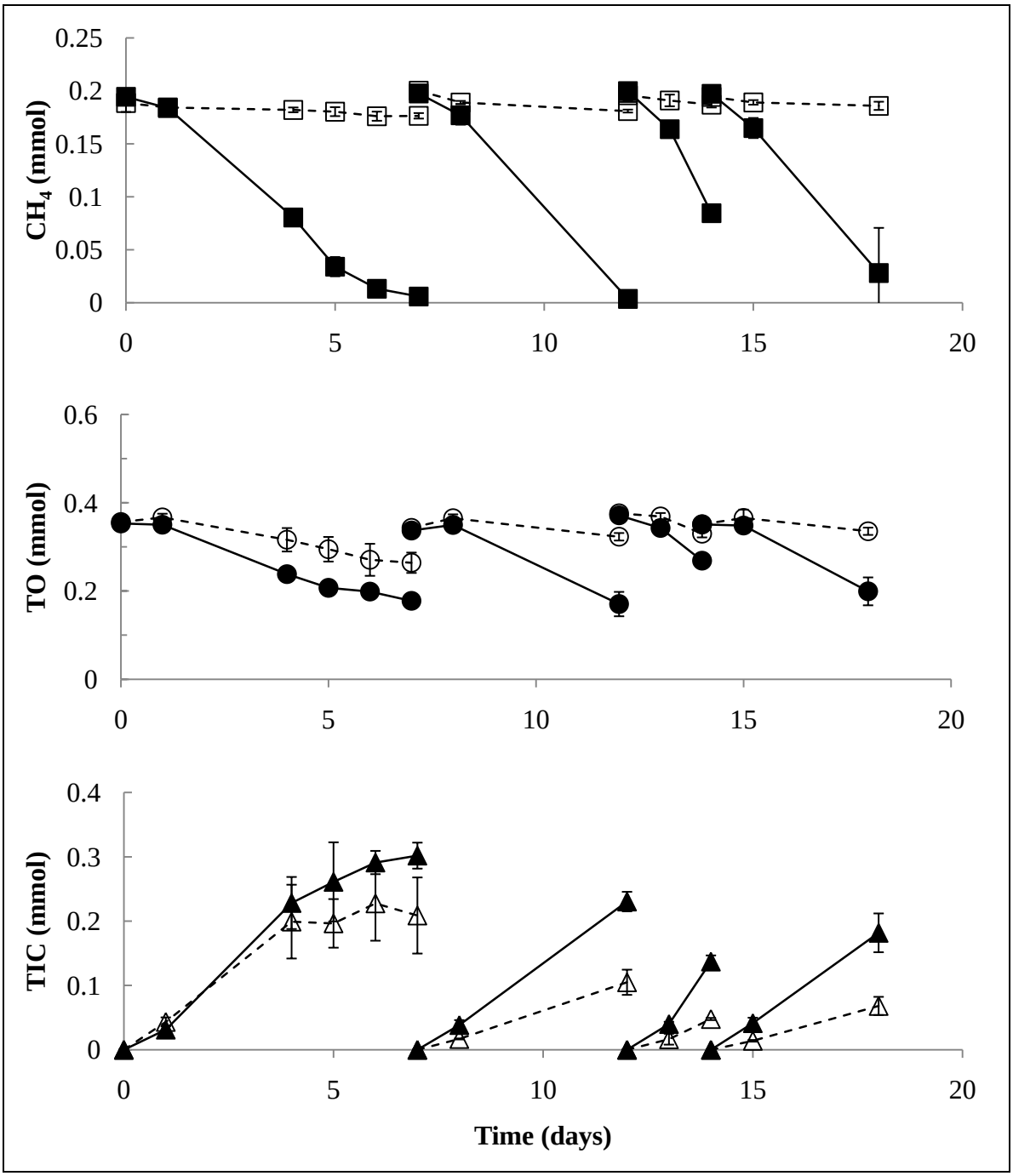

Figure B.4.1 Variations in total mass during *cis*DCE enrichment cycles

Variations in total mass of CH_4, O_2, and IC (mmol) during four enrichment cycles of *cis*DCE experiment; data above for live (black symbols) and control (white symbols) microcosms with CH_4 (mean ± SD, n=3 per treatment).

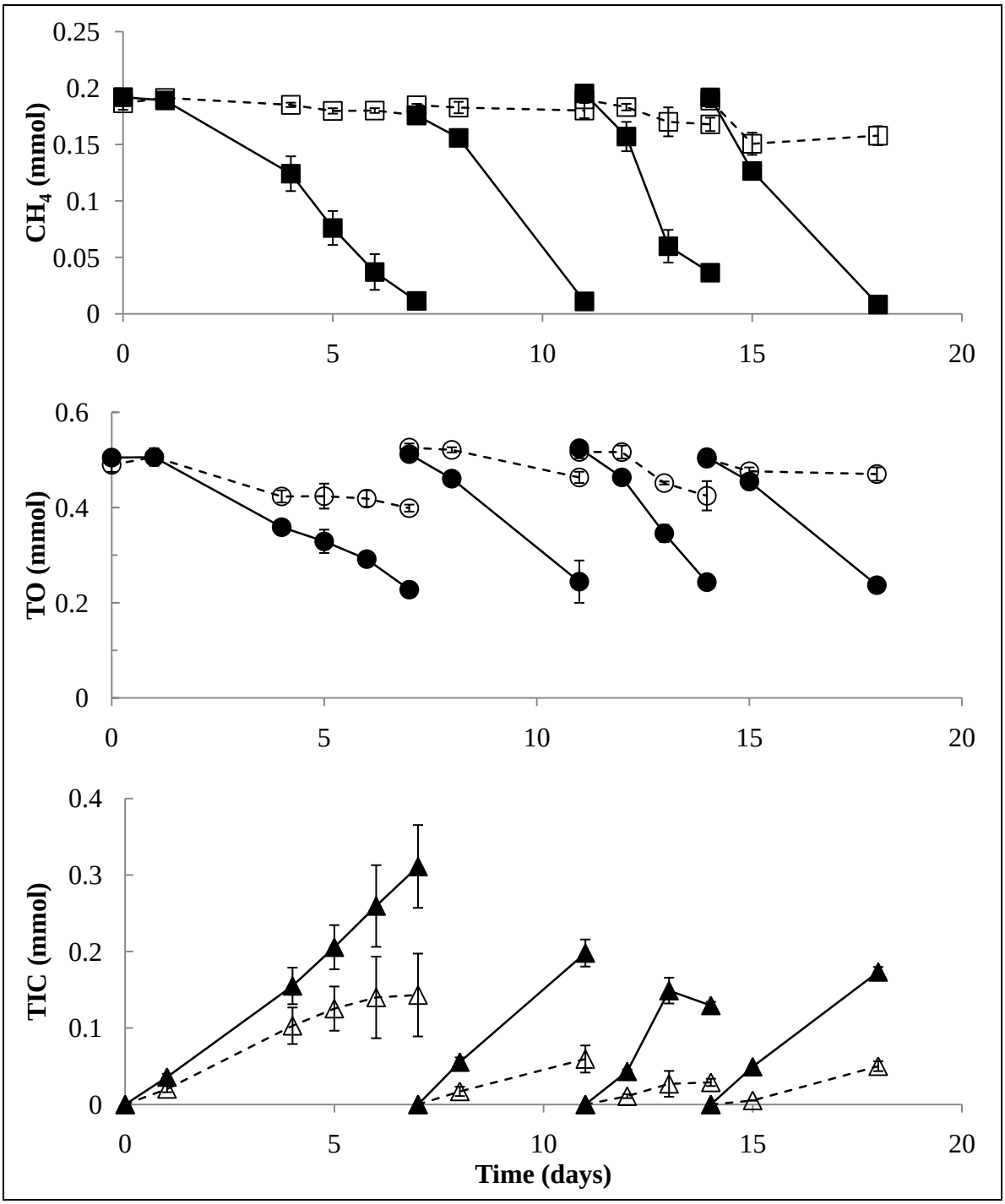

Figure B.4.2 Variations in total mass during TCE enrichment cycles

Variations in total mass of CH_4, O_2, and IC (mmol) during four enrichment cycles of TCE experiment; data above for live (black symbols) and control (white symbols) microcosms with CH_4 (mean ± SD, n=3 per treatment).

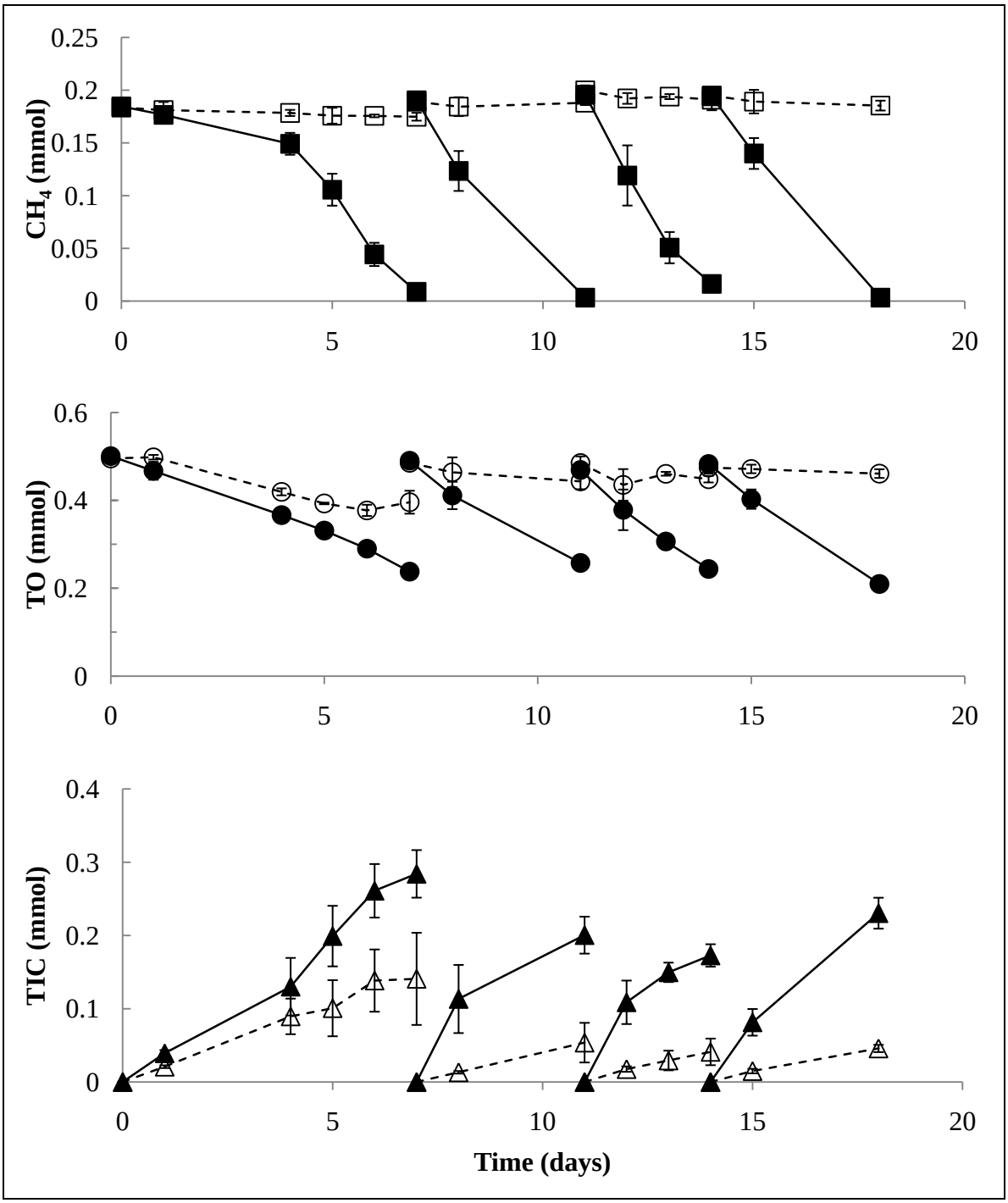

Figure B.4.3 Variations in total mass during 1,1,1TCA enrichment cycles

Variations in total mass of CH_4, O_2, and IC (mmol) during four enrichment cycles of 1,1,1TCA experiment; data above for live (black symbols) and control (white symbols) microcosms with CH_4 (mean ± SD, n=3 per treatment)

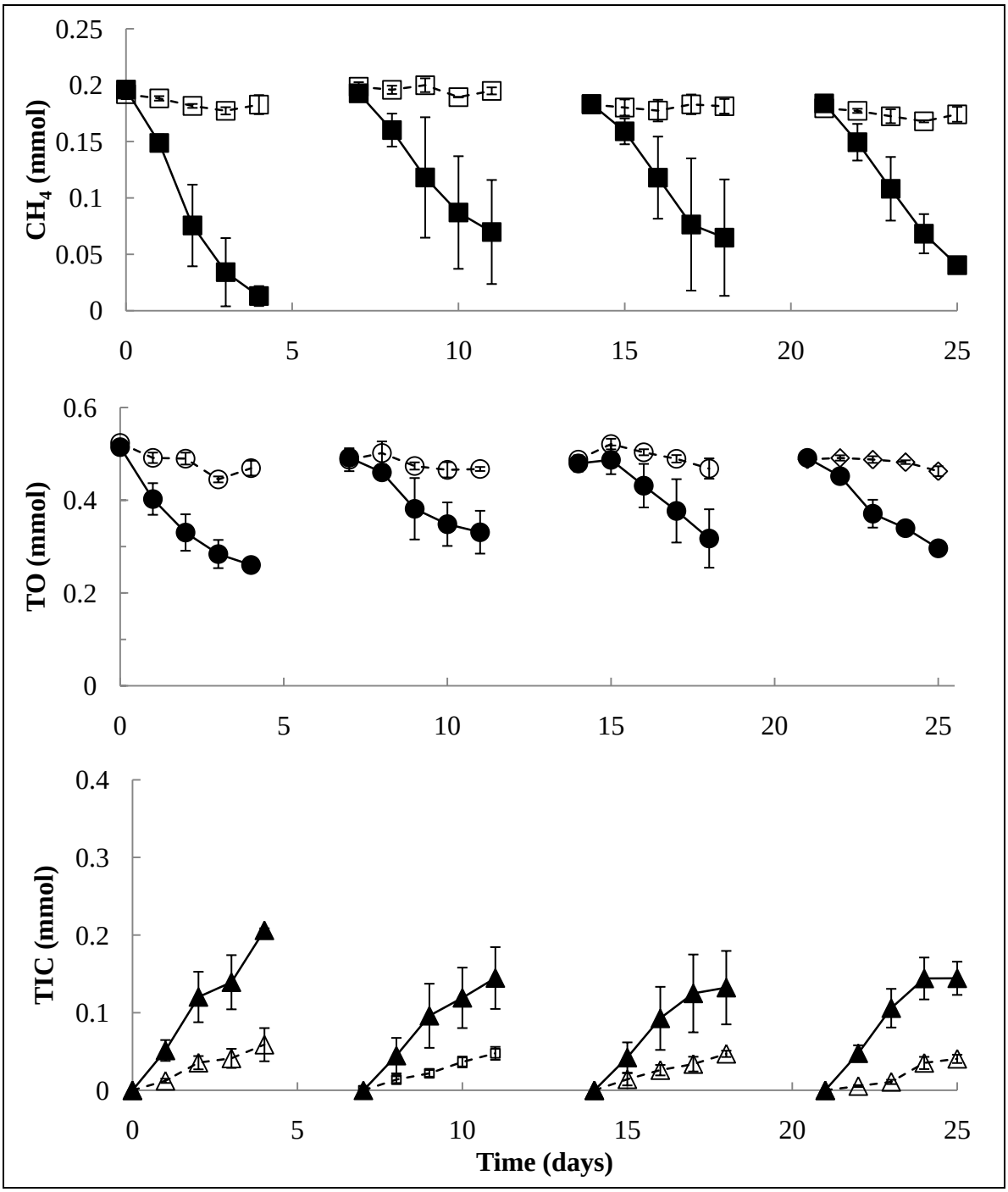

Figure B.4.4 Variations in total mass during *cis*DCE cycles

Variations in total mass of CH_4, O_2, and IC (mmol) during four *cis*DCE cycles of *cis*DCE experiment; data above for live (black symbols) and control (white symbols) microcosms with CH_4 (mean ± SD, n=3 per treatment).

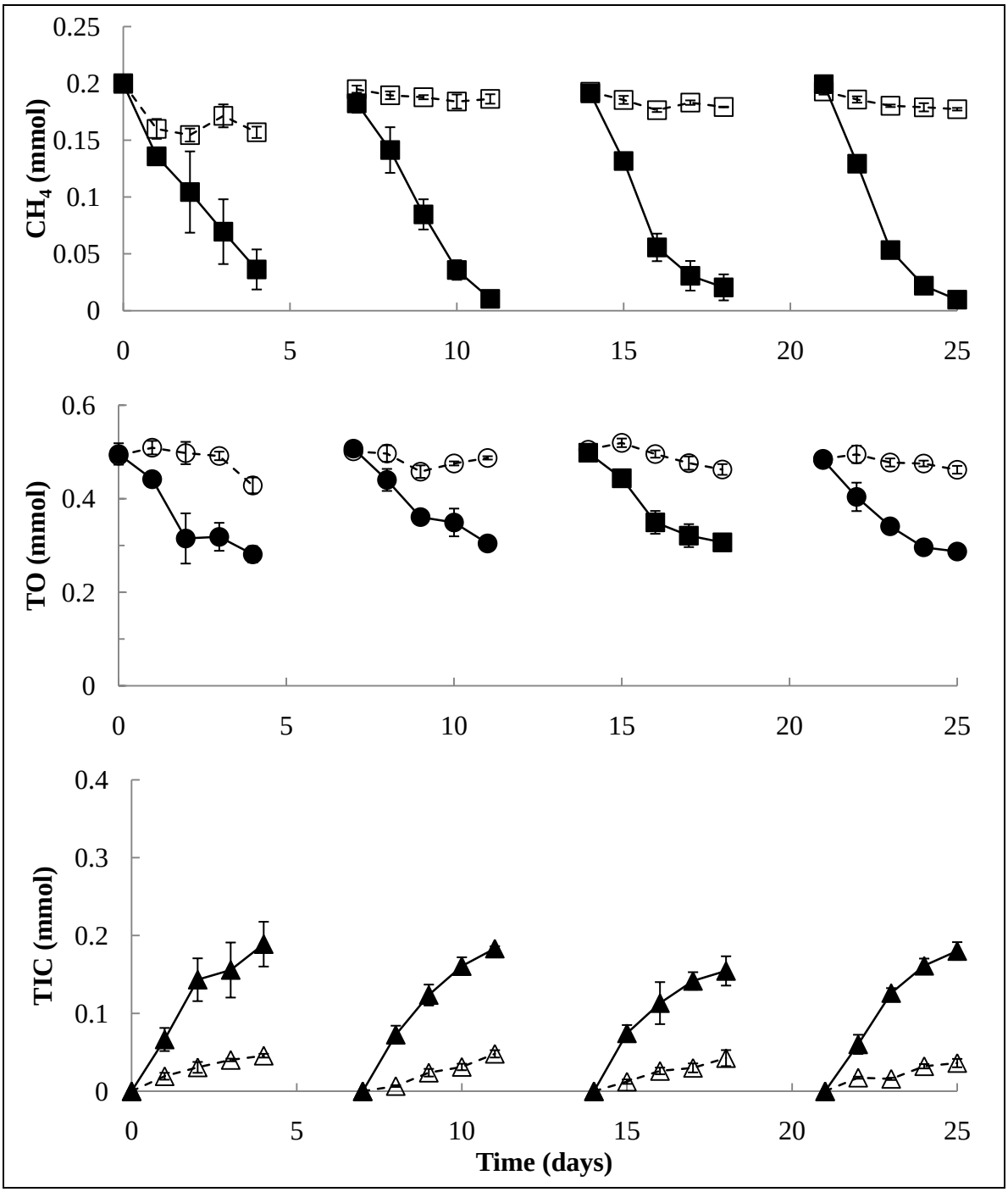

Figure B.4.5 Variations in total mass during TCE cycles

Variations in total mass of CH_4, O_2, and IC (mmol) during four TCE cycles of TCE experiment; data above for live (black symbols) and control (white symbols) microcosms with CH_4 (mean ± SD, n=3 per treatment)**.**

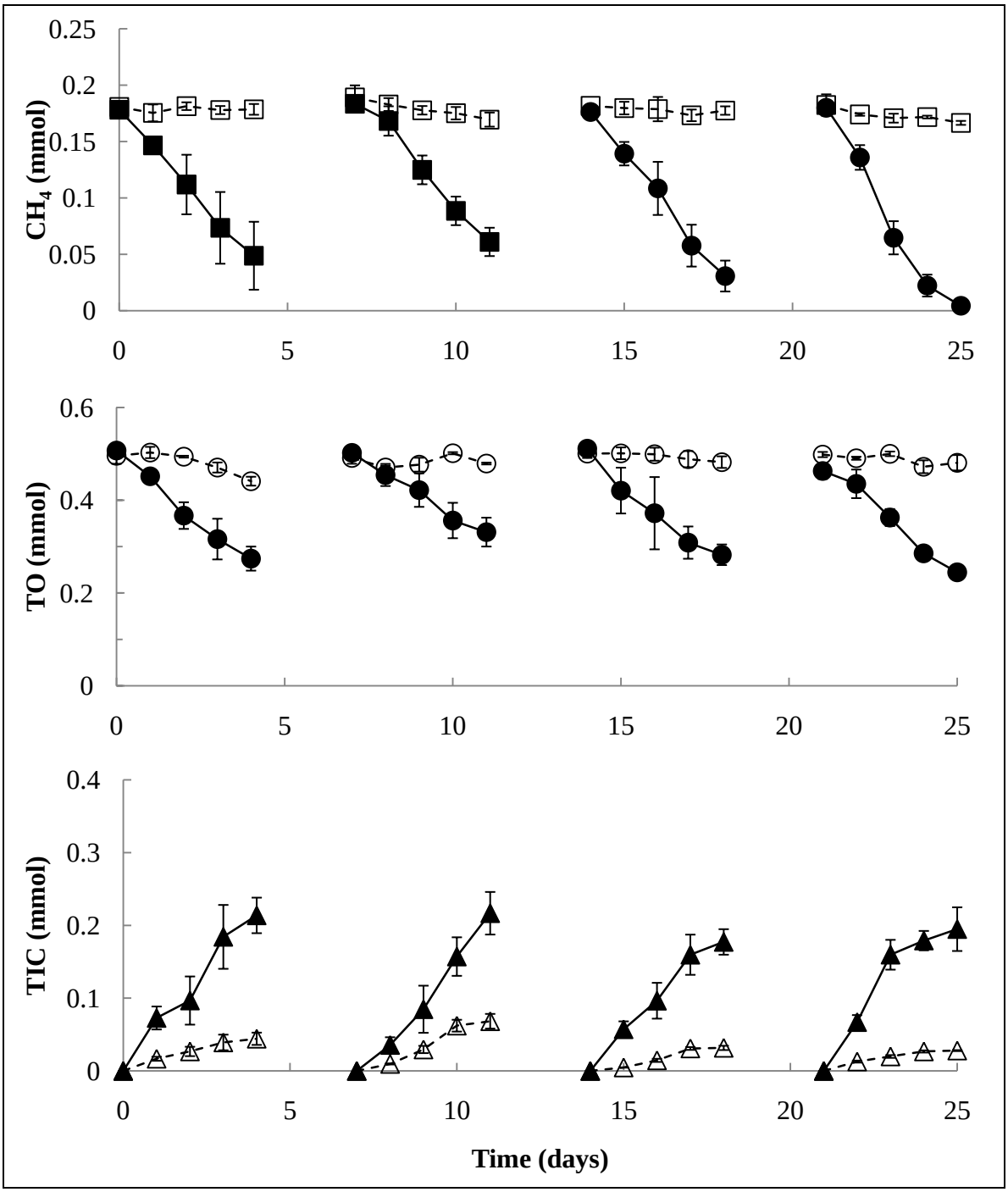

Figure B.4.6 Variations in total mass during 1,1,1TCA cycles

Variations in total mass of CH_4, O_2, and IC (mmol) during four 1,1,1TCA cycles of 1,1,1TCA experiment; data above for live (black symbols) and control (white symbols) microcosms with CH_4 (mean ± SD, n=3 per treatment)**.**

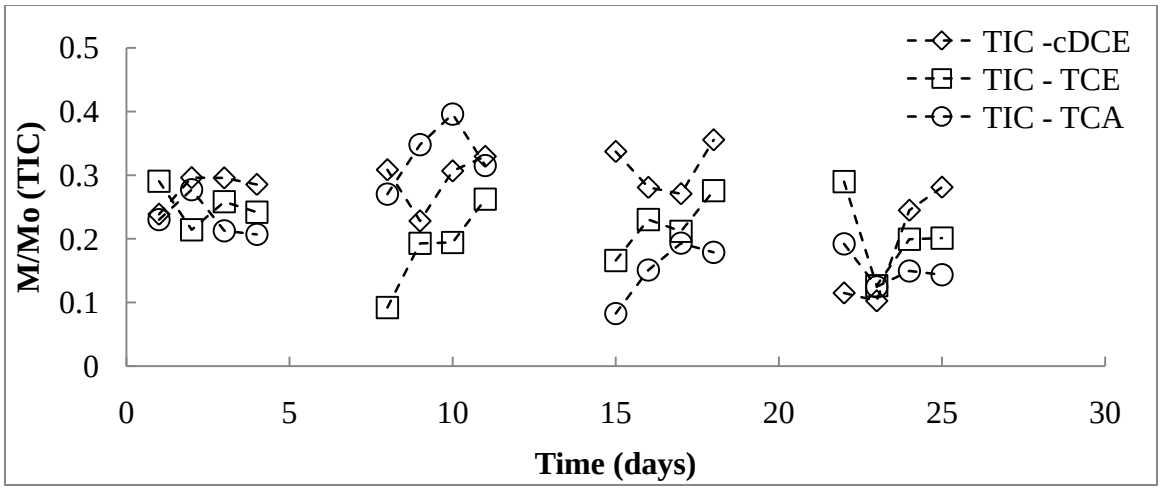

Figure B.4.7 Mean relative changes in mass of total inorganic carbon (TIC) during the kinetics experiments

Mean relative changes in mass of total inorganic carbon (TIC) in the microcosms during the experiments with *cis*DCE, TCE, and 1,1,1TCA.

Table B.4.1 Degradation Rates and Steady-State Biomass for *cis*DCE and TCE.

Degradation rates, $k_{1\text{-}CAH}X_{ss}$ (d^{-1}), and steady-state biomass concentrations, X_{ss} (mmol L^{-1}), for *cis*DCE and TCE. The R^2 values are for an exponential fit to the data.

cycle		*cis*DCE	TCE	TCE (TCA exp)
1	$k_{1\text{-}CAH}X_{ss}$ (d^{-1})	*0.76*	*0.12*	
	R^2	0.99	0.93	
	X_{ss} (mmol L^{-1})	*0.96*	*0.50*	0.58
2	$k_{1\text{-}CAH}X_{ss}$ (d^{-1})	*0.57*	*0.19*	
	R^2	0.99	0.98	
	X_{ss} (mmol L^{-1})	*0.64*	*0.30*	*0.90*
3	$k_{1\text{-}CAH}X_{ss}$ (d^{-1})	*0.58*	*0.13*	*0.10*
	R^2	1	0.98	0.97
	X_{ss} (mmol L^{-1})	*0.59*	*0.47*	*1.07*
4	$k_{1\text{-}CAH}X_{ss}$ (d^{-1})	*0.45*	*0.14*	*0.13*
	R^2	0.99	1	0.98
	X_{ss} (mmol L^{-1})	*0.69*	*0.77*	*1.14*

B.5 REFERENCES

Hinsinger P (1998) How Do Plant Roots Acquire Mineral Nutrients? Chemical Processes Involved in the Rhizosphere. Adv. Agron 64: 225-265

Hinsinger P, Gobran G, Gregory P, Wenzel W (2005) Rhizosphere Geometry and Heterogeneity Arising from Root-Mediated Physical and Chemical Processes. New Phytologist 168: 293-303

Pankow JF (1991) Aquatic Chemistry Concepts. CRC Press, Inc., Boca Raton, FL